AD-A128 965 CHARACTERIZATION OF ULTRASONIC TRANSDUCER THROUGH TRANSMISSION SYSTEMS(U) WEA CAMBRIDGE MA J C BLOUGH ET AL. DEC 82 N00014-81-C-2319 1/3

UNCLASSIFIED F/G 20/3 NL

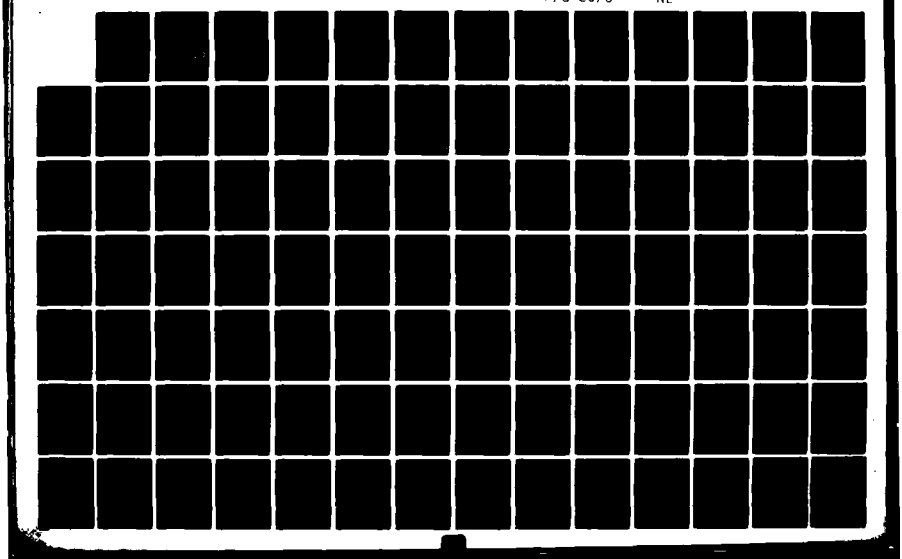

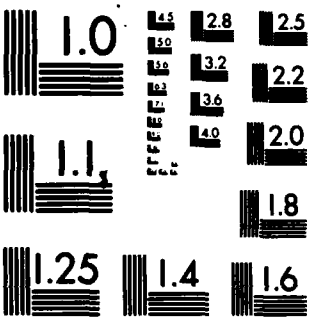

MICROCOPY RESOLUTION TEST CHART
NATIONAL BUREAU OF STANDARDS-1963-A

AD A128965

REPORT DOCUMENTATION PAGE

READ INSTRUCTIONS BEFORE COMPLETING FORM

1. REPORT NUMBER	2. GOVT ACCESSION NO. AD-A128 965 — 3. RECIPIENT'S CATALOG NUMBER
4. TITLE (and Subtitle) CHARACTERIZATION OF ULTRASONIC TRANSDUCER THROUGH-TRANSMISSION SYSTEMS	5. TYPE OF REPORT & PERIOD COVERED FINAL REPORT June 1981 - September 1982
	6. PERFORMING ORG. REPORT NUMBER
7. AUTHOR(s) James C. Blough, Beth Doll, Samson S. Lee & James H. Williams, Jr.	8. CONTRACT OR GRANT NUMBER(s) N00014-81-C-2319
9. PERFORMING ORGANIZATION NAME AND ADDRESS WEA P.O. Box 260, MIT Branch Cambridge, MA 02139	10. PROGRAM ELEMENT, PROJECT, TASK AREA & WORK UNIT NUMBERS
11. CONTROLLING OFFICE NAME AND ADDRESS	12. REPORT DATE December 1982
	13. NUMBER OF PAGES 224
14. MONITORING AGENCY NAME & ADDRESS(if different from Controlling Office) Naval Research Laboratory Washington, D.C. 20375 H.H. Chaskelis, Code 5831	15. SECURITY CLASS. (of this report) UNCLASSIFIED
	15a. DECLASSIFICATION/DOWNGRADING SCHEDULE

16. DISTRIBUTION STATEMENT (of this Report)

Distribution Unlimited

17. DISTRIBUTION STATEMENT (of the abstract entered in Block 20, if different from Report)

Distribution Unlimited

18. SUPPLEMENTARY NOTES

19. KEY WORDS (Continue on reverse side if necessary and identify by block number)

Ultrasonic Transducers
Piezoelectric Transducers
Wave Propagation

20. ABSTRACT (Continue on reverse side if necessary and identify by block number)

Five different designs of broadband piezoelectric ultrasonic transducers are evaluated and compared to determine the effects of various transducer design parameters on the transducer response. The transducers tested include the Acoustic Emission Technology (AET) FC-500 transducer, consisting of a 0.073 cm (0.029 in) lead metaniobate piezoelement, 0.035 cm (0.014 in) titanium carbide wearplate and 0.635 cm (0.250 in) tungsten epoxy backing layer; the AE-101, a prototype identical to the FC-500 except that it has a 0.035 cm (0.014 in) aluminum wearplate; and the AE-100, AE-102, and AE-103, also identical to the

FC-300 except that they have backing layers of 0.0 cm (no backing), 1.270 cm (0.500 in), and 1.905 cm (0.750 in), respectively. Pairs of each of the transducers are clamped face-to-face and tested with narrow-band continuous sinusoids and tone bursts (0.4 to 3.0 MHz), and with a broadband input signal (1.0 μsec pulse).

A model is developed which includes the effects of the generation and detection of stress waves by the piezoelement, the propagation of waves through attenuating transducer elements, and the interaction of stress waves at the interfaces between those elements. The model is used to predict the output signals for each of the two-transducers-together systems, and the predicted results are compared to the measured results for each system.

There are some discrepancies between the measured and predicted results. These discrepancies are eliminated, however, by the introduction of time delays in the model as waves interact at the surfaces of the piezoelement in the output transducer. For the transducers with titanium carbide wearplates, waves which are transmitted across the wearplate-piezoelement interface are delayed by 0.08-0.09 μsec, and reflected waves are delayed by 0.20-0.24 μsec. (By comparison, the transit times of the wearplate and piezoelement are 0.04 and 0.25 μsec, respectively.) These time delays at the wearplate-piezoelement interface are reduced by about 40% when the titanium carbide wearplate is replaced by an aluminum wearplate. A time delay is also introduced for waves traveling through the backing layer, in addition to the transit time of the layer itself; this delay ranges from 0.75 μsec for the AE-101 to 1.50 and 1.60 μsec for the AE-101 and FC-500, respectively.

Two additional factors are shown to influence the correlation between measured and predicted output signals. First, the voltage across the output piezoelement decays exponentially with time due to the flow of current through the oscilloscope. The time constant associated with this decay is found to be 1.0 μsec for the FC-500, and about 5 μsec for the other transducers. Secondly, there is a multiplicative amplitude factor which depends on the piezoelectric constant and capacitance of the piezoelement, which determines the amplitude of the output signal. Since the piezoelectric constant and capacitance are difficult to measure, the amplitude factor is evaluated for each system simply by dividing the amplitudes of the measured and predicted output signals. The amplitude factor is found to be fairly consistent from one transducer to another; over the frequency range 0.4-2.0 MHz, the amplitude factors for all of the transducers fall between 3.5 and 7.0 x 10^{16} N/m^3.

Several other transducer parameters are studied to determine how they influence the output signal for a particular ultrasonic test system. The effects of changes in backing impedance, backing thickness, wearplate impedance and piezoelement thickness are evaluated, and a set of guidelines for transducer design is developed. In addition, the role of couplant layers and adhesive-bonding layers in the system is investigated, and it is found that couplant layers have no effects on wave propagation in the system at the frequencies used (0.4-3.0 MHz).

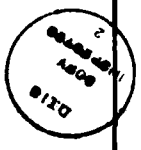

TABLE OF CONTENTS

LIST OF FIGURES

LIST OF TABLES

CHAPTER 1

INTRODUCTION AND LITERATURE REVIEW

1.1 INTRODUCTION

Ultrasonic testing is a means of assessing the mechanical integrity of a structure by studying the propagation of high-frequency stress waves through that structure. An ultrasonic test is performed by applying a known stress waveform at some point on the structure, and then measuring the resulting stress either at that same location or at some other location. The relationship between the input and output stress waveforms can then be used to determine the mechanical integrity of the structure.

A familiar example of ultrasonic testing is the testing of a ping pong ball for cracks. Bouncing the ball on the table introduces a stress impulse to the ball, and the resulting stress waves in the ball produce sound waves which propagate to the ears of the observer. With experience, one can detect even a small crack in the ball by listening to the sound it makes.

Of course, it is easy to detect the presence of overt flaws in a specimen by such a method, but a quantitative determination of strength in unflawed and marginal specimens is much more difficult. Very accurate knowledge of the input and output stress waveforms is required to make such a determination, and the expertise to interpret the results of ultrasonic tests in terms of the strength properties of the specimen is needed as well.

Typically, the correlation of strength properties and ultrasonic test results is performed by fabricating and testing a large number of specimens with varying types and degrees of flaws. The results of the ultrasonic tests are compared to the results of destructive mechanical tests, and a safe limit for certain ultrasonic testing parameters is determined. Unless a thorough analysis accompanies the experiments, however, these empirically-determined "safe" limits can be misleading, incomplete, or even incorrect. Methods must be developed which enable the determination of strength properties directly from the results of ultrasonic tests.

There is clearly a great need for improved quantitative understanding of the behavior of ultrasonic test systems and of the significance of ultrasonic test results. An accurate characterization of broadband piezoelectric ultrasonic transducers is a crucial step toward that goal.

1.2 REVIEW OF THE ANALYSIS AND CHARACTERIZATION OF PIEZOELECTRIC ULTRASONIC TRANSDUCERS

Any attempt to characterize an ultrasonic transducer must begin with an accurate understanding of the behavior of its piezoelement. The fundamental equations describing the piezoelectric effect were first summarized by Voigt in his early volume, "Lehrbuch der Krystallphysik", and appear in a slightly revised form in Cady [1]. A significant contribution to the field was made by Mason [2] with the discovery that the electromechanical behavior of piezoelectric crystals could be

described by an equivalent electric circuit, with one electrical connection and two mechanical connections corresponding to the pair of electrodes and the two faces of the crystal, respectively. Mason's equivalent circuit has since been employed to investigate many transducer phenomena: the coupling between different natural modes of vibration of piezoelectric crystals [3]; the effects of this so-called mode conversion along with impedance-matched backing materials and frequency-tuned wear plates on the frequency response and bandwidth of transducers [4,5,6]; and the nature of the overall transmission coefficient of layered transducers [7], including the effect of adhesive bonding between layers [8]. The strength of Mason's model lies in the application of straightforward, well-understood methods of circuit analysis to an otherwise very difficult electromechanical problem. Unfortunately, many of the equivalent-circuit parameters are not easily measured, and it can be difficult even to estimate values for these quantities [9,10]. In addition, Mason's model provides little if any intuitive insight into the mechanical aspects of transducer operation.

Other electctrical models have been developed to facilitate transducer analysis. A Thevenin-equivalent circuit apprcach has been suggested [11], and a transmission-line model [12] has been employed by Desilets, et. al. [13] to evaluate broadband transducer efficiency, and by Dotti [14] to predict impulse response. Despite such widespread use, however, the value of equivalent circuits in understanding mechanical phenomena is quite limited.

Some work has indeed been done toward predicting transducer

behavior from the principles of applied mechanics. Linear elasticity [15,16] and computational finite-element methods [17] have been applied to analyze the natural modes of piezoelectric plate vibration. The two-dimensional wave equation has been used as a starting point for at least one characterization [18]. These analyses are certainly of value in promoting physical understanding, but provide little aid in describing the interaction of the transducer components with one another.

Among the most significant work in predicting the actual electromechanical behavior of a transducer system is that of Redwood [19,20]. Concerning earlier work based upon the simplified Mason equivalent circuit, Redwood wrote:

> "This equivalent circuit is, however, an approximation, being valid only at frequencies near the mechanical resonance of the transducer, and can therefore be applied only to problems involving continuous waves, and even then only over a very limited band of frequencies. This circuit is certainly of no value in the calculation of transient performance, and here it is necessary to use the exact equivalent circuit. The form of the exact circuit is known, and its derivation can be found in the literature, but it has rarely been discussed or made use of. It incorporates a section of a transmission line, and the basic purpose of this is to represent the time delay which is necessary for mechanical signals to travel from one face of the transducer to the other face." [19]

Redwood observed that the shortcomings of much of the earlier work with resonant transducers were due largely to the simplifying assumptions that had restricted both the bandwidth and the usefulness of Mason's equivalent circuit. In fact, the above-referenced transmission-line models were no more than redevelopments of that portion of Mason's model which had been neglected in the

succeeding resonant-transducer analyses, revived because of the growing interest in broadband transducers in recent years.

Redwood presents an excellent hybrid electrical-mechanical analysis of transducer response, including both the resonant effects from the simplified Mason model and the time delays from the exact circuit. The technique developed in [19] is then utilized in [20] to predict transducer response in the transmission and reception of pulses, and in particular that portion of the response caused by the superposition of reflected waves produced at the faces of the piezoelement. This approach serves as the basis for the present work.

Some additional physical significance may be given to the transmission-line model by considering the actual phenomenon which it describes—the behavior of stress waves at impedance-mismatched interfaces. Altman and Beyer [21] consider the reflections generated at the faces of the piezoelement in a typical transducer, and Hill and El-Dardiry [22] employ a chain-matrix computation to determine the frequency-dependent transmission coefficient for a five-layer transducer. Folds and Loggins [23] treat the oblique incidence of waves on transducer surfaces, and Doll [24] utilizes these concepts to predict the time delays and relative electrical signal amplitudes in an ultrasonic through-transmission test system. Lee and Williams [25] consider such a system and, assuming a thin specimen, obtain a closed-form solution for the steady-state output signal amplitude resulting from an infinite number of reflections of stress waves at the transducer-specimen interfaces. This work provides the tools for

an empirical determination of the maximum ratio of output voltage to input voltage for a given through-transmission system. This is an important step toward the determination of the transduction ratio (stress produced in the specimen per unit voltage introduced to the transducer, and vice-versa) for a particular transducer-specimen system.

In addition to the work in transducer analysis, much effort has also been devoted to better understanding the character of the ultrasonic stress field produced by the transducer. Topics of interest in this area include the effect of the presence of the specimen on the frequency response of the transducer [26]; the effect of piezoelement boundary conditions [27] and the wearplate geometry [28] on the directionality of the stress field; the limitations of the assumption of plane-wave, piston-source wave propagation within the transducer [29]; and the usefulness of finite-element methods in predicting the resulting pressure distribution in the specimen [30].

As it becomes increasingly desirable to attach quantitative significance to ultrasonic measurements, many techniques are being proposed for the evaluation, calibration, and standardization of ultrasonic transducers. Among these are: the use of reciprocity methods to determine the transducer sensitivity in a particular application [31,32]; the theoretical [33] and experimental [34,35] determination of loaded- and unloaded-transducer frequency response; and the experimental measurement of the distribution of ultrasonic stress in the near field of the transducer [36]. Methods for determining the integrity of the transducer-specimen

bond have also been developed [37]. A good treatment of current transducer evaluation procedures may be found in [38].

1.3 SCOPE OF THE PRESENT WORK

The previous section shows that, although some work has been done in the area of transducer analysis and characterization, much of the work uses simplified electrical equivalent circuits and is of little value in gaining quantitative insight into the mechanical aspects of the behavior of ultrasonic test systems. Although some have studied particular mechanical topics such as the propagation of stress waves through layers of dissimilar materials, there is still the need to develop a better quantitative understanding of the effect of transducer geometry and material properties on the behavior of the transducer as a unit and as part of a system.

The present work addresses this need. A theoretical model of a multilayer broadband piezoelectric ultrasonic transducer will be developed, based on the physics of the piezoelectric effect and on the theory of wave propagation in elastic materials. Experiments will be performed on transducers with different geometries and material properties to determine the effects of these factors on the input-output characteristics of the transducers. The results of the experiments will be compared to the predicted results from the model in order to gain additional insight into the operation of piezoelectric transducers and ultrasonic test systems.

CHAPTER 2

ANALYSIS OF ULTRASONIC TEST SYSTEM AND DEVELOPMENT OF MODEL

2.1 INTRODUCTION

A schematic representation of a typical ultrasonic through-transmission test system is shown in Fig. 1. Notice that each transducer consists of three components: (1) the piezoelement, which converts stress to voltage and vice-versa; (2) the wearplate, which protects the piezoelement from direct contact with the specimen; and (3) the backing layer, which absorbs stress waves from the piezoelement. In addition to these three components, each transducer is potted with a urethane plastic. The function of the potting is to protect the wires leading from the piezoelement to the connector, but it is of interest here because it has finite impedance, so that the "free" surface of the backing layer is not entirely free. There is also a thin layer of couplant between the transducers and the specimen, which improves the transmission of stress waves across these interfaces.

An ultrasonic test is initiated by applying a known time-varying voltage signal to the input transducer. This voltage produces a stress waveform, which propagates through the specimen and into the receiving transducer. The receiving transducer then converts the stress waveform back into an output voltage signal, which is measured and compared to the input voltage. These three processes—generation, propagation, and detection of stress waves—are analyzed separately in the following sections, and the

results are then combined to produce a complete system model.

2.2 NOMENCLATURE

In order to keep track of the enormous number of stress waves which are produced within the system, names have been assigned to the waves according to the following rules (see Fig. 2):

(1) The input transducer is designated transducer 1, and the output transducer is called transducer 2.

(2) The backing, piezoelement, and wearplate of each transducer are designated B, P, and W, respectively. The specimen is denoted by the letter S.

(3) Waves traveling to the right are indicated by R; left-traveling waves are named L.

(4) Waves arriving at the interfaces between transducer components or at the wearplate-specimen interfaces have names ending in I; waves which are generated at or reflected from these interfaces and propagate away from them are indicated by the letter O.

These names represent the instantaneous amplitudes of the particular waves to which they correspond. For example, P_2B_2LO refers to one of the waves at the piezoelement-backing interface in the receiving transducer, as indicated by the first part of the name, P_2B_2. The rest of the name, LO, says that the wave travels away from the interface and to the left. Similarly, wave W_2R would be the right-traveling wave in the wearplate of the input transducer.

Some of the other variables that appear in the analysis are listed below, along with the SI units of each:

L_B = thickness of backing layer (cm)

L_P = thickness of piezoelement (cm)

L_W = thickness of wearplate (cm)

L_S = thickness of specimen (cm)

Z_B = acoustic impedance of backing ($gm/cm^2/sec$)

Z_P = acoustic impedance of piezoelement ($gm/cm^2/sec$)

Z_W = acoustic impedance of wearplate ($gm/cm^2/sec$)

Z_S = acoustic impedance of specimen ($gm/cm^2/sec$)

c_B = wavespeed in backing material (cm/sec)

c_P = wavespeed in piezoelement (cm/sec)

c_W = wavespeed in wearplate (cm/sec)

c_S = wavespeed in specimen (cm/sec)

C_o = capacitance of piezoelement (farads)

h = piezoelectric constant (V/m)

S = cross-sectional area of piezoelement (cm^2)

R = input resistance of oscilloscope (ohms)

$\alpha_B(\omega)$ = attenuation of backing material (nepers/cm)

$\alpha_S(\omega)$ = attenuation of specimen (nepers/cm)

The values of some of these parameters vary among the prototype transducers tested in this study. Some of the transducers have titanium carbide wearplates, for example, and some have aluminum wearplates. It is possible, therefore, for the input and output transducers in the same system to have different wearplate impedances, in which case these impedances are denoted by Z_{W_1} and Z_{W_2}, according to the first rule given earlier. No such distinction is made for variables which have the same value in

every transducer, such as piezoelement thickness and backing impedance.

2.3 GENERATION OF STRESS WAVES FROM INPUT VOLTAGE

Applying a step function of voltage across the piezoelement of an ultrasonic transducer produces four stress waves (see Appendix A, section A.7). Using the above nomenclature, the amplitudes of these four waves are given by eqns. (A82) in Appendix A as:

$$
\begin{aligned}
P_1W_1RO &= -\left(\frac{Z_{W_1}}{Z_p + Z_{W_1}}\right)\frac{hC_oV_o}{S}\exp\left(\frac{t}{\tau}\right)\\
P_1W_1LO &= \left(\frac{Z_p}{Z_p + Z_{W_1}}\right)\frac{hC_oV_o}{S}\exp\left(\frac{t}{\tau}\right)\\
B_1P_1RO &= \left(\frac{Z_p}{Z_B + Z_p}\right)\frac{hC_oV_o}{S}\exp\left(\frac{t}{\tau}\right)\\
B_1P_1LO &= -\left(\frac{Z_B}{Z_B + Z_p}\right)\frac{hC_oV_o}{S}\exp\left(\frac{t}{\tau}\right)
\end{aligned}
\qquad (2\text{-}1)
$$

where h is the piezoelectric constant in V/m, C_o is the electrical capacitance in farads, S is the surface area of the piezoelement in cm^2, and V_o is the amplitude of the step input of voltage. The value of the time constant, τ, is given by eqn. (A79) in Appendix A:

$$
\frac{1}{\tau} = \frac{h^2C_o^2}{S}\left\{\frac{\left(Z_B + Z_p\right) + \left(Z_p + Z_{W_1}\right)}{\left(Z_B + Z_p\right)\left(Z_p + Z_{W_1}\right)}\right\} \qquad (2\text{-}2)
$$

Eqns. (2-1) give the amplitudes of the four stress waves produced in the input transducer by a step input of voltage. These may be represented in a general form as:

$$T = KV_o \exp\left(\frac{t}{\tau}\right) \tag{2-3}$$

where T is stress, and K is a constant. In order to extend this step response to a continuous, time-varying input voltage V(t), a stepwise approximation must be used, as shown in Fig. 3. This translates V(t) into a series of n discrete steps, each of amplitude $\Delta V(i)$, which are separated in time by Δt, known as the time interval of the discretization. If each of these steps $\Delta V(i)$ produces a stress response such as that given in eqn. (2-3), the stress at any time $t=k\Delta t$ is simply the superposition of the stress responses produced by all of the preceding voltage steps:

$$\begin{aligned} T(k\Delta t) = K\Bigg\{&\Delta V(1) \exp\left\{(k-1)\frac{\Delta t}{\tau}\right\} \\ &+ \Delta V(2) \exp\left\{(k-2)\frac{\Delta t}{\tau}\right\} + \ldots \\ &+ \Delta V(k-1) \exp\left\{\frac{\Delta t}{\tau}\right\} + \Delta v(k)\Bigg\} \end{aligned} \tag{2-4}$$

It is convenient to write the series as a summation:

$$T(k\Delta\tau) = K \sum_{i=1}^{k} \Delta V(i) \exp\left\{(k-i)\frac{\Delta t}{\tau}\right\} \tag{2-5}$$

This summation gives the time-dependent amplitude of a stress wave generated at the piezoelement of the input transducer for an arbitrary time-varying input voltage, V(t). Evaluating the constant K in eqn. (2-3) for each of the four stress waves

given in eqns. (2-1), and substituting into eqn. (2-5) gives:

$$P_1W_1RO(k\Delta t) = -\left(\frac{Z_{W_1}}{Z_p + Z_{W_1}}\right)\frac{hC_o}{S}\sum_{i=1}^{k}\Delta V(i)\exp\left\{(k-i)\frac{\Delta t}{\tau}\right\}$$

$$P_1W_1LO(k\Delta t) = \left(\frac{Z_p}{Z_p + Z_{W_1}}\right)\frac{hC_o}{S}\sum_{i=1}^{k}\Delta V(i)\exp\left\{(k-i)\frac{\Delta t}{\tau}\right\}$$

$$B_1P_1RO(k\Delta t) = \left(\frac{Z_p}{Z_B + Z_p}\right)\frac{hC_o}{S}\sum_{i=1}^{k}\Delta V(i)\exp\left\{(k-i)\frac{\Delta t}{\tau}\right\}$$

$$B_1P_1LO(k\Delta t) = -\left(\frac{Z_B}{Z_B + Z_p}\right)\frac{hC_o}{S}\sum_{i=1}^{k}\Delta V(i)\exp\left\{(k-i)\frac{\Delta t}{\tau}\right\} \qquad (2\text{-}6)$$

where the stepwise function V(i) is obtained from V(t) by:

$$\Delta V(i) = V(i\Delta t) - V((i-1)\Delta t) \qquad (2\text{-}7)$$

Note that the amplitudes given in eqns. (2-6) are solely those resulting from the application of a voltage to the piezoelement. If other waves are already propagating in the system, their amplitudes must be added to those in eqns. (2-6) to obtain the actual, time-varying amplitudes of waves P_1W_1RO, P_1W_1LO, B_1P_1RO, and B_1P_1LO.

2.4 PROPAGATION OF STRESS WAVES WITHIN THE SYSTEM

As soon as the stress waves are produced at the piezoelement of the input transducer, they begin to propagate through the system. As they propagate, they are affected in several ways: (1) time delays are introduced due to the wave transit times across the transducer and specimen layers; (2) a decrease in amplitude shows up due to attenuation in certain layers; (3) reflections are generated

at impedance-mismatched interfaces between layers. These effects are treated separately below.

2.4.1 Wave Propagation in Piezoelement and Wearplate

The velocity of propagation of plane compressional waves in both piezoelectric and nonpiezoelectric materials is given by eqn. (A5) in Appendix A as:

$$c^2 = \frac{E}{\rho} \tag{2-8}$$

where c is the wavespeed in m/s, E is the elastic modulus of the material in N/m^2, and ρ is the mass density in kg/m^3. If a layer is nonattenuating and nondispersive, it propagates waves at a constant velocity without changing their shape. The only effect on the waves is the introduction of a time delay, λ, where:

$$\lambda = \frac{L}{c} \tag{2-9}$$

Here, λ is the so-called "transit time" of the layer in seconds, L is the thickness of the layer in meters, and c is the wavespeed in m/sec.

Attempts have been made [39] to determine the attenuation of the lead metaniobate piezoelement and the titanium carbide wearplate used in the prototype transducers. Comparatively no attenuation has been observed for the wearplate, and negligible attenuation has been reported for the piezoelement (see Fig. C6). The piezoelement and wearplate may therefore be considered to be nonattenuating for the purposes of this study, so that if λ_{W_1} and λ_{W_2} represent the transit times of wearplates 1 and 2 as found

from eqn. (2-9), and if λ_P represents the piezoelement transit time, the following equations hold for the piezoelements:

$$P_1W_1RI(t + \lambda_P) = B_1P_1RO(t)$$

$$B_1P_1LI(t + \lambda_P) = P_1W_1LO(t)$$

$$P_2B_2RI(t + \lambda_P) = W_2P_2RO(t)$$

$$W_2P_2LI(t + \lambda_P) = P_2B_2LO(t) \qquad (2\text{-}10)$$

and for the wearplates:

$$W_1SRI(t + \lambda_{W_1}) = P_1W_1RO(t)$$

$$P_1W_1LI(t + \lambda_{W_1}) = W_1SLO(t)$$

$$W_2P_2RI(t + \lambda_{W_2}) = SW_2RO(t)$$

$$SW_2LI(t + \lambda_{W_2}) = W_2P_2LO(t) \qquad (2\text{-}11)$$

Eqns. (2-10) and (2-11) account for the time delays introduced by the nonattenuating piezoelements and wearplates, respectively. For example, the first of eqns. (2-11) shows that the wave leaving the piezoelement-wearplate interface in the input transducer at time t, $P_1W_1RO(t)$, arrives at the interface between wearplate and specimen (W_1SRI) at time $t+\lambda_{W_1}$, that is, after the transit time required to pass through the wearplate.

2.4.2 Wave Propagation in Backing Material and Specimen

In addition to introducing a time delay, some materials also attenuate the waves which pass through them, thereby reducing their amplitude. Fig. C6 shows that the backing material used in the

prototype transducers exhibits significant attenuation at all frequencies, with a very strong frequency-dependence above 1.0 MHz.

The attenuation of stress waves in material layers is described by the following equation:

$$\frac{T_o}{T_i} = \exp\{-\alpha(\omega)L\} \tag{2-12}$$

where T_i is the amplitude of the stress wave that enters the layer, T_o is the amplitude of the exiting wave, $\alpha(\omega)$ is the frequency-dependent attenuation parameter in nepers/m (where ω is the radian frequency), and L is the thickness of the layer in meters.

Using eqns. (2-9) and (2-12), the equations describing wave propagation through the attenuating backing layers may be written:

$$\begin{aligned}
B_1P_1RI(t + \lambda_{B_1}) &= B_1RO_o(t)\ \exp\ (-\alpha_B(\omega)L_{B_1}) \\
B_1LI_o(t + \lambda_{B_1}) &= B_1P_1LO(t)\ \exp(-\alpha_B(\omega)L_{B_1}) \\
B_2RI_o(t + \lambda_{B_2}) &= P_2B_2RO(t)\ \exp(-\alpha_B(\omega)L_{B_2}) \\
P_2B_2LI(t + \lambda_{B_2}) &= B_2LO_o(t)\ \exp\ (-\alpha_B(\omega)L_{B_2})
\end{aligned} \tag{2-13}$$

Here, $\alpha_B(\omega)$ is the attenuation of the backing material in nepers/m, λ_{W_1} and λ_{W_2} represent the transit times, in seconds, of the backing layers, and L_{W_1} and L_{W_2} are the thicknesses of the layers in meters. The wave names subscripted Ø denote those waves at the rear surface of the backing layer, that is, the surface farthest away from the piezoelement.

In general, the specimen will also exhibit frequency-dependent attenuation, with attenuation parameter $\alpha_S(\omega)$. If the impedance,

wavespeed, and thickness of the specimen are known, eqn. (2-9) can be used to obtain the transit time λ_S for the specimen and the following propagation equations may be written:

$$SW_2RI(t + \lambda_S) = W_1SRO(t) \exp(-\alpha_S(\omega)L_S)$$

$$W_1SLI(t + \lambda_S) = SW_2LO(t) \exp(-\alpha_S(\omega)L_S) \qquad (2\text{-}14)$$

Here, as in eqns. (2-13), $\alpha_S(\omega)$ is the attenuation of the specimen in nepers/m, λ_S is the transit time of the specimen layer in seconds, and L_S is the thickness of the specimen in meters.

2.4.3 Reflection at Impedance-Mismatched Interfaces

Whenever a wave strikes an interface between two materials of different acoustic impedance, a portion of its amplitude is transmitted across the interface, and a portion is reflected back (see Appendix A, section A.4). If a stress wave with amplitude T_i traveling in a medium with impedance Z_1 encounters a medium with impedance Z_2, eqns. (A31) in Appendix A give the amplitudes of the resulting reflected and transmitted waves:

$$T_{tr} = \frac{2 Z_2}{Z_1 + Z_2} T_i$$

$$T_r = \frac{Z_2 - Z_1}{Z_1 + Z_2} T_i \qquad (2\text{-}15)$$

where T_{tr} represents the wave transmitted across the interface, and T_r represents the reflected wave.

Applying eqns. (2-15) to the impedance-mismatched interfaces between wearplates and piezoelements gives the following:

$$P_1W_1RO = \frac{2\,Z_{W_1}\,(P_1W_1RI) + (Z_P - Z_{W_1})(P_1W_1LI)}{(Z_P + Z_{W_1})}$$

$$P_1W_1LO = \frac{(Z_{W_1} - Z_P)(P_1W_1RI) + 2\,Z_P\,(P_1W_1LI)}{(Z_P + Z_{W_1})}$$

$$W_2P_2RO = \frac{2\,Z_P\,(W_2P_2RI) + (Z_{W_1} - Z_P)(W_2P_2LI)}{(Z_{W_2} + Z_P)}$$

$$W_2P_2LO = \frac{(Z_P - Z_{W_2})(W_2P_2RI) + 2\,Z_{W_2}(W_2P_2RI)}{(Z_{W_2} + Z_P)} \qquad (2\text{-}16)$$

At the wearplate-specimen interfaces, the equations are:

$$W_1SRO = \frac{2\,Z_s\,(W_1SRI) + (Z_{W_1} - Z_s)(W_1SLI)}{(Z_{W_1} + Z_s)}$$

$$W_1SLO = \frac{(Z_s - Z_{W_1})(W_1SRI) + 2\,Z_{W_1}(W_1SLI)}{(Z_{W_1} + Z_s)}$$

$$SW_2RO = \frac{2\,Z_{W_2}\,(SW_2RI) + (Z_s - Z_{W_2})(SW_2LI)}{(Z_s + Z_{W_2})}$$

$$SW_2LO = \frac{(Z_{W_2} - Z_s)(SW_2RI) + 2\,Z_s\,(SW_2LI)}{(Z_s + Z_{W_2})} \qquad (2\text{-}17)$$

And at the rear face of the backing layer:

$$B_1RO_o = \left(\frac{Z_u - Z_B}{Z_u + Z_B}\right) B_1LI_o$$

$$B_2LO_o = \left(\frac{Z_u - Z_B}{Z_B + Z_u}\right) B_2RI_o \qquad (2\text{-}18)$$

Note that each of the waves produced at an interface depends on

both of the waves arriving at that interface. For example, the first of eqns. (2-16) says that the right-traveling wave leaving the interface between piezoelement and wearplate in the input transducer, P_1W_1RO, is the sum of the transmitted part of the incident right-traveling wave at that interface, P_1W_1RI, and the reflected part of the left-traveling wave, P_1W_1LI. For simplicity, the time-dependence of these quantities is not explicitly stated here, although they do represent instantaneous values of continuous time-dependent stresses.

2.5 DETECTION OF STRESS WAVES AND PRODUCTION OF OUTPUT VOLTAGE

The output voltage V_{out} produced by a step input of stress in the wearplate of a transducer is obtained from eqn. (A57) in Appendix A:

$$V_{out}(t) = \frac{-2\ h\ W_2P_2RI_o}{(Z_{W_2} + Z_p)}\left\{\frac{\exp\left(\frac{-t}{\tau_1}\right) - \exp\left(\frac{-t}{\tau_2}\right)}{\frac{1}{\tau_2} - \frac{1}{\tau_1}}\right\} \tag{2-19}$$

where $W_2P_2RI_o$ is the amplitude in N/m^2 of the step input of stress, and R is the resistance in ohms connected across the piezoelement of the transducer. The values of the time constants τ_1 and τ_2 are given in eqn. (A56):

$$\frac{1}{\tau_1}, \frac{1}{\tau_2} = \frac{1}{2RC_o} \pm \left\{\left(\frac{1}{2RC_o}\right)^2 + \left(\frac{h^2}{RS(Z_{W_2} + Z_p)}\right)\right\} \tag{2-20}$$

where C_o is the capacitance of the piezoelement in farads, h is the piezoelectric constant in V/m, and Z_{W_2} and Z_P are the

characteristic impedances of the wearplate and piezoelement, respectively.

It will later prove useful to write the output voltage in terms of the stress waves inside the piezoelement. If W_2P_2RI is the only stress wave entering the transducer, eqn. (2-16)(b) gives

$$\frac{2\ W_2P_2RI}{Z_{W_2} + Z_P} = \frac{W_2P_2RO}{Z_P} \tag{2-21}$$

Making this substitution for W_2P_2RI in eqn. (2-19) gives the output voltage in terms of stress wave W_2P_2RO, inside the piezoelement:

$$V_{out}(t) = \frac{-h\ W_2P_2RO_o}{Z_P} \left\{ \frac{\exp\left(\frac{-t}{\tau_1}\right) - \exp\left(\frac{-t}{\tau_2}\right)}{\frac{1}{\tau_2} - \frac{1}{\tau_1}} \right\} \tag{2-22}$$

The term in brackets in this equation is a complicated function of time, especially for values of τ_1 and τ_2 which are close to one another. A simplifying assumption may be made, however. Eqn. (2-20) shows that the difference between the time constants depends on $\{h^2/[RS(Z_{W_2}+Z_P)]\}^{\frac{1}{2}}$, which is estimated to be an order of magnitude less than $1/RC_o$ for the transducers used in this study. Neglecting this term in eqn. (2-20) then gives $1/\tau_1 = 1/RC_o$, and $1/\tau_2 = 0$. Substituting these values back into eqn. (A55) and reinverting the Laplace transform [40] produces the final result:

$$V_{out}(t) = \frac{-h\, W_2 P_2 RO_o}{Z_P} \int_0^t \exp\left(\frac{-\tau}{RC_o}\right) d\tau \qquad (2\text{-}23)$$

This equation gives the output voltage in terms of the stress inside the piezoelement. Although considerably simpler than the previous equation, it nonetheless shows some interesting behavior.

First observe that if the time constant RC_o is large, the term $\exp(-t/RC_o)=1$, and the integral is simply equal to t. This corresponds to a ramp of voltage for a step input of stress, so that the voltage is simply the time-integral of the stress inside the piezoelement. Fig. 4 shows a rectangular pulse of stress as it propagates through the piezoelement, and the voltage which is generated as a result. Note from Fig. 4 that the voltage is determined only by the stress inside the piezoelement--when the stress wave leaves the piezoelement, the voltage returns to zero.

Secondly, note what happens if $RC_o=0$. This can only be realized if R=0, corresponding to a short circuit across the piezoelement. The exponential in eqn. (2-23) then goes to $\exp(-\infty)=0$, so that V_{out} is always 0. No voltage is accumulated across the piezoelement because of the short circuit.

The third case is the most interesting, where RC_o is somewhere between 0 and ∞. For this case, the voltage is also an integral, but it is not precisely the integral of the stress waveform. It is, instead, the convolution of the stress waveform with an exponentially-decaying function of time. A closed-form solution of the integral gives:

$$\int_0^t \exp\left(\frac{-\tau}{RC_o}\right) d\tau = RC_o\left\{1 - \exp\left(\frac{-t}{RC_o}\right)\right\} \tag{2-24}$$

so that, rather than a ramp, the output voltage shows an inverted exponential rise converging to a maximum value (see Fig. 5). At the maximum, a steady-state condition exists, where the decay of voltage is exactly compensated by the increase in voltage due to the additional stress continually entering the piezoelement.

Thus, the voltage across the output resistance R is a rather complicated function of the stress inside the piezoelement. Eqn. (2-23) indicates that waves entering the piezoelement produce a negative voltage, so that those waves leaving the piezoelement must conversely produce a positive voltage. Including the effects of all of the waves entering and leaving the piezoelement then gives the total output voltage:

$$V_{out}(t) = \frac{-h\,RC_o}{Z_P}\left\{W_2P_2RO_o - W_2P_2LI_o - P_2B_2RI_o + P_2B_2LO_o\right\}\left\{1 - \exp\left(\frac{-t}{RC_o}\right)\right\} \tag{2-25}$$

Here the subscript o denotes the amplitude of a step function of stress, arriving at the surface of the piezoelement at time t=0.

An equation analogous to eqn. (2-7) can be used to obtain a stepwise approximation of each of the continuous time-varying stress waves which contribute to the output voltage. The superposition method of section 2.3 then gives the total, time-varying output voltage resulting from the combination of all of these stress waves:

$$V_{out}(k\Delta t) = \frac{-\,h\,RC_o}{Z_P} \sum_{i=1}^{k} \Big\{ \Delta W_2P_2RO(i) - \Delta W_2P_2LI(i) - \Delta P_2B_2RI(i) + \Delta P_2B_2LO(i) \Big\} \left\{ 1 - \exp\left((k-i)\,\frac{\Delta t}{RC_o} \right) \right\} \quad (2\text{-}26)$$

This equation is used in the model to obtain the output voltage produced by a known set of stress waves $W_2P_2RO(t)$, $W_2P_2LI(t)$, $P_2B_2RI(t)$, and $P_2B_2LO(t)$.

2.6 DEVELOPMENT OF OVERALL SYSTEM MODEL

The equations of the previous three sections describe all phases of the conversion from input voltage to output voltage in an ultrasonic test system. All that remains is to combine these equations into a sufficiently general, yet convenient form for application to particular systems. This is a straightforward task, except for the bookkeeping involved in tracking the many waves generated within the system. This section introduces the algorithm used to solve this problem.

In Section 2.3 it was shown that each specimen and transducer layer has a characteristic transit time λ, given by eqn. (2-9). If the transit times of all of the layers were the same, this transit time could be used as the time step Δt for the discretization of the input signal (see eqn. (2-7)), so that it would be a simple matter to account for all of the waves in the system by applying the interface equations at times Δt, $2\Delta t$, $3\Delta t$, and so on. Each of the individual transit times is different, however, so that a few multiple reflections can generate a very large number of waves which, rather than superimposing upon one another, fall

between one another in time. The number of waves produced increases as time passes, so that for long simulations literally thousands of waves must be considered.

A simple solution is to mathematically discretize each of the transducer and specimen layers into small segments of equal transit time λ_o, as shown in Fig. 6. This transit time becomes the time step for the simulation, and may be arbitrarily chosen as small as desired. If, for example, the piezoelement has 50 segments, it is a simple matter for the digital computer to keep track of the amplitudes of the stress waves at each of the 49 locations between the segments, and to shift the amplitudes from one location to another to represent an elapsed time of one transit time λ_o. For instance, recall the first of eqns. (2-10):

$$P_1W_1RI(t + \lambda_p) = B_1P_1RO(t) \tag{2-27}$$

If the array $P_1R\{i\}$ contains the amplitudes of the right-traveling stress waves between the segments of the input piezoelement, and λ_o is the transit time of each segment, eqn. (2-22) becomes a system of equations:

$$\begin{aligned}
P_1R\{1\}(t + \lambda_o) &= B_1P_1RO(t) \\
P_1R\{2\}(t + \lambda_o) &= P_1R\{1\}(t) \\
P_1R\{3\}(t + \lambda_o) &= P_1R\{2\}(t) \\
&\vdots \\
P_1R\{50\}(t + \lambda_o) &= P_1R\{49\}(t) \\
P_1W_1RI(t + \lambda_o) &= P_1R\{50\}(t)
\end{aligned} \tag{2-28}$$

Although this method increases the number of equations involved

in a short simulation, it offers the advantage that waves produced at the same interface at the same time are simply added together, rather than being tracked separately. As a consequence, the number of calculations which must be performed is not affected by the production of multiple reflections, and the complexity of the problem does not increase with time. There is a slight error ε introduced by discretizing the transit times of the layers (see Fig. 6), but the error can be made arbitrarily small by reducing λ_0 and increasing the number of segments in each layer. Writing eqns. (2-10), (2-11), (2-13) and (2-14) in this fashion completes the system model.

Appendix B contains a listing, a flow chart, and a sample simulation session using the BASIC program that has been written to perform the input-output simulation of a general ultrasonic through-transmission test system.

CHAPTER 3

EXPERIMENTS

In an ultrasonic through-transmission test system, a specimen is clamped between the faces of the transmitting and receiving transducers. An electrical waveform known as the input signal excites the piezoelement in the transmitting transducer, which in turn generates ultrasonic stress waves in the specimen. These waves propagate through the specimen and eventually arrive at the piezoelement of the receiving transducer, which generates a corresponding electrical signal known as the output signal. Both the input and output signals are monitored simultaneously with a digital oscilloscope, and the data stored for later analysis.

3.1 PROTOTYPE TRANSDUCERS

Five different transducer designs are evaluated in this study. The Acoustic Emission Technology (AET) FC-500 broadband transducer serves as the standard after which the other four designs are patterned. As shown in Fig. C1 (see Appendix C), the FC-500 consists of a lead metaniobate piezoelement sandwiched between a protective wearplate of titanium carbide and a highly-attenuating tungsten epoxy backing layer.

Three transducers have been fabricated for this work which are identical to the FC-500 except for the thickness of the backing. The standard backing layer is 0.635 cm (0.250 in) thick, and the prototype transducers have backing thicknesses of

0 cm (no backing), 1.270 cm (0.500 in), and 1.905 cm (0.750 in). These transducers are identified by the numbers AE-100, AE-102, and AE-103, respectively, and the manufacturer (Panametrics, Inc., 221 Crescent St., Waltham, MA 02154) claims that they are identical to the standard AET FC-500 transducer, except for the thickness of the backing.

In addition, a transducer has been fabricated which has a different wearplate than the standard. In order to minimize the reflections generated at the piezoelement-wearplate and wearplate-specimen interfaces, aluminum was chosen as the material for the wearplate of this transducer, designated AE-101. This aluminum wearplate is the same thickness as the standard titanium carbide wearplate, so that transducer AE-101 is again identical to the FC-500, except for the wearplate material.

The dimensions and material properties of all five of these prototype transducer designs are summarized in Fig. C2.

3.2 ELECTRONIC TEST EQUIPMENT

A pulsed oscillator (Arenberg model PG-650C) was used to generate the input signals for the experiments. This signal generator is capable of producing continuous and gated sinusoids ranging in frequency from 0 to 4 MHz, and broadband pulses as short as 1 usec in duration. The peak-to-peak amplitude of these waveforms is continuously variable from 0 to 100 volts.

The input and output signals were monitored and stored on a Nicolet model 2090 digital oscilloscipe, capable of sampling two channels simultaneously at 20 MHz and with 8-bit resolution. The

digitized waveforms were then transferred through an RS-232 data link to an IBM Personal Computer for permanent storage, analysis and plotting.

3.3 SPECIMENS AND EXPERIMENTAL PROCEDURES

Transducers and specimens to be tested were clamped together at a constant pressure of 0.4 MPa (twice the "saturation pressure" of 0.2 MPa reported in [41]) on a pneumatic test stand. A layer of ultrasonic couplant (AET SC-6) was applied at all interfaces between transducers and specimens to improve the transmission of stress waves across those interfaces. An electrical attenuator was installed between the signal generator and the oscilloscope to avoid overloading the oscilloscope. Fig. C3 is a schematic of the system used for broadband pulse experiments; Fig. C4 shows the system set up for tone burst experiments.

Two categories of experiments were performed. First, all transducers were clamped face-to-face and tested with broadband pulses (1 μsec duration), and with gated and continuous sinusoids at frequencies of 0.4, 0.6, 1.0, 1.5, 2.0, 2.4, and 3.0 MHz. Next, some specimens were clamped between transducers and tested with the same input signals, to investigate the effect of couplant layers and adhesive bonds on the propagation of stress waves within the system. Fig. C5 shows a sketch of the three specimens tested in the experiments.

Specimen A (see Fig. C5) is simply a 1.270 cm (0.500 in) thick aluminum plate. It was tested between both AE-103 and AE-101 transducers, to observe the difference in output caused by

impedance-matching the wearplate to the specimen. (The AE-101 has an aluminum wearplate, while the AE-103 has the standard titanium carbide wearplate.) Specimen B consists of two 0.635 cm (0.250 in) thick aluminum plates separated by a couplant layer, and in specimen C the couplant layer is replaced by a thin (0.005 cm) epoxy layer. Both of these specimens were tested between AE-101 transducers, and the results compared to those for the solid 1.270 cm plate to determine the effect of the intermediate layers on the output of the system.

3.4 EXPERIMENTAL RESULTS

Appendix D gives the measured output of each of the systems for broadband pulse and tone burst inputs. No output signals corresponding to tone burst inputs above 1.0 MHz are shown, because the backing attenuation is so large above this frequency that the amplitude of the backing wave is negligible. The results of the continuous-wave experiments are also given, in Table 7.

CHAPTER 4

RESULTS AND DISCUSSION

In this chapter, the results of the evaluations of each of the transducer designs are presented and discussed. First, the experimental results for each transducer are compared with the predicted results obtained from the wave propagation model developed in Chapter 2, which makes possible the quantitative evaluation of time delays and piezoelectric constants in the system. Next, the experimental results for each of the transducers are studied to determine the role of each transducer design parameter on the output of the system. The conclusions are confirmed with the wave propagation model, and the model is then used to predict the effects of additional parameters on the output. The results of experiments to determine the effects of couplant layers and adhesive-bonding layers are discussed, and, finally, a scheme is presented which enables the model to predict complete output signals for broadband input signals.

4.1 RESULTS OF CHARACTERIZATION USING THE WAVE PROPAGATION MODEL

The wave propagation model developed in Chapter 2 can be used to characterize an ultrasonic test system. In order to obtain good correlation between the predicted results (from the model) and the measured results, it is found that several time delays must be introduced into the model. These time delays, along with the time constant RC_o for exponential decay of the

output voltage, and the backing attenuation parameter $\alpha_B(\omega)$, make up the list of what are called "modeling parameters" in the following discussion. These are parameters whose values may be arbitrarily varied to optimize the correlation between measured and predicted results. The characterization of an ultrasonic test system, then, consists of finding the values of each of the modeling parameters that give the best agreement between measured and predicted output signals.

Appendix E shows how the optimum values of each of the modeling parameters may be determined for a particular ultrasonic system. The procedure is an iterative one, in which the value of a particular parameter, say ϕ_i, is repeatedly altered in the simulation until the predicted output signal matches the measured signal as closely as possible. This value is taken to be the correct, or optimum value of ϕ_i for the particular system under consideration. The optimum value is then used as an input to the model while the next parameter is varied, and so on until all of the parameters have been optimized. Table 1 lists the values of the modeling parameters for each of the predicted curves in Appendix E, and Fig. 7 shows a flow chart of the characterization process, where ϕ_i represents the particular parameter being optimized at any given time.

Two requirements must be met in order for this scheme to work. First, the model itself must be accurate, so that good correlation between measured and predicted output signals can, indeed, be obtained if the correct values of the modeling parameters are used as input data. Also, the effects of the

parameters on the output of the system must be independent, so that changing one parameter does not change the optimum value of a parameter which has already been optimized.

It is easy to demonstrate that the model satisfies the first requirement. Figs. E8, E13, and E15 (see Appendix E) show the excellent correlation between measured and predicted results which is obtained for carefully-chosen values of the modeling parameters. These cases correspond to broadband pulse, 0.4 MHz tone burst, and 0.6 MHz tone burst input signals, respectively, for the system of two FC-500 transducers clamped face-to-face. The independence of the modeling parameters is not so easily established, but the discussion of Appendix E shows that, if the parameters are optimized in the proper order (δ, β, RC_o, α, γ, h^2C_o/S), the effect of changing one parameter on other parameters which have already been optimized is minimal.

Four systems are characterized using this procedure. Each of the systems consists of a pair of transducers clamped face-to-face, the four systems corresponding to the FC-500, AE-101, AE-102, and AE-103 transducers. The results of the characterizations are shown along with the experimental results for each system in Tables 2-5; Table 6 contains a summary of the optimum values of the modeling parameters for each system. The effects of each of the parameters on the output of the system are discussed in the following paragraphs.

4.1.1 Wearplate-Piezoelement Time Delay, δ

As mentioned earlier, several time delays must be included

in the wave propagation model in order to obtain good correlation between measured and predicted results for a given system. The particular time delay discussed here, called δ, is introduced as waves pass through the interfaces between the wearplates and piezoelements in the system. The effect of this time delay is simply to increase the time interval between the application of the input signal and the first appearance of the output signal, as discussed in Appendix E (subsection E.1.2). This time delay does not affect the shape or amplitude of the output signal in any way.

The values of δ in Table 6 are all within 0.01 μsec of each other, except for transducer AE-101, which is the only transducer with an aluminum wearplate. It appears that a softer wearplate material like aluminum reduces the value of the time delay. Otherwise, the value of δ seems to be fairly constant for transducers of similar construction (same wearplate and piezoelement). In addition, no variation of δ with frequency is observed over the range from 0.4-3.0 MHz.

4.1.2 Wearplate-Piezoelement Time Delay, β

This time delay is introduced as waves are reflected back into the wearplates from the wearplate-piezoelement interfaces in the system. Fig. E3 shows schematically the propagation of stress waves through the system, where the solid black lines represent the wavefronts. Observe that the waves bounce back and forth between the wearplate-piezoelement interfaces several times, and that this results in an echo in the output signal. The effect

of β is to increase the time between the echoes, as described in Appendix E (subsection E.1.3). Predicted output signals corresponding to several different values of β are shown in Fig. 8 (reproduced from Fig. E6); these should be compared with the measured broadband pulse output signals for each of the systems, shown in Fig. 9.

The value of β varies considerably from transducer to transducer; the FC-500 shows a value of 0.24 μsec, while β for the AE-101 is only slightly greater than half of that (0.125 μsec). Note that the 37.5% reduction in β associated with the aluminum wearplate is exactly the same as the reduction in δ. Clearly, both of the time delays at the wearplate-piezoelement interface depend strongly on the wearplate impedance.

Observe from Table 6 that both the AE-102 and the AE-103 have identical values for β. This is significant, because these are the only two transducers with matched backing layers and titanium wearplates that were made at the same time. Thus the time delay β seems to be consistent from one transducer to another, if the transducers have identical wearplates and piezoelements and were manufactured under the same conditions. The discrepancy between the AE-102 and AE-103 versus the FC-500 is probably attributable to differences is materials or manufacturing.

The optimization of β was initially carried out using only the broadband pulse input signal. However, the optimum values obtained for the broadband pulse were also found to be the optimum values for tone burst input signals over the entire frequency range of the experiments, indicating no dependence of β upon the

frequency of the input signal.

4.1.3 The Time Constant, RC_o

The parameter RC_o can have a very significant effect on the output signal for a particular ultrasonic test system, as described in Appendix E (subsection E.1.4). RC_o is the time constant of the series R-C circuit made up of the output piezoelement and the oscilloscope. The value of RC_o determines how fast the output voltage decays from the piezoelement; if RC_o is small (on the order of 0.1 μsec), the output signal is proportional to the stress inside the piezoelement, and if RC_o is large (5.0 μsec), the signal is proportional to the integral of stress. This effect is discussed in more detail in Chapter 2 (section 2.5); Fig. E7 shows predicted output signals corresponding to several different values of RC_o.

Transducers AE-101, AE-102, and AE-103 all show a time constant of approximately 5.0 μsec, indicating that the output voltage is virtually the exact integral of the stress inside the piezoelement. The output for the FC-500, however, shows a slight decay with time, indicating a value for the time constant of about 1.0 μsec. This difference is almost certainly a result of variations in transducer materials; the lead metaniobate used for the FC-500 piezoelement apparently has a lower relative dielectric constant than that used in the new prototype transducers, resulting in a lower value for the capacitance C_o.

4.1.4 Backing Wave Time Delay, γ

The function of the backing layer in an ultrasonic transducer is to broaden the bandwidth of the transducer by suppressing the development of standing waves in the piezoelement. There is an additional effect of the backing layer, however. Fig. 10 shows the broadband pulse response for each of the prototype transducers that has a matched backing layer; observe that waves travel through the backing layer and eventually return to the piezoelement at a reduced amplitude, producing a contribution to the output voltage at that time. The FC-500 and AE-101 transducers have 0.635 cm (0.250 in) backing layers with a transit time of 3.7 sec, so that the backing waves for these transducers are delayed by at least 7.4 sec. The AE-102 has twice the backing thickness of the AE-101 and the AE-103 three times the thickness, giving arrival times for the backing waves of at least 14.6 and 22 sec, respectively. The measured arrival times exceed the predicted times in every case, indicating the introduction of a time delay, γ, as waves travel across the backing layer. Fig. E11 shows four predicted output signals corresponding to four different values of the time delay, γ.

Table 6 shows values for γ ranging from 0.75 μsec for transducer AE-101 to 1.60 μsec for the FC-500. Again the FC-500 shows substantially different behavior than the others, but note that the ratio of the γ values for the AE-101 and AE-102 is identical to the ratio of their backing thicknesses. This correlation with backing thickness would indicate that, rather than being an interfacial effect, the time delay has something to

do with wave propagation through the backing layer itself.

The highest frequency at which a backing wave can be detected is 1.0 MHz, and this only for the transducers with 0.635 cm (0.250 in) backings. Over this limited range (0.4-1.0 MHz), no frequency-dependence is observed for the time delay γ.

4.1.5 Backing Attenuation, $\alpha_B(\omega)$

The effect of the attenuation of the backing material is to reduce the amplitude of the backing wave in the output signal for the system. Fig. E12 shows four predicted output signals corresponding to four different values of backing attenuation, α_B.

Fig. 11 shows a plot of the measured attenuation of the backing material (taken from Fig. B6), and the values of $\alpha_B(\omega)$ obtained from the characterization of the transducers are also shown. Note that the predicted values of α_B are slightly greater than the measured values, indicating that the measured backing waves are actually smaller in amplitude than one would expect, based on the values of backing attenuation reported in [24].

The probable explanation of this slight discrepancy is that there is some other source of attenuation in the system in addition to the backing layer itself. This would mean that the stress waves entering the backing layer would already have been attenuated somewhat. Perhaps the source of this attenuation is the conversion of stress to voltage in the piezoelement of the output transducer. It seems reasonable to expect that the production of electrical energy at the surfaces of the piezo-element might be accompanied by a corresponding reduction in

the mechanical strain energy inside the piezoelement. An experiment is recommended in the next chapter to confirm this hypothesis.

4.1.6 The Amplitude Factor, h^2C_o/S

The predictions from the wave superposition model do not include the amplitude factor h^2C_o/S, where h, C_o and S represent the piezoelectric constant, capacitance, and surface area of the piezoelement, respectively. Both h and C_o are difficult to measure, because they tend to vary significantly even from one "identical" piezoelement to another [10]. In this analysis, therefore, the amplitude factor h^2C_o/S is found by dividing the measured output amplitude by the predicted output amplitude, resulting in the value of the amplitude factor that gives a predicted output signal exactly equal in amplitude to the measured signal. The values for h^2C_o/S found in this manner are given in Tables 2 through 5.

Fig. 12 shows a plot of h^2C_o/S versus frequency for four of the transducer systems tested in this study. (The correlation between the predicted and measured output signals for the unbacked transducer (AE-100) was not good enough to allow the calculation of the amplitude factor.) These curves correspond to the steady-state output amplitude produced by a continuous sinusoidal input signal. All of the curves fall fairly close to one another over the range 0.4-2.0 MHz; the average values of the amplitude factor over this range for each of the transducers are reported in Table 6.

Observe from Fig. 12 that transducers AE-102 and AE-103 again show qualitatively very similar behavior, with h^2C_o/S for the AE-102 exceeding that for the AE-103 by a fairly constant amount over the entire frequency range. This seems to indicate that, all other factors being equal, the sensitivity of a transducer (which is proportional to the amplitude factor) decreases for increasing backing thickness. Referring back to the transient results for the broadband pulse input in Fig. 10 shows that they confirm this observation, with the AE-102 (1.270 cm (0.500 in) backing) showing almost a 25% greater output amplitude than the AE-103 (1.905 cm (0.750 in) backing).

This correlation of output amplitude with backing thickness is surprising. At relatively low frequencies, where the backing wave makes a significant contribution to the output, it is understandable that a transducer with a thin backing layer might produce a larger steady-state output signal, because of the contribution of the backing wave to the output. This is not the case here, however, for the difference in amplitude between the AE-102 and AE-103 transducers is approximately constant over the entire frequency range of the experiments. In addition, the pulse response shows the same behavior, and the backing wave does not enter into the first peak of the pulse response. This effect cannot be adequately explained without further research.

The AE-101 transducer shows a sharp rise in amplitude factor above 2.0 MHz. This is probably due to a change in the transit time of the piezoelement which is caused by the presence of the aluminum wearplate. This effect is discussed in detail in

Appendix F (section F.2).

4.1.7 Characterization of the Unbacked Transducer

The differences between the behavior of backed and unbacked transducers are so great that a separate discussion is required for the unbacked transducer (AE-100) tested in this study. The difference is actually the difference between a damped system and a resonant system, corresponding to the backed and unbacked transducers, respectively. Some of the particular complexities of a resonant system are alluded to in the discussion of steady-state output amplitude in Appendix F (expecially section F.2).

In an unbacked transducer, waves are reflected from the rear surface of the piezoelement rather than being transmitted across it, so that there are two more possible time delays to evaluate than for the backed transducer. These two time delays correspond to the reflection of waves back into the piezoelement from each of its faces. Also, since no attenuating materials are present in the unbacked system except the slightly attenuating piezo-element, the only loss of stress-wave energy from the system is by transmission into the potting material from the rear surface of the piezoelement and by conversion into electrical energy by the piezoelement itself. In a backed transducer, these effects are insignificant compared to the attenuation of the backing layer, but when no backing is present, they become very important. In fact, in the AE-100, some waves undergo as many as 30 reflections before their amplitudes are small enough to be neglected. This means that the time delays, transit times, impedances, and all

other parameters must be evaluated much more precisely for an unbacked transducer than for a transducer with a backing layer, or errors will accumulate and eventually dominate the predicted results. As the frequency of the input signal nears the resonant frequency of the piezoelement, this problem becomes increasingly more severe.

Fig. 13 shows four predicted output signals for the AE-100 transducer, corresponding to one broadband pulse and three tone burst input signals. These predictions are the best predictions that can be obtained without changing the model to include the time delays and attenuation factors which are peculiar to the unbacked case. Fig. 13 should be compared with to Fig. 14 (taken from Fig. D3), which contains the corresponding measured output signals for the AE-100. Because of the enormous number of reflections in the unbacked transducer, it is difficult to explain the differences between the measured and predicted results in terms of particular transducer parameters, but some observations can be made nonetheless.

Observe for the pulse response (plot (a) in Figs. 13 and 14) that the measured output shows appreciably more damping than the predicted output. The measured signal only rings for about 10 μsec, compared to a 30 μsec duration for the predicted output signal. Plot (d) illustrates this highly-resonant behavior even more dramatically; as the input frequency nears the resonant frequency of the piezoelement, the predicted output amplitude increases by six orders of magnitude compared to the measured output. Plots (b) and (c) in Figs. 13 and 14 show slight

qualitative similarity for measured and predicted results, but correlation is rather poor without including the two time delays mentioned earlier.

4.2 EFFECTS OF OTHER PARAMETERS ON THE OUTPUT OF THE SYSTEM

During the characterization of an ultrasonic system, it becomes necessary to investigate the effects of factors other than merely the time delays and time constants discussed in the previous section. These other factors are not modeling parameters in the sense that their values cannot be arbitrarily varied to improve the accuracy of the predicted results, but they certainly affect the output of the system and it is helpful to understand their role in the behavior of the system as a whole. Each of these factors is discussed in detail in Appendices F through J, and a summary of their effects on the output signal is presented in the following paragraphs.

4.2.1 Effect of Wearplate Impedance and Backing Impedance

Appendices F and G discuss the influence of these two quantities on the output of an ultrasonic test system; Appendix F draws conclusions based on the measured steady-state output amplitude, and Appendix G corroborates the conclusions with theoretical predictions. The results show that impedance mismatch between wearplate and piezoelement reduces the efficiency of a transducer; maximum transmission of stress-wave energy across the wearplate-piezoelement interface requires that the two layers be impedance-matched.

The effect of impedance mismatch at the piezoelement-backing interface is more dramatic. If the backing layer is not impedance-matched to the piezoelement, standing waves can develop in the piezoelement and cause it to resonate. A piezoelement which is free to resonate is much more sensitive to excitement at or near its resonant frequency than at other frequencies, so that its bandwidth is relatively narrow compared to that of a piezoelement with a matched backing layer.

4.2.3 Effect of Backing Thickness

Appendix F also discusses the effect of backing thickness on steady-state output amplitude of the system. The result is the interesting and confounding observation that the steady-state output amplitude, and consequently the sensitivity of a transducer, decreases with increasing backing thickness. This observation was also made in the previous section during the discussion of the amplitude factor $h^2 C_o/S$, where it was pointed out that even in the transient case, where a broadband pulse input signal is used, the amplitude of the output signal for the AE-103 transducer (1.905 cm (0.750 in) backing thickness) is 25% less than that for the AE-102 (1.270 cm (0.500 in) backing). This effect cannot be explained except by some peculiar behavior of stress waves at the piezoelement-backing interface. Further investigation is required to confirm and explain this result.

4.2.4 Effect of Piezoelement Thickness

In addition to considering the effects of wearplate impedance

and backing impedance on the output of an ultrasonic test system, Appendix G also uses the wave propagation model to predict the effect of changing the piezoelement thickness. Increasing the thickness of the piezoelement is shown to increase the amplitude of the output signal, but at the cost of losing some bandwidth. Since the piezoelement integrates the stress inside it to produce the output voltage, a thicker piezoelement integrates over a longer time interval and consequently filters out some of the higher-frequency components of the stress waveform. The best piezoelement is that which has a short enough transit time so as not to filter useful information out of the output signal, yet is thick enough to give a reasonable output amplitude.

There is another effect of piezoelement thickness which is important in resonant transducers. The resonant frequency of a piezoelement is inversely proportional to its transit time, so increasing the thickness of the piezoelement will lower its resonant frequency, and vice-versa.

4.2.4 Effect of Intermediate Couplant and Bonding Layers

Appendix H describes the experiments used to isolate the effects of couplant layers and adhesive-bonding layers between transducer components and at transducer-specimen interfaces in the system. The results show that the behavior of stress waves at impedance-mismatched interfaces where a couplant layer is present is exactly as predicted by the impedance model of Chapter 2 (see subsection 2.3.1), and that only a very small reflection (less than 2% of incident amplitude) is produced at an impedance-matched

interface where couplant is used. No time delays are observed at the couplant layer in either case, although other researchers have reported them at higher frequencies [42].

The presence of an intermediate epoxy bonding layer is shown to have two significant and easily-quantified effects: reduction of the amplitude of the transmitted wave, and production of large-amplitude reflections at the layer. Both are due to impedance mismatch between the epoxy and the adjacent layers.

4.2.5 Effect of Frequency-Dependent Attenuation on Output for Broadband Input Signal

Since the attenuation of the backing material used in the transducers is frequency-dependent, the wave superposition model does not give an accurate prediction of the backing wave when a broadband input signal is used. One way to solve this problem is to use a digital signal processing program such as the Fast Fourier Transform (FFT) to transform the input signal into the frequency domain, and then to selectively attenuate different frequency components as required by the frequency-dependent attenuation parameter $\alpha_B(\omega)$ [24].

A simpler procedure involves the use of a digital low-pass filter to simulate the increase in attenuation at higher frequencies. Appendix I discusses this procedure, which gives satisfactory results for the broadband pulse used in this study.

CHAPTER 5

CONCLUSIONS AND RECOMMENDATIONS

5.1 CONCLUSIONS

Five different transducer designs were evaluated in this study. One of the designs is sold commercially, the Acoustic Emission Technology (AET) FC-500 transducer, manufactured by Panametrics, Inc. of Waltham, MA (model V105). This transducer consists of a lead metaniobate piezoelement which converts stress to voltage and vice-versa, a titanium carbide wearplate which protects the piezoelement from direct contact with the specimen during testing, and a tungsten epoxy backing layer which broadens the bandwidth of the transducer by damping out standing waves in the piezoelement. The other prototype transducer designs are similar to the FC-500, differing only in backing thickness and wearplate impedance.

The transducers were evaluated by comparing the results of through-transmission experiments to theoretical results predicted by a mathematical model of a general ultrasonic test system. The model was developed specifically for this study, and is based on the theory of wave propagation in elastic materials and on the physics of the piezoelectric effect. Once the accuracy of the model was verified, it was then used as an aid in understanding the effects of certain transducer parameters on the output of an ultrasonic system. The conclusions which can be drawn from this study are summarized below.

Items (1) through (8) are the results of the comparison of measured and predicted results:

(1) In order to obtain good correlation between measured and predicted results, it was found necessary to account for three time delays in the model. One delay, δ, is introduced as waves are transmitted across the interface between the wearplate and piezoelement of the output transducer; another delay, β, is introduced as waves are reflected back into the wearplate from the same interface; and a third delay, γ, is introduced as waves propagate through the backing layer and are reflected from the interface between the backing layer and the potting material. All of these time delays are in addition to the time delays (transit times) assiciated with the transducer elements themselves.

(2) The values for the time delay δ were found to be 0.08 μsec for those transducers with titanium carbide wearplates, and 0.05 μsec for those with aluminum wearplates.

(3) The values for the time delay β were found to be 0.20 μsec for those transducers with titanium carbide wearplates, and 0.125 μsec for those with aluminum wearplates.

(4) The values for the time delay γ were found to be 0.75 μsec for the AE-101 transducer, with 0.635 cm (0.250 in)

backing thickness, and 1.50 μsec for the AE-102, with 1.270 cm (0.500 in) backing thickness. The FC-500 has a backing thickness of 0.635 cm (0.250 in), and showed a time delay of 1.60 μsec.

(5) No frequency-dependence was observed for any of the time delays over the frequency range 0.4-3.0 MHz.

(6) It was found that the decay of voltage across the output piezoelement due to the flow of current through the oscilloscope played an important role in determining the shape of the output signal. The value of the time constant RC_o corresponding to this decay was found to be 1.0 μsec for the standard AET FC-500 transducer, and 5.0 μsec for the prototype transducers with matched backing layers (AE-101, AE-102, AE-103).

(7) The amplitude factor h^2C_o/S, where h, C_o and S represent the piezoelectric constant, capacitance and surface area of the piezoelement, respectively, was found to be approximately constant between 0.4 and 2.0 MHz, falling between 3.5 and 7.0 x 10^{15} N/m^3 for each of the transducers over that range.

(8) Excellent correlation between predicted results from the wave propagation model and measured results was found for all of the transducers except the AE-100, provided the correct time delays and time constant were known.

Items (9) through (11) are further observations and conclusions based on these results:

(9) Replacing the titanium wearplate with an aluminum wearplate reduced both of the wearplate-piezoelement time delays by exactly the same proportion—37.5%. This shows clearly that these time delays are functions of the wearplate impedance; a decrease in wearplate impedance results in a decrease in the values of the time delays at the interface between wearplate and piezoelement. This also causes an increase in the resonant frequency of the piezoelement (see item (13), below).

(10) The ratio between the backing-wave time delays for the AE-101 and AE-102 transducers is exactly the same as the ratio of the backing thicknesses for these transducers. This indicates that perhaps this time delay does not represent an interfacial effect, but rather a correction for errors in the measured values for wavespeed and/or thickness of the backing layers.

(11) Using the measured values of backing attenuation in the model gave predicted backing waves that were too large by a factor of two. Either the measurements were inaccurate, or some other source of backing-wave attenuation exists, in addition to wave propagation through the backing layer.

Items (12) through (17) are statements concerning the influence of certain transducer parameters and conditions on the output of an ultrasonic test system.

(12) The presence of a layer of ultrasonic acoustic couplant at interfaces within the system has a negligible effect on the propagation of stress waves within the system over the frequency range from 0.4 to 3.0 MHz. Neither the amplitude nor the phase of the stress waves is affected by the presence of the couplant layer.

(13) A mismatch in acoustic impedance between the wearplate and piezoelement in a transducer results in a decrease in output amplitude and the production of spurious reflected waves at those interfaces in the system. An impedance-mismatched wearplate can also affect the resonant frequency of the piezoelement by altering the time delays at the piezoelement-wearplate interfaces.

(14) Impedance mismatch between wearplate and specimen also reduces the amplitude of the output signal and creates spurious reflections in the output signal.

(15) Impedance mismatch at the rear surface of the piezoelement in an ultrasonic transducer allows the presence of a large-amplitude resonant peak in the frequency response of the transducer.

(16) Increasing the thickness of the backing layer in a transducer reduces the sensitivity of the transducer.

(17) Increasing the thickness of the piezoelement in a transducer increases the amplitude of the output signal, but reduces the bandwidth of the signal.

5.2 RECOMMENDATIONS

Based on the conclusions of the preceding section, several sets of recommendations can be made. These are summarized in the paragraphs which follow.

5.2.1 Recommendations for Future Work

This study raised several questions which deserve further experimentation and analysis:

(1) Further investigation is required to experimentally establish the existence of time delays and amplitude reductions at the surfaces of the piezoelement in an ultrasonic transducer. A specimen for this purpose could be made by bonding a piezoelement between two layers of a material with low attenuation, such as titanium carbide. The entire specimen could then be tested between two transducers, and the output signal analyzed for evidence of time delays and amplitude reduction. At the same time, the effect of changing the electrical load across the piezoelement on these parameters could be determined as well.

(2) A statistical study should be performed on a number of allegedly "identical" transducers to determine the correspondence between the values of the time delays, capacitances, and piezoelectric constants for these transducers. This would help to establish whether the values of these parameters could be predicted in advance

for a particular transducer, or whether the manufacturing process introduces so many variables that each transducer must be evaluated individually.

(3) An analysis similar to that employed here should be applied to resonant transducers, such as the AE-1MM used in this study. The increased precision required in the resonant case would give additional insight into the behavior of ultrasonic transducers in general.

5.2.2 Recommendations for Transducer Design

Based on the results of this study, the following guidelines are suggested for the design of broadband piezoelectric ultrasonic transducers:

(1) A broadband ultrasonic transducer should be designed with a backing layer that has the same acoustic impedance as the piezoelement. If possible, the round-trip transit time of the backing layer should be larger than the expected duration of the output signal. This eliminates the possibility of interference between the backing wave and the primary wave in the output signal.

(2) The thickness of the piezoelement should be chosen so that the round-trip transit time of the piezoelement is equal to the desired time-resolution of the output signal. This gives the best compromise between amplitude and bandwidth in the output signal.

(3) The impedance of the wearplate should also be chosen to

match either the piezoelement or the specimen. This gives the largest-amplitude output signal, and also reduces the production of spurious reflected waves in the system. In addition, the wearplate should be designed as thin as is practical, so that its thickness-mode resonant frequency is well above the upper limit of the bandwidth of the transducer.

5.2.3 Recommendations for Reporting of Ultrasonic Test Results

One of the implications of this study is that there are many factors which influence the output of a particular ultrasonic test system. When results of ultrasonic tests are reported, the information given is often incomplete and vague, so that it is difficult for the reader to determine exactly what has been done, and even more difficult to reproduce the work himself. To avoid this problem, the following information should be included when reporting the results of ultrasonic tests:

(1) The acoustic impedance, wavespeed, and dimensions of the test specimen should be reported with the test results.

(2) A description of the transducer used should be included, along with either a frequency response curve or a plot of the impulse response of the transducer.

(3) The method of attaching the transducer to the specimen should be described, particularly if an adhesive is used.

(4) A description of the device used to measure the output voltage should be given.

REFERENCES

[1] Cady, W.G., "Piezoelectricity", McGraw-Hill Book Company, Inc., 1st edition, 1946.

[2] Mason, W.P., "Electromechanical Transducers and Wave Filters", D. Van Nostrand Company, Inc., 2nd edition, 1948.

[3] Rhyne, T.L., "An Improved Interpretation of Mason's Model for Piezoelectric Plate Transducers", IEEE Transactions on Sonics and Ultrasonics, Vol. SU-25, No. 2, March 1978, pp. 98-103.

[4] Smith, W.M.R., and Awojobi, A.O., "Factors in the Design of Ultrasonic Probes", Ultrasonics, Vol. 17, pp. 20-26.

[5] Kossoff, G., "The Effects of Backing and Matching on the Performance of Piezoelectric Ceramic Transducers", IEEE Transactions on Sonics and Ultrasonics, Vol. SU-13, No. 1, March 1966, pp. 20-30.

[6] Goll, J.H., and Auld, B.A., "Multilayer Impedance Matching Schemes for Broadbanding of Water Loaded Piezoelectric Transducers and High Q Electric Resonators", IEEE Transactions on Sonics and Ultrasonics, Vol. SU-22, No. 1, January 1975, pp. 52-53.

[7] Sittig, E.K., "Transmission Parameters of Thickness-Driven Piezoelectric Transducers Arranged in Multilayer Configurations", IEEE Transactions on Sonics and Ultrasonics, Vol. SU-14, No. 4, October 1967, pp. 167-174.

[8] Sittig, E.K., "Effects of Bonding and Electrode Layers on the Transmission Parameters of Piezoelectric Transducers Used in Ultrasonic Digital Delay Lines", IEEE Transactions on Sonics and Ultrasonics, Vol. SU-16, No. 1, January 1969, pp. 2-10.

[9] Gusev., O.B., "Experimental Determination of Electric Equivalent-Circuit Parameters of a Loaded Piezoelectric Transducer", Soviet Journal of Nondestructive Testing, Vol. 12, No. 2, pp. 159-162.

[10] Fox, M.D., and Donnelly, J.F., "Simplified Method for Determining Piezoelectric Constants for Thickness Mode Transducers", Journal of the Acoustical Society of America, Vol. 64, No. 5, November 1978, pp. 1261-1265.

[11] Martin, R.W., and Sigelmann, R.A., "Force and Electrical Thevenin Equivalent Circuits and Simulations for Thickness Mode Piezoelectric Transducers", Journal of the Acoustical Society of America, Vol. 58, No. 2, August 1975, pp. 475-489.

[12] Krimholtz, R., Leedom, D., and Matthaei, G., "New Equivalent Circuits for Elementary Piezoelectric Transducers", Electronics Letters, Vol. 6, June 1970, pp. 398-399.

[13] Desilets, C.S., Fraser, J.D., and Kino, G.S., "The Design of Efficient Broad-Band Piezoelectric Transducers", IEEE Transactions on Sonics and Ultrasonics, Vol. SU-25, No. 3, May 1978, pp. 115-125.

[14] Dotti, D., "A New Model of a Piezoelectric Transducer for Direct Impulse Response Evaluation", IEEE Transactions on Sonics and Ultrasonics, Vol. SU-22, No. 3, May 1975, pp. 202-205.

[15] Tiersten, H.F., "Linear Piezoelectric Plate Vibrations", Plenum Press, 1969.

[16] Shaw, E.A.G., "On the Resonant Vibrations of Thick Barium Titanate Disks", Journal of the Acoustical Society of America, Vol. 28, No. 1, January 1956, pp. 38-50.

[17] Cowdrey, D.R., and Willis, J.R., "Applications of the Finite Element Method to the Vibrations of Quartz Plates", Journal of the Acoustical Society of America, Vol. 56, No. 1, July 1974, pp. 94-98.

[18] Korolev, M.V., and Karpelson, A.E., "Transient, Pulse, and Amplitude-Frequency Characteristics of Surface-Excited Thick Piezoelectric Transducers", Soviet Journal of Nondestructive Testing, Vol. 15, No. 12, pp. 1019-1024.

[19] Redwood, M., "Transient Performance of a Piezoelectric Transducer", Journal of the Acoustical Society of America, Vol. 33, No. 4, April 1961, pp. 527-536.

[20] Redwood, M., "A Study of Waveforms in the Generation and Detection of Short Ultrasonic Pulses", Applied Materials Research, Vol. 2, April 1963, pp. 76-84.

[21] Hill, R., and El-Dardiry, S.M.A., "A Theory for Optimization in the use of Acoustic Emission Transducers", Journal of the Acoustical Society of America, Vol. 67, No. 2, February 1980, pp. 673-682.

[22] Altman, H.E., and Beyer, R.T., "Effect of the Parallel Reflecting Surfaces of a Transducer on the Resulting Pulse Shape", Journal of the Acoustical Society of America, Vol. 59, No. 3, March 1976, pp. 545-550.

[23] Folds, D.L., and Loggins, C.D., "Transmission and Reflection of Ultrasonic Waves in Layered Media", Journal of the Acoustical Society of America, Vol. 62, No. 5, November 1977, pp. 1102-1109.

[24] Doll, B., "Input-Output Characterization of Ultrasonic Transducer-Uniaxial Graphite Fiber Composite System", S.M. Thesis, Department of Mechanical Engineering, Massachusetts Institute of Technology, January 1981.

[25] Lee, S.S., and Williams, J.H., Jr., "Stress-Wave Attenuation in Thin Structures by Ultrasonic Through-Transmission", Journal of Nondestructive Evaluation, Vol. 1, No. 4, April 1980, pp. 277-285.

[26] Merkulov, L.G., Federov, V.A., and Yakovlev, L.A., "Operation of a Piezoelectric Transducer into an Elastically Anisotropic Solid Medium", Journal of Soviet Physics-Acoustics, Vol. 19, No. 1, July-August 1973, pp. 36-40.

[27] Dekker, D.L., Piziali, R.L., and Dong, E., Jr., "Effect of Boundary Conditions on the Ultrasonic-Beam Characteristics of Circular Disks", Journal of the Acoustical Society of America, Vol. 56, No. 1, July 1974, pp. 87-93.

[28] Hayman, A.J., and Weight, J.P., "Transmission and Reception of Short Ultrasonic Pulses by Circular and Square Transducers", Journal of the Acoustical Society of America, Vol. 66, No. 4, October 1979, pp. 945-951.

[29] Papadakis, E.P., and Fowler, K.A., "Broad-Band Transducers: Radiation Field and Selected Applications", Journal of the Acoustical Society of America, Vol. 50, No. 3, 1971, pp. 729-745.

[30] Kagawa, Y., and Yamabuchi, T., "Finite Element Simulation of a Composite Piezoelectric Ultrasonic Transducer", IEEE Transactions on Sonics and Ultrasonics, Vol. SU-26, No. 2, March 1979, pp. 81-88.

[31] Hatano, H., and Mori, E., "Acoustic-Emission Transducer and its Absolute Calibration", Journal of the Acoustical Society of America, Vol. 59, No. 2, Februa y 1976, pp. 344-349.

[32] Melkanovich, A.F., and Liventsova, L.B., "Measuring the Sensitivity of Piezoelectric Transducers", Soviet Journal of Nondestructive Testing, Vol. 12, No. 4, pp. 406-412.

[33] Papadakis, E.P. "Theoretical and Experimental Methods to Evaluate Ultrasonic Transducers for Inspection and Diagnostic Applications", IEEE Transactions on Sonics and Ultrasonics, Vol. SU-26, No. 1, January 1979, pp. 14-27.

[34] Gericke, O.R., "Experimental Determination of Ultrasonic Transducer Frequency Response", Materials Evaluation, Vol. 24, August 1966, pp. 409-411.

[35] Panin, V.I., "Calculation of the Amplitude-Frequency and Phase-Frequency Curves of Ultrasonic Piezoelectric Transducers", Soviety Journal of Nondestructive Testing, Vol. 14, No. 8, pp. 685-691.

[36] Mansour, T.M., "Evaluation of Ultrasonic Transducers by Cross-Sectional Mapping of the Near Field Using a Point Reflector", Materials Evaluation, Vol. 37, No. 7, June 1979, pp. 50-54.

[37] Timofeev, V.M., "Checking the Condition of Piezoelectric Transducers Attached to the Object", Soviet Journal of Nondestructive Testing, Vol. 15, No. 1, pp. 44-48.

[38] Miller, E.B., and Eitzen, D.G., "Ultrasonic Transducer Characterization at the NBS", IEEE Transactions on Sonics and Ultrasonics, Vol. SU-26, No. 1, January 1979, pp. 28-37.

[39] Williams, J.H., Jr., and Doll, B., "A Simple Wave Propagation Analysis of Piezoceramic Ultrasonic Transducer Response", (to appear in Materials Evaluation), April 1982.

[40] Kreyszig, E., "Advanced Engineering Mathematics", John Wiley & Sons, 4th edition, 1979, pp. 200-215.

[41] Williams, J.H., Jr., Nayeb-Hashemi, H., and Lee, S.S., "Ultrasonic Attenuation and Velocity in AS/3501-6 Graphite Fiber Composite", Journal of Nondestructive Evaluation, Vol. 1, No. 2, 1980, pp. 137-148.

[42] Vary, A., "Simulation of Transducer-Couplant Effects on Broadband Ultrasonic Signals", NASA Technical Memorandum 81489, 1980.

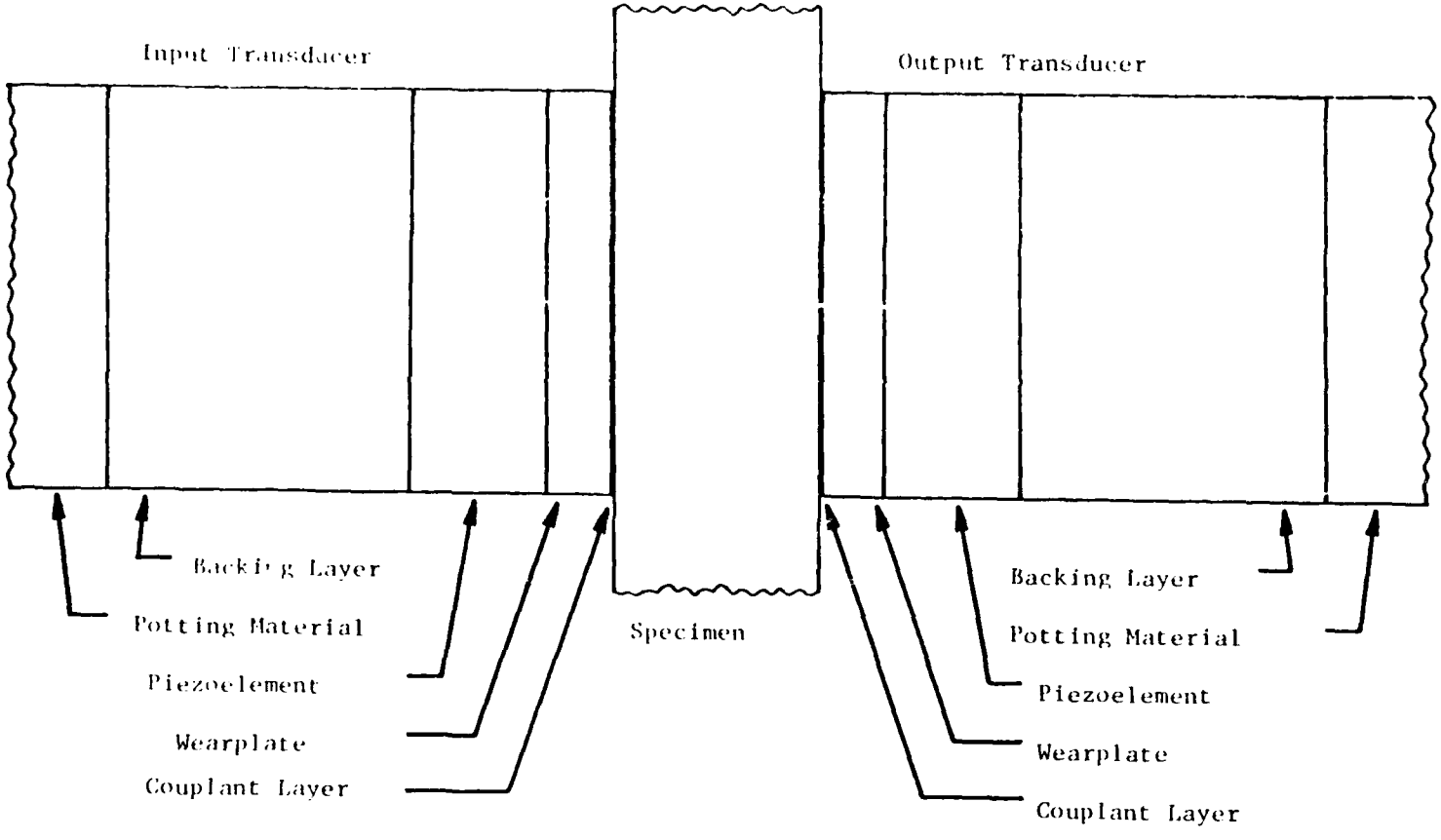

Fig. 1 Schematic representation of a typical ultrasonic through-transmission test system showing transducer and specimen layers.

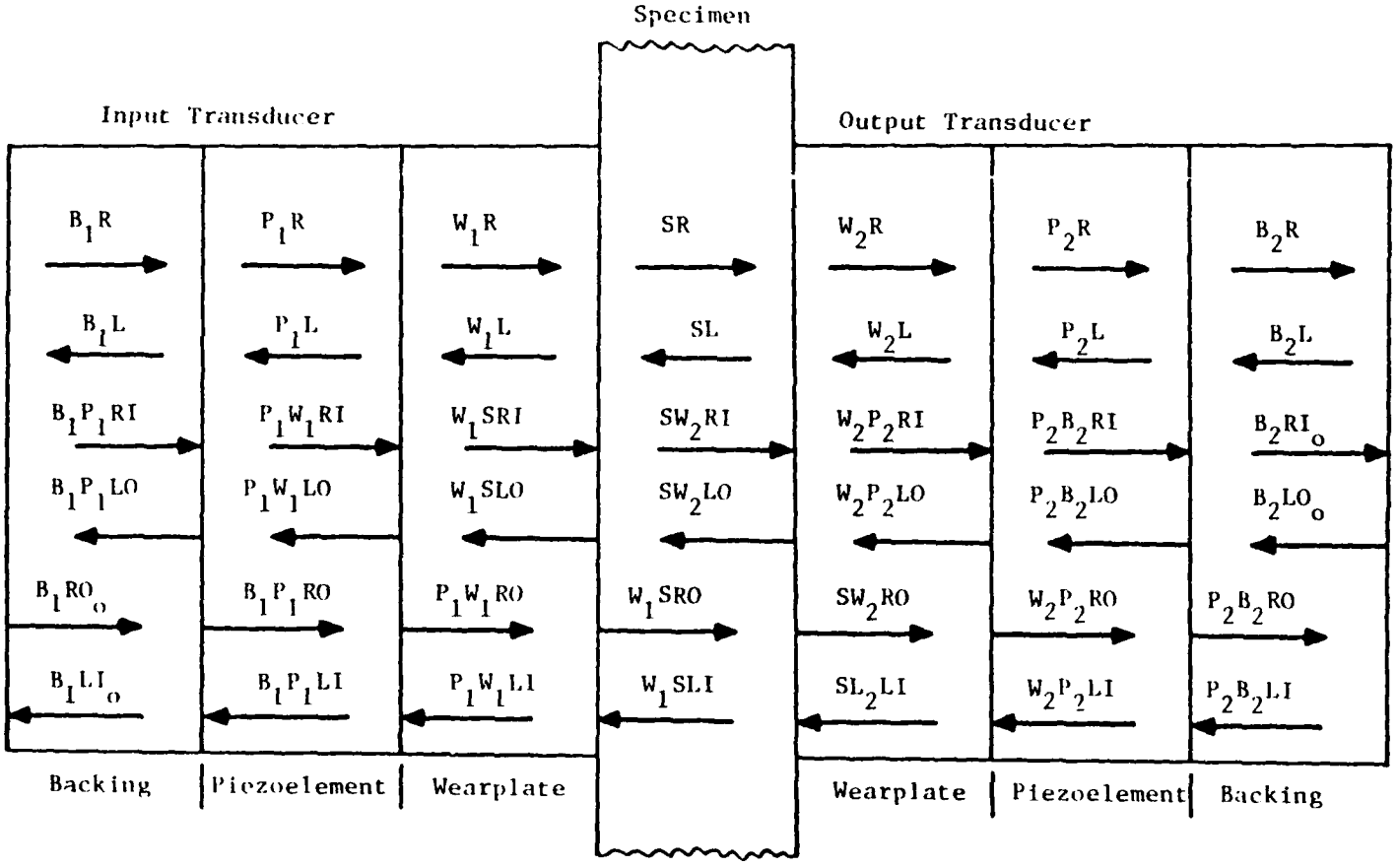

Fig. 2 System of nomenclature for stress waves in ultrasonic through-transmission test system.

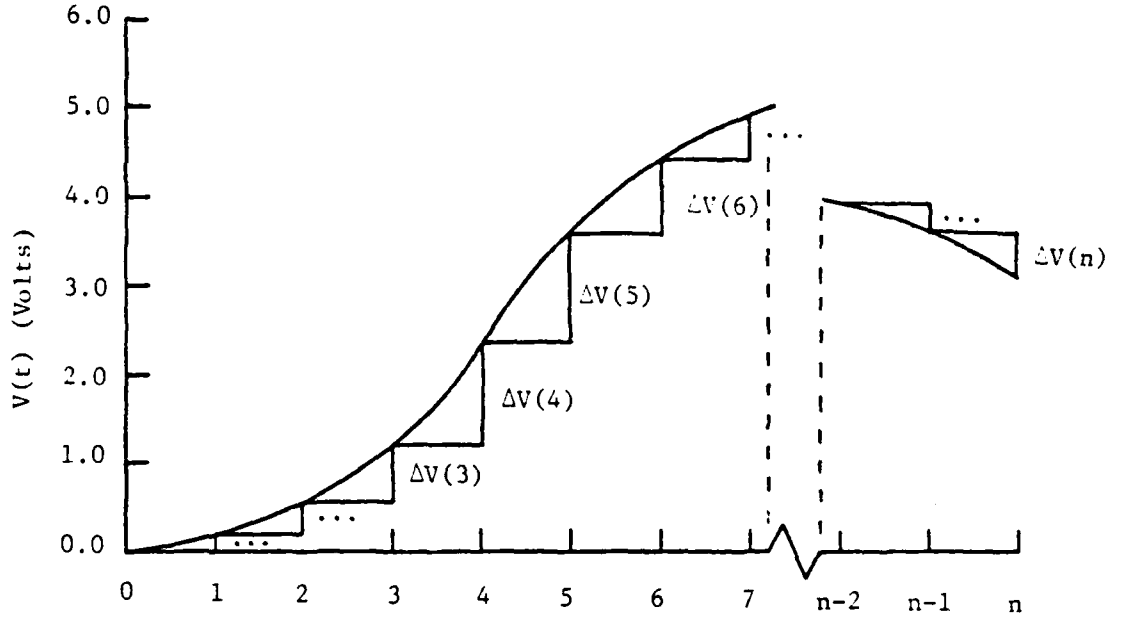

(a) Dimensionless Time, $t/\Delta t$

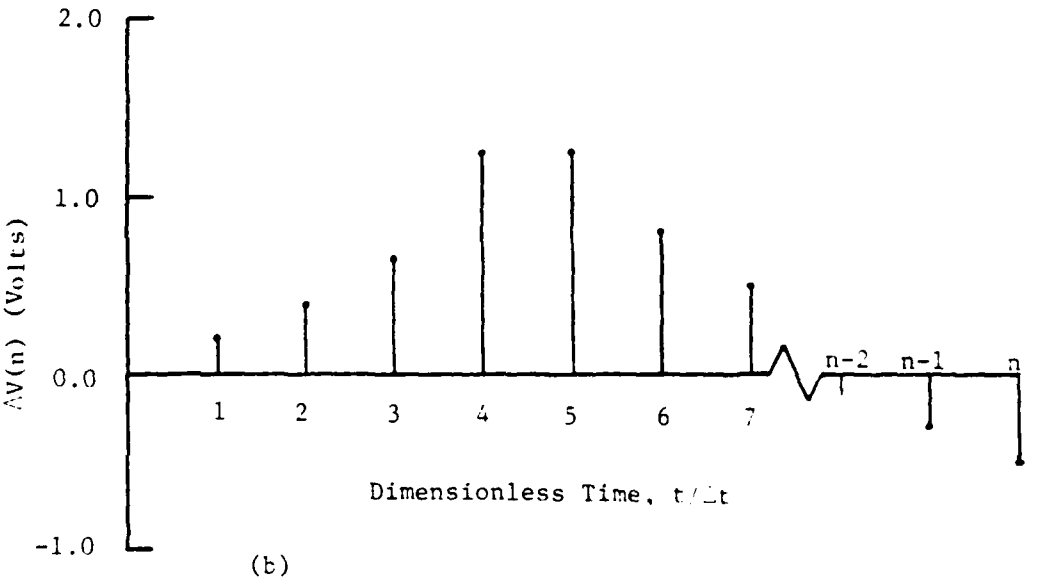

(b)

Fig. 3 Stepwise approximation $\Delta V(n)$ of a continuous time-varying voltage waveform V(t).

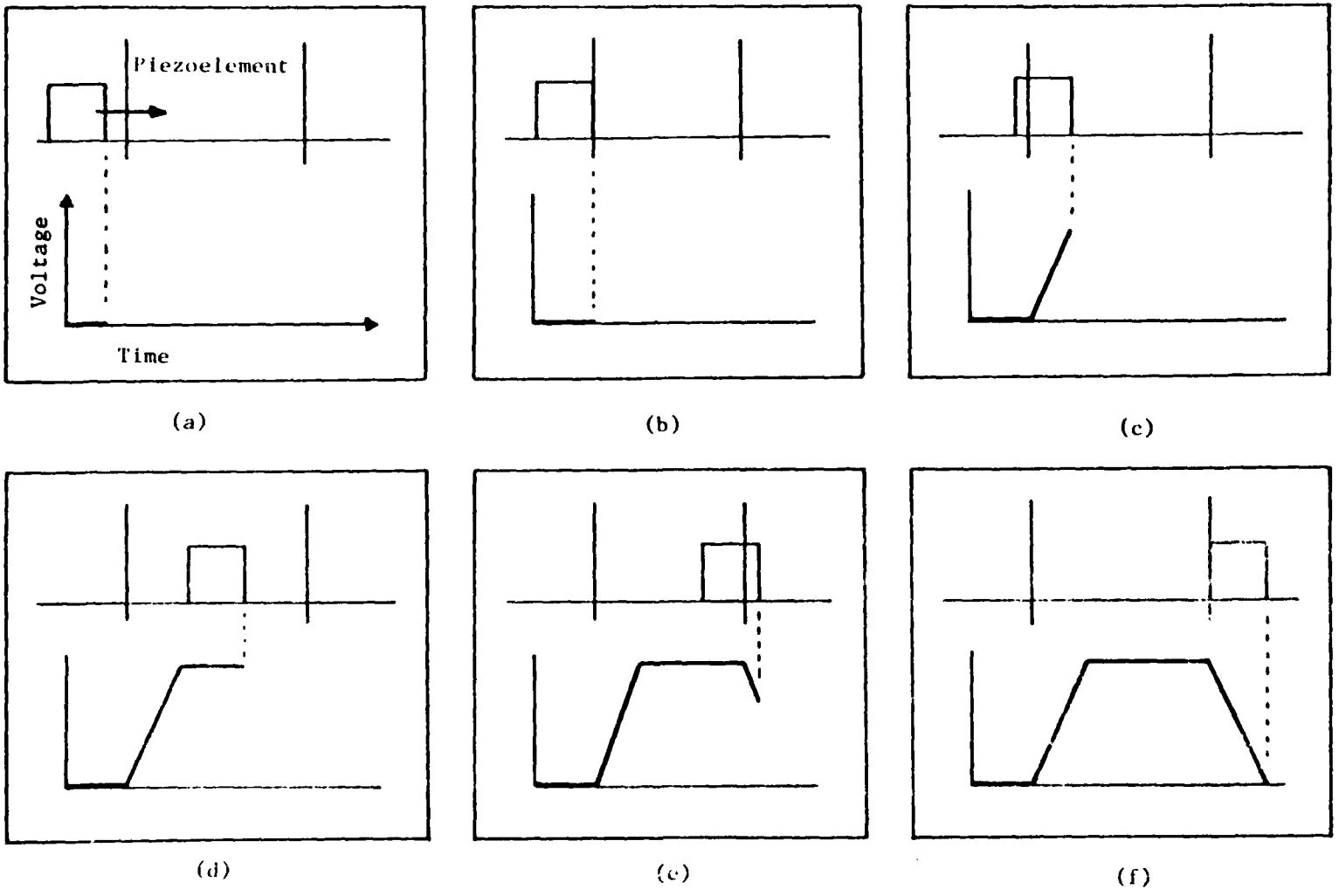

Fig. 4 Voltage produced by a rectangular stress pulse propagating through the piezoelement of an ultrasonic transducer

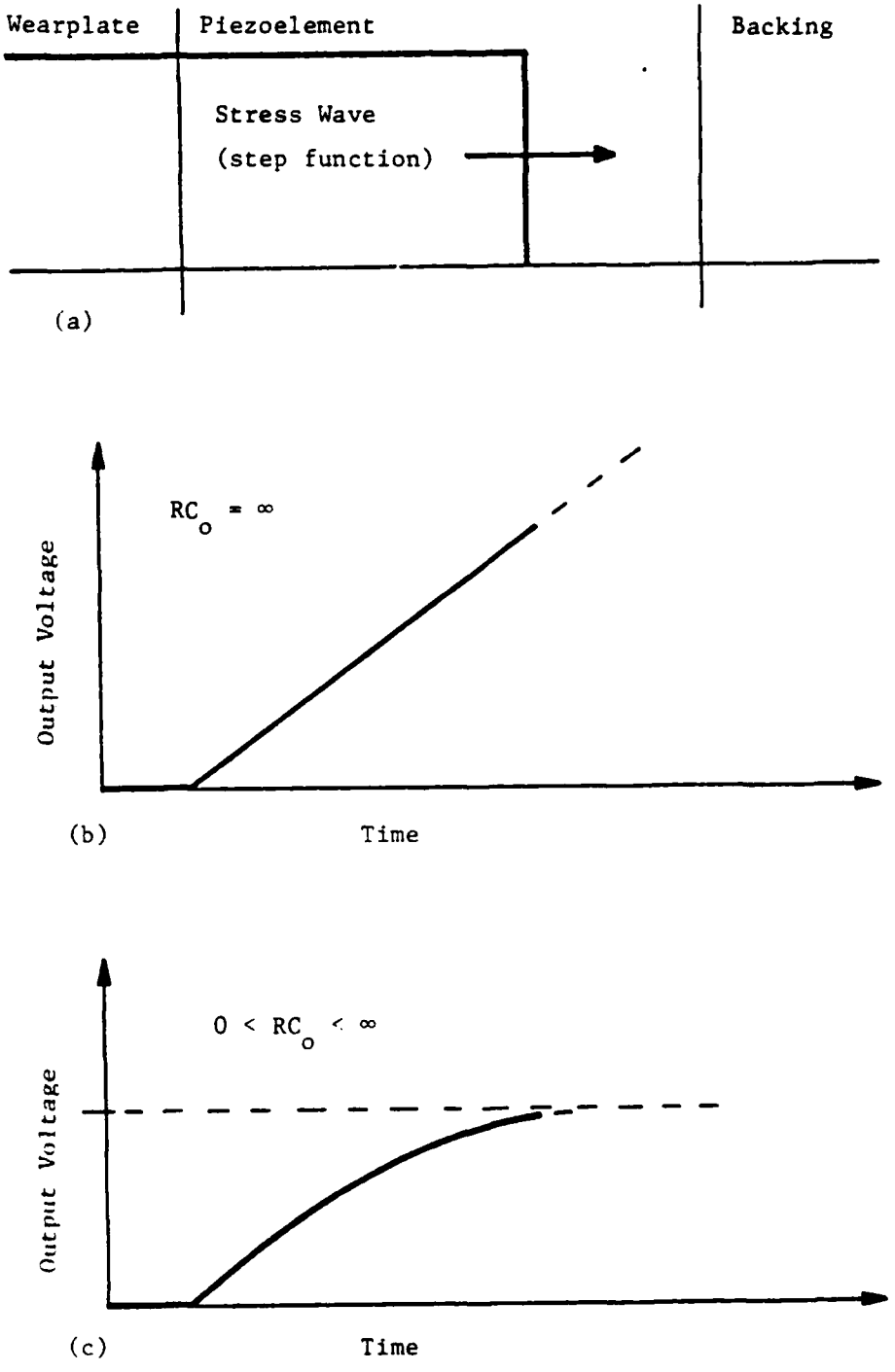

Fig. 5 Effect of a finite time constant RC_o on the voltage produced by a step function of stress in the piezoelement of an ultrasonic transducer.

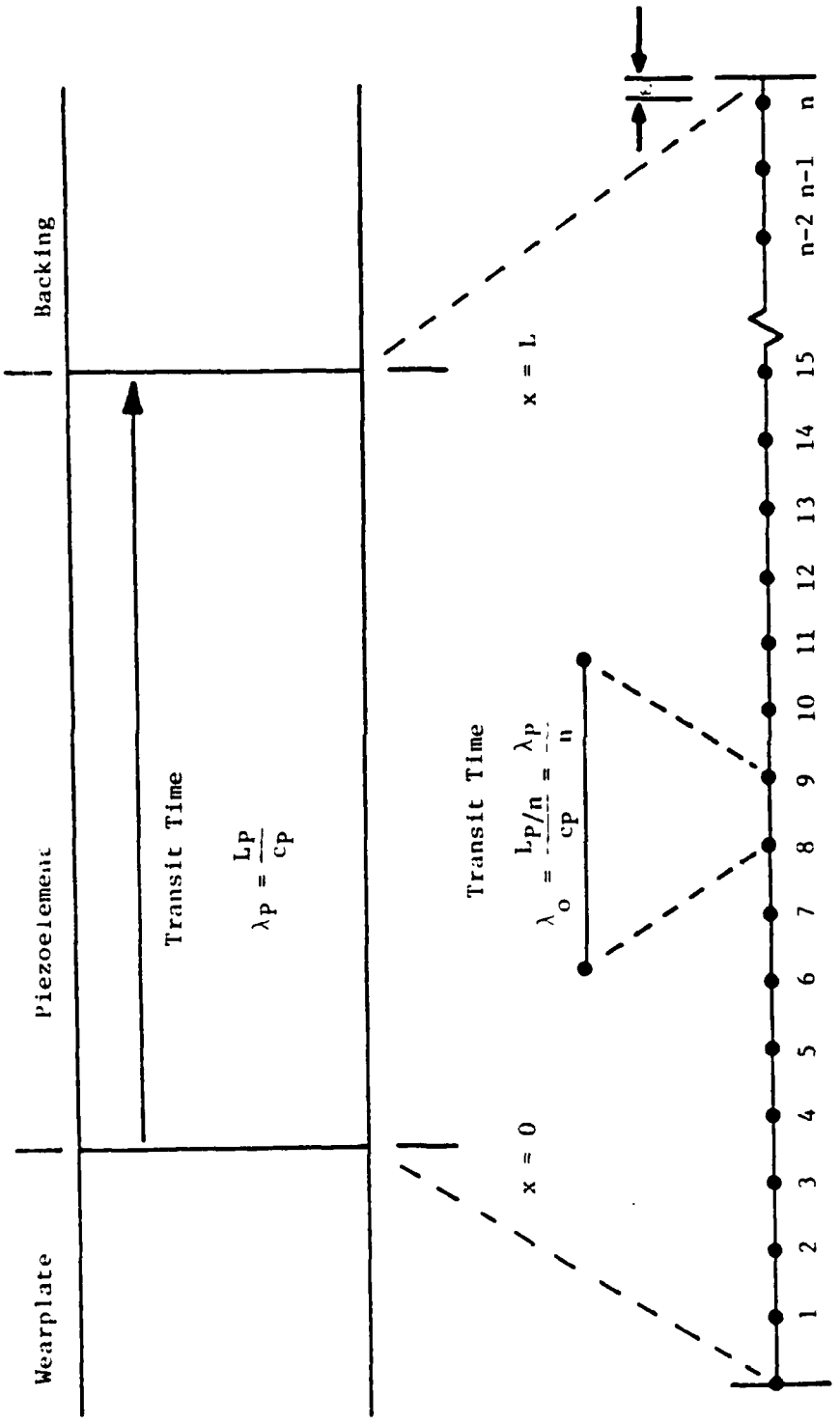

Fig. 6 Discretization of the piezoelement of an ultrasonic transducer into n segments, each having transit time λ_o.

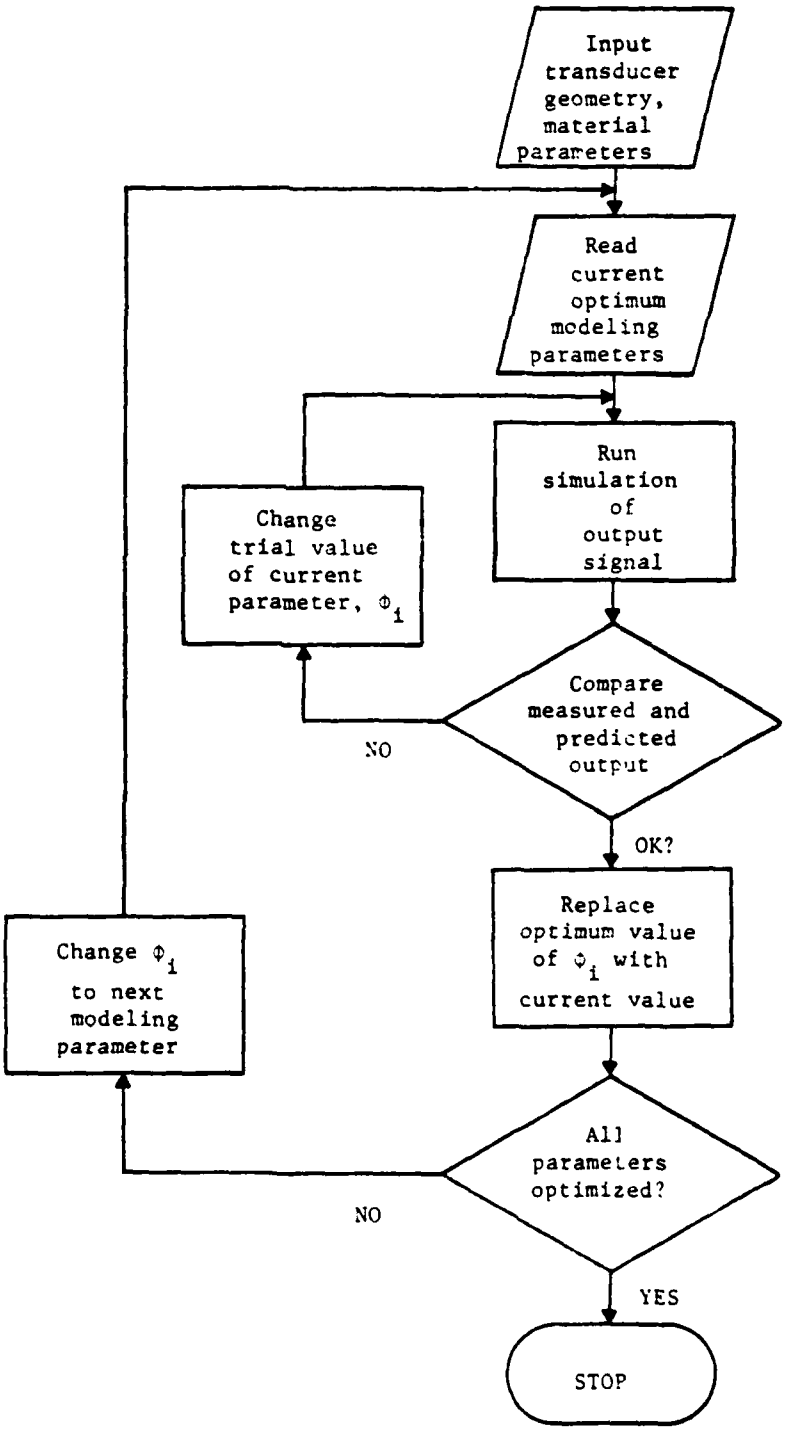

Fig. 7 Flowchart of the procedure for characterizing an ultrasonic test system using the wave propagation model.

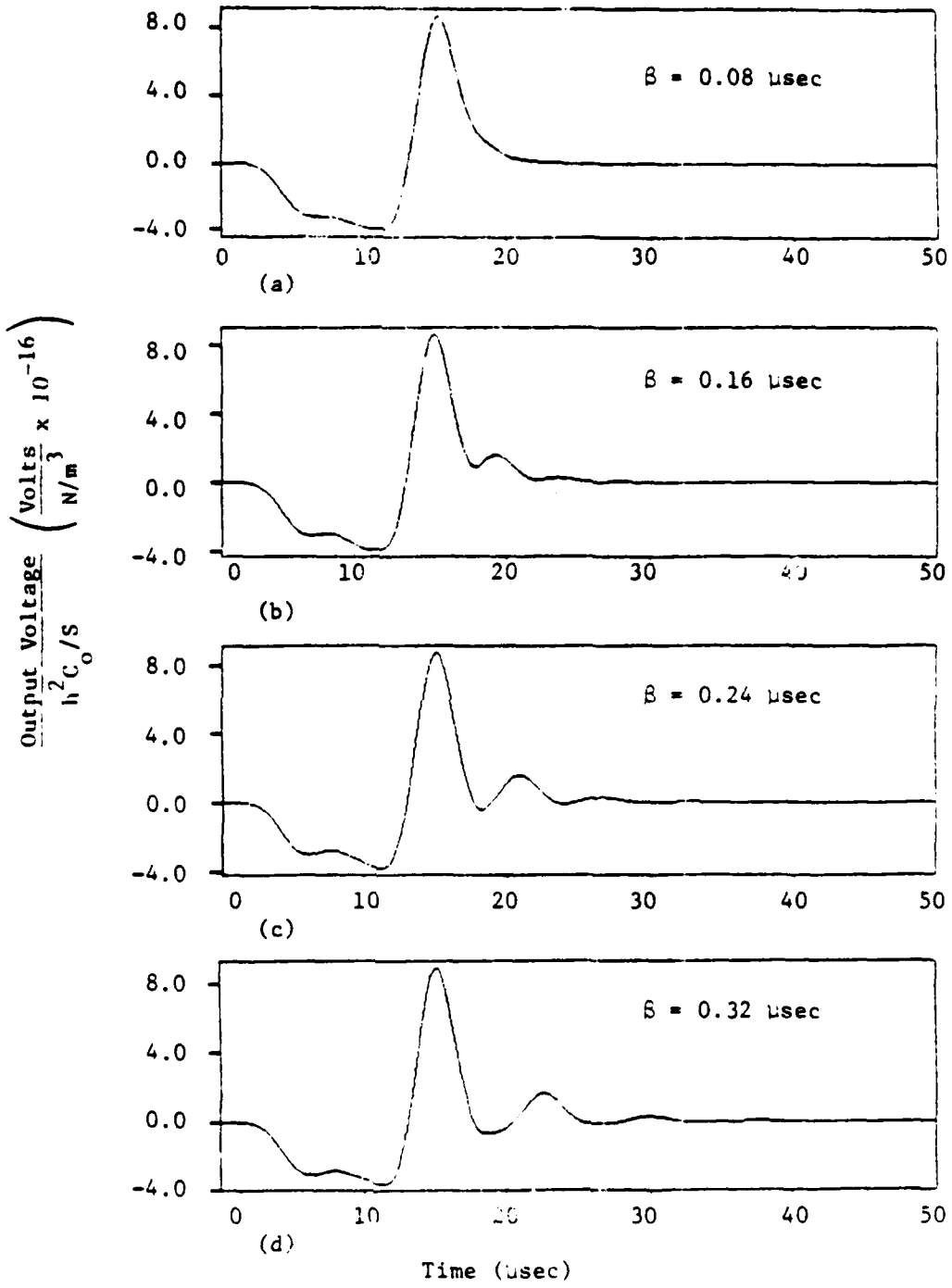

Fig. 8 Predicted broadband pulse response of two FC-500 transducers clamped face-to-face as a function of the time delay β.

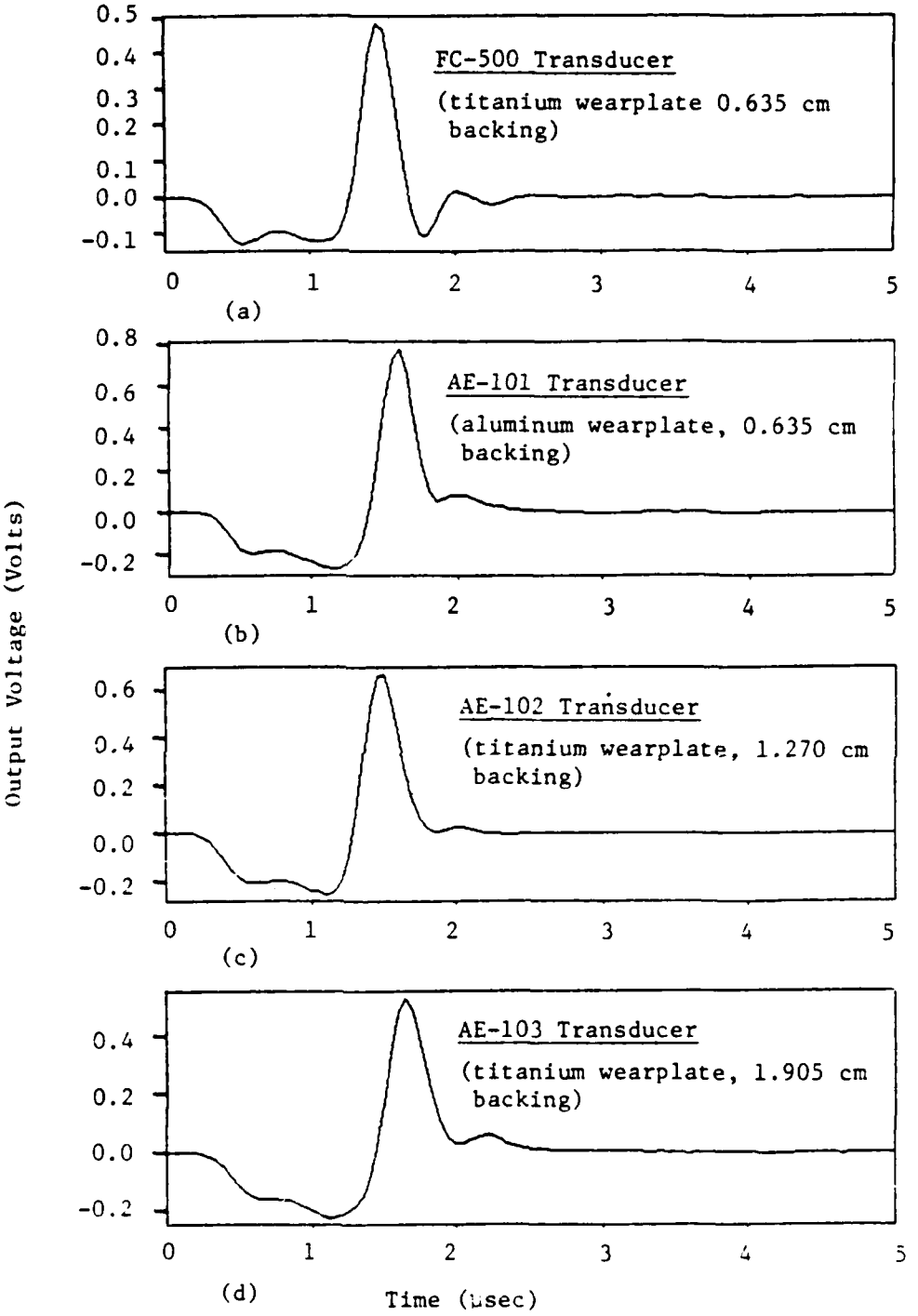

Fig. 9 Measured broadband pulse response of (a) FC-500, (b) AE-101, (c) AE-102, and (d) AE-103 transducers clamped face-to-face (expanded time scale).

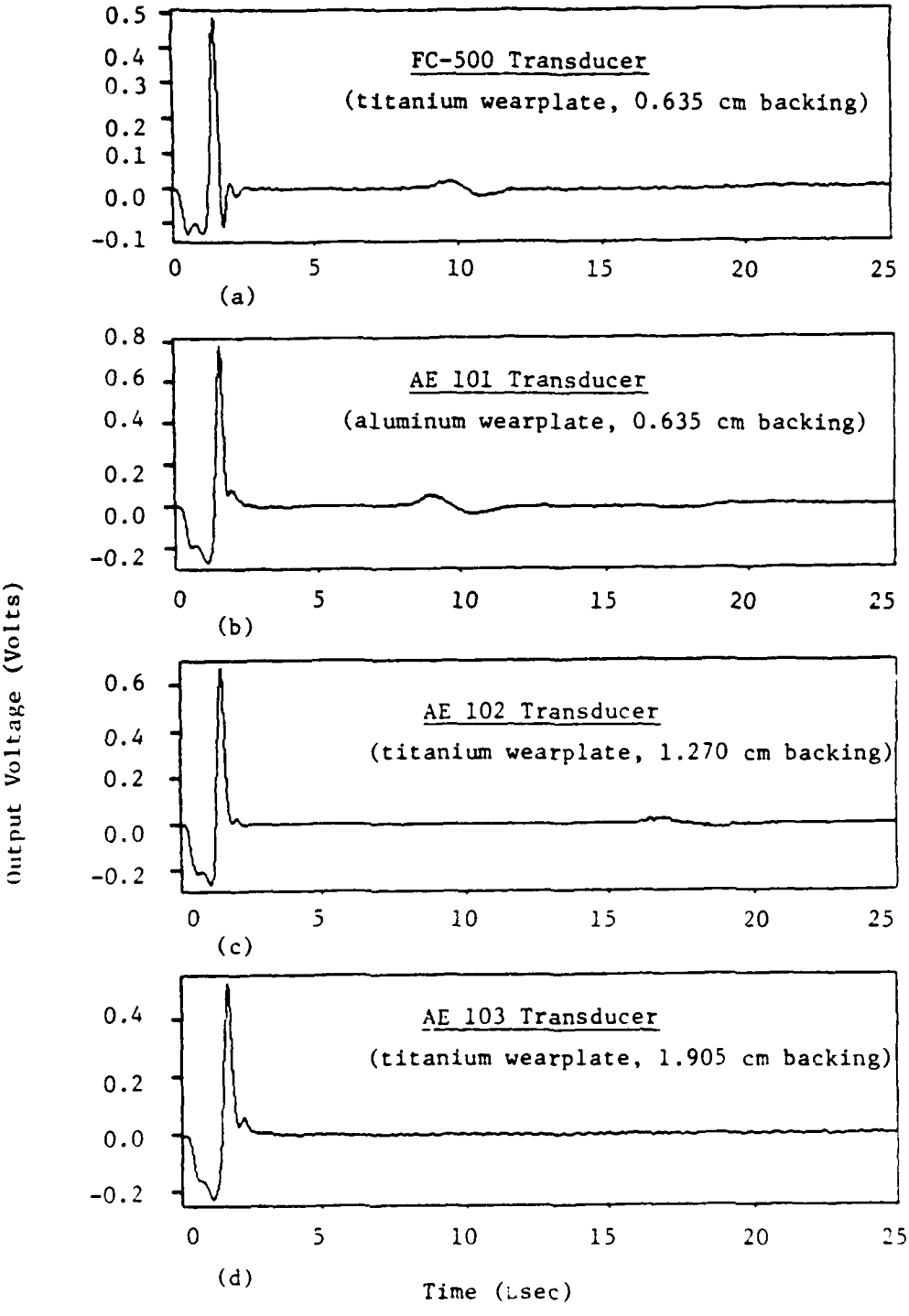

Fig. 10 Measured broadband pulse response of (a) FC-500, (b) AE-101, (c) AE-102, and (d) AE-103 transducers clamped face-to-face.

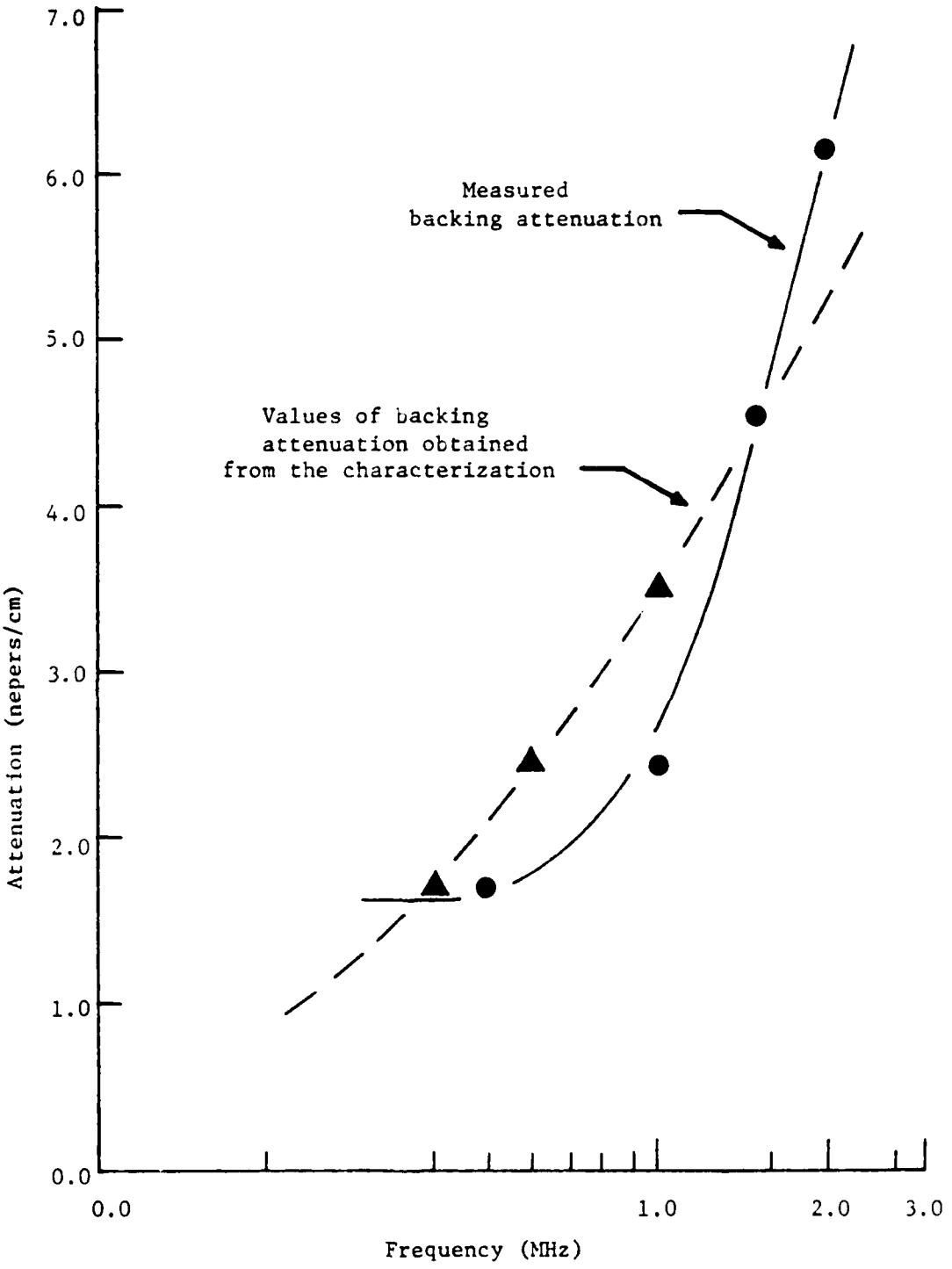

Fig. 11 Comparison of measured backing attenuation with values of attenuation obtained from the characterization.

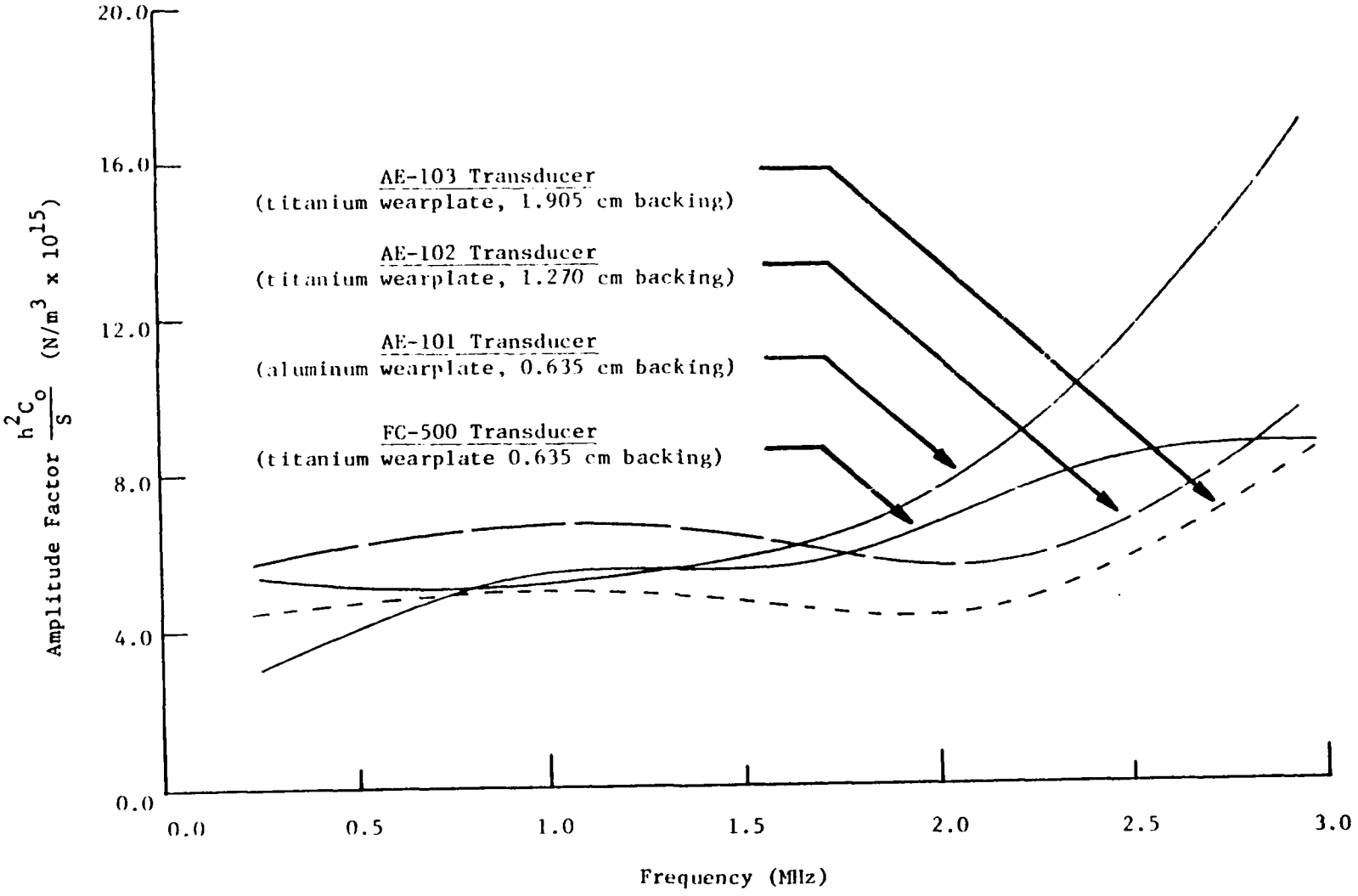

Fig. 12 Plot of amplitude factor h^2C_o/S vs. frequency for FC-500, AE-101, AE-102, AE-103 transducers.

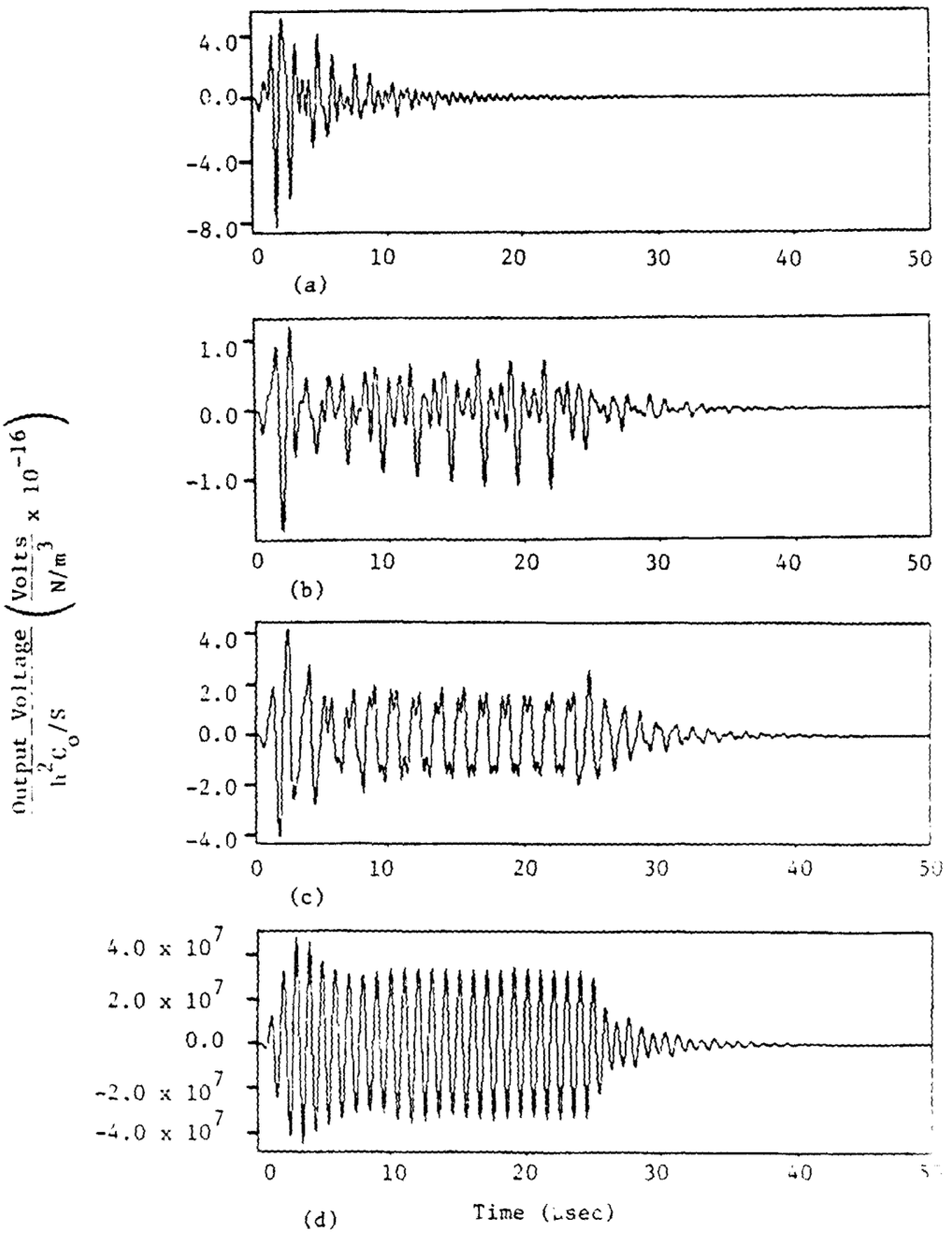

Fig. 13 Predicted output signals corresponding to (a) broadband pulse input, (b) 0.4 MHz tone burst input, (c) 0.6 MHz tone burst input, and (d) 1.0 MHz tone burst input; two AE-100 transducers face-to-face.

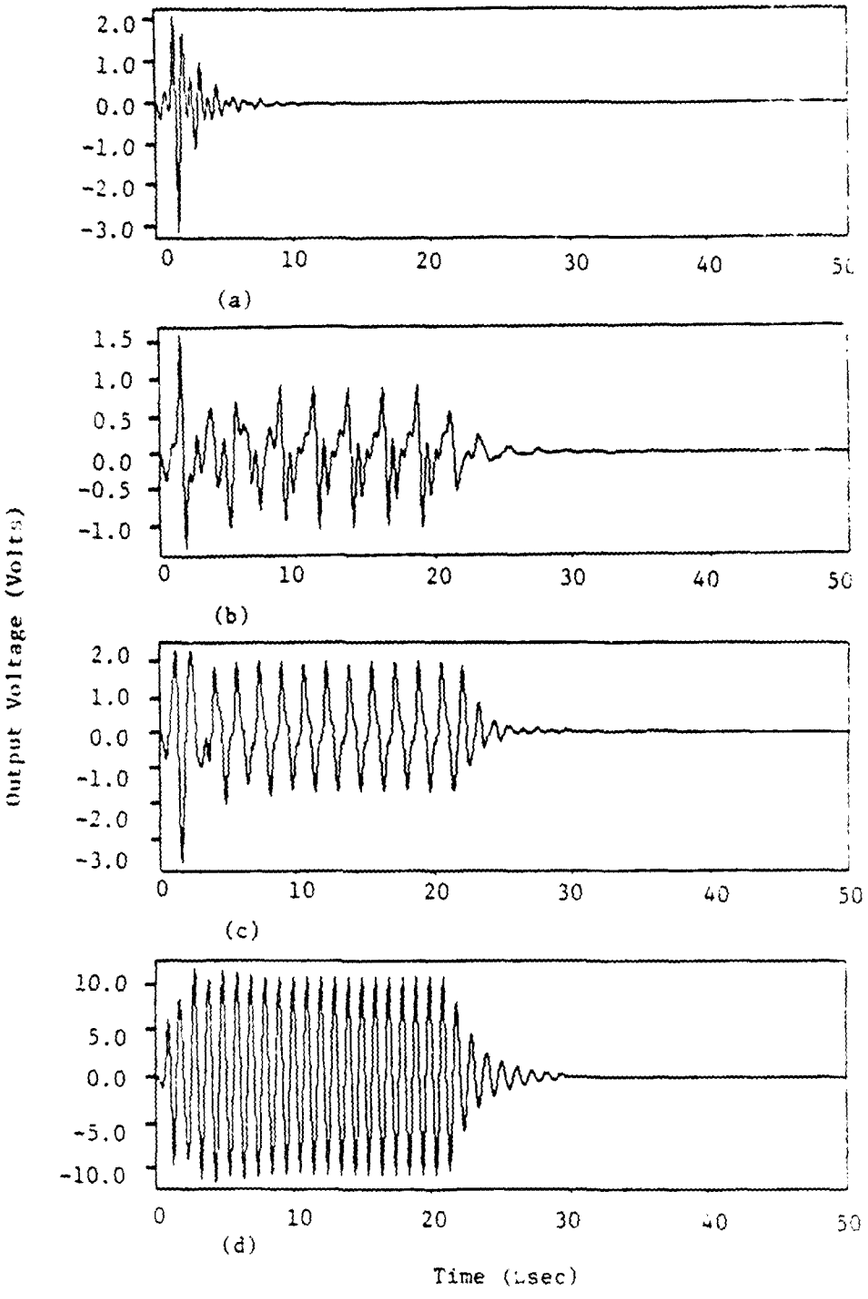

Fig. 14 Measured output signals corresponding to (a) broadband pulse input, (b) 0.4MHz tone burst input, (c) 0.6 MHz tone burst input, and (d) 1.0 MHz tone burst input; two AE-100 transducers face-to-face.

Figure containing prediction	Modeling Parameters					
	Wearplate-piezoelement time delay, β (μsec)	Wearplate piezoelement time delay, δ (μsec)	Backing layer time delay, γ (μsec)	Electrical time constant, RC_o (μsec)	Attenuation parameter, $\alpha_b \left(\frac{\text{nepers}}{\text{cm}}\right)$	Attenuation filtering parameter Λ (dimensionless)
Fig. E5	0	0	0	∞	---	---
Fig. E6	---	0.08	0		---	---
Fig. E7	0.24	0.08	0	---	---	---
Fig. E8	0.24	0.08	0	1	---	---
Fig. E10	0.24	0.08	0	1	1.6	0
Fig. E11	0.24	0.08	---	1	1.6	0
Fig. E12	0.24	0.08	1.40	1	---	---
Fig. E13	0.24	0.08	1.40	1	1.8	0
Fig. E14	0.24	0.08	1.40	1	2.5	0
Fig. G1	0.24	0.08	---	1	---	---
Fig. G2	0.24	0.08	---	1	---	---
Fig. G3	0.24	0.08	---	1	---	---
Fig. I3	0.24	0.08	1.60	1	1.8	0
Fig. I1	0.24	0.08	1.60	1	1.8	0
Fig. I2	0.24	0.08	1.60	1	1.8	---
Fig. I3	0.24	0.08	1.60	1	1.3	0.975

Table 1 Values of the modeling parameters corresponding to each predicted output signal.

Modeling Parameters	Input Signals							
	Pulse	Frequency of Tone Burst Input (MHz)						
		0.4	0.6	1.0	1.5	2.0	2.4	3.0
wearplate-piezoelement time delay, δ(μsec)	0.08 (constant with frequency)							
wearplate-piezoelement time delay, β(μsec)	0.24 (constant with frequency)							
Backing layer time delay γ(μsec)	1.60 (constant with frequency)							
Electrical time constant, RC_o (μsec)	1.0 (constant with frequency)							
Attenuation parameter, α_B(nepers/cm)	--	1.8	2.5	3.5	> 3.5	> 3.5	> 3.5	> 3.5
Measured steady-state output (Volts)	0.625	2.41	4.16	6.45	8.91	9.58	7.19	4.43
Predicted output (Volts/N/m^3 x 10^{-16})	1.14	6.34	8.82	11.78	18.07	14.52	8.83	5.10
Amplitude factor h^2C_o/S (N/m^3 x 10^{15})	5.47	3.80	4.72	5.48	4.92	6.61	8.15	8.69

Table 2 Results of the testing and characterization of the FC-500 transducer.

Modeling Parameters	Input Signals							
	Pulse	Frequency of Tone Burst Input (MHz)						
		0.4	0.6	1.0	1.5	2.0	2.4	3.0
wearplate-piezoelement time delay, δ(μsec)	0.05 (constant with frequency)							
wearplate-piezoelement time delay, β(μsec)	0.125 (constant with frequency)							
Backing layer time delay, γ(μsec)	0.75 (constant with frequency)							
Electrical time constant, RC_o(μsec)	5.0 (constant with frequency)							
Attenuation parameter, α_B(nepers/cm)	--	1.6	2.5	3.6	> 3.6	> 3.6	> 3.6	> 3.6
Measured steady-state output (Volts)	1.084	4.75	5.99	8.44	10.86	12.65	12.65	10.18
Predicted output (Volts/N/m^3 x 10^{-16})	1.459	8.48	11.74	15.91	18.64	16.60	11.71	5.99
Amplitude factor h^2C_o/S (N/m^3 x 10^{15})	7.43	5.61	5.10	5.30	5.83	7.62	10.81	17.00

Table 3 Results of the testing and characterization of the AE-101 transducer

Modeling Parameters	Input Signals							
	Pulse	Frequency of Tone Burst Input (MHz)						
		0.4	0.6	1.0	1.5	2.0	2.4	3.0
wearplate-piezoelement time delay, δ(μsec)	0.06 (constant with frequency)							
wearplate-piezoelement time delay, β(μsec)	0.20 (constant with frequency)							
Backing layer time delay, γ(μsec)	1.50 (constant with frequency)							
Electrical time constant, RC_o(μsec)	5.0 (constant with frequency)							
Attenuation parameter, α_B(nepers/cm)	---	1.6	2.5	> 2.5	> 2.5	> 2.5	> 2.5	> 2.5
Measured steady-state output (Volts)	0.926	4.02	5.86	8.13	9.71	9.01	6.57	4.63
Predicted output (Volts/N/m^3 x 10^{-16})	1.143	6.53	9.17	11.9	15.3	16.5	10.4	4.54
Amplitude factor h^2C_o/S (N/m^3 x 10^{16})	8.10	6.16	6.40	6.85	6.36	6.45	6.29	10.20

Table 4 Results of the testing and characterization of the AE-102 transducer.

Modeling Parameters	Input Signals							
	Pulse	Frequency of Tone Burst Input (MHz)						
		0.4	0.6	1.0	1.5	2.0	2.4	3.0
wearplate-piezoelement time delay, δ(μsec)	0.09 (constant with frequency)							
wearplate-piezoelement time delay, β(μsec)	0.20 (constant with frequency)							
Backing layer time delay, γ(μsec)	(no backing wave was observed for this transducer)							
Electrical time constant, RC_o(μsec)	5.0 (constant with frequency)							
Attenuation parameter, α_B (nepers/cm)	(no backing wave was observed for this transducer)							
Measured steady-state output (Volts)	0.748	3.11	4.54	5.90	7.24	7.04	5.73	4.00
Predicted output (Volts/N/m^3 x 10^{-16})	1.14	6.53	4.17	11.9	15.3	16.5	10.4	4.54
Amplitude factor h^2C_o/S (N/m^3 x 10^{15})	6.54	4.77	4.95	4.98	4.74	4.26	5.49	8.80

Table 5 Results of the testing and characterization of the AE-102 transducer.

Transducer	Modeling Parameters							
	Time Delay δ (μsec)	Time Delay β(μsec)	Time Delay γ(μsec)	Time Constant RC_o (μsec)	Amplitude Factor $\frac{h^2 C_o}{S}\left(\frac{N}{m^3}\right)$*	Backing Attenuation α(nepers/cm)		
						0.4 MHz	0.6 MHz	1.0 MHz
FC-500	0.08	0.24	1.60	1.0	5.11×10^{15}	1.8	2.5	3.5
AE-100	0.09	*(not characterized due to poor correlation between measured and predicted signals)*						
AE-101	0.05	0.125	0.75	5.0	5.89×10^{15}	1.6	2.5	3.6
AE-101	0.08	0.20	1.50	5.0	6.24×10^{15}	1.6	2.5	> 2.5
AE-103	0.09	0.20	†	5.0	4.74×10^{15}	†	†	†

* For frequencies from 0.4 - 1.0 MHz.

† No backing wave observed.

Table 6 Optimum values of the modeling parameters for each transducer.

Transducer	Steady-State Peak-to-Peak Output Amplitude (Volts)						
	0.4 MHz	0.6 MHz	1.0 MHz	1.5 MHz	2.0 MHz	2.4 MHz	3.0 MHz
FC-500	2.41	4.16	6.45	8.91	9.58	7.19	4.43
AE-100	1.50	4.75	19.50	53.50	30.60	20.25	10.14
AE-101	4.75	5.99	8.44	10.86	12.65	12.65	10.18
AE-102	4.02	5.86	8.13	9.71	9.01	6.57	4.63
AE-103	3.11	4.54	5.90	7.24	7.04	5.73	4.00

Table 7 Results of the continuous-wave experiments.

APPENDIX A

BEHAVIOR OF ONE-DIMENSIONAL PLANE COMPRESSIONAL WAVES IN PIEZOELECTRIC AND NONPIEZOELECTRIC MATERIALS

This analysis is patterned after that of Redwood [19]. One-dimensional plane-wave propagation in both piezoelectric and non-piezoelectric materials is investigated; the equations relating stress and voltage in piezoelectric materials are also developed.

A.1 WAVE PROPAGATION IN NONPIEZOELECTRIC MATERIALS

In this section, the one-dimensional, plane compressional wave equation is derived for nonpiezoelectric materials. Consider a uniform elastic bar extending along the x-axis and propagating plane compressional waves as shown in Fig. A1. The momentum equation for a differential element of the bar may be written as follows:

$$S\left\{\left(T + \frac{\partial T}{\partial x}\,dx\right) - T\right\} = \left\{\rho S\,dx\right\}\frac{\partial^2 u}{\partial t^2} \tag{A1}$$

where S is the cross-sectional area of the bar in m^2, ρ is its mass density in kg/m^3, and T and u are the stress in N/m^2 and displacement in m, respectively, in the x-direction. This equation simplifies to

$$\rho\frac{\partial^2 u}{\partial t^2} = \frac{\partial T}{\partial x} \tag{A2}$$

In addition, the relationship between stress and displacement in the bar may be written by Hooke's law:

$$T = E \frac{\partial u}{\partial x} \tag{A3}$$

where E is Young's modulus. Substituting eqn. (A3) into eqn. (A2) then yields the one-dimensional wave equation for plane compressional wave propagation in a nonpiezoelectric material:

$$\frac{\partial^2 u}{\partial t^2} = \frac{E}{\rho} \frac{\partial^2 u}{\partial x^2} \tag{A4}$$

Note that the coefficient E/ρ corresponds to the square of the wavespeed, c, in the bar:

$$c^2 = \frac{E}{\rho} \tag{A5}$$

A.2 WAVE PROPAGATION IN PIEZOELECTRIC MATERIALS

In this section, the equation for wave propagation in piezoelectric materials is derived. The momentum equation (A2) is unaffected by the piezoelectric effect, but the Hooke's law relationship requires an additional term:

$$T = E \frac{\partial u}{\partial x} - hD \tag{A6}$$

This equation shows that the presence of an electric flux D in the x-direction produces a so-called "piezoelectric stress" hD, where h is the piezoelectric constant of the material in V/m. Substituting eqn. (A6) into the momentum equation (A2) yields

$$\frac{\partial^2 u}{\partial t^2} = \frac{E}{\rho} \frac{\partial^2 u}{\partial x^2} - \frac{h}{\rho} \frac{\partial D}{\partial x} \tag{A7}$$

This equation can be simplified by obtaining an alternative expression for D. If there is no free charge in the material,

Gauss' law may be written as follows:

$$\frac{\partial D_x}{\partial x} + \frac{\partial D_y}{\partial y} + \frac{\partial D_z}{\partial z} = 0 \tag{A8}$$

where D_x, D_y, and D_z are the electric flux densities in the x-, y-, and z-directions, respectively. However, the plane-wave assumption (that plane waves remain plane) requires that the x- and y- dimensions of the specimen be much larger than the z-dimension, so that all derivatives with respect to x and y must vanish. Eqn. (A8) then becomes

$$\frac{\partial D}{\partial x} = 0 \tag{A9}$$

and eqn. (A7) reduces to

$$\frac{\partial^2 u}{\partial t^2} = \frac{E}{\rho} \frac{\partial^2 u}{\partial x^2} \tag{A10}$$

which is the one-dimensional plane compressional wave equation for piezoelectric materials. Note that this equation is identical to eqn. (A4), which holds for nonpiezoelectric materials.

A.3 SOLUTION TO THE WAVE EQUATION

In this section, expressions are obtained for stress and displacement which satisfy the wave equation (A10). Operational calculus is used to simplify the mathematics. Recall that the Laplace transform is defined by

$$\{g(t)\} = g'(p) = \int_0^\infty e^{-pt}\, g(t)\, dt \tag{A11}$$

where $g'(p)$ represents the Laplace transform of the time-domain function $g(t)$, and p is the Laplace transform variable. For the

remainder of this analysis, Laplace transforms of quantities will be referred to by the names of the quantities themselves; for example, u' will be referred to as displacement, and so on. It will be understood from the superscript ' that it is actually the Laplace transform of the variable that is being considered, rather than the variable itself.

If the value of the function f(t) is 0 at t=0, it may be easily shown [40] that

$$\left\{\frac{dg(t)}{dt}\right\} = pg'(p) \tag{A12}$$

and consequently that

$$\left\{\frac{d^2g(t)}{dt^2}\right\} = p^2g'(p) \tag{A13}$$

Applying this operation to eqn. (A10) yields the transformed one-dimensional plane-wave equation:

$$\frac{\partial^2 u'}{\partial x^2} = \frac{p^2}{E/\rho}\, u' \tag{A14}$$

where u' is the Laplace transform of u(t).

The solution to eqn. (A14) can be written as the sum of two exponentials:

$$u' = A \exp\left(\frac{-px}{c}\right) + B \exp\left(\frac{px}{c}\right) \tag{A15}$$

where c is the wavespeed from eqn. (A5), and p is the Laplace transform variable. The first term of u' represents a wave traveling in the positive x-direction, and the second a wave in the negative x-direction; A and B are amplitude factors that are

evaluated from the boundary conditions. Substituting eqn. (A15) into eqn. (A3) gives the corresponding solution in terms of stress waves:

$$T' = E \frac{p}{c} \left\{ -A \exp\left(\frac{-px}{c}\right) + B \exp\left(\frac{px}{c}\right) \right\} \tag{A16}$$

where T' is stress in the x-direction. Substituting $\rho c^2 = E$ gives the following:

$$T' = \rho c \, p \left\{ -A \exp\left(\frac{-px}{c}\right) + B \exp\left(\frac{px}{c}\right) \right\} \tag{A17}$$

The coefficient ρc is seen to be the ratio of stress to particle velocity in the material, and is called the "characteristic impedance", Z:

$$Z = \rho c \tag{A18}$$

Eqn. (A17) may now be written in terms of Z:

$$T' = pZ \left\{ -A \exp\left(\frac{-px}{c}\right) + B \exp\left(\frac{px}{x}\right) \right\} \tag{A19}$$

This is the equation for stress in the x-direction of a nonpiezoelectric material which satisfies the one-dimensional, plane compressional wave equation.

A.4 WAVE INTERACTION AT IMPEDANCE-MISMATCHED INTERFACES

In this section, the amplitudes of the waves which are produced when a stress wave strikes an interface between two materials of different characteristic impedance are found. Consider the interface between two layers of nonpiezoelectric material with impedances Z_1 and Z_2, as shown in Fig. A2. The

right-traveling displacement wave with amplitude A_1 strikes the interface, and produces a reflected wave, B_1, and a transmitted wave, A_2. The boundary conditions require that displacement and stress be continuous across the boundary:

$$u_1'\Big|_{x=0} = u_2'\Big|_{x=0}$$

$$T_1'\Big|_{x=0} = T_2'\Big|_{x=0} \tag{A20}$$

where the subscripts 1 and 2 refer to layers 1 and 2, respectively. Substituting eqn. (A15) into the displacement boundary condition gives

$$A_1 + B_1 = A_2 + B_2 \tag{A21}$$

and substituting eqn. (A19) into the stress condition gives

$$pZ_1\left(-A_1 + B_1\right) = pZ_2\left(-A_2 + B_2\right) \tag{A22}$$

If the analysis is restricted to values of time less than that required for wave A_2 to reach the far end of layer 2, wave B_2 will never show up and it may be struck from eqns. (A21) and (A22). Then, from eqn. (A22):

$$A_2 = -\frac{Z_1}{Z_2}\left(-A_1 + B_1\right) \tag{A23}$$

and from eqn. (A21):

$$B_1 = A_2 - A_1 \tag{A24}$$

Substituting eqn. (A24) into eqn. (A23) gives

$$A_2 = -\frac{Z_1}{Z_2}\left(A_2 - 2A_1\right) \tag{A25}$$

which simplifies to

$$\frac{A_2}{A_1} = \frac{2Z_1}{Z_1 + Z_2} \tag{A26}$$

This equation gives the amplitude of the reflected displacement wave in terms of the amplitude of the incident wave and the impedances of the two layers. The amplitude of the transmitted wave, B_1, can also be found:

$$\frac{B_1}{A_1} = \frac{Z_1 - Z_2}{Z_1 + Z_2} \tag{A27}$$

Eqns. (A26) and (A27) may be written in terms of stress by comparing eqns. (A15) and (A19). These show that the relationship between stress T' and displacement u' is expressed by

$$T' = pZu' \tag{A28}$$

for a right-traveling wave, and

$$T' = -pZu' \tag{A29}$$

for a left-traveling wave. If T'_i, T'_r and T'_{tr} represent the amplitudes of the incident, reflected, and transmitted stress waves, respectively, then these amplitudes are related to the corresponding displacement amplitudes A_1, B_1, and A_2 by:

$$\begin{aligned} T'_i &= pZ_1A_1 \\ T'_r &= -pZ_1B_1 \\ T'_{tr} &= pZ_2A_2 \end{aligned} \tag{A30}$$

AD-A128 965 CHARACTERIZATION OF ULTRASONIC TRANSDUCER THROUGH TRANSMISSION SYSTEMS(U) WEA CAMBRIDGE MA J C BLOUGH ET AL. DEC 82 N00014-81-C-2319

23

UNCLASSIFIED F/G 20/3 NL

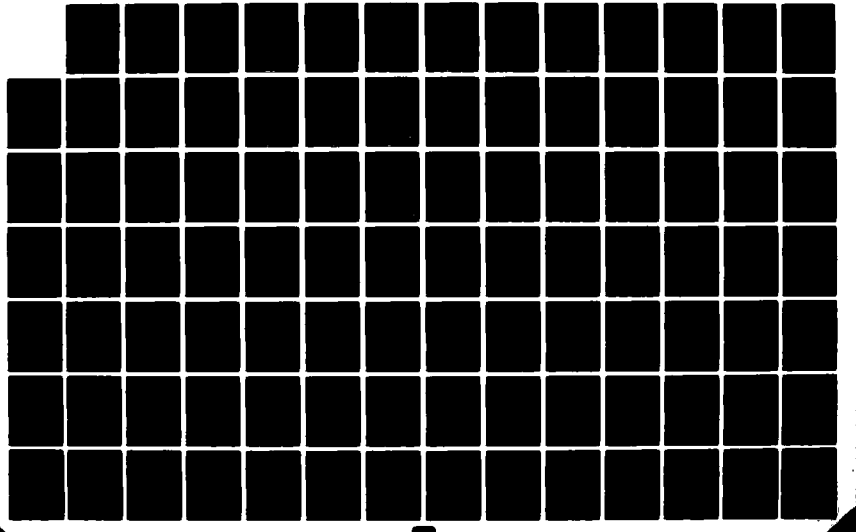

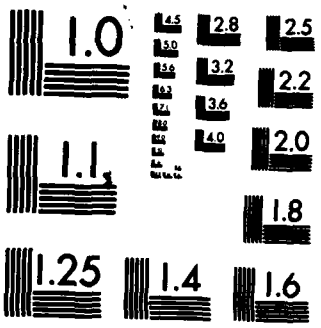

MICROCOPY RESOLUTION TEST CHART
NATIONAL BUREAU OF STANDARDS-1963-A

Making the appropriate substitutions of eqns. (A30) into eqns. (A26) and (A27) gives the following:

$$\frac{T'_r}{T'_i} = \frac{Z_2 - Z_1}{Z_1 + Z_2} \qquad \frac{T'_{tr}}{T'_i} = \frac{2Z_2}{Z_1 + Z_2} \tag{A31}$$

These equations give the amplitudes of the reflected (T'_r) and transmitted (T'_{tr}) stress waves which are produced when a stress wave of amplitude T'_i traveling in a medium with impedance Z_1 strikes another medium with impedance Z_2. Although the equations are given in terms of the Laplace transforms of the amplitudes, they hold for the time-domain amplitudes as well. Since the waves differ only by an amplitude factor, their time-dependent parts will be identical, and will cancel out of the numerator and denominator of eqns. (A31).

A.5 RELATIONSHIP BETWEEN ELECTRICAL AND MECHANICAL QUANTITIES IN A PIEZOELECTRIC PLATE

In this section, the fundamental equation relating displacement and voltage in piezoelectric materials is derived. The piezoelectric plate under consideration, henceforth referred to as the piezoelement, is depicted in Fig. A3.

To obtain a relation between stress and electric flux in the piezoelement, substitute eqn. (A15) into the Laplace transform of eqn. (A6):

$$T' + hD' = E\frac{p}{c}\left\{-A \exp\left(\frac{-px}{c}\right) + B \exp\left(\frac{px}{c}\right)\right\} \tag{A32}$$

The flux density D' in the transducer is a constant function of x, as shown in eqn. (A9), and is related to the charge Q' by Gauss' law:

$$D' = \frac{Q'}{S} \tag{A33}$$

where S represents the surface area of the plate. Substituting eqn. (A33) into eqn. (A32) gives the following general equation for stress in the piezoelement:

$$T' + \frac{hQ'}{S} = pZ\left\{-A\ epx\left(\frac{-px}{c}\right) + B\ exp\left(\frac{px}{c}\right)\right\} \tag{A34}$$

where, as in eqn. (A18), Z= c.

To determine the voltage across the piezoelement, the following fundamental equation must be used:

$$\frac{\partial \phi'(x,p)}{\partial x} = -h\frac{\partial u'}{\partial x} + \frac{D'}{\varepsilon} \tag{A35}$$

where $\phi'(x,p)$ is the local potential in the piezoelement, and ε is the absolute permittivity of the piezoelectric material in farads/m. To solve for V', the total voltage across the piezoelement, eqn. (A35) must be integrated along the x-axis from Ø to L (see Fig. A3):

$$V' = \int_o^L \frac{\partial \phi'(x,p)}{\partial x}\,dx = -hu'\Big|_{x=0}^{x=L} + \frac{D'L}{\varepsilon} \tag{A36}$$

The second term in eqn. (A36) can be simplified by realizing that Gauss' law can again be used to determine the capacitance C_o of the unstressed piezoelement:

$$C_o = \frac{\varepsilon S}{L} \tag{A37}$$

Substituting eqns. (A37) and (A33) into eqn. (A36) gives the

transducer voltage in terms of charge:

$$V' = -hu'\Big|_{x=0}^{x=L} + \frac{Q'}{C_o} \tag{A38}$$

This is the fundamental equation relating the quantities of displacement, voltage and charge in a piezoelectric transducer.

A.6 ELECTRICAL RESPONSE OF A PIEZOELECTRIC TRANSDUCER TO AN INCIDENT STRESS WAVE

In this section, a step input of stress is applied to a piezoelectric transducer and the resulting voltage is found. Consider a piezoelement and wearplate bonded together as in Fig. A4. A_1 is the displacement associated with the incident wave in the wearplate, and B_1 and A are the amplitudes of the reflected and transmitted displacement waves, respectively, which are produced when wave A_1 strikes the interface between the layers. Eqn. (A20) gives the boundary conditions at x=0:

$$u_1'\Big|_{x=0} = u_2'\Big|_{x=0}$$

$$T_1'\Big|_{x=0} = T_2'\Big|_{x=0} \tag{A39}$$

where quantities without subscripts refer to the transducer, and those subscripted 1 refer to the wearplate. Substituting eqns. (A15) and (A34), the boundary conditions (A39) become

$$A_1 + B_1 = A + B$$

$$pZ_1(-A_1 + B_1) = pZ(-A + B) - \frac{hQ'}{S} \tag{A40}$$

If the analysis is restricted to values of time less than that required for wave A to reach the far side of the transducer, wave

B may be ignored. Eqns. (A40) then become

$$A_1 + B_1 = A \tag{A41}$$

and

$$pZ_1(-A_1 + B_1) = -pZA - \frac{hQ'}{S} \tag{A42}$$

and solving eqn. (A41) for B_1 and substituting into eqn. (A42) then gives

$$-2A_1pZ_1 + A\,Z_1 = -A\,Z - \frac{hQ'}{S} \tag{A43}$$

This equation relates mechanical quantities A_1 and A to the charge Q' on the piezoelement. If a resistance R is connected across the piezoelement, the voltage V'_{out} may be expressed as

$$V'_{out} = I'R = -pQ'R \tag{A44}$$

where I' represents the current in amperes through the resistance R, Q' is the charge on the transducer in coulombs, and p is the Laplace transform variable. Substituting eqn. (A44) into eqn. (A43) and collecting terms yields:

$$Ap(Z_1 + Z) = \frac{hV'_{out}}{pRS} + 2A_1pZ_1 \tag{A45}$$

or, solving for A:

$$A = \left\{\frac{hV'_{out}}{pRS} + 2pZ_1A_1\right\}\left\{p(Z_1 + Z)\right\}^{-1} \tag{A46}$$

This equation relates the amplitude of the displacement wave A and the voltage V'_{out} produced in the piezoelement to the amplitude of the incident displacement wave, A_1.

Eqn. (A38), reproduced here, gives the voltage across the plate in terms of the displacements at its faces:

$$V'_{out} = -hu'\Big|_{x=0}^{x=L} + \frac{Q'}{C_o} \tag{A47}$$

Substituting eqns. (A15) and (A39), the voltage becomes

$$V'_{out} = -h\left\{A \exp\left(\frac{-pL}{c}\right) - 1\right\} - \frac{V'_{out}}{pRC_o} \tag{A48}$$

Note that L/c is the "transit time" of the transducer, the time required for a wave to pass through it. Denoting this transit time by λ, eqn. (A48) becomes

$$V'_{out} = -hA\left\{\exp\left(-p\lambda\right) - 1\right\} - \frac{V'_{out}}{pRC_o} \tag{A49}$$

and substituting eqn. (A46) gives

$$V'_{out} = \frac{-h}{p(Z_1 + Z)}\left\{\frac{hV'_{out}}{pRS} + 2pZ_1A_1\right\}\left\{\exp\left(-p\lambda\right) - 1\right\} - \frac{V'_{out}}{pRC_o} \tag{A50}$$

Solving for V'_{out} gives the final result:

$$V'_{out} = 2hA_1\left\{\frac{Z_1}{Z_1 + Z}\right\}\left\{\frac{p^2\{1 - \exp(-p\lambda)\}}{p^2 + \frac{p}{RC_o} - \frac{h^2\{1 - \exp(-p\lambda)\}}{RS(Z_1 + Z)}}\right\} \tag{A51}$$

V'_{out} here is the voltage generated across the piezoelement when a displacement wave of amplitude A_1 enters it from an adjacent wearplate of impedance Z_1. R is the resistance across the piezoelement, and h, Z, C_o and S are the piezoelectric constant, characteristic impedance, clamped capacitance and surface area of the transducer, respectively.

Eqn. (A51) may be cast in terms of stress, if desired. If T_i represents the amplitude of the incident step function of stress in the wearplate, the Laplace transform of the step [40] is T_i/p, so that the stress in the wearplate is expressed by

$$\frac{T_i}{p} = -pZ_1A_1, \tag{A52}$$

Solving for A_1 in terms of T_i gives

$$A_1 = \frac{-T_i}{p^2Z_1} \tag{A53}$$

Substituting this value for A_1 into eqn. (A51) results in

$$V'_{out} = \frac{-2hT_i}{(Z_1 + Z)} \left\{ \frac{\{1 - \exp(-p\lambda)\}}{p^2 + \frac{p}{RC_o} - \frac{h^2\{1 - \exp(-p\lambda)\}}{RS(Z_1 + Z)}} \right\} \tag{A54}$$

which gives V'_{out} in terms of the amplitude T_i of a step function of stress in the wearplate.

Examination of eqn. (A54) shows that the factor $\exp(-p\lambda)$ appears twice. This factor represents a time delay [40] equal to λ, so that the terms which it multiplies do not show up at the same time as the rest of the terms in eqn. (A54). Since the analysis was restricted to values of time less than the transit time of the piezoelement, these time delay terms must be struck from the equation. Taking only those terms which show up immediately:

$$V'_{out} = \frac{-2hT_i}{(Z_1 + Z)} \left\{ p^2 + \frac{p}{RC_o} - \frac{h^2}{RS(Z_1 + Z)} \right\}^{-1} \tag{A55}$$

The denominator of eqn. (A55) may be written as $(p+1/\tau_1)(p+1/\tau_2)$,

where

$$\frac{1}{\tau_1}, \frac{1}{\tau_2} = \left(\frac{1}{2RC_o}\right) \pm \left\{\left(\frac{1}{2RC_o}\right)^2 + \left(\frac{h^2}{RS(Z_1 + Z)}\right)\right\}^{\frac{1}{2}} \tag{A56}$$

The inverse Laplace transform is then easily found in terms of the time constants τ_1 and τ_2:

$$V_{out}(t) = \frac{-2hT_i}{(Z_1 + Z)} \left\{\frac{\exp\left(-\frac{t}{\tau_1}\right) - \exp\left(-\frac{t}{\tau_2}\right)}{\frac{1}{\tau_2} - \frac{1}{\tau_1}}\right\} \tag{A57}$$

This equation gives the time-dependent output voltage which is produced across the piezoelement by a step input T_i of stress from the adjacent wearplate. The impedances of the wearplate and piezoelement are Z_1 and Z, respectively, and h is the piezoelectric constant.

A.7 MECHANICAL RESPONSE OF A PIEZOELECTRIC TRANSDUCER TO AN INPUT VOLTAGE

In this section, the equations are developed which give the time-dependent amplitudes of the stress waves produced by a step input of voltage to a piezoelectric transducer. Consider a piezoelement bonded to a wearplate on one face and a backing layer on the other face as seen in Fig. A5. As shown in the drawing, wave B_1 propagates into the wearplate, wave A_2 propagates into the backing, and waves A and B are the right- and left-traveling waves generated inside the piezoelement itself. The impedances of the wearplate, backing, and piezoelement are designated Z_1, Z_2, and Z, respectively.

The boundary conditions at the front face of the piezoelement

are given in eqn. (A41):

$$B_1 = A + B$$

$$pZ_1 B = pZ(-A + B) - \frac{hQ'}{S} \tag{A58}$$

The boundary conditions at the back face are obtained by evaluating eqns. (A15) and (A34) at x=L and equating stresses and displacements in the two layers:

$$A_2 = A \exp(-p\lambda) + B \exp(p\lambda)$$

$$pZ\left\{-A \exp(-p\lambda) + B \exp(p\lambda)\right\} - \frac{hQ'}{S} = -pZ_2 A_2 \tag{A59}$$

Here, as in section A.6, λ represents the transit time of the piezoelement, L/c. Combining eqns. (A58) gives

$$\frac{hQ'}{S} = -p\left\{A(Z_1 + Z) + B(Z_1 - Z)\right\} \tag{A60}$$

and eqns. (A59) combine to

$$\frac{hQ'}{S} = p\left\{A(-Z_1 + Z_2) \exp(-p\lambda) + B(Z + Z_2) \exp(p\lambda)\right\} \tag{A61}$$

In order to reduce the amount of algebra in the derivation, the following substitutions will be made:

$$m = \exp(-p\lambda) \; ; \quad n = \exp(p\lambda) \tag{A62}$$

so that eqn. (A61) becomes

$$\frac{hQ'}{S} = p\left\{A\,m(-Z_1 + Z_2) + B\,n(Z + Z_2)\right\} \tag{A63}$$

Eliminating hQ' from eqns. (A60) and (A63) then yields

$$A\left\{m(Z - Z_2) - (Z_1 + Z)\right\} = B\left\{n(Z + Z_2) + (Z_1 - Z)\right\} \tag{A64}$$

This gives the relationship between the amplitudes of the two displacement waves produced inside the transducer.

The voltage across the transducer is introduced by recalling eqn. (A38):

$$V' = -hu'\Big|_{x=0}^{x=L} + \frac{Q'}{C_o} \tag{A65}$$

Evaluating eqn. (A15) at x=L and substituting gives

$$\frac{V_o}{p} = -h\left\{Am + Bn - (A + B)\right\} + \frac{Q'}{C_o} \tag{A66}$$

Here, the input voltage has been taken to be a step of amplitude V_o, so that $V'=V_o/p$. Multiplying through by hC_o/S and collecting terms gives

$$\frac{h\,C_o\,V_o}{Sp} = -\frac{h^2 C_o}{S}\left\{A(m - 1) + B(n - 1)\right\} + \frac{hQ'}{S} \tag{A67}$$

Eliminating hQ' from eqns. (A60) and (A67) then gives

$$\frac{h\,C_o\,V_o}{Sp} = A\left\{\frac{h^2 C_o}{S}(1 - m) - p(Z_1 + Z)\right\} + B\left\{\frac{h^2 C_o}{S}(1 - n) + p(Z - Z_1)\right\} \tag{A68}$$

Solving eqn. (A64) for A and inserting into eqn. (A68):

$$\frac{h\,C_o\,V_o}{Sp} = \frac{B}{\{m(Z - Z_2) - (Z_1 + Z)\}} \left\{\left\{n(Z + Z_2) + (Z_1 - Z)\right\}\left\{\frac{h^2 C_o}{S}(1 - m) - p(Z_1 + Z)\right\} + \left\{m(Z - Z_2) - (Z_1 + Z)\right\}\left\{\frac{h^2 C_o}{S}(1 - n) + p(Z - Z_1)\right\}\right\} \tag{A69}$$

Combining terms then results in

$$\frac{hC_oV_o}{Sp} = \frac{B}{\left\{m(Z - Z_2) - (Z_1 + Z)\right\}}$$

$$\left\{\frac{h^2C_o}{S}\left\{Z_1(n - m) + 2Z(m + n - 2) + Z_2(n - m)\right\}\right.$$

$$\left. + p\left\{m(Z - Z_2)(Z - Z_1) - n(Z + Z_2)(Z_1 + Z)\right\}\right\} \qquad \text{(A70)}$$

or, solving for B:

$$B = \frac{hC_oV_o}{S}\frac{\left\{m(Z - Z_2) - (Z_1 + Z)\right\}}{\{CD\}} \qquad \text{(A71)}$$

where

$$\{CD\} = p\left\{(Z + Z_2)(Z_1 + Z) - (Z - Z_2)(Z - Z_1)\exp(-2p\lambda)\right\}$$

$$+ \frac{h^2C_o}{S}\left\{(Z_1 + Z_2)\exp(-2p\lambda) - 1 - 2Z\left\{\exp(-2p\lambda) - 2\exp(-p\lambda) + 1\right\}\right\} \qquad \text{(A72)}$$

Eqn. (A71) gives the amplitude of the left-traveling displacement wave produced in the transducer by a step input of voltage, V_o. Similarly, solving eqn. (A64) for B and substituting into eqn. (A68) gives the amplitude of the right-traveling wave:

$$A = \frac{hC_oV_o}{S}\frac{\left\{n(Z + Z_2) + (Z_1 - Z)\right\}}{\{CD\}} \qquad \text{(A73)}$$

Now, since $u'(0,p)=A+B$:

$$u'\Big|_{x = 0} = \frac{hC_oV_o}{S}\frac{\left\{Z(m + n - 2) + Z_2(n - m)\right\}}{\{CD\}} \qquad \text{(A74)}$$

Eqn. (A74) gives the displacement at the front face of the transducer due to a step input of voltage. It may be expanded by noting from eqns. (A62) that $mn=1$ and that $\frac{m}{n} = \exp(-2p\lambda)$. Multiplying by m/m and making these substitutions:

$$u'\Big|_{x=0} = \frac{\frac{hC_oV_o}{S}\left\{Z\left\{\exp(-2p\lambda) - 2\exp(-p\lambda) - 1\right\} + Z_2\left\{1 - \exp(-2p\lambda)\right\}\right\}}{p\{CD\}} \tag{A75}$$

Eqn. (A75) is similar to eqn. (A54) in that several of the terms are delayed in time, some by λ and some by 2λ. These delays arise from the propagation of waves A and B through the piezoelement. After a delay of λ, wave B has reached the front face of the piezoelement and will affect the displacement there. After a delay of 2λ, wave A will have been partially reflected from the rear face and will have returned to the front face, where it too will affect the displacement. At this point, however, only the waves actually produced at the surfaces of the transducer by the applied voltage are of interest. The effects of waves propagating through the system will be considered later. Therefore, taking only the part of eqn. (A75) which shows no delay, and substituting for {CD} from eqn. (A72) gives:

$$u'\Big|_{x=0} = \frac{hC_oV_o}{S}(Z + Z_2)\left\{p^2\left\{(Z_1 + Z)(Z + Z_2)\right\} - \frac{ph^2C_o}{S}\left\{Z_1 + 2Z + Z_2\right\}\right\}^{-1} \tag{A76}$$

Dividing by $(Z_1+Z)(Z+Z_2)$ above and below:

$$u'\Big|_{x=0} = \frac{hC_oV_o}{S(Z_1 + Z)}\left\{p^2 - \frac{ph^2C_o}{S}\left\{\frac{(Z_1 + Z) + (Z + Z_2)}{(Z_1 + Z)(Z + Z_2)}\right\}\right\}^{-1} \tag{A77}$$

This gives the displacement at the front face of a piezoelectric transducer due to a step voltage input of amplitude V_o. The corresponding displacement at the back face may be obtained by analogy. If the backing and wearplate are exchanged with one

another, the front face then becomes the back face and vice-versa. Therefore, interchanging Z_1 and Z_2 in eqn. (A77):

$$u'\Big|_{x=L} = \frac{hC_oV_o}{S(Z+Z_2)}\left\{p^2 - \frac{ph^2C_o}{S}\left\{\frac{(Z_1+Z)+(Z+Z_2)}{(Z_1+Z)(Z+Z_2)}\right\}\right\}^{-1} \tag{A78}$$

This equation then gives the displacement at the rear face of the transducer caused by a step input of voltage. Note that a sign change occurs when the surfaces of the transducer are reversed, because the direction of +x is effectively reversed as well.

A time constant, τ, may be extracted from the denominator of eqns. (A77) and (A78):

$$\frac{1}{\tau} = h^2C_o\left\{\frac{(Z_1+Z)+(Z+Z_2)}{(Z_1+Z)(Z+Z_2)}\right\} \tag{A79}$$

so that eqns. (A77) and (A78) become, respectively:

$$u'\Big|_{x=0} = \frac{\dfrac{hC_oV_o}{S(Z_1+Z)}}{p^2 - p/\tau}$$

$$u'\Big|_{x=L} = \frac{\dfrac{hC_oV_o}{S(Z+Z_2)}}{p^2 - p/\tau} \tag{A80}$$

These equations show that applying a voltage across the piezoelement produces a displacement at each of its faces. These displacements then cause four stress waves to be propagated, one in each direction from each face. The amplitudes of these waves are obtained from the stress-displacement relationships of eqns. (A28) and (A29). If T_1L' and T_2R' represent the amplitudes

of the stress waves produced in the wearplate and backing, respectively, and if TR' and TL' represent the right- and left-traveling waves in the transducer, then:

$$TL_1' = -pZ_1 u'\Big|_{x=0} = -\frac{hC_o V_o}{S}\left\{\frac{Z_1}{Z_1 + Z_2}\right\}\left\{\frac{1}{p^2 - p/\tau}\right\}$$

$$TR' = pZ\, u'\Big|_{x=0} = \frac{hC_o V_o}{S}\left\{\frac{Z}{Z_1 + Z}\right\}\left\{\frac{1}{p^2 - p/\tau}\right\}$$

$$TL' = -pZ\, u'\Big|_{x=L} = \frac{hC_o V_o}{S}\left\{\frac{Z}{Z + Z_2}\right\}\left\{\frac{1}{p^2 - p/\tau}\right\}$$

$$TR_2' = pZ_2 u'\Big|_{x=L} = -\frac{hC_o V_o}{S}\left\{\frac{Z_2}{Z + Z_2}\right\}\left\{\frac{1}{p^2 - p/\tau}\right\} \qquad \text{(A81)}$$

Finally, taking the inverse transform of each:

$$TL_1(t) = \frac{-hC_o V_o}{S}\left\{\frac{Z_1}{Z_1 + Z}\right\} \exp\,(t/\tau)$$

$$TR(t) = \frac{hC_o V_o}{S}\left\{\frac{Z}{Z_1 + Z}\right\} \exp\,(t/\tau)$$

$$TL(t) = \frac{hC_o V_o}{S}\left\{\frac{Z}{Z + Z_2}\right\} \exp\,(t/\tau)$$

$$TR_2(t) = \frac{-hC_o V_o}{S}\left\{\frac{Z_2}{Z + Z_2}\right\} \exp\,(t/\tau) \qquad \text{(A82)}$$

These equations give the time-dependent amplitudes of the four stress waves produced by a step input of voltage to a piezoelectric transducer. The value of the time constant τ is found from eqn. (A79).

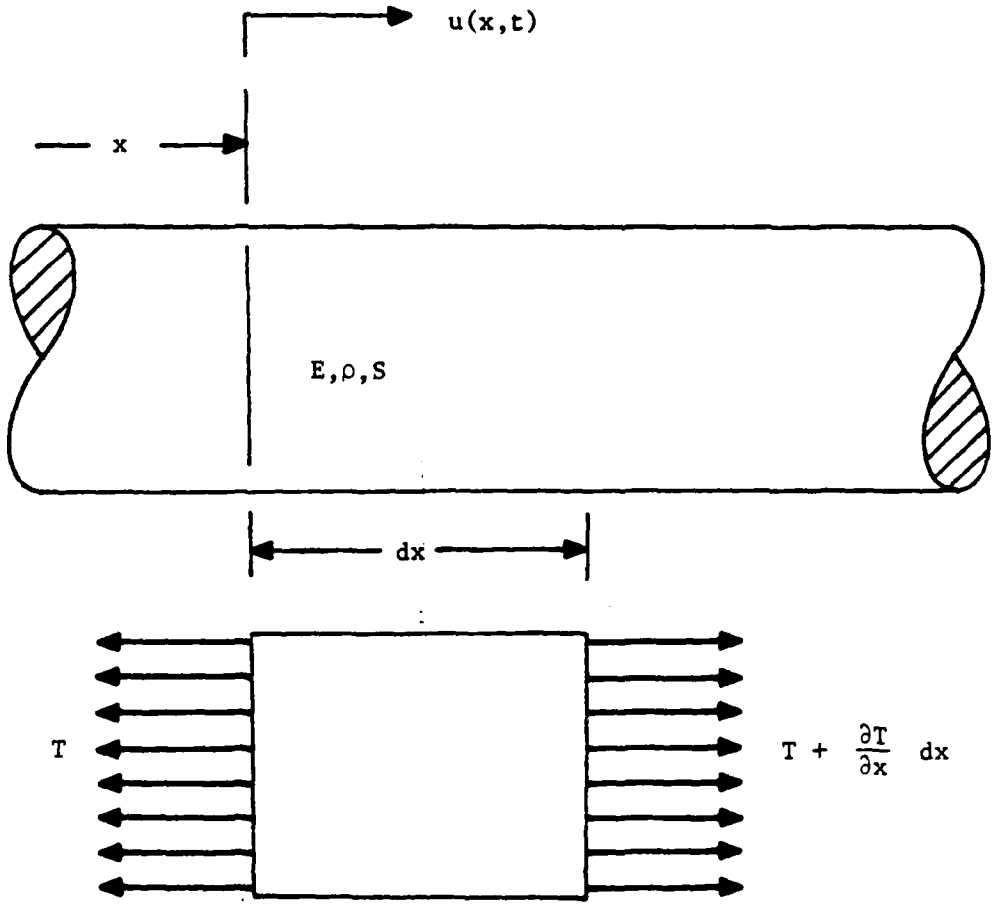

Fig. A1 Elastic bar supporting longitudinal wave propagation in the x-direction.

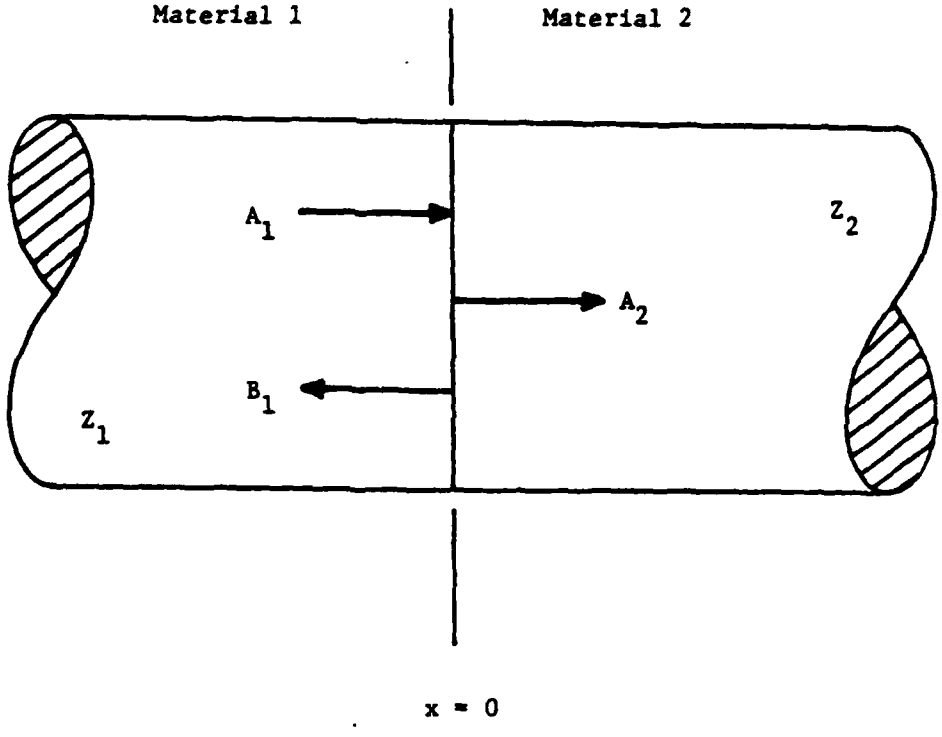

Fig. A2 The production of reflected and transmitted waves at the interface between two materials of different characteristic impedance.

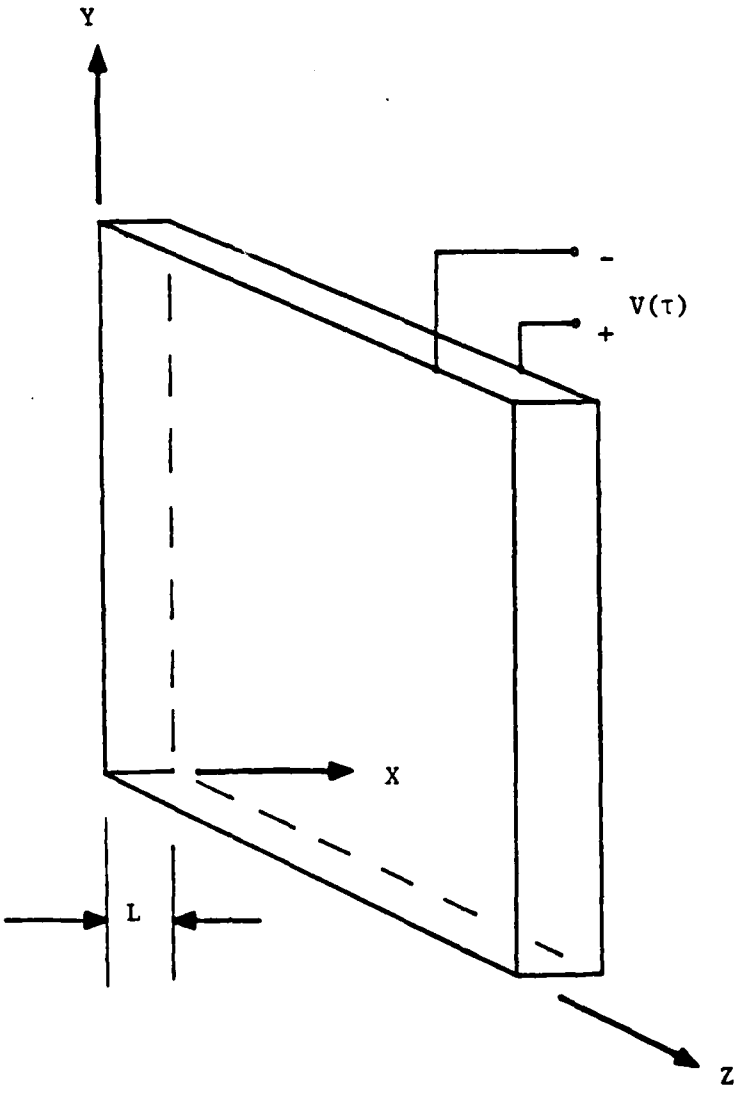

Fig. A3 Sketch of piezoelectric plate perpendicular to the x-axis.

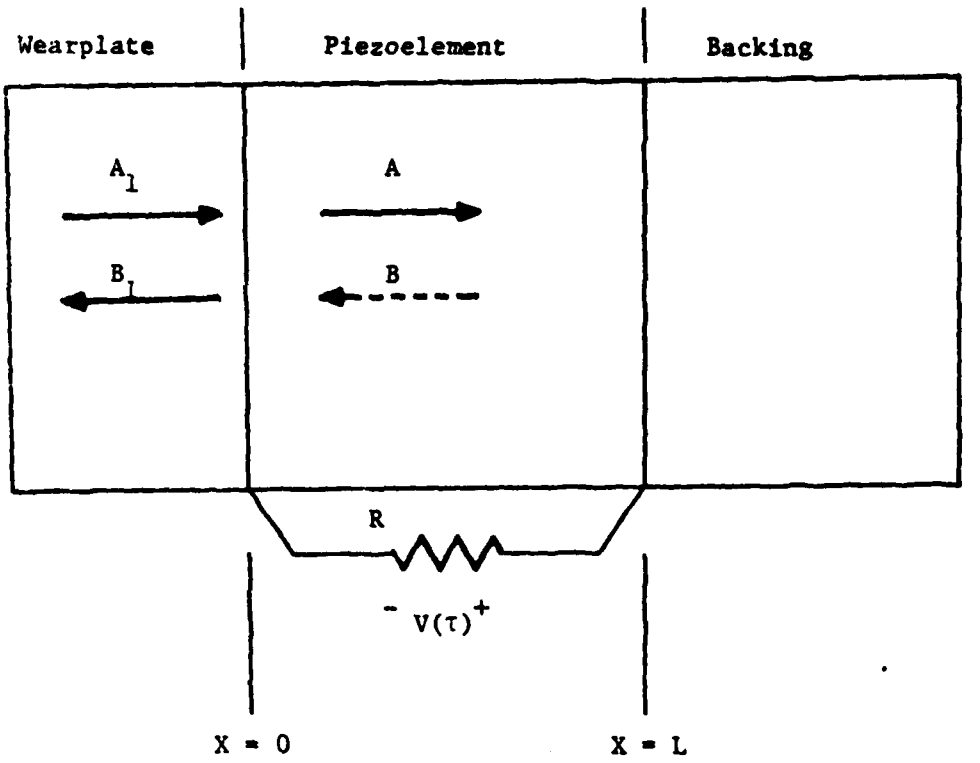

Fig. A4 Multilayer piezoelectric transducer used to detect ultrasonic stress waves

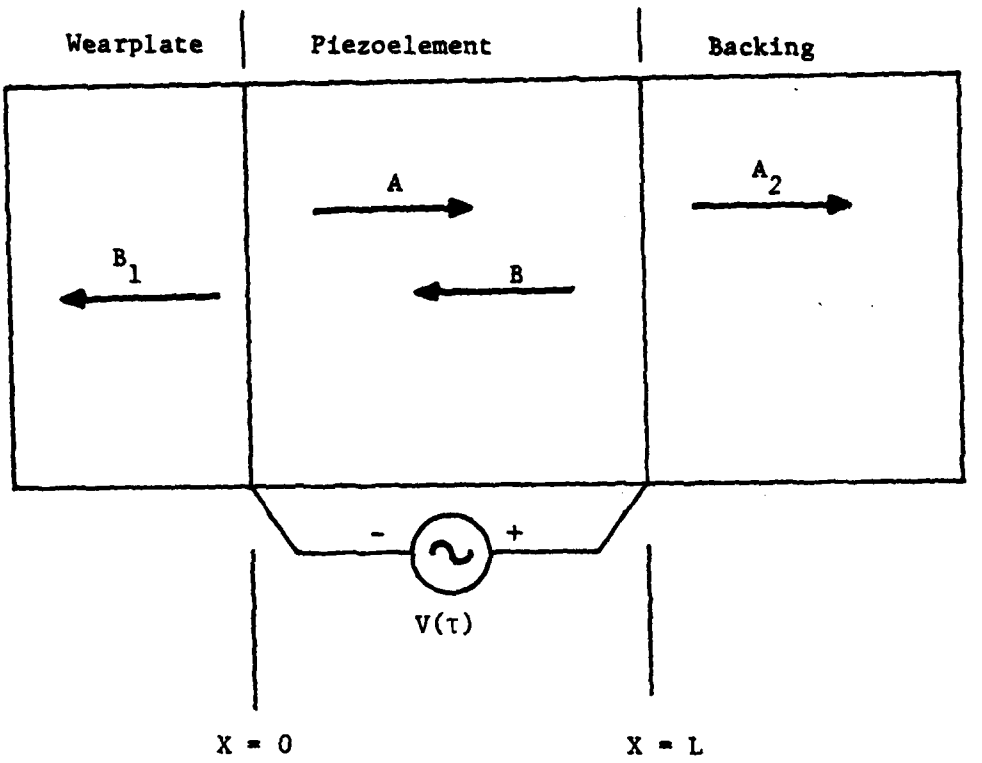

Fig. A5 Multilayer piezoelectric transducer used to generate ultrasonic stress waves.

APPENDIX B

COMPUTER IMPLEMENTATION OF THE WAVE PROPAGATION MODEL

ATTACHMENT B1

LISTING OF THE BASIC MODELING PROGRAM

```
 1:*DIM B1R(850),B1L(850),B2R(850),B2L(850)
 2: DIM P1R(275),P1L(275),P2R(275),P2L(275)
 3: DIM W1R(75),W1L(75),W2R(75),W2L(75)
 4: DIM S1R(250),S1L(250),S2R(125),S2L(125)
 5: DIM S3R(125),S3L(125),VIN(4000),VOUT(4000)
 6:
 7: ' INPUT DATA
 8:
 9: CP=274000
10: ZP=1800000
11: CB=173000
12: ZU=160000
13:
14: ' INTERACTIVE INPUT
15:
16: 1 PRINT "ENTER INPUT DATA (PRESS RETURN FOR DEFAULT VALUE)"
17: PRINT "*****************************************************"
18: PRINT " "
19: PRINT "DATA FOR BACKING LAYERS:"
20: PRINT "-------------------------"
21: INPUT"BACKING THICKNESS OF INPUT TRANSDUCER IN CM (DEF=0): ",LB1
22: INPUT"BACKING THICKNESS OF OUTPUT TRANSDUCER IN CM (DEF=0): ",LB2
23: INPUT"IMPEDANCE OF BACKING LAYERS IN GM/CM2/SEC (DEF=1.8E06): ",ZB
24: IF ZB=0 THEN ZB=1.8E06
25: INPUT"ATTENUATION OF BACKING LAYERS, ALPHA (DEF=1.6): ",ALPHA
26: IF ALPHA=0 THEN ALPHA=1.6
27: INPUT"FREQUENCY FILTERING PARAMETER, DELTA (DEF=0): ",DELTA
28: PRINT " "
29: PRINT "DATA FOR WEARPLATES:"
30: PRINT "--------------------"
31: INPUT"WEARPLATE THICKNESS OF TRANSDUCERS IN CM (DEF=0.035): ",LW
32: IF LW=0 THEN LW=0.035
33: INPUT"WEARPLATE WAVESPEED OF INPUT IN CM/SEC (DEF=8.64E05): ",CW1
34: IF CW1=0 THEN CW1=8.64E05
35: INPUT"WEARPLATE WAVESPEED OF OUTPUT IN CM/SEC (DEF=8.64E05): ",CW2
36: IF CW2=0 THEN CW2=864000
37: INPUT"WEARPLATE IMPEDANCE OF INPUT IN GM/CM2/SEC (DEF=4.5E06): ",ZW1
38: IF ZW1=0 THEN ZW1=4500000
39: INPUT"WEARPLATE IMPEDANCE OF OUTPUT IN GM/CM2/SEC (DEF=4.5E06): ",ZW2
40: IF ZW2=0 THEN ZW2=4500000
```

```
41: PRINT " "
42: PRINT "DATA FOR PIEZOELEMENTS:"
43: PRINT "-----------------------"
44: INPUT"THICKNESS OF PIEZOELEMENTS IN CM (DEF=0.073): ",LP
45: IF LP=0 THEN LP=0.073
46: INPUT"TIME CONSTANT OF INPUT TRANSDUCER, TAU (DEF=LARGE): ",TAU
47: IF TAU=0 THEN TAU=1E10
48: INPUT"TIME CONSTANT OF OUTPUT TRANSDUCER, RCO (DEF=1E-06): ",RCO
49: IF RCO=0 THEN RCO=1E-06
50: PRINT " "
51: PRINT "DATA FOR SPECIMEN(S):"
52: PRINT "---------------------"
53: INPUT "ARE THERE ANY SPECIMENS PRESENT? [Y/N]: ",SPEC$
54: IF SPEC$="N" OR SPEC$="n" THEN 10
55: INPUT"HOW MANY SPECIMEN LAYERS? [1,2,3]: ",NSPEC%
56: INPUT"THICKNESS OF LAYER 1 IN CM (DEF=0.635): ",LS1
57: IF LS1=0 THEN LS1=0.635
58: INPUT"WAVESPEED OF LAYER 1 IN CM/SEC (DEF=4.81E05): ",CS1
59: IF CS1=0 THEN CS1=4.81E06
60: INPUT"IMPEDANCE OF LAYER 1 IN GM/CM2/SEC (DEF=1.30E06): ",ZS1
61: IF ZS1=0 THEN ZS1=1.303E06
62: INPUT"ATTENUATION OF LAYER 1 IN NEPERS/CM (DEF=0): ",ALPHA1
63: IF NSPEC%=1 THEN 10
64: INPUT"THICKNESS OF LAYER 2 IN CM (DEF=0): ",LS2
65: INPUT"WAVESPEED OF LAYER 2 IN CM/SEC (DEF=0): ",CS2
66: INPUT"IMPEDANCE OF LAYER 2 IN GM/CM2/SEC (DEF=0): ",ZS2
67: INPUT"ATTENUATION OF LAYER 2 IN NEPERS/CM (DEF=0): ",ALPHA2
68: IF NSPEC%=2 THEN 10
69: INPUT"THICKNESS OF LAYER 3 IN CM (DEF=0): ",LS3
70: INPUT"WAVESPEED OF LAYER 3 IN CM/SEC (DEF=0): ",CS3
71: INPUT"IMPEDANCE OF LAYER 3 IN GM/CM2/SEC (DEF=0): ",ZS3
72: INPUT"ATTENUATION OF LAYER 3 IN NEPERS/CM (DEF=0): ",ALPHA3
73: 10 PRINT " "
74: PRINT "DATA FOR INPUT WAVEFORM:"
75: PRINT "------------------------"
76: INPUT"INPUT AUTOMATICALLY OR FROM FILE? [A/F]: ",INP$
77: IF INP$="A" OR INP$="a" THEN 20
78: INPUT"NAME OF INPUT DATA FILE: ",NIMP$ : GOTO 30
79: 20 INPUT"INPUT WAVEFORM (S,G,P,I) (NO DEFAULT): ",ANS$
80: IF ANS$="I" OR ANS$="i" THEN 30
81: IF ANS$="P" OR ANS$="p" THEN FREQ=0.50 : GOTO 30
82: INPUT"FREQUENCY OF INPUT IN MHZ (DEF=1.0): ",FREQ
83: IF FREQ=0 THEN FREQ=1.0
84: 30 PRINT " "
85: PRINT "NAMES OF OUTPUT FILES:"
86: PRINT "----------------------"
87: INPUT"OUTPUT FILE NAME FOR INPUT WAVEFORM: ",IN$
88: INPUT"OUTPUT FILE NAME FOR OUTPUT WAVEFORM: ",OUT$
89: PRINT " "
90: PRINT "NUMERICAL DATA FOR SIMULATION:"
```

```
 91: PRINT "_____"
 92: 40 INPUT"SIZE OF TIME STEP IN SEC (DEF=1.333E-08): ",DELTAT
 93: IF DELTAT=0 THEN DELTAT=1.33333E-08
 94: INPUT"FINAL TIME IN MICROSEC (DEF=50): ",TMAX
 95: IF TMAX=0 THEN TMAX=50
 96: NEND%=CINT(TMAX/DELTAT/1000000)
 97: IF NEND%>4000 THEN NEND=4000
 98:
 99: ' PRELIMINARY CALCULATIONS
100:
101: NP%=CINT(LP/(DELTAT*CP))-1
102: IF LP=0 THEN NP%=1
103: NW1%=CINT(LW/(DELTAT*CW1))-1
104: IF LW=0 THEN NW1%=1
105: NW2%=CINT(LW/(DELTAT*CW2))-1
106: IF LW=0 THEN NW2%=1
107: NB1%=CINT(LB1/(DELTAT*CB))-1
108: IF LB1=0 THEN NB1%=0
109: NB2%=CINT(LB2/(DELTAT*CB))-1
110: IF LB2=0 THEN NB2%=0
111: IF NSPEC%=0 THEN 45
112: NS1%=CINT(LS1/(DELTAT*CS1))-1
113: IF NSPEC%=1 THEN 45
114: NS2%=CINT(LS2/(DELTAT*CS2))-1
115: IF NSPEC%=2 THEN 45
116: NS3%=CINT(LS3/(DELTAT*CS3))-1
117: 45 IF NP%>275 THEN PRINT "NP EXCEEDS MAXIMUM ARRAY SIZE!" : GOTO 50
118: IF NW1%>75 THEN PRINT "NW1 EXCEEDS MAXIMUM ARRAY SIZE!" : GOTO 50
119: IF NW2%>75 THEN PRINT "NW2 EXCEEDS MAXIMUM ARRAY SIZE!" : GOTO 50
120: IF NB1%>850 THEN PRINT "NB1 EXCEEDS MAXIMUM ARRAY SIZE!" : GOTO 50
121: IF NB2%>850 THEN PRINT "NB2 EXCEEDS MAXIMUM ARRAY SIZE!" : GOTO 50
122: IF NS1%>250 THEN PRINT "NS1 EXCEEDS MAXIMUM ARRAY SIZE!" : GOTO 50
123: IF NS2%>125 THEN PRINT "NS2 EXCEEDS MAXIMUM ARRAY SIZE!" : GOTO 50
124: IF NS3%>125 THEN PRINT "NS3 EXCEEDS MAXIMUM ARRAY SIZE!" : GOTO 50
125: GOTO 60
126: 50 PRINT "DELTAT IS TOO SMALL.  TRY A LARGER VALUE. . ." : GOTO 40
127: 60 NMAX%=NP%
128: IF NW1%>NMAX% THEN NMAX%=NW1%
129: IF NW2%>NMAX% THEN NMAX%=NW2%
130: IF NB1%>NMAX% THEN NMAX%=NB1%
131: IF NB2%>NMAX% THEN NMAX%=NB2%
132: IF NS1%>NMAX% THEN NMAX%=NS1%
133: IF NS2%>NMAX% THEN NMAX%=NS2%
134: IF NS3%>NMAX% THEN NMAX%=NS3%
135: PRINT " "
136: PRINT "************************************************"
137: PRINT " "
138: PRINT "NUMBER OF ITERATIONS REQUIRED (NEND) = ",NEND%
139: PRINT "NUMBER OF SEGMENTS IN PIEZOELEMENTS (NP) = ",NP%
140: PRINT "NUMBER OF SEGMENTS IN WEARPLATES (NW1,NW2) = ",NW1%;NW2%
```

```
141: PRINT "SEGMENTS IN BACKING LAYERS (NB1,NB2) = ",NB1%;NB2%
142: PRINT "SEGMENTS IN SPECIMEN LAYERS (NS1,NS2,NS3) = ",NS1%;NS2%;NS3%
143: TIMET=(NMAX%+1)*DELTAT
144: IF LB1=0 THEN ERRB1=0 : GOTO 70
145: ERRB1=(ABS(((NB1%+1)*DELTAT)-(LB1/CB))/TIMET)*100
146: 70 IF LB2=0 THEN ERRB2=0 : GOTO 80
147: ERRB2=(ABS(((NB2%+1)*DELTAT)-(LB2/CB))/TIMET)*100
148: 80 IF LS1=0 THEN ERRS1=0 : GOTO 90
149: ERRS1=(ABS(((NS1%+1)*DELTAT)-(LS1/CS1))/TIMET)*100
150: 90 IF LS2=0 THEN ERRS2=0 : GOTO 100
151: ERRS2=(ABS(((NS2%+1)*DELTAT)-(LS2/CS2))/TIMET)*100
152: 100 IF LS3=0 THEN ERRS3=0 : GOTO 110
153: ERRS3=(ABS(((NS3%+1)*DELTAT)-(LS3/CS3))/TIMET)*100
154: 110 ERRW1=(ABS(((NW1%+1)*DELTAT)-(LW/CW1))/TIMET)*100
155: ERRW2=(ABS(((NW2%+1)*DELTAT)-(LW/CW2))/TIMET)*100
156: ERRP=(ABS(((NP%+1)*DELTAT)-(LP/CP))/TIMET)*100
157: PRINT " "
158: PRINT "************************************************************"
159: PRINT " "
160: PRINT "ERRORS IN TRANSIT TIMES OF ELEMENTS: "
161: PRINT "-------------------------------------"
162: PRINT "BACKING OF TRANSMITTER:   ";ERRB1;"%"
163: PRINT "BACKING OF RECEIVER:      ";ERRB2;"%"
164: PRINT "WEARPLATE OF TRANSMITTER: ";ERRW1;"%"
165: PRINT "WEARPLATE OF RECEIVER:    ";ERRW2;"%"
166: PRINT "PIEZOELEMENT OF EACH:     ";ERRP;"%"
167: PRINT "SPECIMEN LAYER 1:         ";ERRS1;"%"
168: PRINT "SPECIMEN LAYER 2:         ";ERRS2;"%"
169: PRINT "SPECIMEN LAYER 3:         ";ERRS3;"%"
170: PRINT " "
171: INPUT"ARE THESE ERRORS ACCEPTABLE? [Y/N]: ",OK$
172: IF OK$="Y" OR OK$="y" THEN 120
173: PRINT "TRY ANOTHER TIME STEP. . . " : GOTO 40
174: 120 PRINT " "
175: PRINT "******************************************"
176: RHO1=EXP(-ALPHA*LB1)
177: RHO2=EXP(-ALPHA*LB2)
178: SRHO1=EXP(-ALPHA1*LS1)
179: SRHO2=EXP(-ALPHA2*LS2)
180: SRHO3=EXP(-ALPHA3*LS3)
181:
182: ' INPUT WAVEFORM AS A FUNCTION OF TIME
183:
184: PRINT " "
185: IF INP$="A" OR INP$="a" THEN 130
186: PRINT "     * READING INPUT DATA FILE"
187: OPEN "I",1,NIMP$ : INPUT#1,NI%
188: FOR I%=1 TO NI% : INPUT#1,VIN(I%) : NEXT I% : CLOSE #1
189: GOTO 150
190: 130 PRINT "     * CREATING INPUT WAVEFORM"
```

```
191: VIN(1)=100
192: IF ANS$="I" OR ANS$="i" THEN 150
193: FOR I%=1 TO NEND%
194: IF (ANS$="P" OR ANS$="p") AND I%>=150 THEN 150
195: IF (ANS$="G" OR ANS$="g") AND I%>=750 THEN 150
196: VIN(I%)=-1000*COS(I%*DELTAT*FREQ*6283200)
197: IF (ANS$="P" OR ANS$="p") THEN VIN(I%)=500+VIN(I%)/2
198: 140 NEXT I%
199:
200: ' CONVERSION OF INPUT VOLTAGE TO STRESS
201:
202: 150 PRINT "     * CONVERTING INPUT VOLTAGE TO STRESS"
203: VIN(0)=0
204: FOR I%=1 TO NEND%
205: VIN(NEND%+1-I%)=VIN(NEND%+1-I%)-VIN(NEND%-I%)
206: NEXT I%
207: FOR I%=1 TO NEND%
208: VIN(I%)=VIN(I%)+(EXP(DELTAT/TAU)*VIN(I%-1))
209: NEXT I%
210:
211: ' ITERATION TO CALCULATE TIME RESPONSE
212:
213: PRINT "     * WAVE PROPAGATION     % COMPLETED"
214: FOR IT%=1 TO NEND%
215: PDONE%=INT(IT%/NEND%*100)
216: LOCATE 23,24 : PRINT PDONE%
217:
218: ' REFLECTIONS AT IMPEDANCE-MISMATCHED INTERFACES
219:
220: IF NB1%=0 THEN 160
221: B1RO0=((ZU-ZB)/(ZU+ZB))*B1LI0
222: B1P1RO=(((2*ZP)*B1P1RI)+((ZB-ZP)*B1P1LI)+(ZP*VIN(IT%)))/(ZB+ZP)
223: B1P1LO=(((ZP-ZB)*B1P1RI)+((2*ZB)*B1P1LI)-(ZB*VIN(IT%)))/(ZB+ZP)
224: GOTO 170
225: 160 P1RO0=(((ZU-ZP)*P1LI0)+(ZP*VIN(IT%)))/(ZU+ZP)
226: 170 P1W1RO=(((2*ZW1)*P1W1RI)+((ZP-ZW1)*P1W1LI)-(ZW1*VIN(IT%)))/(ZP+ZW1)
227: P1W1LO=(((ZW1-ZP)*P1W1RI)+((2*ZP)*P1W1LI)+(ZP*VIN(IT%)))/(ZP+ZW1)
228: IF NS1%=0 THEN 200
229: W1S1RO=((2*ZS1)*W1S1RI+(ZW1-ZS1)*W1S1LI)/(ZW1+ZS1)
230: W1S1LO=((ZS1-ZW1)*W1S1RI+(2*ZW1)*W1S1LI)/(ZW1+ZS1)
231: IF NS2%>0 THEN 180
232: S1W2RO=((2*ZW2)*S1W2RI+(ZS1-ZW2)*S1W2LI)/(ZS1+ZW2)
233: S1W2LO=((ZW2-ZS1)*S1W2RI+(2*ZS1)*S1W2LI)/(ZS1+ZW2)
234: GOTO 210
235: 180 S1S2RO=((2*ZS2)*S1S2RI+(ZS1-ZS2)*S1S2LI)/(ZS1+ZS2)
236: S1S2LO=((ZS2-ZS1)*S1S2RI+(2*ZS1)*S1S2LI)/(ZS1+ZS2)
237: IF NS3%>0 THEN 190
238: S2W2RO=((2*ZW2)*S2W2RI+(ZS2-ZW2)*S2W2LI)/(ZS2+ZW2)
239: S2W2LO=((ZW2-ZS2)*S2W2RI+(2*ZS2)*S2W2LI)/(ZS2+ZW2)
240: GOTO 210
```

```
241: 190 S2S3RO=((2*ZS3)*S2S3RI+(ZS2-ZS3)*S2S3LI)/(ZS2+ZS3)
242: S2S3LO=((ZS3-ZS2)*S2S3RI+(2*ZS2)*S2S3LI)/(ZS2+ZS3)
243: S3W2RO=((2*ZW2)*S3W2RI+(ZS3-ZW2)*S3W2LI)/(ZS3+ZW2)
244: S3W2LO=((ZW2-ZS3)*S3W2RI+(2*ZS3)*S3W2LI)/(ZS3+ZW2)
245: GOTO 210
246: 200 W1W2RO=((2*ZW2)*W1W2RI+(ZW1-ZW2)*W1W2LI)/(ZW1+ZW2)
247: W1W2LO=((ZW2-ZW1)*W1W2RI+(2*ZW1)*W1W2LI)/(ZW1+ZW2)
248: 210 W2P2RO=((2*ZP)*W2P2RI+(ZW2-ZP)*W2P2LI)/(ZW2+ZP)
249: W2P2LO=((ZP-ZW2)*W2P2RI+(2*ZW2)*W2P2LI)/(ZW2+ZP)
250: IF NB2%=0 THEN 220
251: P2B2RO=((2*ZB)*P2B2RI+(ZP-ZB)*P2B2LI)/(ZP+ZB)
252: P2B2LO=((ZB-ZP)*P2B2RI+(2*ZP)*P2B2LI)/(ZP+ZB)
253: B2LO0=((ZU-ZB)/(ZB+ZU))*B2RI0
254: GOTO 230
255: 220 P2LO0=((ZU-ZP)/(ZP+ZU))*P2RI0
256:
257: ' DELAY LINE EQUATIONS
258:
259: 230 FOR I%=1 TO NMAX%-1
260: IF I%>=NS1% THEN 240
261: S1R(NS1%+1-I%)=S1R(NS1%-I%)
262: S1L(I%)=S1L(I%+1)
263: 240 IF I%>=NS2% THEN 250
264: S2R(NS2%+1-I%)=S2R(NS2%-I%)
265: S2L(I%)=S2L(I%+1)
266: 250 IF I%>=NS3% THEN 260
267: S3R(NS3%+1-I%)=S3R(NS3%-I%)
268: S3L(I%)=S3L(I%+1)
269: 260 IF I%>=NP% THEN 270
270: P1R(NP%+1-I%)=P1R(NP%-I%)
271: P1L(I%)=P1L(I%+1)
272: P2R(NP%+1-I%)=P2R(NP%-I%)
273: P2L(I%)=P2L(I%+1)
274: 270 IF I%>=NW1% THEN 280
275: W1R(NW1%+1-I%)=W1R(NW1%-I%)
276: W1L(I%)=W1L(I%+1)
277: 280 IF I%>=NW2% THEN 290
278: W2R(NW2%+1-I%)=W2R(NW2%-I%)
279: W2L(I%)=W2L(I%+1)
280: 290 IF I%>=NB1% THEN 300
281: B1R(NB1%+1-I%)=B1R(NB1%-I%)
282: B1L(I%)=B1L(I%+1)
283: 300 IF I%>=NB2% THEN 310
284: B2R(NB2%+1-I%)=B2R(NB2%-I%)
285: B2L(I%)=B2L(I%+1)
286: 310 NEXT I%
287:
288: ' BOUNDARIES OF DELAY LINES
289:
290: IF NB1%=0 THEN 320
```

```
291: B1R(1)=B1RO0
292: B1LI0=(1-DELTA)*(B1L(1)*RHO1)+DELTA*B1LI0
293: B1P1RI=(1-DELTA)*(B1R(NB1%)*RHO1)+DELTA*B1P1RI
294: B1L(NB1%)=B1P1LO
295: P1R(1)=B1P1RO
296: B1P1LI=P1L(1)
297: GOTO 330
298: 320 P1R(1)=P1RO0
299: P1LI0=P1L(1)
300: 330 P1W1RI=P1R(NP%)
301: P1L(NP%)=P1W1LO
302: W1R(1)=P1W1RO
303: P1W1LI=W1L(1)
304: IF NS1%=0 THEN 360
305: W1S1RI=W1R(NW1%)
306: W1L(NW1%)=W1S1LO
307: S1R(1)=W1S1RO
308: W1S1LI=S1L(1)*SRHO1
309: IF NS2%>0 THEN 340
310: S1W2RI=S1R(NS1%)*SRHO1
311: S1L(NS1%)=S1W2LO
312: W2R(1)=S1W2RO
313: S1W2LI=W2L(1)
314: GOTO 370
315: 340 S1S2RI=S1R(NS1%)*SRHO1
316: S1L(NS1%)=S1S2LO
317: S2R(1)=S1S2RO
318: S1S2LI=S2L(1)*SRHO2
319: IF NS3%>0 THEN 350
320: S2W2RI=S2R(NS2%)*SRHO2
321: S2L(NS2%)=S2W2LO
322: W2R(1)=S2W2RO
323: S2W2LI=W2L(1)
324: GOTO 370
325: 350 S2S3RI=S2R(NS2%)*SRHO2
326: S2L(NS2%)=S2S3LO
327: S3R(1)=S2S3RO
328: S2S3LI=S3L(1)*SRHO3
329: S3W2RI=S3R(NS3%)*SRHO3
330: S3L(NS3%)=S3W2LO
331: W2R(1)=S3W2RO
332: S3W2LI=W2L(1)
333: GOTO 370
334: 360 W1W2RI=W1R(NW1%)
335: W1L(NW1%)=W1W2LO
336: W2R(1)=W1W2RO
337: W1W2LI=W2L(1)
338: 370 W2P2RI=W2R(NW2%)
339: W2L(NW2%)=W2P2LO
340: P2R(1)=W2P2RO
```

```
341: W2P2LI=P2L(1)
342: IF NB2%=0 THEN 380
343: P2B2RI=P2R(NP%)
344: P2L(NP%)=P2B2LO
345: B2R(1)=P2B2RO
346: P2B2LI=(1-DELTA)*(B2L(1)*RHO2)+DELTA*P2B2LI
347: B2RI0=(1-DELTA)*(B2R(NB2%)*RHO2)+DELTA*B2RI0
348: B2L(NB2%)=B2LO0
349: VOUT(IT%)=(W2P2LI-W2P2RO)+(P2B2RI-P2B2LO)
350: GOTO 390
351: 380 P2RI0=P2R(NP%)
352: P2L(NP%)=P2LO0
353: VOUT(IT%)=(W2P2LI-W2P2RO)+(P2RI0-P2LO0)
354: 390 NEXT IT%
355:
356: ' CONVERSION OF STRESS TO OUTPUT VOLTAGE
357:
358: PRINT "      * CONVERTING STRESS TO OUTPUT VOLTAGE"
359: FOR I%=1 TO NEND%
360: VOUT(I%)=(2*DELTAT*VOUT(I%)/ZP)+(VOUT(I%-1)*EXP(-DELTAT/RCO))
361: NEXT I%
362:
363: ' WRITING OF OUTPUT DATA FILES
364:
365: PRINT "      * WRITING OUTPUT DATA FILES"
366: OPEN "O",1,IN$ : WRITE#1,NEND%
367: FOR I%=1 TO NEND% : WRITE#1,VIN(I%) : NEXT I% : CLOSE #1
368: OPEN "O",1,OUT$ : WRITE#1,NEND%
369: FOR I%=1 TO NEND% : WRITE#1,VOUT(I%) : NEXT I% : CLOSE #1
370: PRINT " "
371: PRINT "*****************************************"
372: PRINT " "
373: INPUT"WANT ANOTHER SIMULATION? [Y/N] : ",REDO$
374: IF REDO$="Y" OR REDO$="y" THEN 1
375: END
```

ATTACHMENT B2

SAMPLE SIMULATION USING THE MODELING PROGRAM

```
ENTER INPUT DATA (PRESS RETURN FOR DEFAULT VALUE)
**************************************************

DATA FOR BACKING LAYERS:
------------------------

BACKING THICKNESS OF INPUT TRANSDUCER IN CM (DEF=0): .635
BACKING THICKNESS OF OUTPUT TRANSDUCER IN CM (DEF=0): .635
IMPEDANCE OF BACKING LAYERS IN GM/CM2/SEC (DEF=1.8E06):
ATTENUATION OF BACKING LAYERS, ALPHA (DEF=1.6): 1.8
FREQUENCY FILTERING PARAMETER, DELTA (DEF=0):

DATA FOR WEARPLATES:
--------------------

WEARPLATE THICKNESS OF TRANSDUCERS IN CM (DEF=0.035):
WEARPLATE WAVESPEED OF INPUT IN CM/SEC (DEF=8.64E05):
WEARPLATE WAVESPEED OF OUTPUT IN CM/SEC (DEF=8.64E05):
WEARPLATE IMPEDANCE OF INPUT IN GM/CM2/SEC (DEF=4.5E06):
WEARPLATE IMPEDANCE OF OUTPUT IN GM/CM2/SEC (DEF=4.5E06):

DATA FOR PIEZOELEMENTS:
-----------------------

THICKNESS OF PIEZOELEMENTS IN CM (DEF=0.073):
TIME CONSTANT OF INPUT TRANSDUCER, TAU (DEF=LARGE):
TIME CONSTANT OF OUTPUT TRANSDUCER, RCO (DEF=1E-06):

DATA FOR SPECIMEN(S):
---------------------

ARE THERE ANY SPECIMENS PRESENT? [Y/N]: N

DATA FOR INPUT WAVEFORM:
------------------------

INPUT AUTOMATICALLY OR FROM FILE? [A/F]: F
NAME OF INPUT DATA FILE: IN.DAT

NAMES OF OUTPUT FILES:
----------------------

OUTPUT FILE NAME FOR INPUT WAVEFORM: IN.OUT
OUTPUT FILE NAME FOR OUTPUT WAVEFORM: OUT.OUT
```

```
NUMERICAL DATA FOR SIMULATION:
------------------------------

SIZE OF TIME STEP IN SEC (DEF=1.333E-08):
FINAL TIME IN MICROSEC (DEF=50): 10

************************************************

NUMBER OF ITERATIONS REQUIRED (NEND) =     750
NUMBER OF SEGMENTS IN PIEZOELEMENTS (NP) =                19
NUMBER OF SEGMENTS IN WEARPLATES (NW1,NW2) =              2  2
SEGMENTS IN BACKING LAYERS (NB1,NB2) =     274  274
SEGMENTS IN SPECIMEN LAYERS (NS1,NS2,NS3) =               0  0  0

************************************************************

ERRORS IN TRANSIT TIMES OF ELEMENTS:
------------------------------------

BACKING OF TRANSMITTER:     .1053446 %
BACKING OF RECEIVER:        .1053446 %
WEARPLATE OF TRANSMITTER:   1.389166E-02 %
WEARPLATE OF RECEIVER:      1.389166E-02 %
PIEZOELEMENT OF EACH:       6.618141E-03 %
SPECIMEN LAYER 1:           0 %
SPECIMEN LAYER 2:           0 %
SPECIMEN LAYER 3:           0 %

ARE THESE ERRORS ACCEPTABLE? [Y/N]: Y

*****************************************

     * READING INPUT DATA FILE
     * CONVERTING INPUT VOLTAGE TO STRESS
     * WAVE PROPAGATION 100 % COMPLETED
     * CONVERTING STRESS TO OUTPUT VOLTAGE
     * WRITING OUTPUT DATA FILES

*****************************************

WANT ANOTHER SIMULATION? [Y/N] : N
```

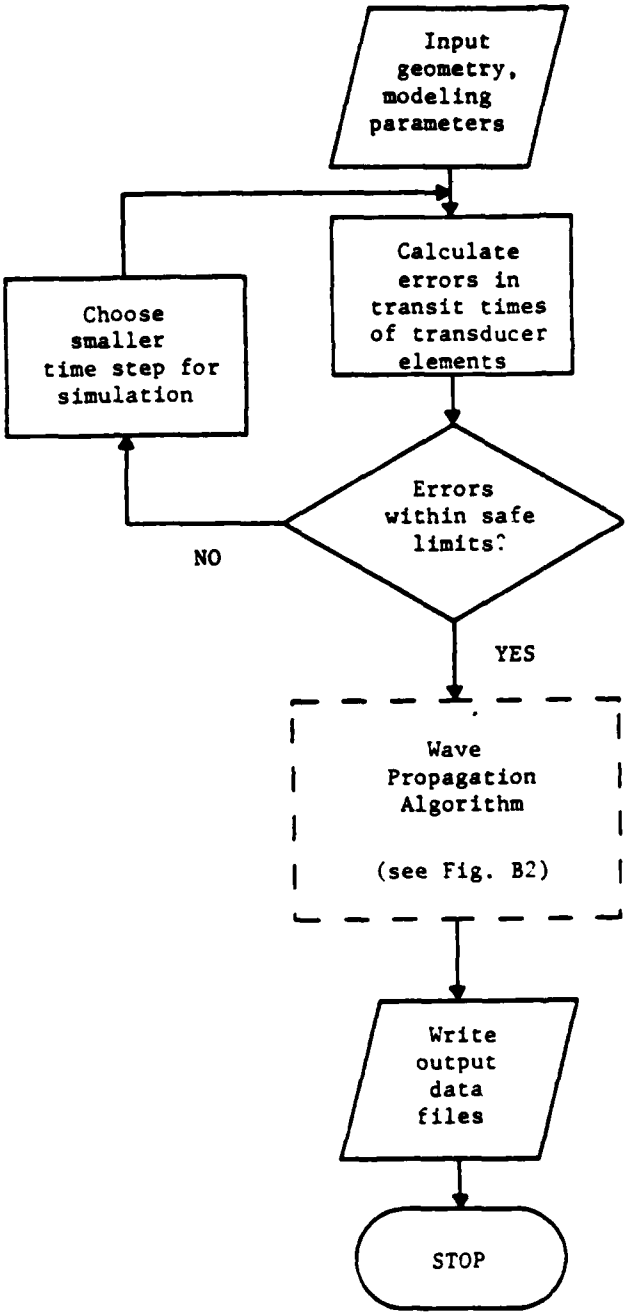

Fig. B1 Flowchart of BASIC modeling program.

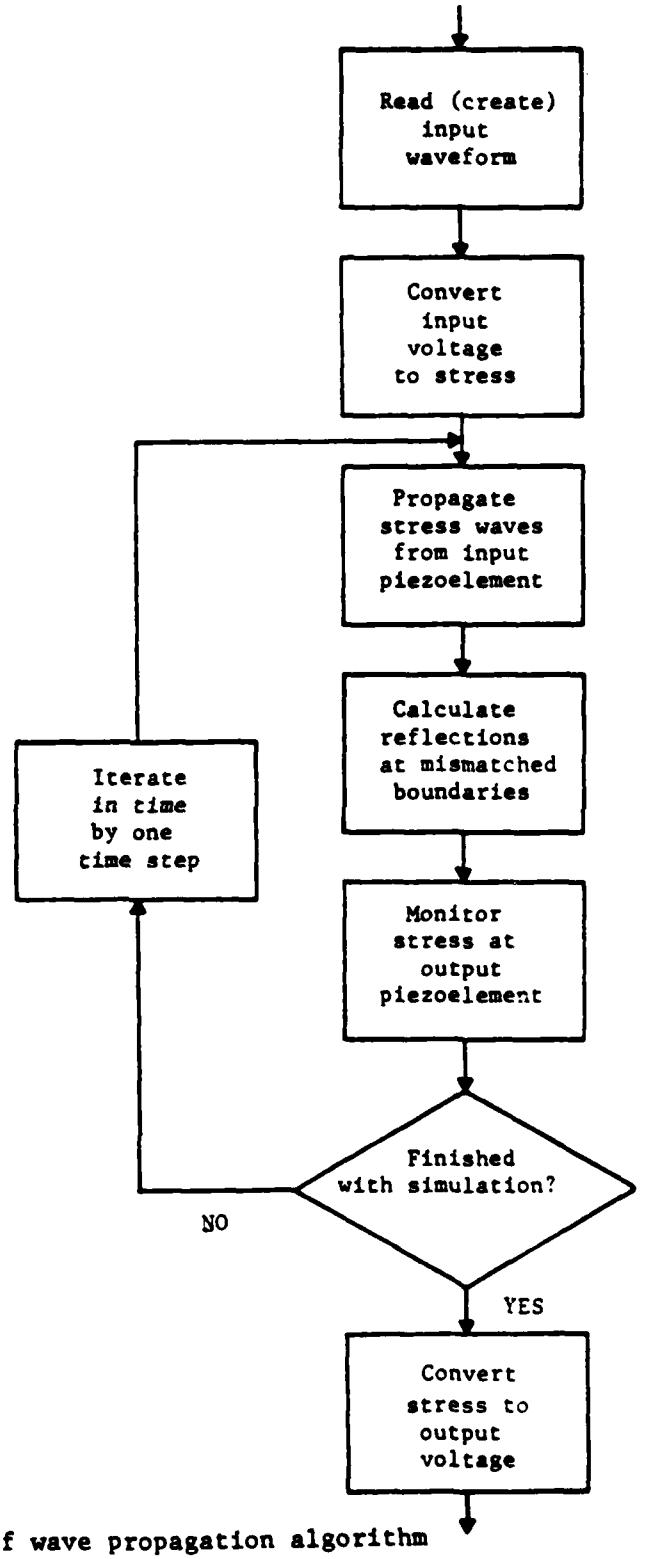

Fig. B2 Flowchart of wave propagation algorithm used in modeling program

APPENDIX C

DESCRIPTION OF TRANSDUCERS AND SPECIMENS

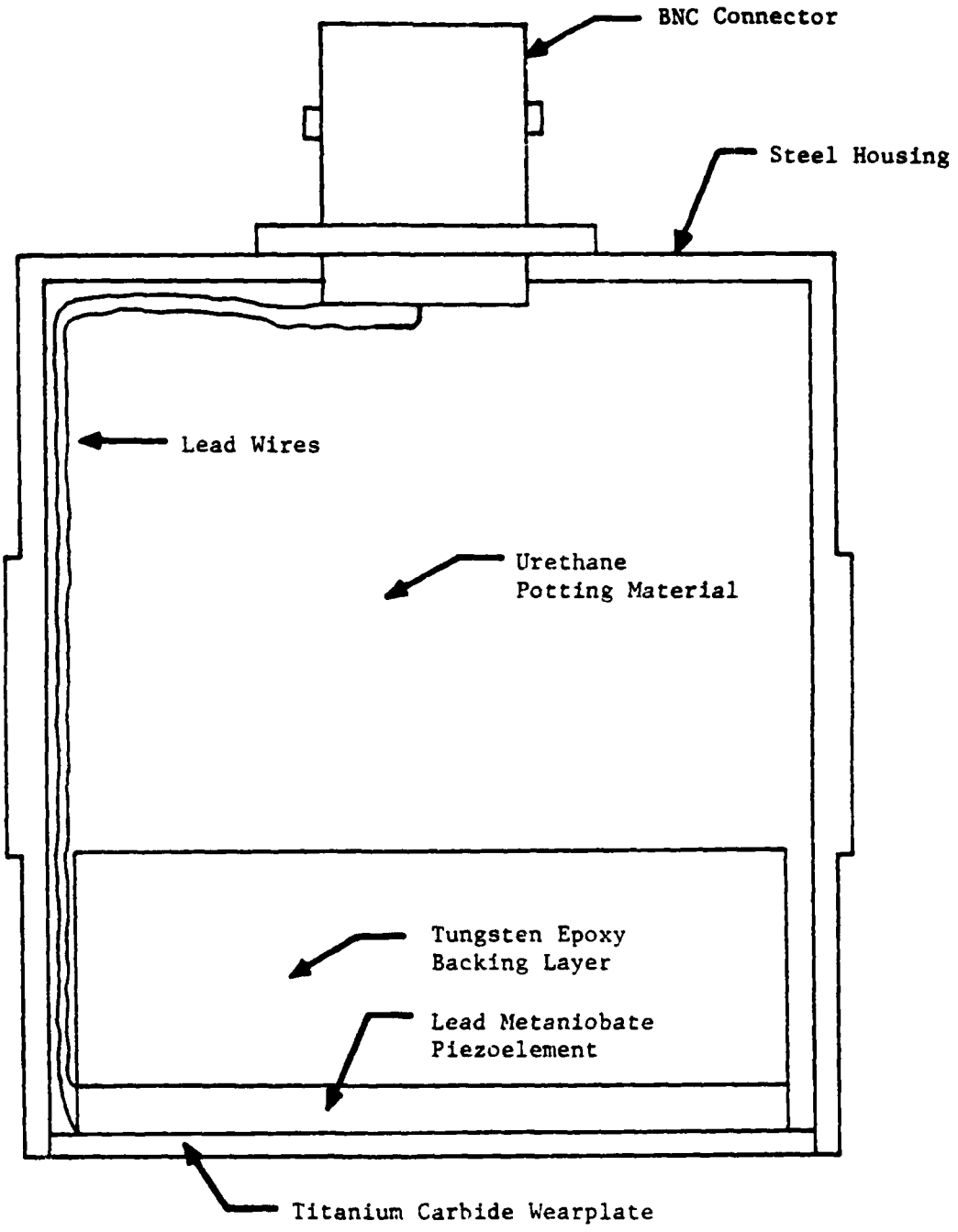

Fig. C1 Sketch of Acoustic Emission Technology (AET) FC-500 broadband ultrasonic transducer.

Design Parameter	Transducer				
	AE-103	AE-102	AE-101	FC-500	AE-100
L_B (cm)	1.905	1.270	0.635	0.635	0
Z_B (gm/cm^2/sec)	1.8×10^6	1.8×10^6	1.8×10^6	1.8×10^6	---
c_B (cm/sec)	1.73×10^5	1.73×10^5	1.73×10^5	1.73×10^5	---
L_W (cm)	0.035	0.035	0.035	0.035	0.035
Z_W (gm/cm^2/sec)	4.5×10^6	4.5×10^6	1.3×10^6	4.5×10^6	4.5×10^6
c_W (cm/sec)	8.64×10^5	8.64×10^5	4.8×10^5	8.64×10^5	8.64×10^5
L_P (cm)	0.073	0.073	0.073	0.073	0.073
Z_P (gm/cm^2/sec)	1.8×10^6	1.8×10^6	1.8×10^6	1.8×10^6	1.8×10^6
c_P (cm/sec)	2.74×10^5	2.74×10^5	2.74×10^5	2.74×10^5	2.74×10^5

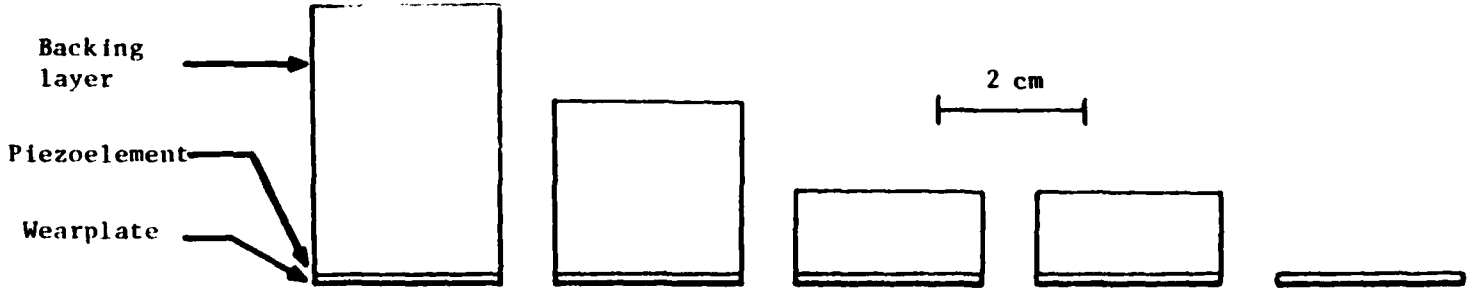

Fig. C2 Dimensions and properties of transducer elements for FC-500, AE-100, AE-101, AE-102, and AE-103 transducers.

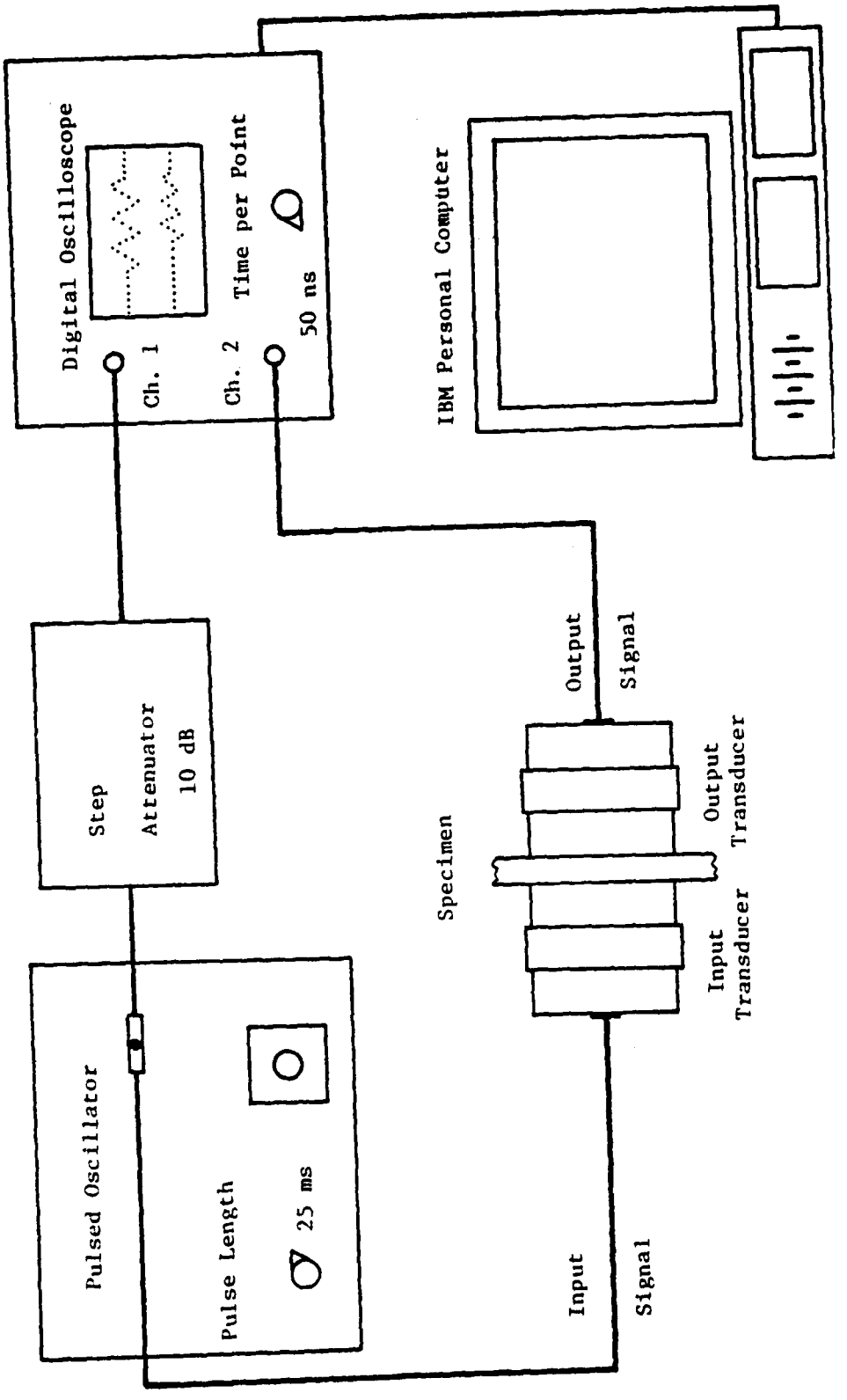

Fig. C3 Ultrasonic test system set up for tone burst and continuous sinusoidal input signals.

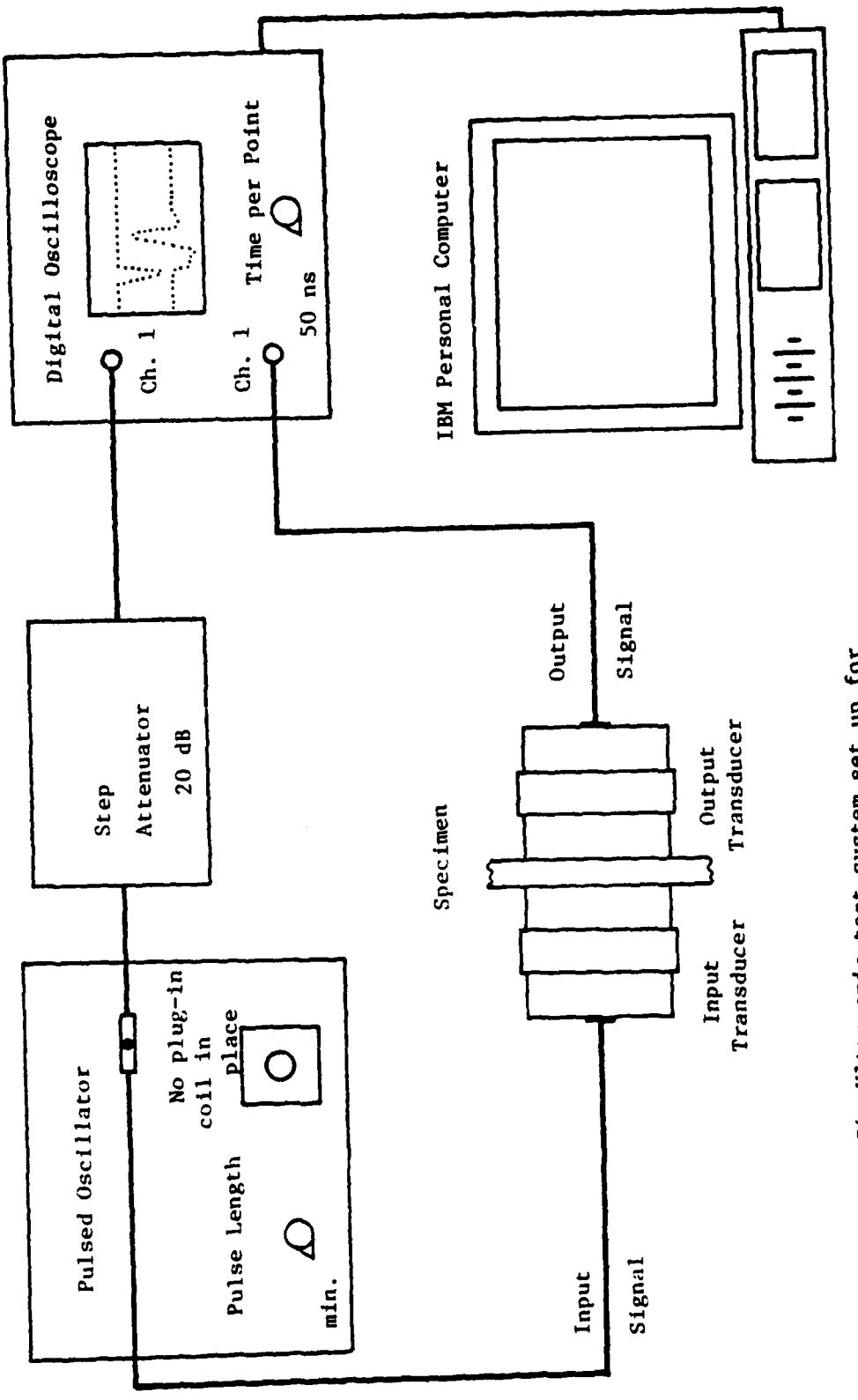

Fig. C4 Ultrasonic test system set up for broadband pulse input signals.

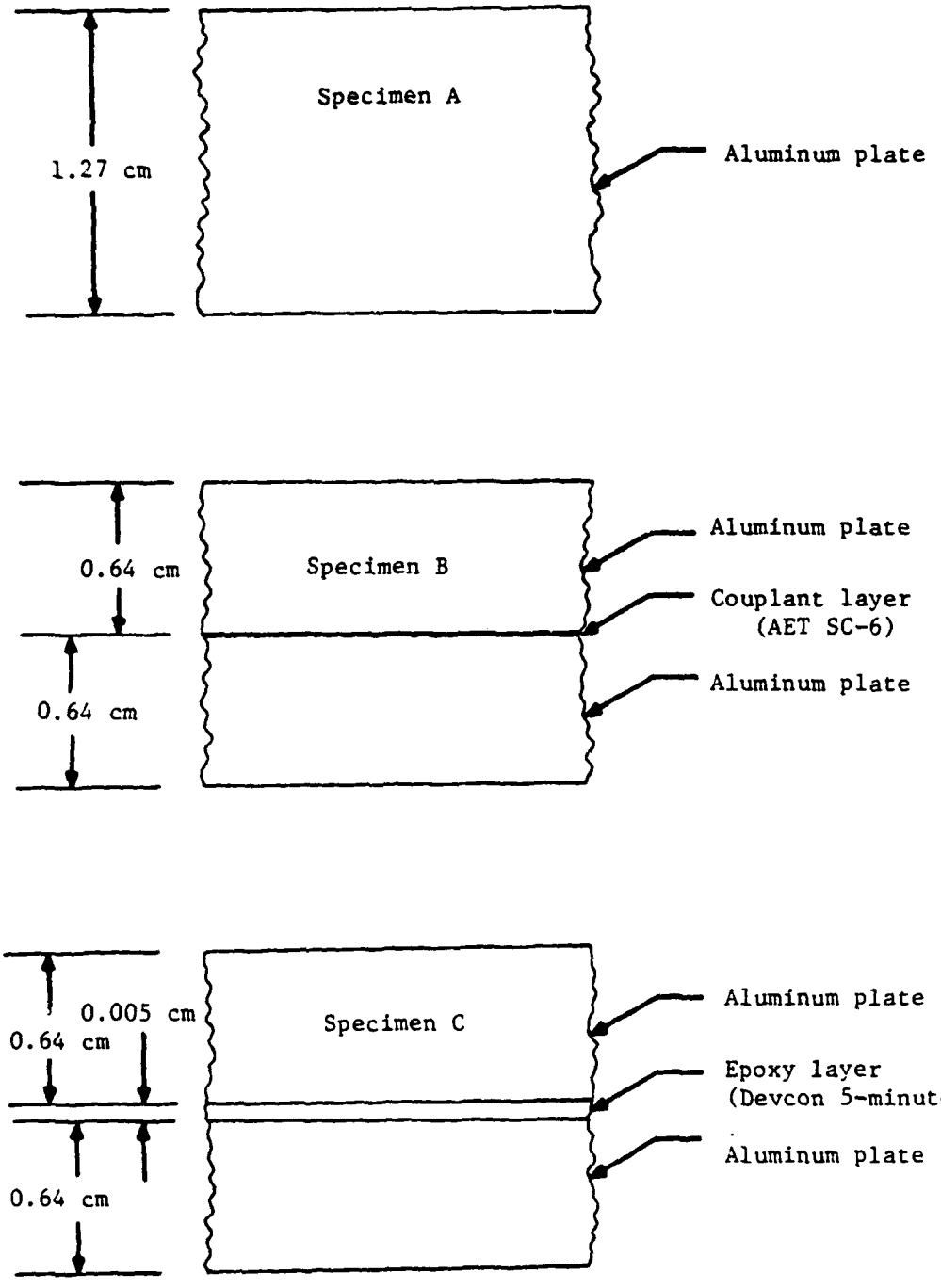

Fig. C5 Sketch of specimens used to study effects of couplant and adhesive-bonding layers in an ultrasonic test system.

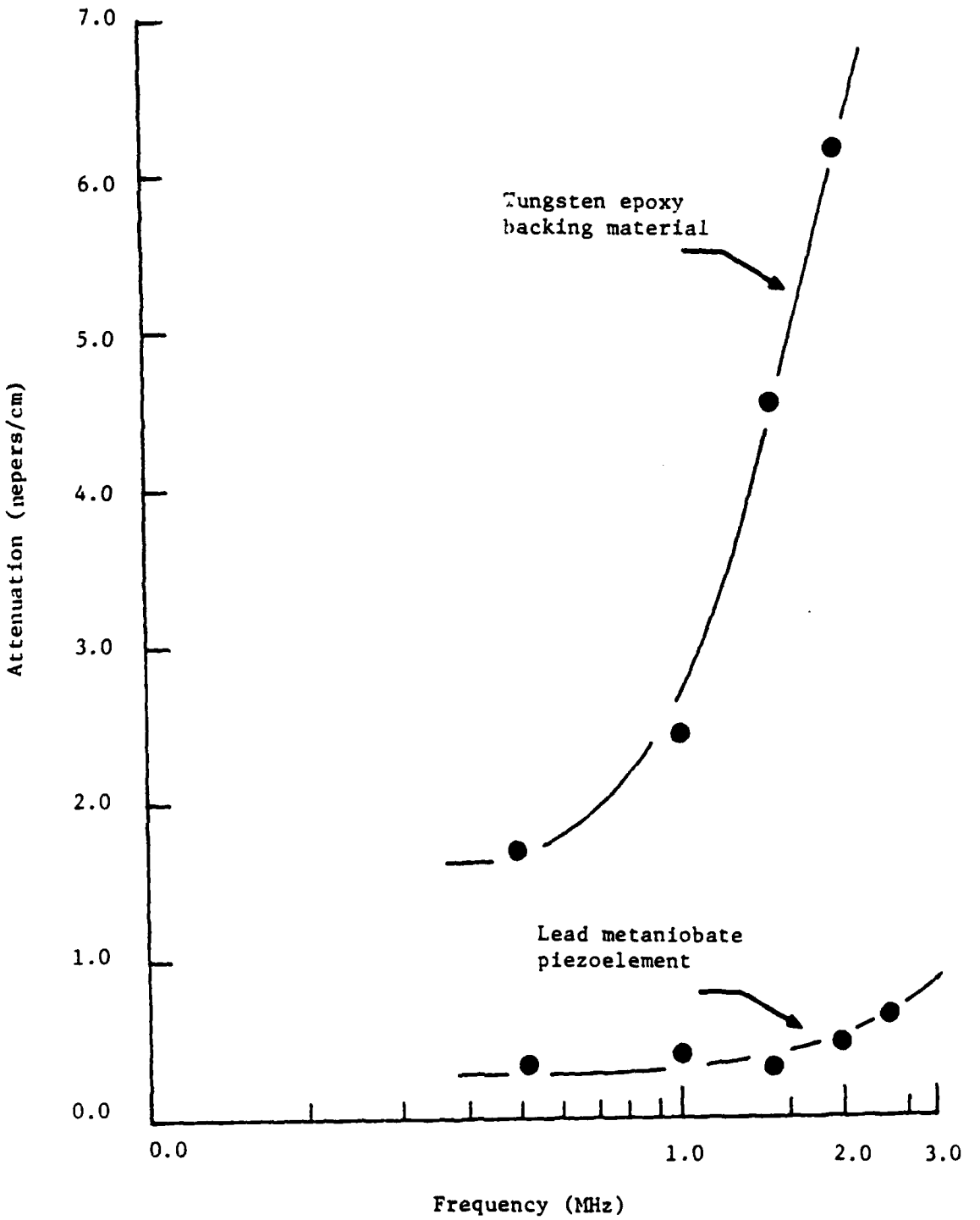

Fig. C6 Plot of measured backing attenuation vs. frequency for tungsten epoxy backing material and titanium carbide wearplate (from [24]).

APPENDIX D

RESULTS OF TRANSDUCER EXPERIMENTS

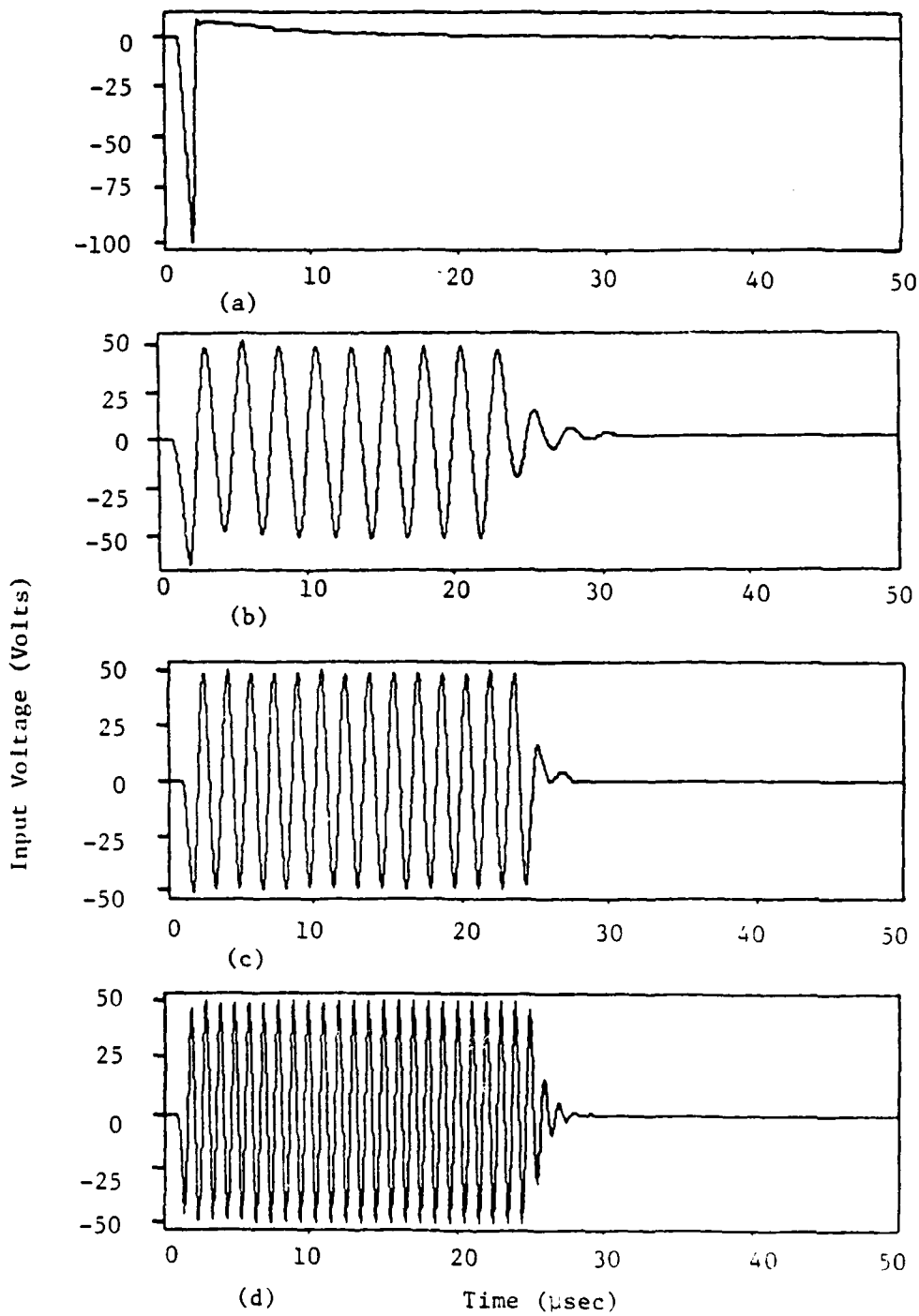

Fig. D1 Measured (a) broadband pulse, (b) 0.4 MHz tone burst, (c) 0.6 MHz tone burst, and (d) 1.0 MHz tone burst input signals used in transducer experiments.

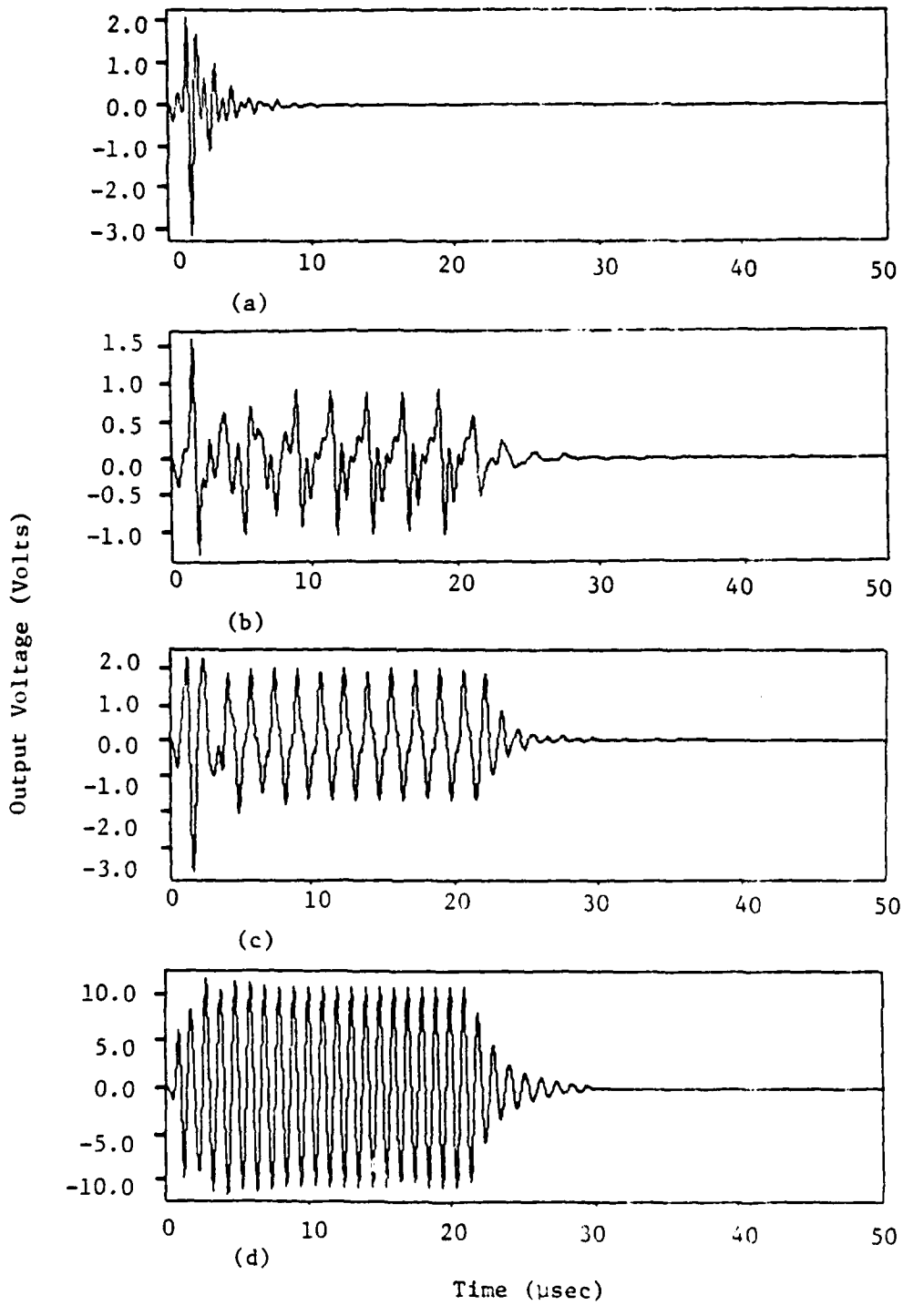

Fig. D2 Measured ouput signals corresponding to (a) broadband pulse, (b) 0.4 MHz tone burst, (c) 0.6 MHz tone burst, and (d) 1.0 MHz tone burst input signals for two AE-100 transducers clamped face-to-face.

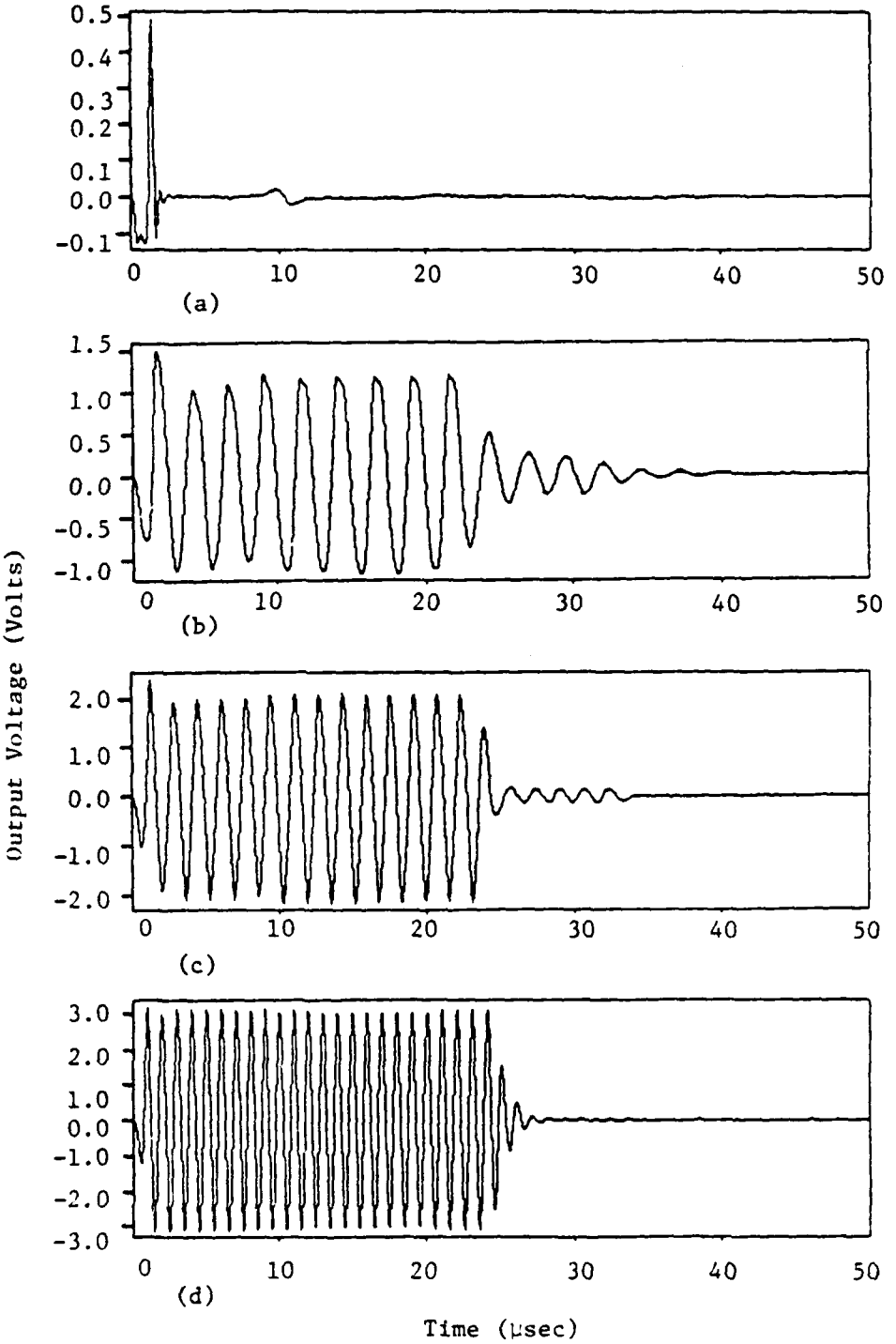

Fig. D3 Measured output signals corresponding to (a) broadband pulse, (b) 0.4 MHz tone burst, (c) 0.6 MHz tone burst, and (d) 1.0 MHz tone burst input signals for two FC-500 transducers clamped face-to-face.

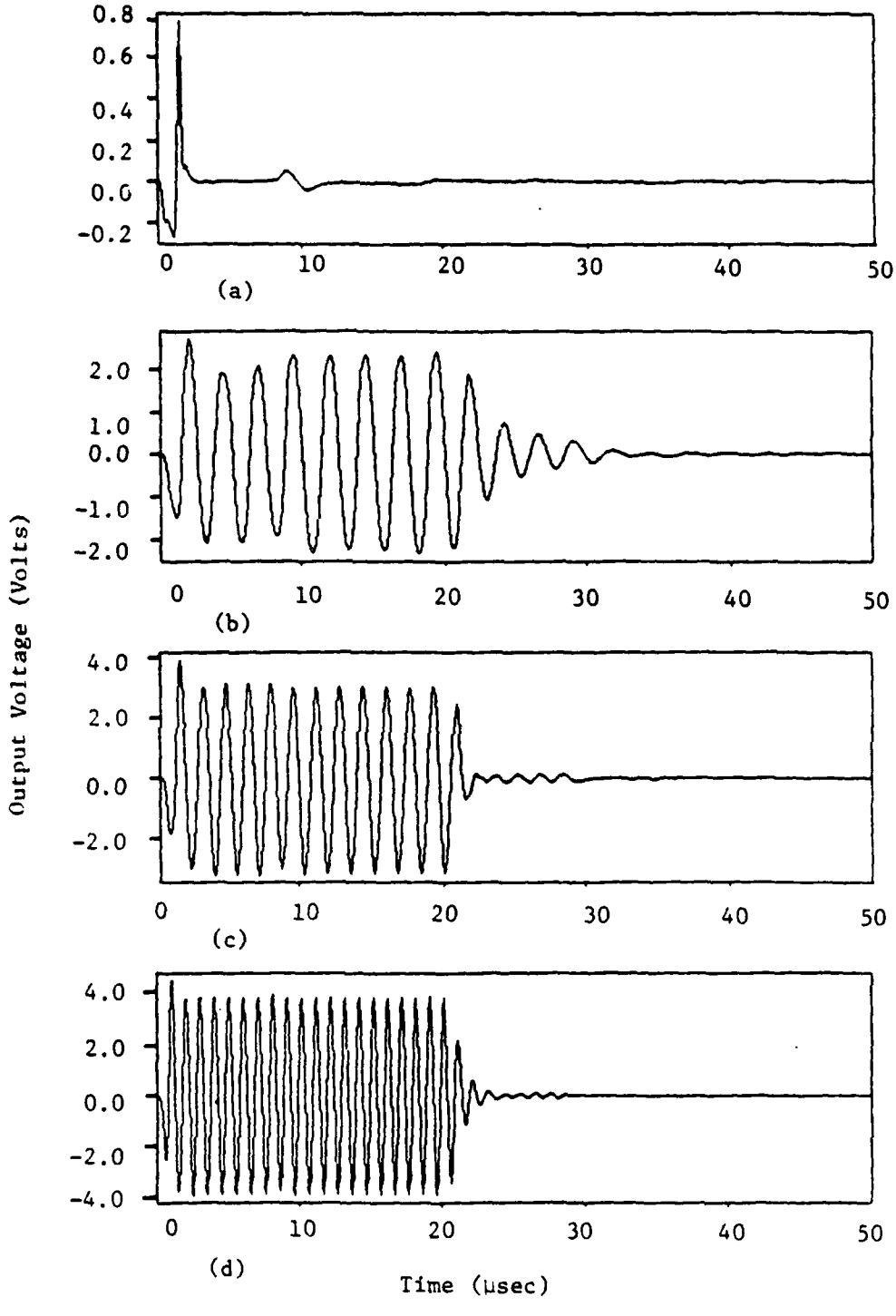

Fig. D4 Measured output signals corresponding to (a) broadband pulse, (b) 0.4 MHz tone burst, (c) 0.6 MHz tone burst, and (d) 1.0 MHz tone burst input signals for two AE-101 transducers clamped face-to-face.

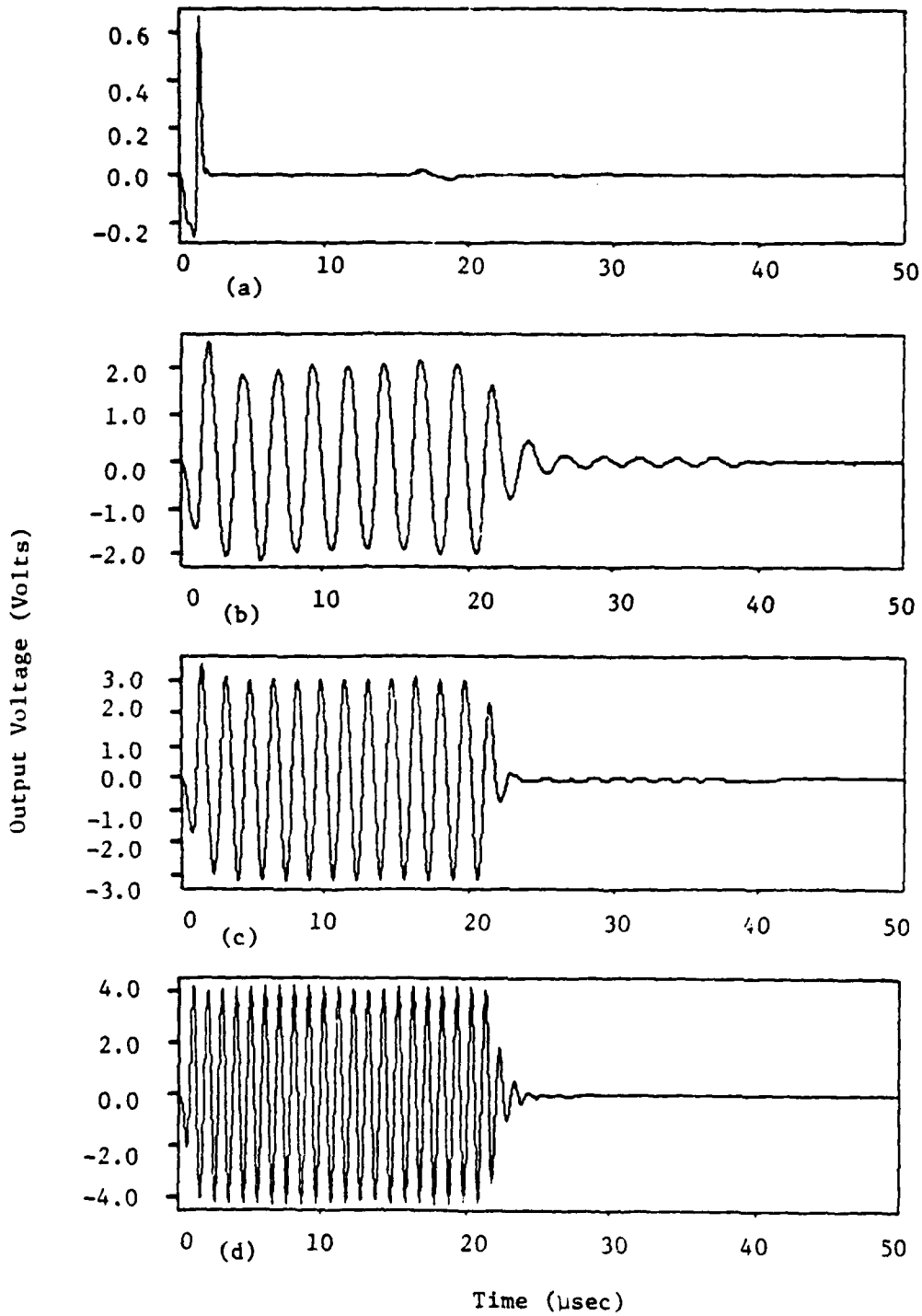

Fig. D5 Measured output signals corresponding to (a) broadband pulse, (b) 0.4 MHz tone burst, (c) 0.6 MHz tone burst, and (d) 1.0 MHz tone burst input signals for two AE-102 transducers clamped face-to-face.

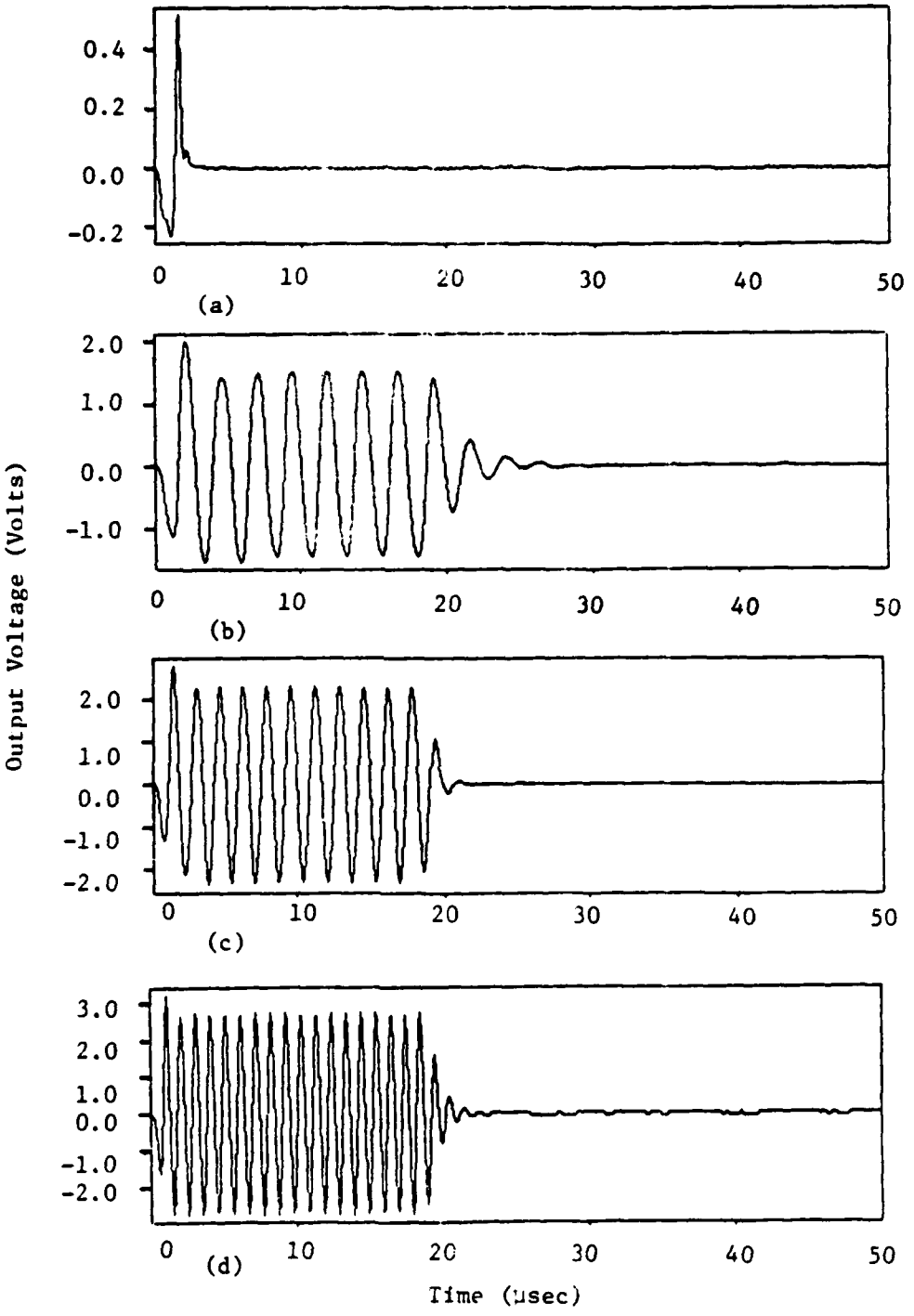

Fig. D6 Measured output signals corresponding to (a) broadband pulse, (b) 0.4 MHz tone burst, (c) 0.6 MHz tone burst, and (d) 1.0 MHz tone burst input signals for two AE-103 transducers clamped face-to-face.

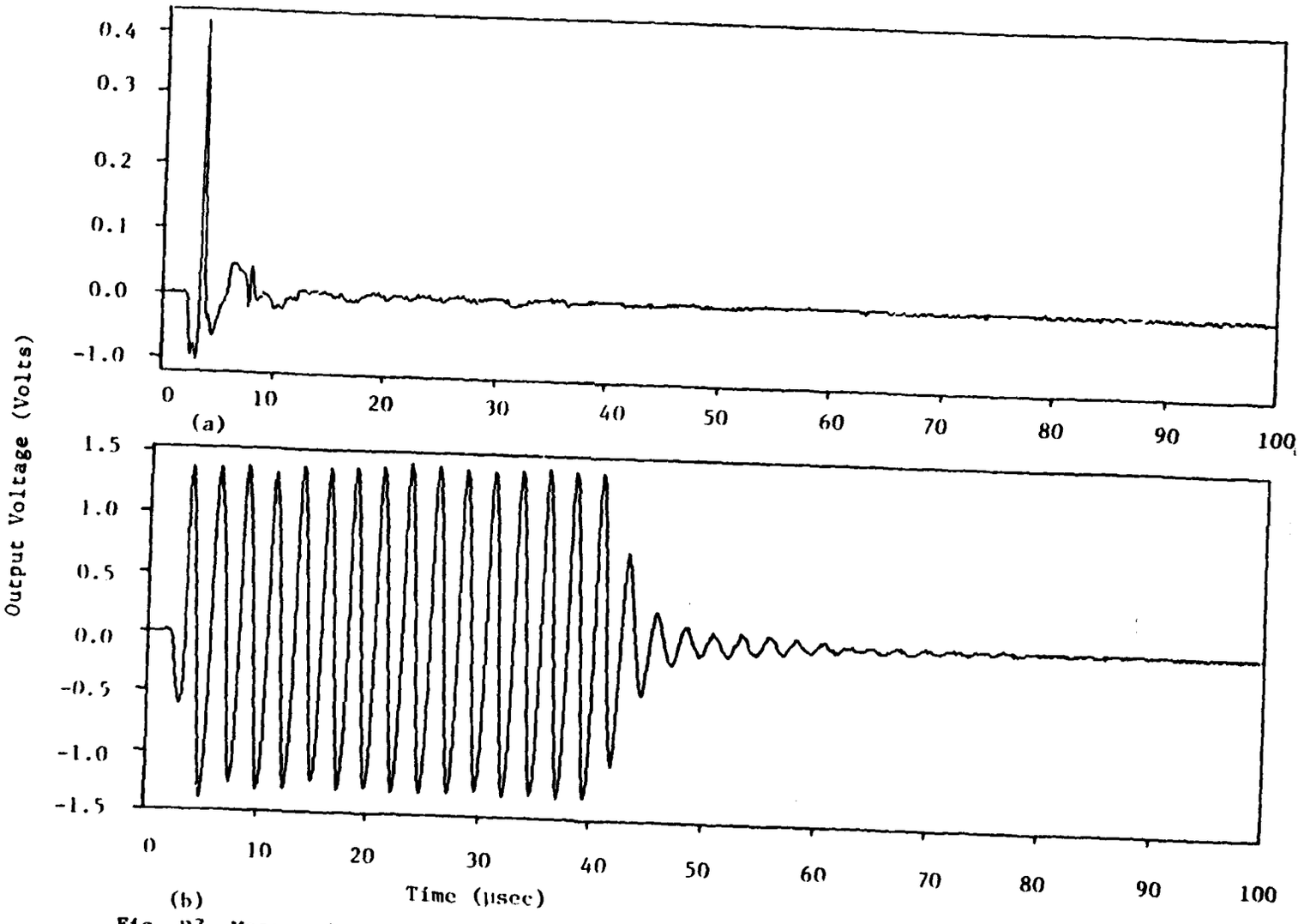

Fig. D7 Measured output signals corresponding to (a) broadband pulse and (b) 0.4 MHz tone burst input signals for 1.270 cm (0.500 in) aluminum plate clamped between two AE-103 transducers.

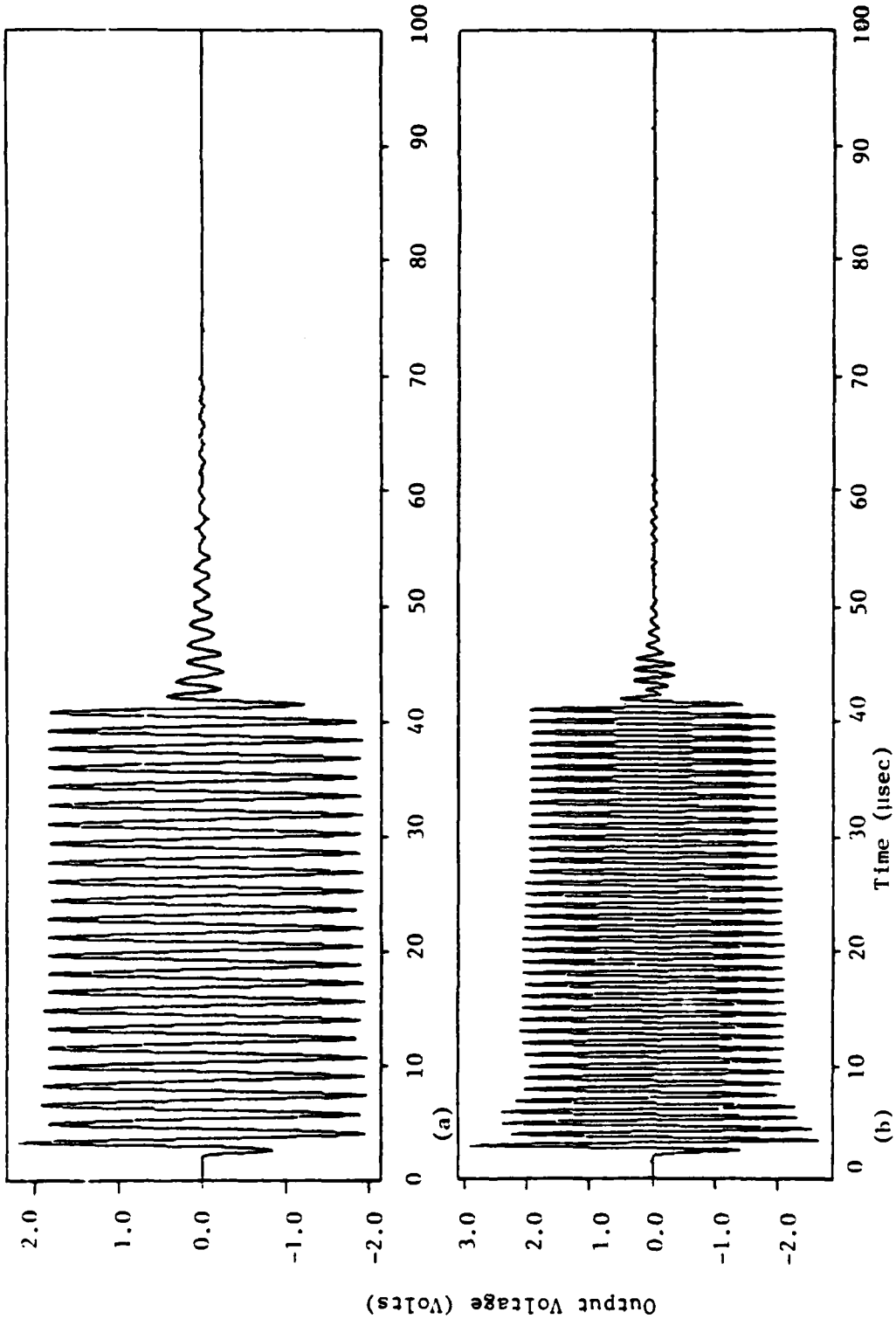

Fig. D8 Measured output signals corresponding to (a) 0.6 MHz and (b) 1.0 MHz tone burst input signals for 1.270 cm (0.500 in) aluminum plate clamped between two AE-103 transducers.

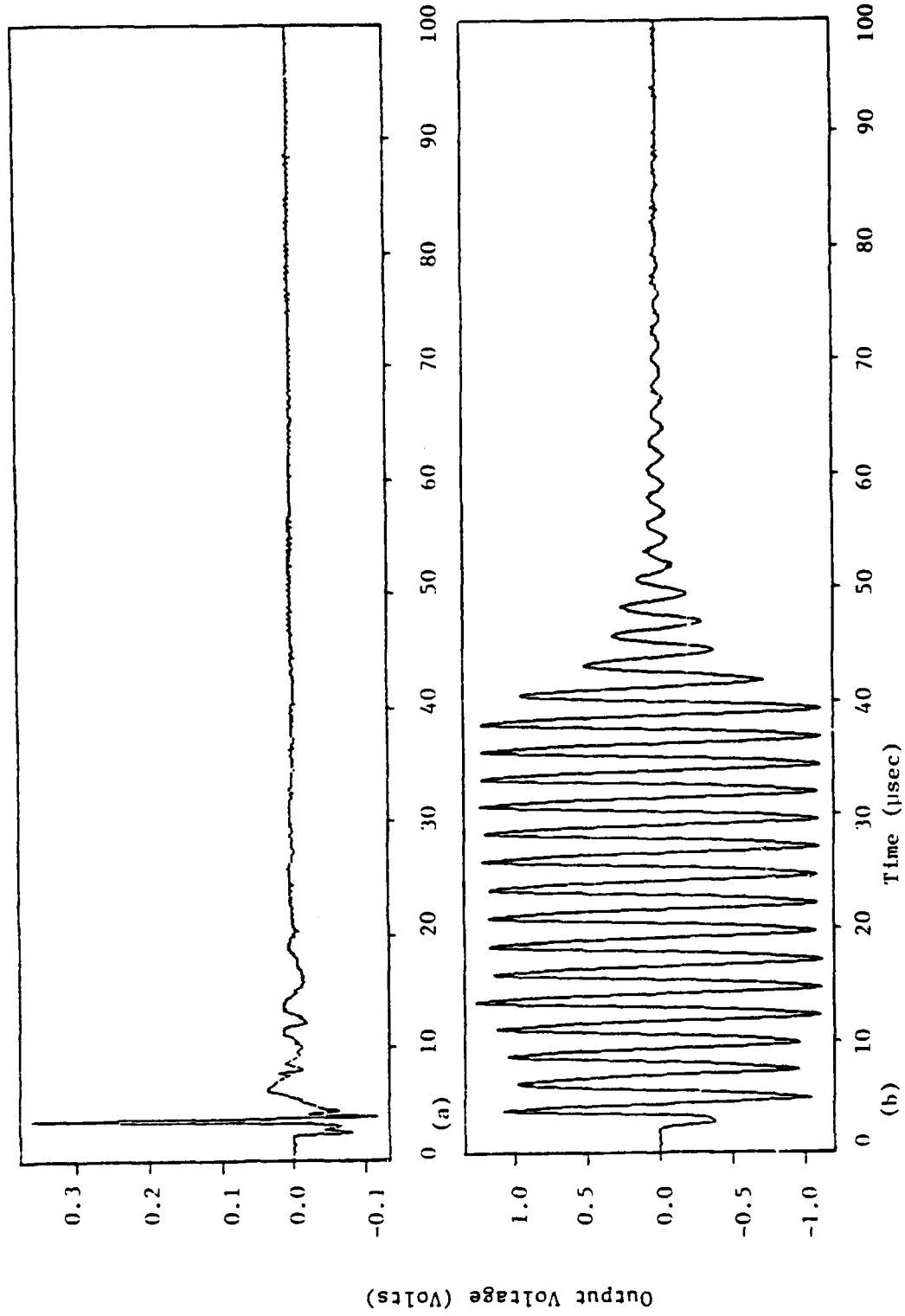

Fig. D9 Measured output signals corresponding to (a) broadband pulse and (b) 0.4 MHz tone burst input signals for 1.270 cm (0.500 in) aluminum plate clamped between two FC-500 transducers.

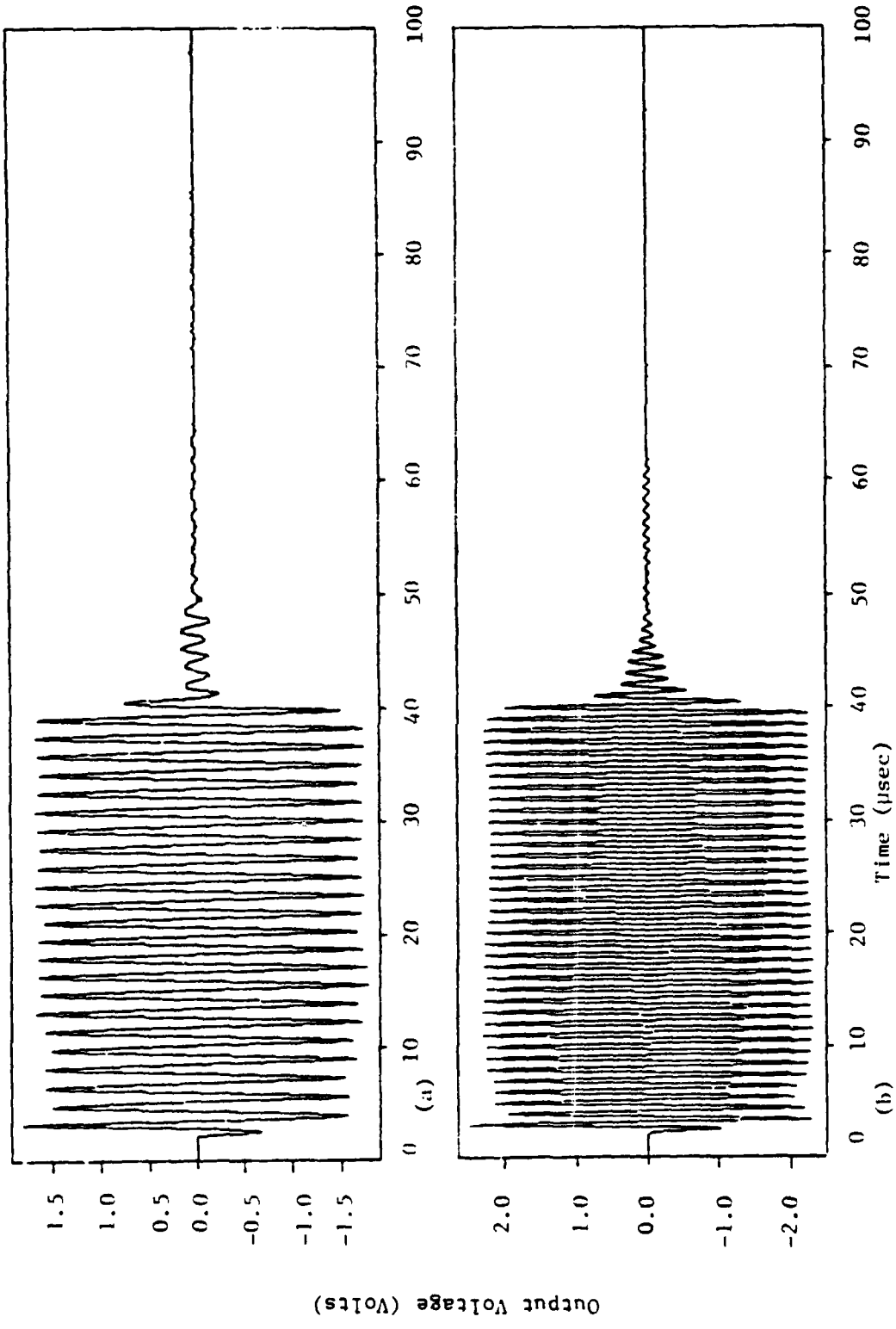

Fig. 4.10 Measured output signals corresponding to (a) 0.6 MHz and (b) 1.0 MHz tone burst input signals for 1.270 cm (0.500 in) aluminum plate clamped between two FC-500 transducers.

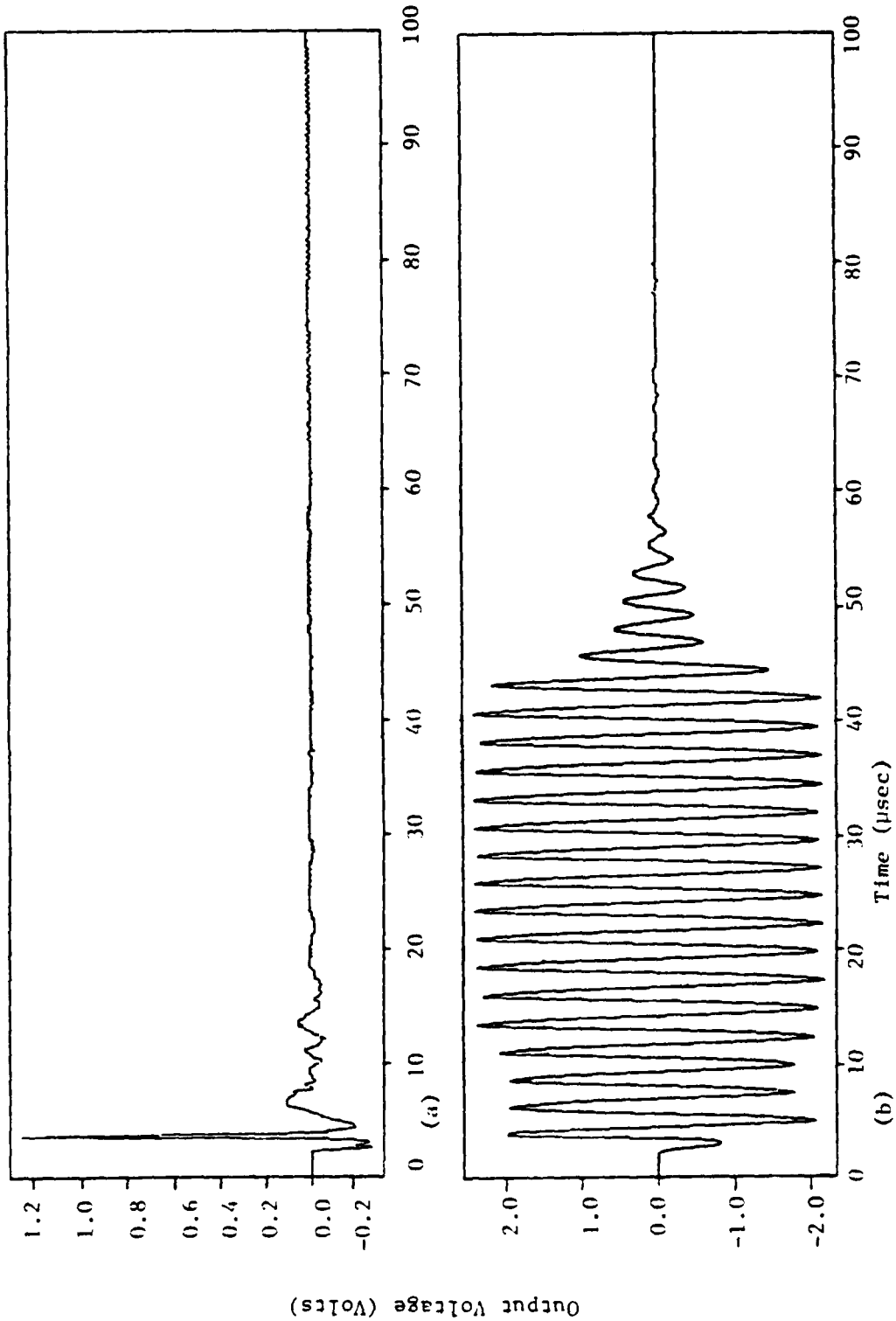

Fig. 511 Measured output signals corresponding to (a) broadband pulse and (b) 0.4 MHz tone burst input signals for 1.270 cm (0.500 in) aluminum plate clamped between two AE-101 transducers.

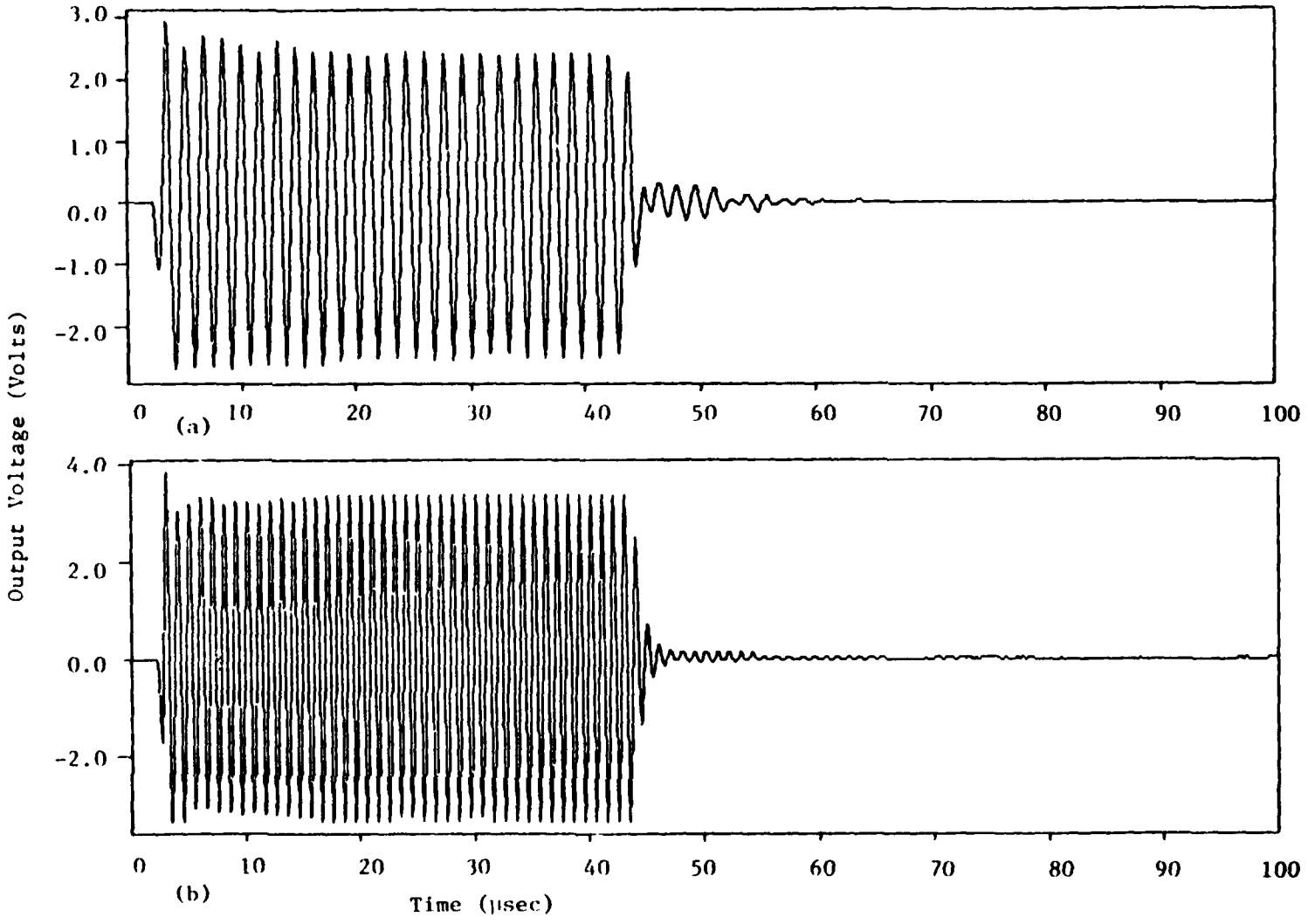

Fig. D12 Measured output signals corresponding to (a) 0.6 MHz and (b) 1.0 MHz tone burst input signals for 1.270 cm (0.500 in) aluminum plate clamped between two AE-101 transducers.

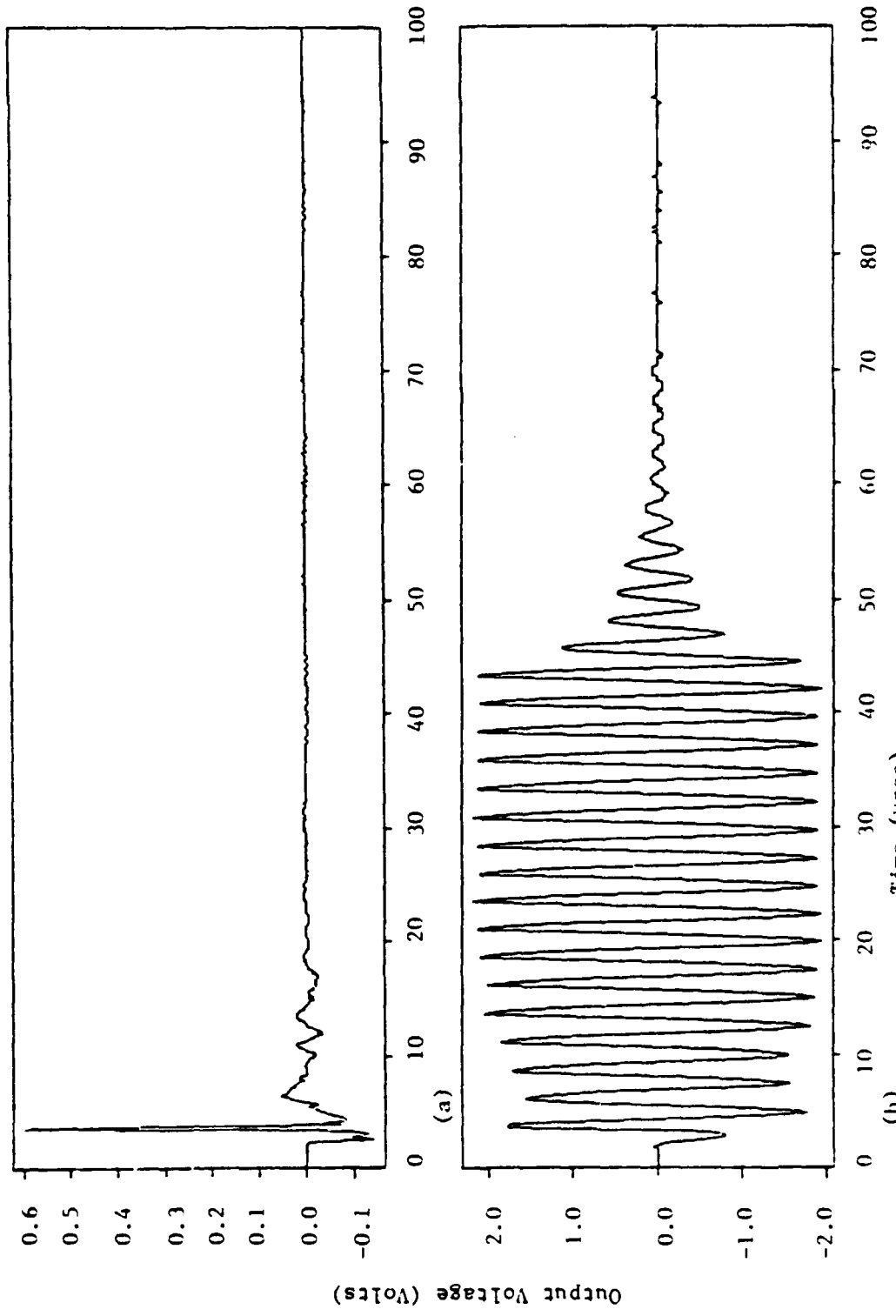

Fig. D13 Measured output signals corresponding to (a) broadband pulse and (b) 0.4 MHz tone burst input signals for two 0.635 cm (0.250 in) aluminum plates with intermediate couplant layer clamped between two AE-101 transducers.

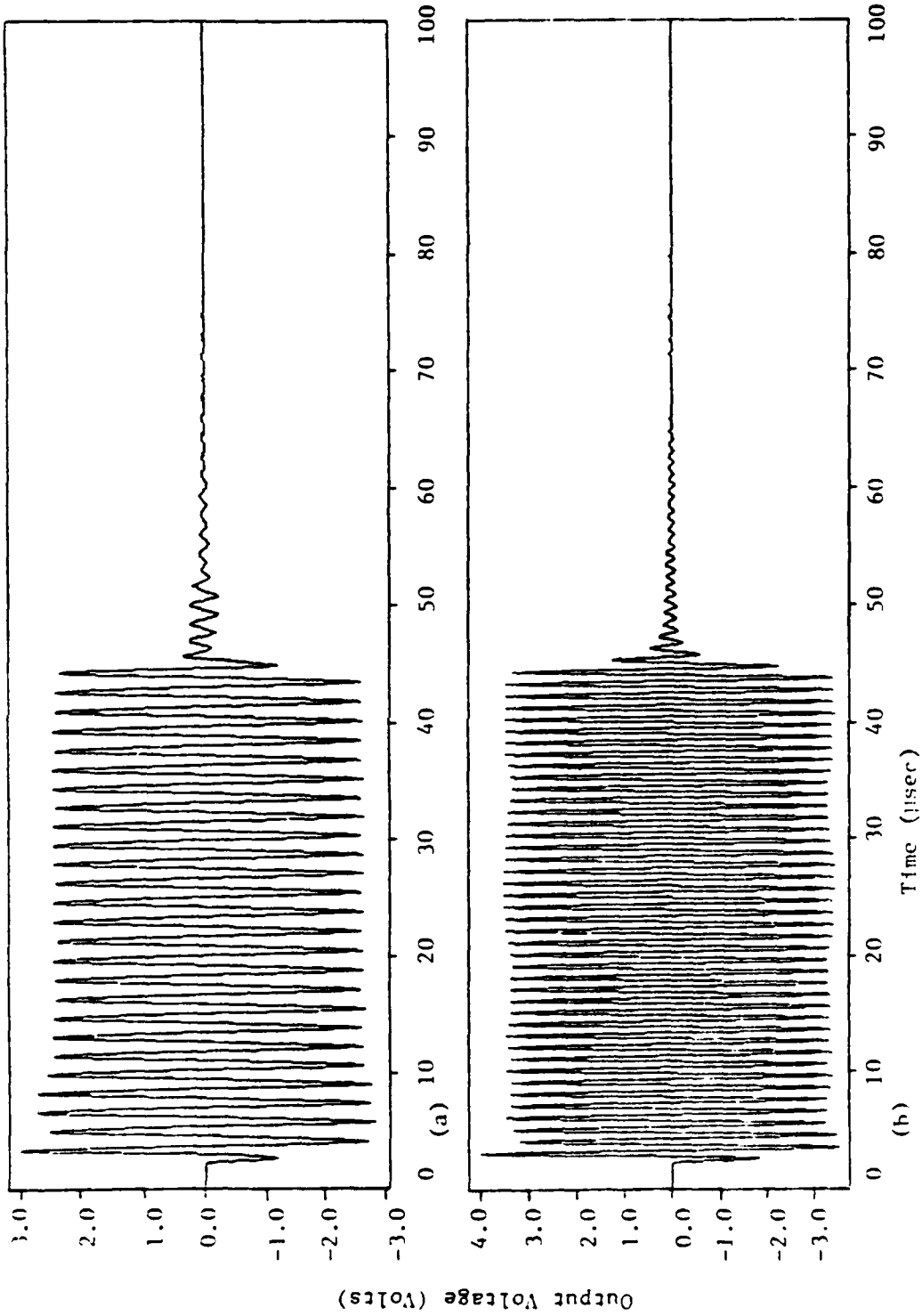

Fig. D14 Measured output signals corresponding to (a) 0.6 MHz and (b) 1.0 MHz tone burst input signals for two 0.635 cm (0.250 in) aluminum plates with intermediate couplant layer clamped between two AE-101 transducers.

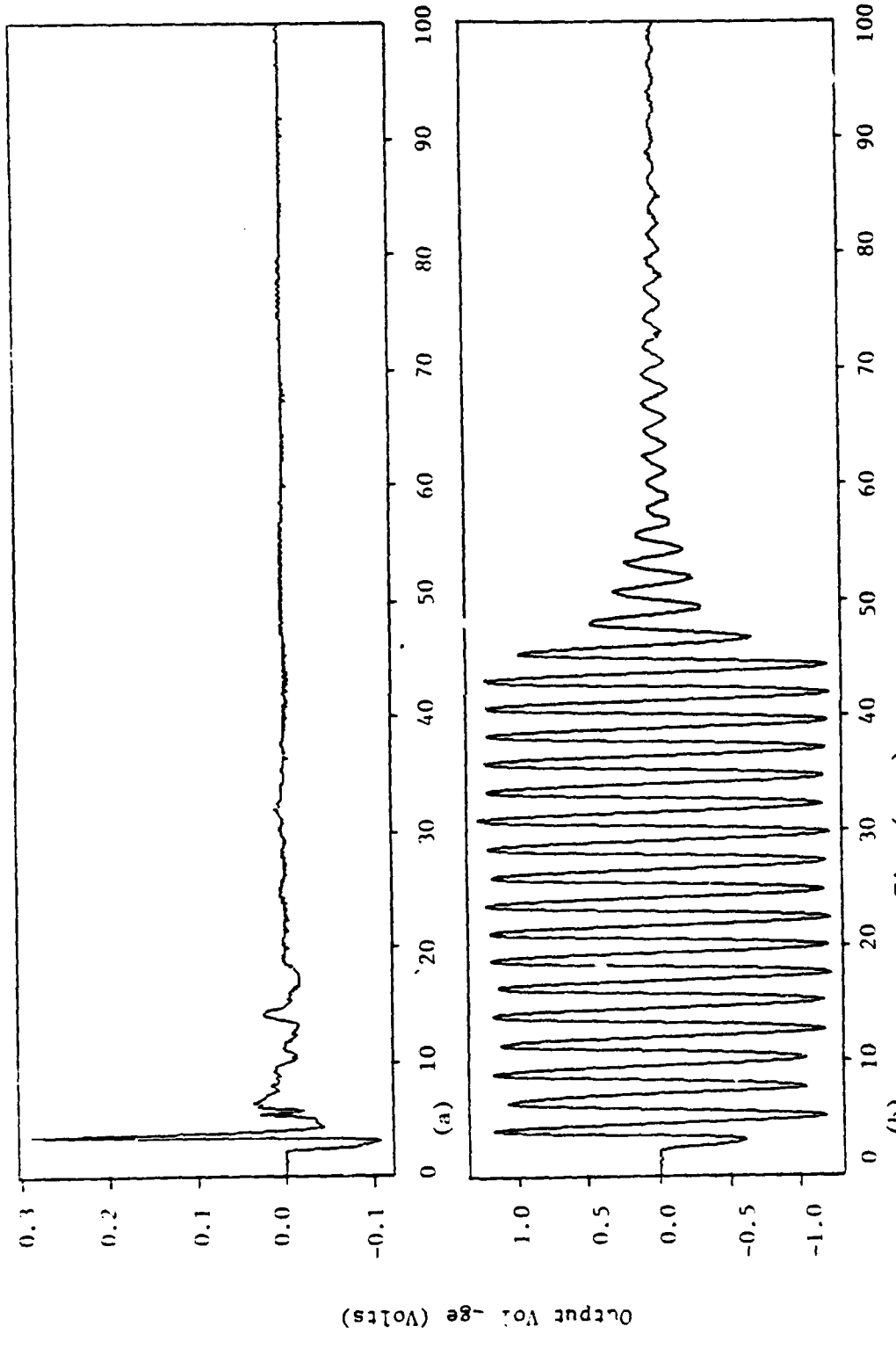

Fig. D15 Measured output signals corresponding to (a) broadband pulse and (b) 0.4 MHz tone burst input signals for two 0.635 cm (0.250 in) aluminum plates with intermediate epoxy layer clamped between two AE-101 transducers.

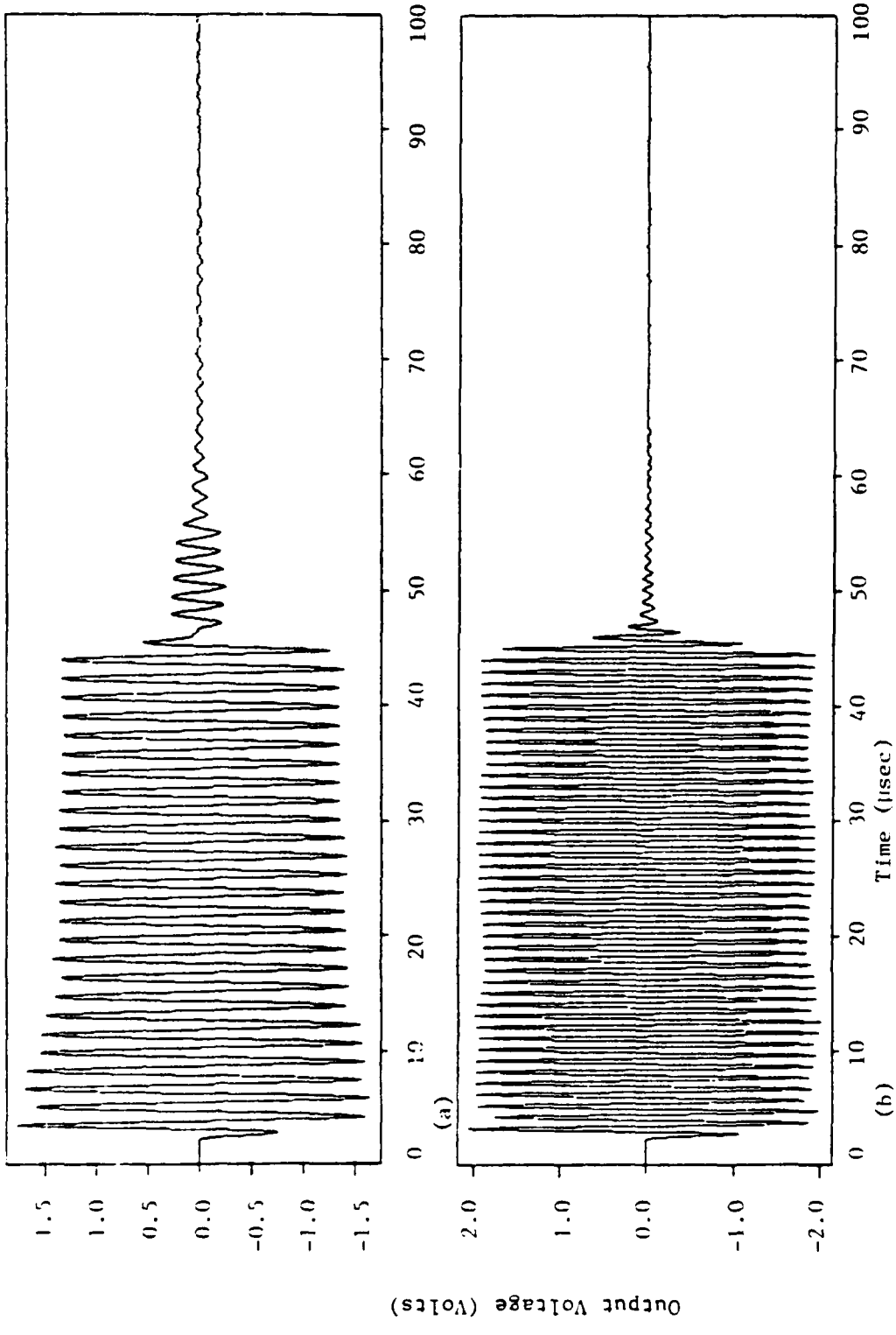

Fig. D16 Measured output signals corresponding to (a) 0.6 MHz and (b) 1.0 MHz tone burst input signals for two 0.635 cm (0.250 in) aluminum plates with intermediate epoxy layer clamped between two AE-101 transducers.

APPENDIX E

CHARACTERIZATION OF AN ULTRASONIC TEST SYSTEM USING THE WAVE PROPAGATION MODEL

In this appendix, the wave propagation model developed in Chapter 2 is used to characterize a particular ultrasonic through-transmission test system, consisting of two AET FC-500 transducers clamped face-to-face. The characterization is accomplished by using the wave propagation model to predict the output signal for a particular input signal, and then comparing that predicted output signal to the measured output. The values of various parameters which serve as inputs to the model are then changed one at a time to obtain the best agreement between predicted and measured output signals. In the following sections, this process will be referred to as "correlation."

Fig. E1 shows the measured output of the system for a broadband pulse input. Observe that the output consists of two distinct wave packets, called the primary wave and backing wave, respectively. The primary wave corresponds to wave interaction in the piezoelements and wearplates of the system, and the backing wave is a result of waves traveling through the backing layers [24]. Since the two wave packets represent the influence of different transducer components, they can be correlated separately.

The correlation of each wave packet takes place in four steps:

(1) Experimental observations are made concerning the

particular wave under consideration.

(2) The wave propagation model is used to generate a preliminary prediction, based on the current best estimates for all modeling parameters.

(3) The values of various parameters are selectively changed to improve the correlation between predicted and measured results.

(4) A "best" prediction is made, which represents the best correlation which can be obtained between measured and predicted results without adding additional parameters to the model.

These four steps make up the subsections of the following primary-wave and backing-wave studies for the characterization of two FC-500 transducers face-to-face.

E.1 CORRELATION OF PRIMARY WAVE USING BROADBAND PULSE INPUT

The primary wave is correlated using the broadband pulse as an input signal. The short duration of the pulse makes it the best signal to use for studying the primary wave, and the fact that it covers a relatively broad range of frequencies does not matter, since the properties of the wearplate and piezoelement are not frequency-dependent.

E.1.1 Experimental Observations Concerning the Primary Wave

Fig. E1 shows the broadband input pulse and the resulting output signal for the system. The first wave packet of the output is of interest here, and is shown on an expanded time scale in Fig. E2. It is evident from these plots that the conversion of input to output in the system is not a trivial process. A logical first step toward accurately predicting this output signal is the

development of an intuitive feel for the input-output behavior of the system.

Fig. E3 is a schematic of the propagation of stress waves through the system. The solid lines represent the paths of the various wavefronts in the system as they are generated at the surfaces of the input piezoelement, propagated through the various transducer layers, reflected from impedance-mismatched interfaces, and finally detected at the surfaces of the output piezoelement. Since this section deals only with the primary wave, waves entering the backing layer are ignored and are shown as dotted arrows in the drawing.

In Chapter 2 (section 2.1) it is shown that applying a voltage impulse to the input transducer at time t=0 causes four stress impulses to be generated at the surfaces of the piezoelement at that instant. Observe from Fig. E3 that the stress impulse produced at the front face of the input piezoelement (P_1W_1) which strikes the front face of the output piezoelement (W_2P_2) produces a positive voltage A(11), the first impulse of the output signal. This wave then propagates through the output piezoelement and strikes its rear surface (P_2B_2), producing a negative voltage A(21) at precisely the same instant as the wave from the rear of the input piezoelement reaches the front surface of the output piezoelement. This last wave then continues on into the output piezoelement, producing a positive voltage A(31) as it strikes the rear surface (P_2B_2). Fig. E4 shows schematically how the primary wave may be constructed by simply superposing the input pulse weighted by A(11), A(21),

and A(31) at the appropriate arrival times.

Note also the presence of multiple reflections produced at the wearplate-piezoelement interfaces, which are called A(12), A(13), and so on. Analysis shows that, for the FC-500, only the first two of these reflections make a significant contribution (greater than 1% of the amplitude of the first impulse) to the output signal. It is, therefore, the nine wavefronts shown in Fig. E3 which combine to produce the output signal seen in Fig. E2.

E.1.2 Preliminary Predictions of the Primary Wave

Fig. E5 shows the broadband pulse response of the system as predicted by the model, using the measured values given in Fig. C2 as inputs to the model. The values of all modeling parameters used in each simulation are given in Table 1; in general, only the particular parameters of interest will be mentioned in the discussion.

Fig. E5 shows fair agreement between predicted and measured output signals. The predicted initial time delay is only 0.06 μsec, as compared to the measured delay of 0.22 μsec. This discrepancy of 0.16 μsec could be the result of an error in the calculated wearplate transit time (wavespeed or thickness), since the initial time delay is simply twice the wearplate transit time, as seen in Fig. E3. An alternative explanation would involve a time delay introduced at either the couplant layer or at the wearplate-piezoelement interfaces. It is also possible that the piezoelement takes some time to respond to stress and produce a voltage.

Other than the time delay, the most obvious discrepancy in Fig. E5 occurs after 2 μsec, with the appearance of disturbances in the measured signal that do not show up in the predicted signal. Because of the similarity between the first 2 μsec of the two signals, however, it seems that the three main peaks (corresponding to A(11), A(21), and A(31) in Fig. E3) fall at about the right times and with reasonably correct amplitudes in the predicted output. The only source for disturbances after 2 sec would be the multiple reflections A(12), A(13), A(22), A(23), A(32) and A(33) which are generated at the wearplate-piezoelement interfaces. These do not appear in the predicted output of Fig. E5 because of the extremely short transit time of the wearplates (0.04 μsec), so that the predicted multiple reflections are only 0.16 μsec apart, whereas those in the measured output are almost 0.6 μsec apart. It seems likely that a time delay is introduced as the waves are reflected from the wearplate-piezoelement interfaces.

E.1.3 Effect of Wearplate-Piezoelement Time Delays on the Primary Wave

Fig. E6 illustrates the effect of including a time delay, β, in the simulation, showing predicted output signals for values of β from 0.08 to 0.32 μsec. These curves do indeed show disturbances beyond 2 μsec, as expected. In particular, the signal for which β=0.24 μsec bears a marked resemblance to the measured output signal of Fig. E5.

It is interesting to note the effects of introducing these

time delays. If only the reflected waves are delayed, as is the case in Fig. E6, the arrival times of wavefronts A(11), A(21), and A(31) remain unchanged, because none of these waves undergoes any reflection (see Fig. E3). The time interval between A(11) and A(12) is affected, however, and so is the interval between A(12) and A(13), A(21) and A(22), and so on.

Now consider delaying the transmitted waves at the wearplate-piezoelement interfaces. This has the effect of delaying every wavefront by precisely the same amount, since each wave is transmitted across each interface once and only once. A time delay, δ, of 0.08 μsec for the transmitted waves therefore resolves the discrepancy in the initial time delay noted earlier. It is concluded, then, that waves reflected from the wearplate-piezoelement interfaces are delayed by 0.24 μsec, and that waves transmitted across these interfaces are delayed by 0.08 μsec.

E.1.4 Effect of the Time Constant RC_o on the Primary Wave

The predicted output signal of Fig. E5 is based on the assumption that the output piezoelement produces a voltage proportional to the integral of the stress inside it. This is a good approximation if the resistance across the piezoelement is large, because electrically the piezoelement behaves like a capacitor, and will continue to accumulate voltage if no path is provided for current to flow from one plate of the capacitor to the other. If, however, there is a relatively small resistance across the piezoelement, the voltage will decay with time according to the factor $\exp(-t/RC_o)$, where C_o is the capacitance

of the piezoelement, and R is the resistance across it. The output voltage is then no longer proportional to the integral of the stress inside the piezoelement, but to the convolution of stress with an exponentially-decaying function of time (see Chapter 2, section 2.5).

If the value of RC_o in the simulation is decreased, the shape of the output signal changes drastically, as seen in Fig. E7. A time constant which is of the same order of magnitude as other time parameters in the system allows the output voltage to decay in "real time," so that it does not accumulate as fast as it would if RC were larger. If the time constant is made small enough, the voltage never accumulates at all, and the output voltage is proportional to the stress itself rather than to the integral of stress, as shown in Fig. E7(a). The other three curves of Fig. E7 show that increasing the time constant has two effects: it increases the amplitude of the peak at 1.1 μsec, and decreases the amplitude of the peak at 1.8 μsec. Comparing these predicted output signals to the measured output of Fig. E5 indicates that the value of the time constant for the system under consideration is about 1.0 μsec.

E.1.5 Best Prediction of the Primary Wave

The best predicted output signal corresponding to a broadband pulse input is presented for comparison with the measured output signal in Fig. E8. The important parameters used in the simulation are the time delays β=0.24 μsec and δ=0.08 μsec, and the time constant RC_o=1.0 μsec. Qualitatively, the measured and

predicted curves appear to correlate very well. Quantitatively, they indicate that the amplitude parameter h^2C_o/S has the value 5.47×10^{15} N/m^3 for this case.

E.2 CORRELATION OF THE BACKING WAVE USING TONE BURST INPUT

It is easier to correlate the backing wave using a tone burst input signal for several reasons. First, the attenuation of the backing material used in the transducers is frequency-dependent, and the narrow bandwidth of the tone burst signals enables the determination of attenuation at several different frequencies. Second, it is easier to determine the exact time delay associated with the backing wave when a tone burst is used, since the time delay directly affects the phase angle between the primary wave and the backing wave. Although the primary wave has been correlated with a broadband input pulse, the optimum values for δ, S, and RC_o have been found to be the same for tone bursts across the entire frequency range (0.4-2.0 MHz) as for the pulse.

E.2.1 Experimental Observations Concerning the Backing Wave

Fig. E9 shows the measured 0.4 MHz tone burst input and output signals for two FC-500 transducers face-to-face. Observe that the input signal takes three full cycles to settle down to a steady amplitude, and that this transient shows up in the output signal as well. Note also, however, that the output shows other disturbances at about 10 μsec after the input is first applied. Recall from Fig. E1 that 10 μsec is the observed time delay associated with the backing layer, so that both the disturbance at

10 μsec and the reduced-amplitude oscillation from 25 to 35 μsec are due to waves traveling through the backing layer.

E.2.2 Preliminary Predictions Including the Backing Wave

Fig. E10 shows the measured output signal and the predicted output, the latter obtained by using the measured values for thickness and attenuation of the backing material at 0.4 MHz. Observe that the first three cycles of the predicted output compare very favorably with the measured output, but that when the backing wave arrives at about 10 μsec, the amplitude of the predicted output is greatly reduced. One would suspect that the value of backing attenuation is too high—that the predicted amplitude of the backing wave is too small. The plot shows, however, that when everything except the backing wave has died out (30 μsec), the predicted backing wave actually has a larger amplitude that the measured one. Observe also that the last full-amplitude peak of the measured output (before the amplitude begins to taper off) occurs at about 31 μsec, but only at 29.5 μsec for the predicted output. These observations indicate that the predicted backing wave arrives about 1.5 μsec too early, necessitating the introduction of a time delay similar to those used in the previous section.

E.2.3 Effect of Time Delays on the Backing Wave

Fig. E11 shows the predicted output signals for several values of time delay, γ, introduced as waves propagate through the backing layer and reflect from the backing-potting interface.

These time delays were simulated by increasing the value of backing thickness in the input data for the model, in order to also illustrate the dependence of the amplitude of the backing wave on the thickness of the backing layer itself. The difference in amplitude over the range of backing thickness shown in Fig. E11 is quite small, but one can see that the backing wave decreases slightly in amplitude for increasing backing thickness.

The more important effect seen in Fig. E11 is the rather strong dependence of the steady-state output amplitude on the time delay. Note that the variation in steady-state amplitude as a result of changes in the time delay is much greater than the variation in the amplitude of the backing wave itself. This is due to the effect of the time delay, γ, on the phase angle between the primary wave and the backing wave. A change of 0.1 μsec in the time delay is equivalent to a 15 degree shift in phase at 0.4 MHz, so that over the range of time delays in Fig. E11, the phase angle between the primary and backing waves varies by 45 degrees. This can make the difference between the backing wave having a strong effect on the steady-state amplitude, as in plot (a), and, as in plot (d), the steady-state signal being virtually independent of the backing wave, depending only on the primary-wave amplitude.

Fig. E10 shows quite graphically the extreme case, that of nearly totally destructive interference between the backing and primary waves. Note that the output shows a drastic decrease in amplitude due to the arrival of the backing wave at 10 μsec, and that it exhibits a sort of phase reversal at about 25 μsec, when

the primary wave dies out and the backing wave takes over. Comparing Fig. E10 and Fig. E11(a) shows the sort of effect that relatively small changes in the time delay can have on the output of the system. This effect is, of course, frequency-dependent as well, because the phase angle corresponding to a particular time delay is a function of the frequency.

It is concluded, then, that there is a time delay introduced as waves are propagated through the backing layer and reflected from the backing-potting interface. This time delay is particularly significant in that it affects the phase angle between the primary wave and the backing wave, and consequently can affect the steady-state output amplitude to a great extent. More discussion of the steady-state output amplitude is given in Appendix G.

E.2.4 Effect of Backing Attenuation on the Backing Wave

Fig. E12 shows the result of varying the attenuation parameter, α_B, of the backing material. As expected, the only effect on the output is a change in the amplitude of the backing wave and, to a lesser degree, the steady-state amplitude. From these two studies it is concluded that the best correlation between theory and experiment at 0.4 MHz is obtained for the values γ=1.40 μsec and α_B=1.8 nepers/cm.

E.2.5 Best Prediction Including the Backing Wave

Fig. E13 shows the best predicted output signal for a 0.4 MHz tone burst input, along with the measured output for

comparison. Once again, the correlation is impressive, and the value of h^2C_o/S is found to be 3.80×10^{15} N/m^3, only slightly smaller than that found from the broadband pulse results.

To complete the characterization, the backing wave can be correlated at as many frequencies as desired, using the same procedure as described in this section. For example, Fig. E14 shows the measured input and output signals for a 0.6 MHz tone burst input, and Fig. E15 shows the best prediction, obtained from the parameter values γ=1.40 μsec and α_B=2.5 nepers/cm. The amplitude factor h^2C_o/S=4.72×10^{15} N/m^3 for this case.

The values of the modeling parameters for the FC-500, as well as for all of the other transducers, are presented in Tables 2 through 6 and are discussed in Chapter 4.

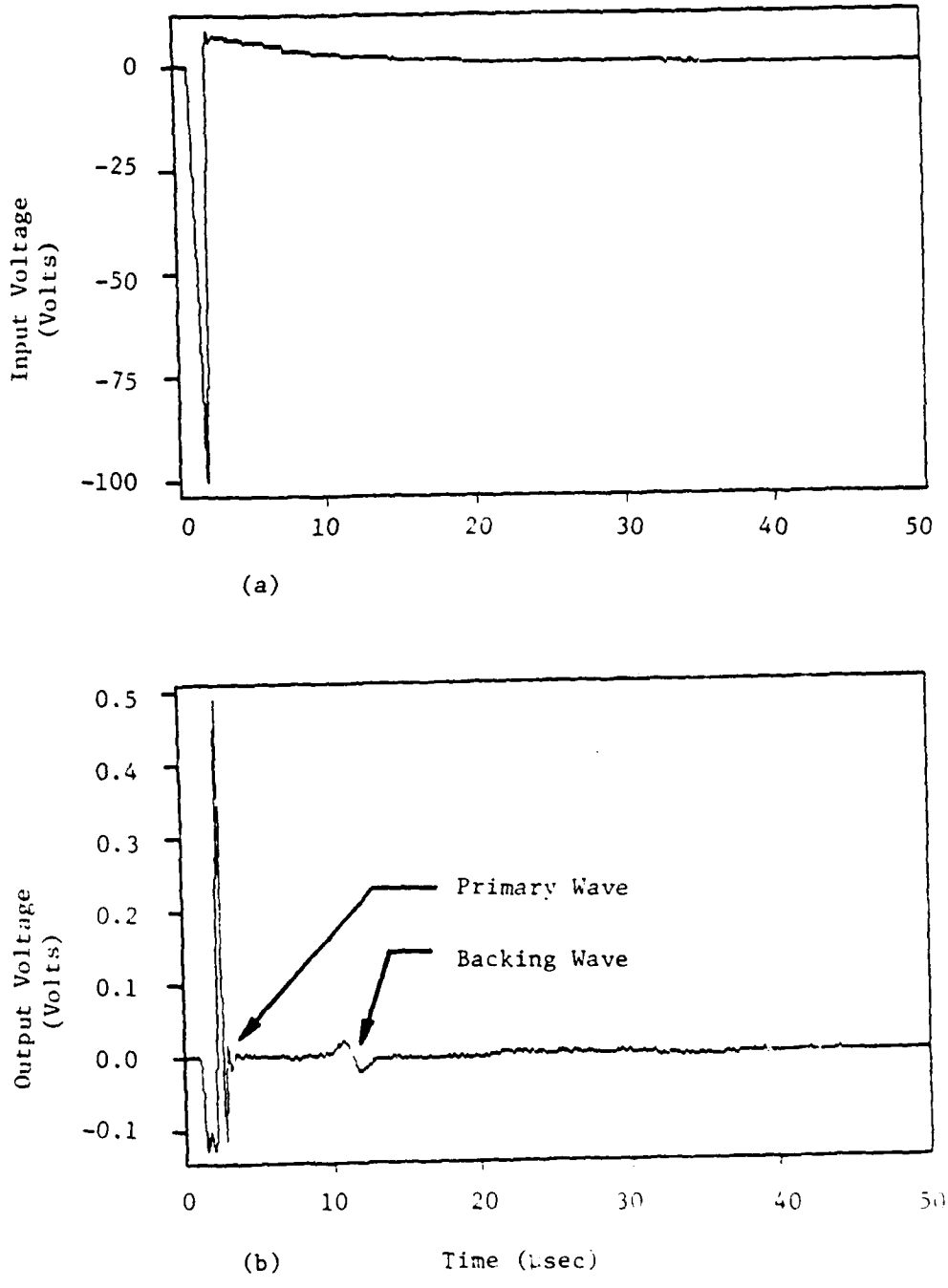

Fig. E1 Measured broadband pulse (a) input and (b) output signals for two FC-500 transducers clamped face-to-face.

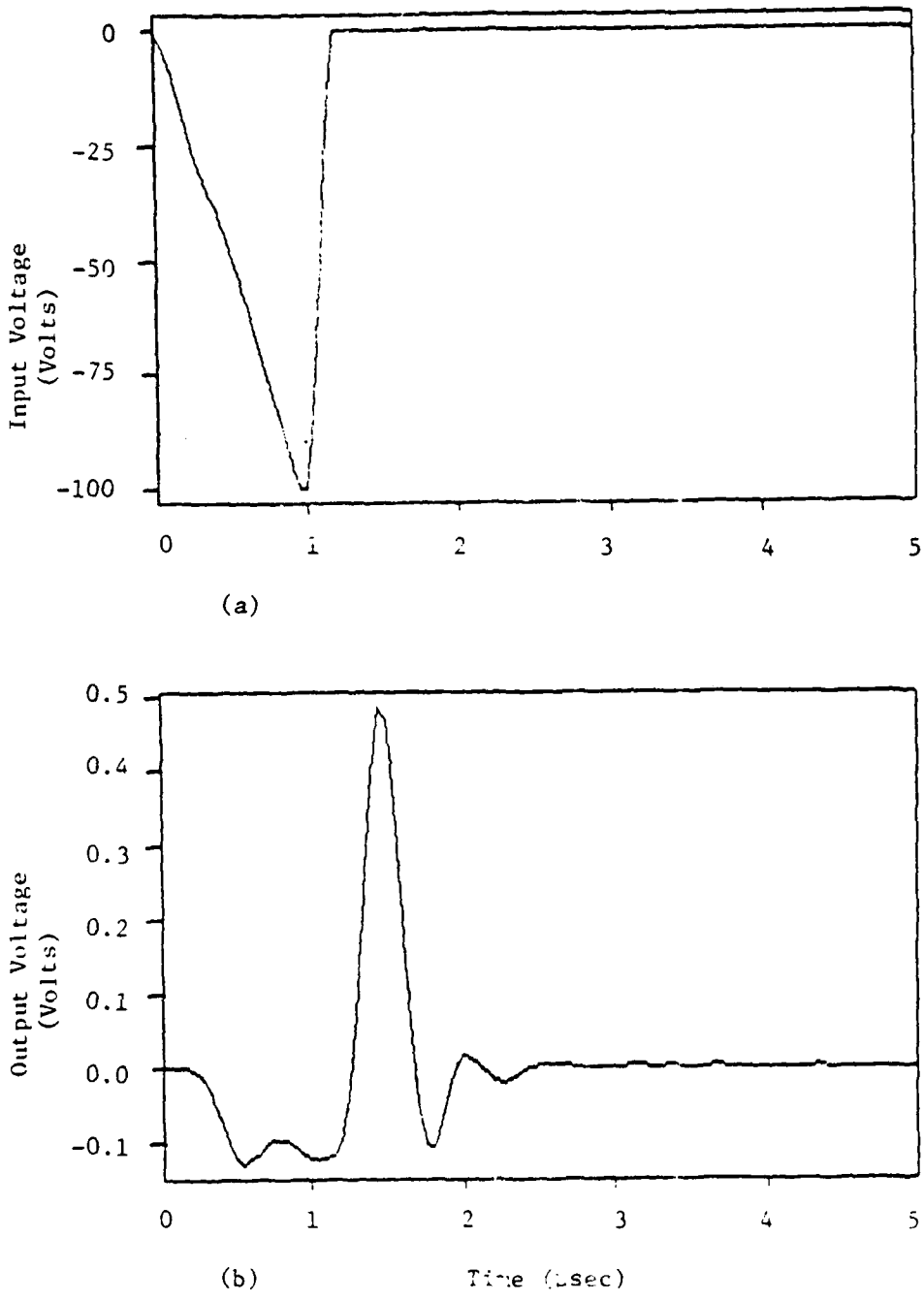

Fig. E2 Measured broadband pulse (a) input and (b) output signals for two FC-500 transducers clamped face-to-face (expanded time scale).

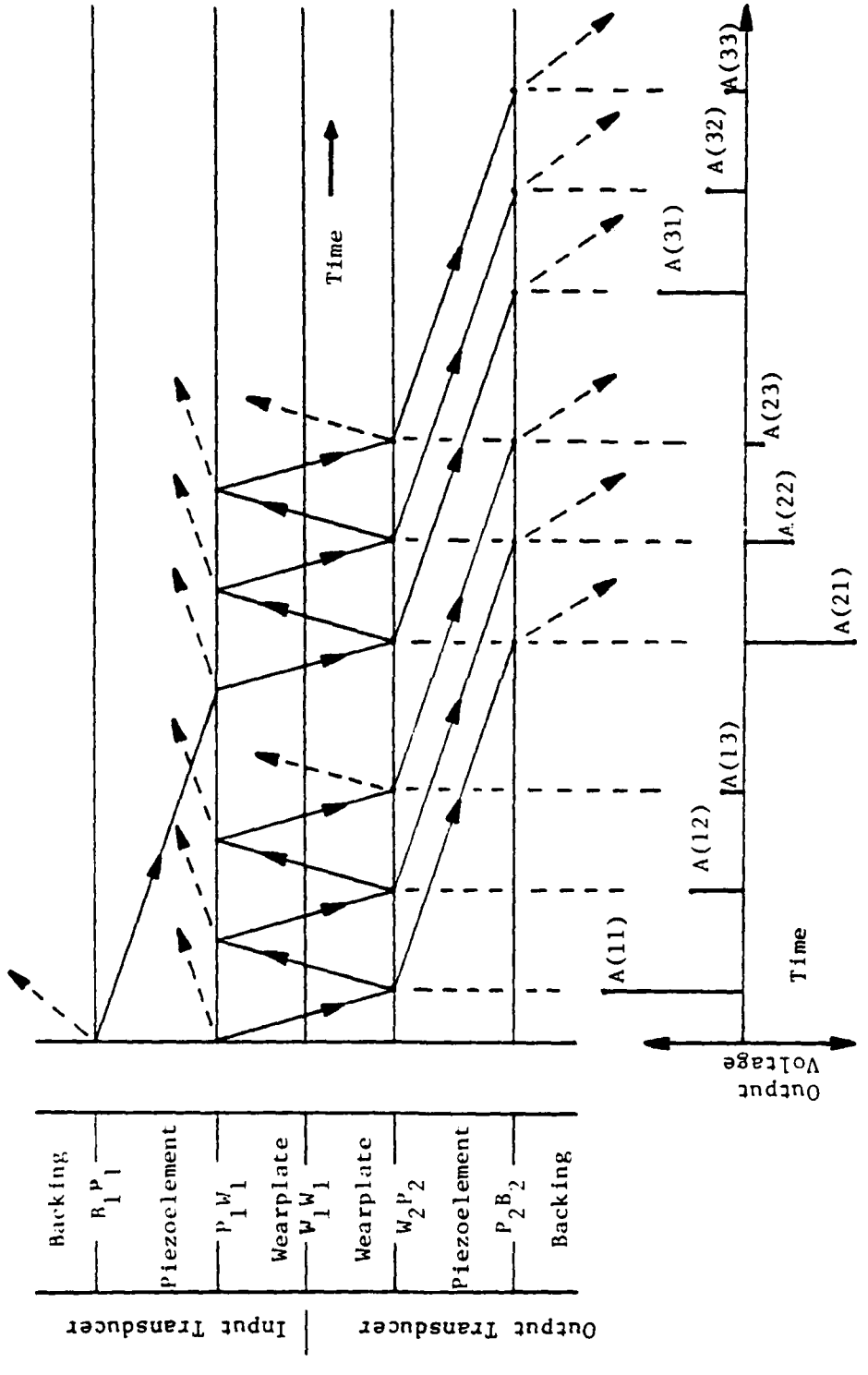

Fig. E3 Schematic of (a) the propagation of stress waves and (b) the production of output voltage in an ultrasonic test system consisting of two transducers clamped face-to-face.

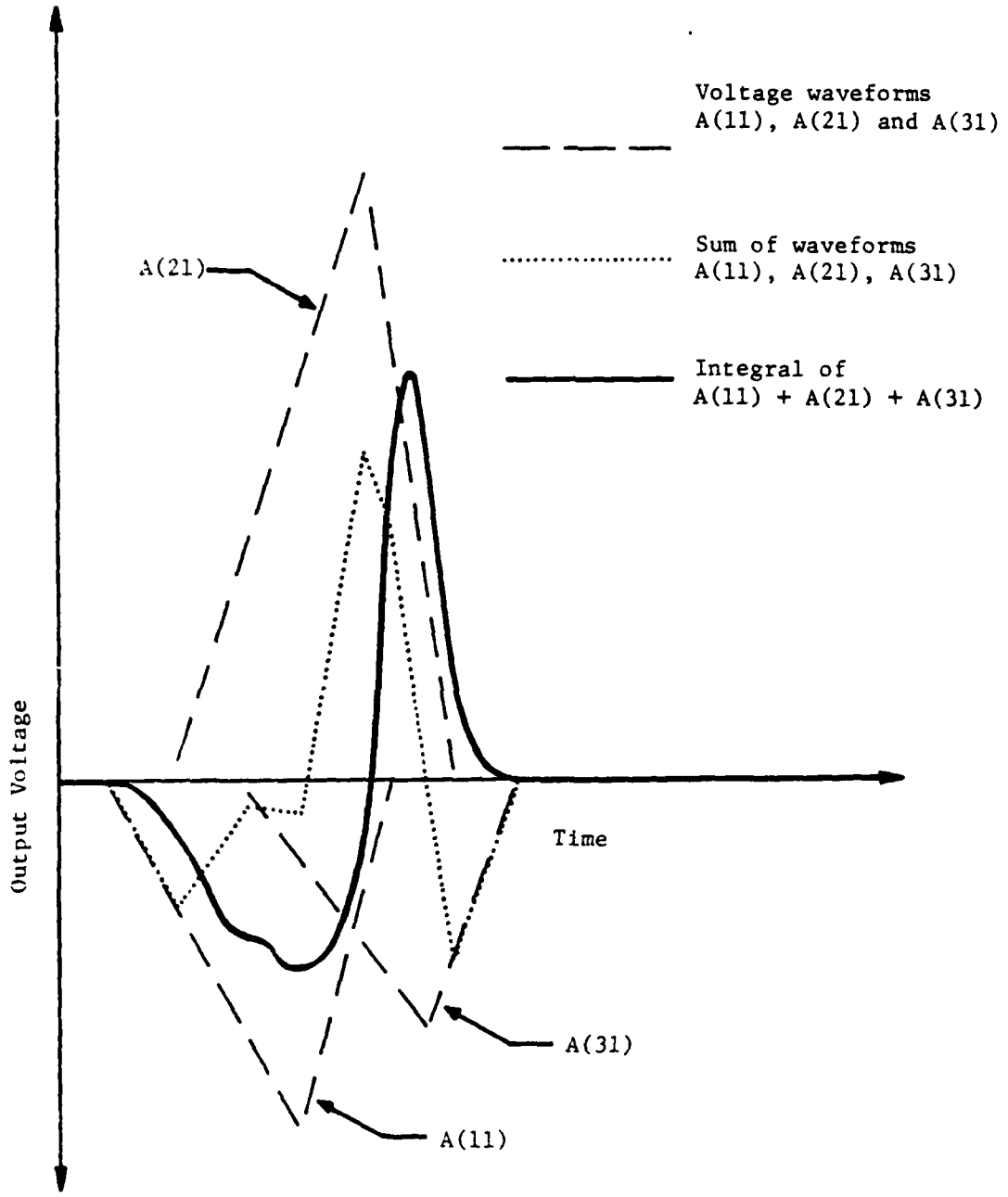

Fig. E4 Construction of output pulse from primary stress waves A(11), A(21), and A(31).

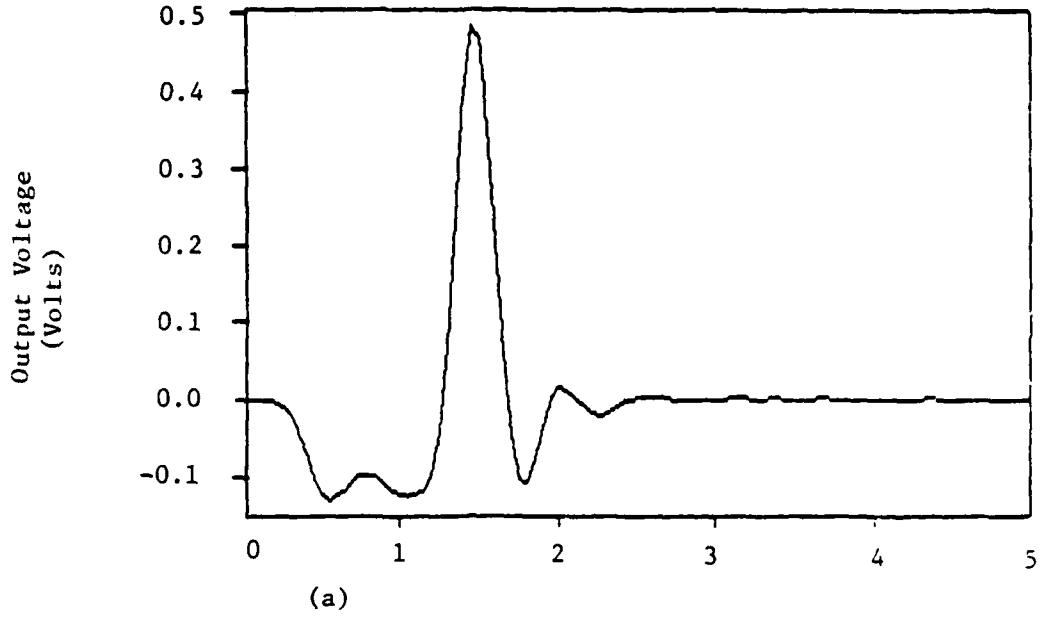

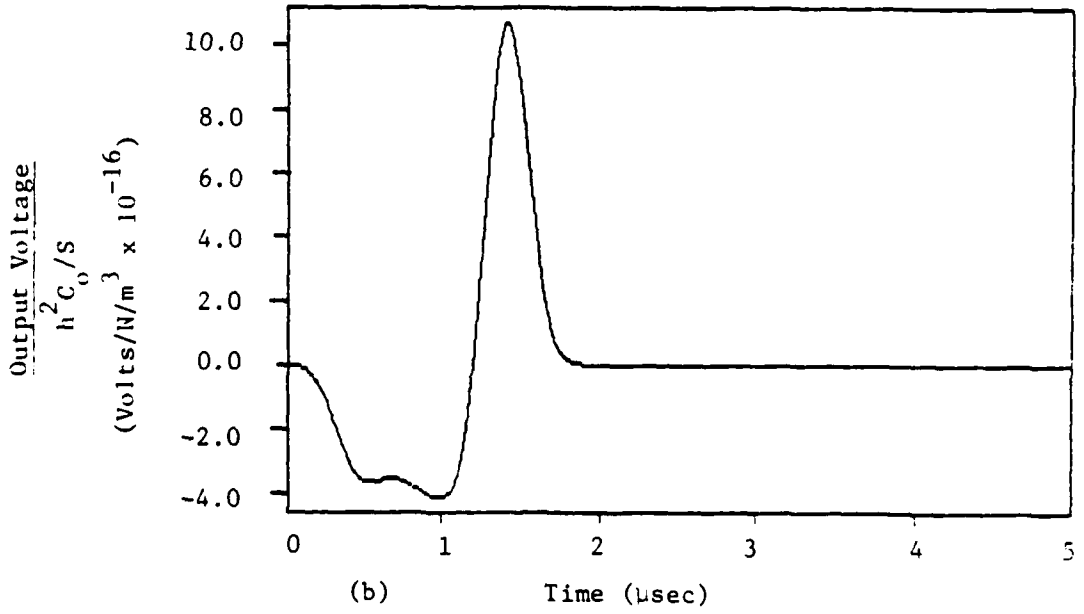

Fig. E5 Comparison of (a) measured and (b) predicted output signals corresponding to broadband pulse input for two FC-500 transducers clamped face-to-face (δ=0, β=0, RC_o=0).

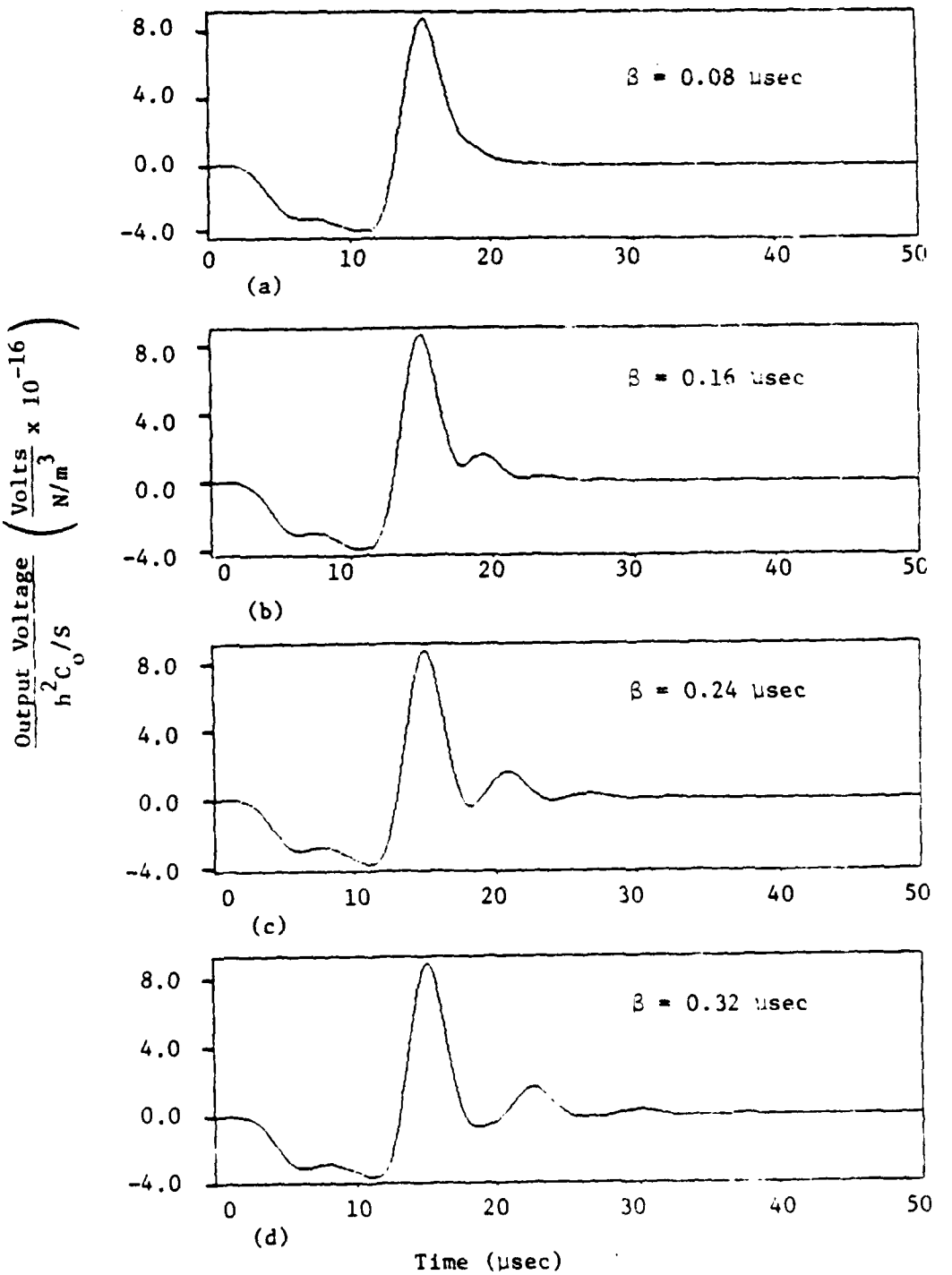

Fig. E6 Predicted broadband pulse response of two FC-500 transducers clamped face-to-face as a function of the time delay β.

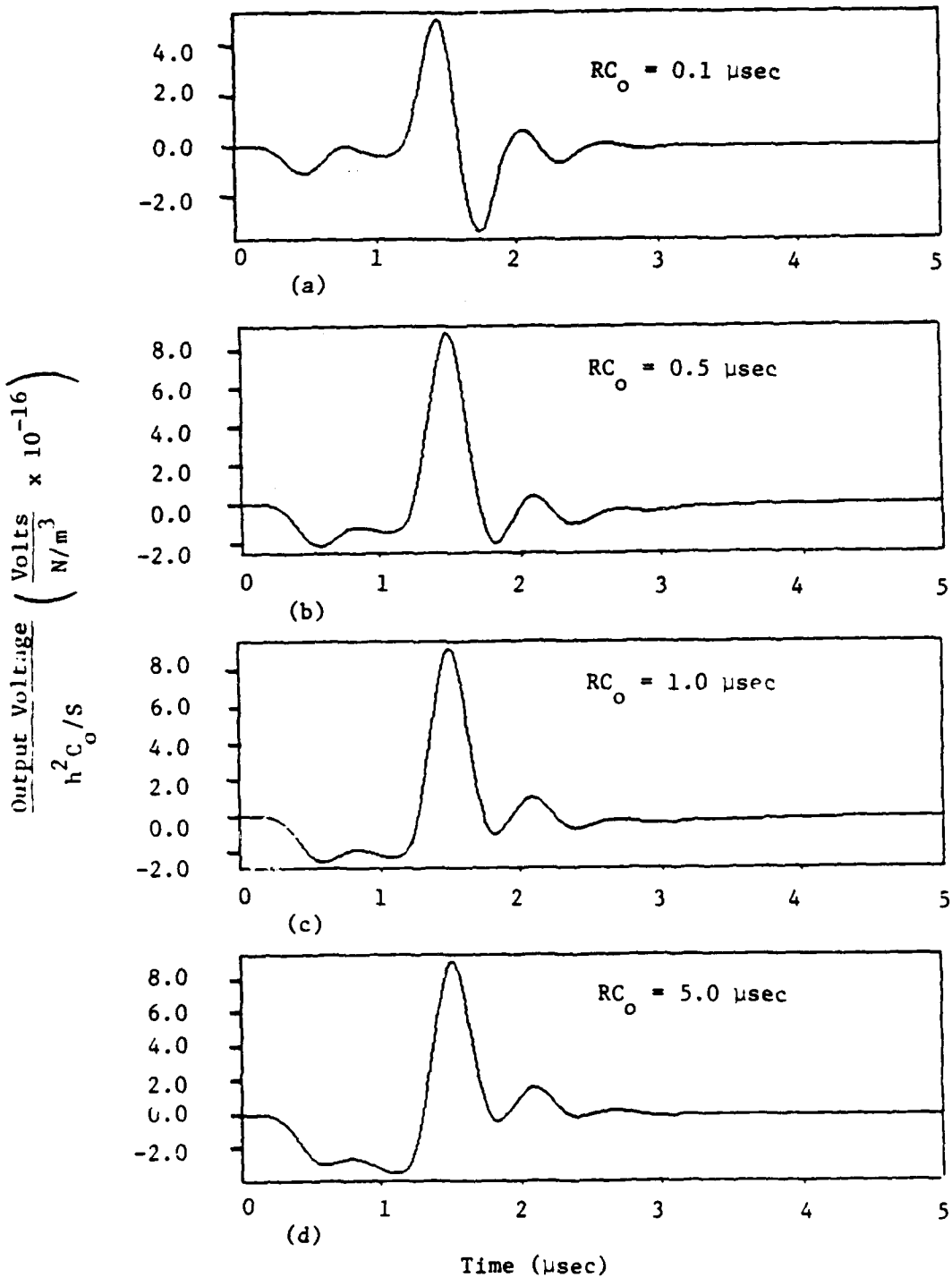

Fig. E7 Predicted broadband pulse response of two FC-500 transducers clamped face-to-face as a function of the time constant RC_o.

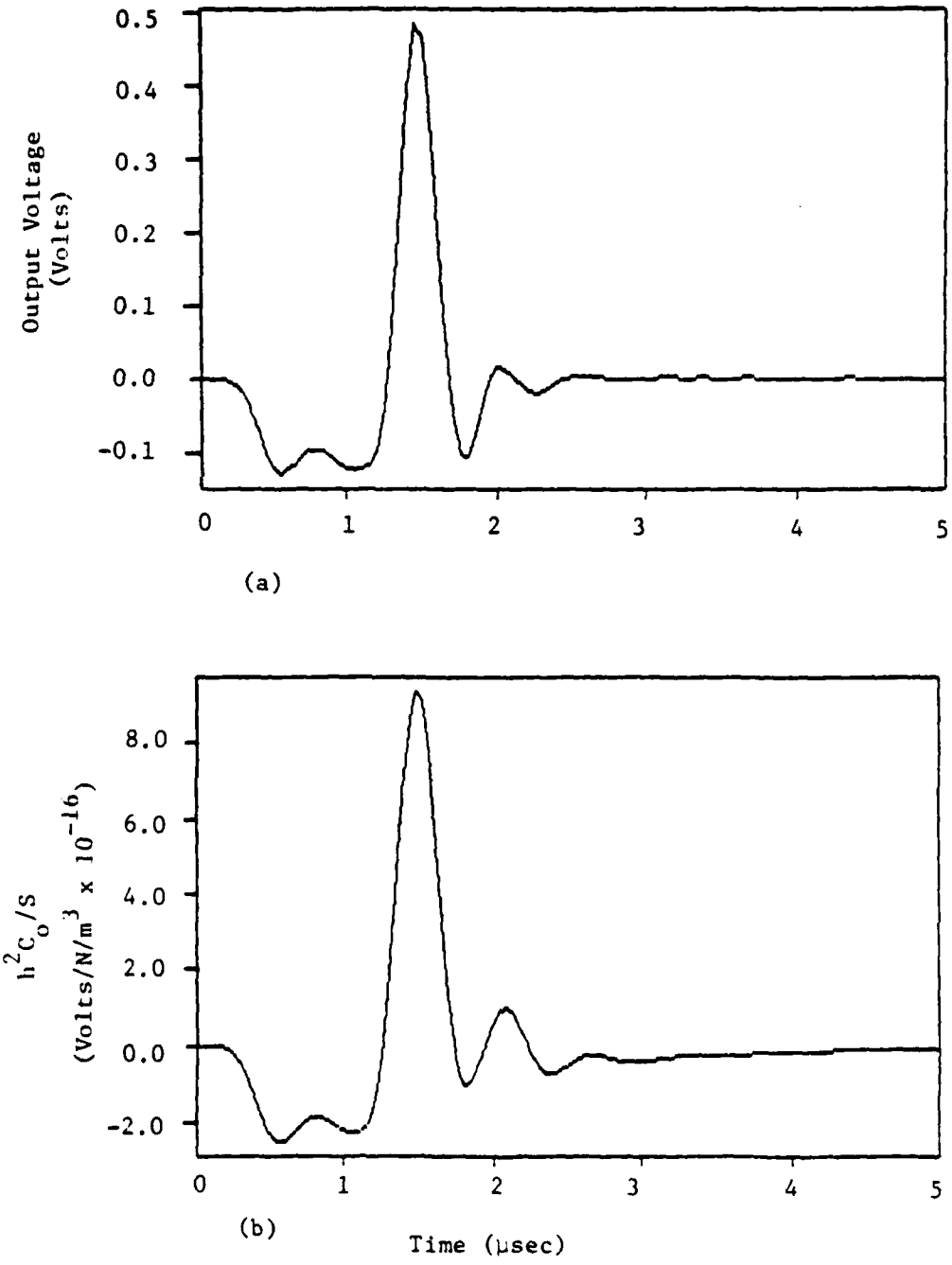

Fig. E8 Comparison of (a) measured and (b) predicted output signals corresponding to broadband pulse input for two FC-500 transducers clamped face-to-face (δ=0.08 μsec, β=0.24 μsec, RC_o=1.0 μsec)

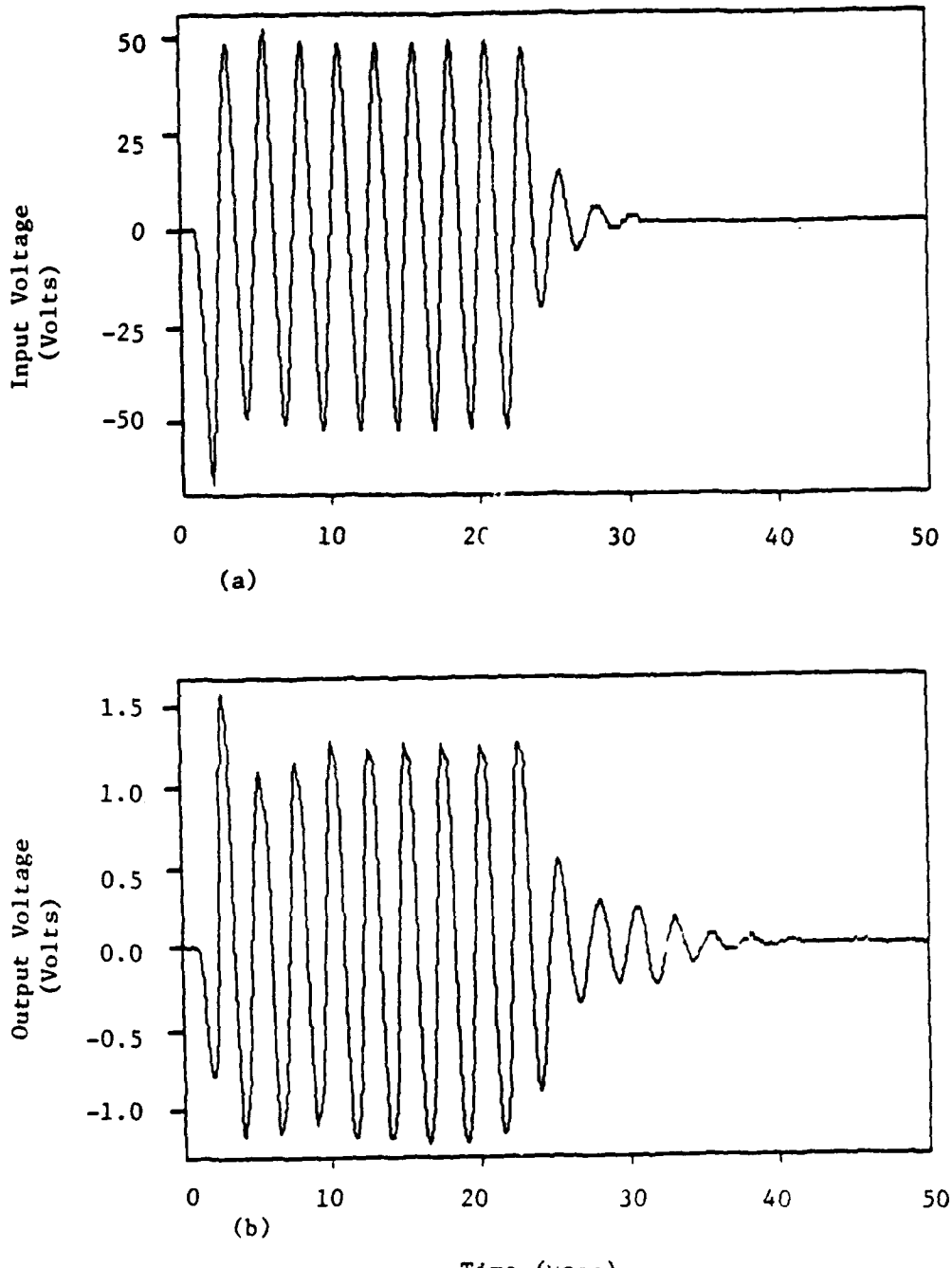

Fig. E9 Measured 0.4 MHz tone burst (a) input and (b) output signals for two FC-500 transducers clamped face-to-face.

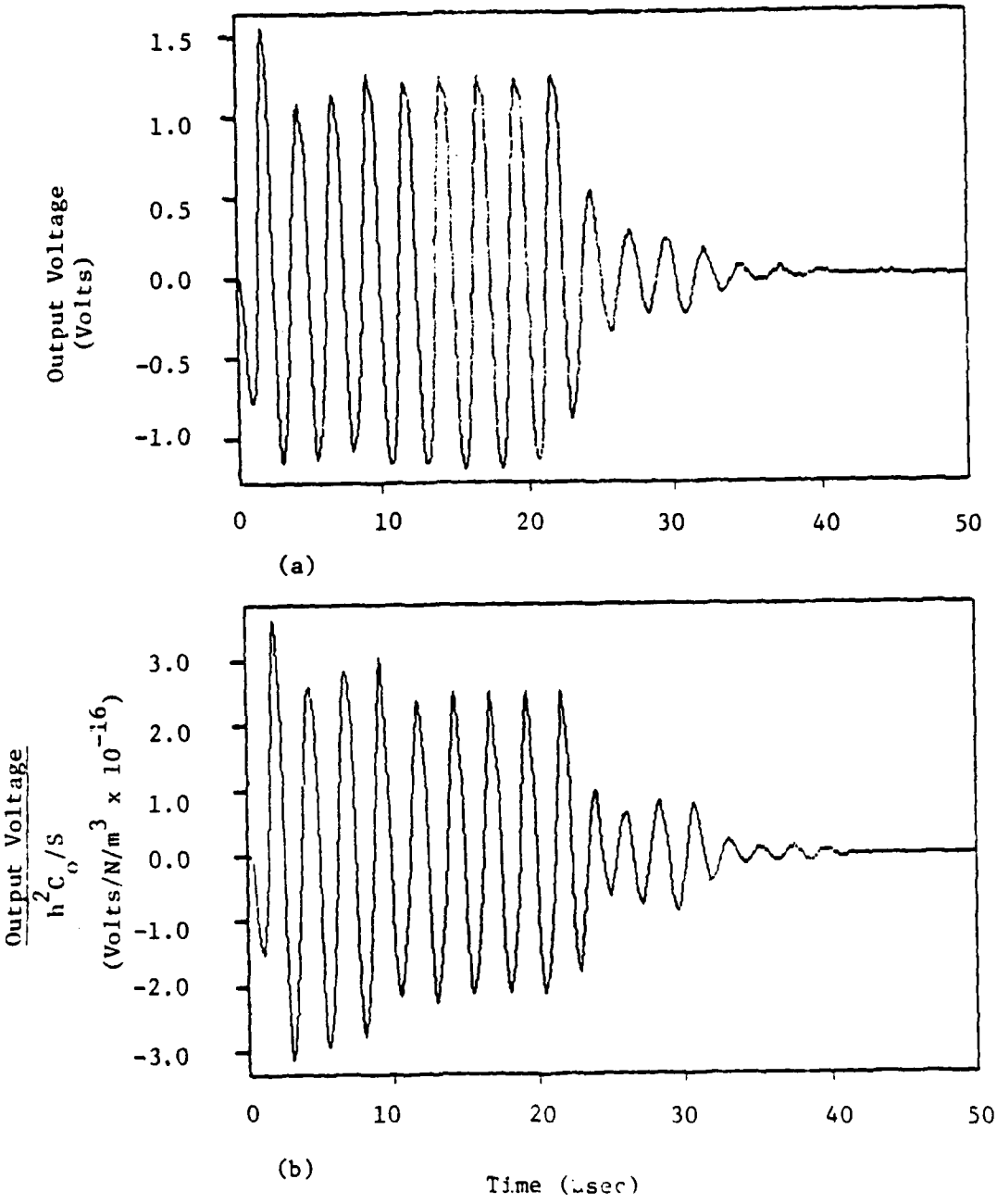

Fig. E10 Comparison of (a) measured and (b) predicted output signals corresponding to 0.4 MHz tone burst input for two FC-500 transducers clamped face-to-face (λ=0, α_B=1.6 nepers/cm).

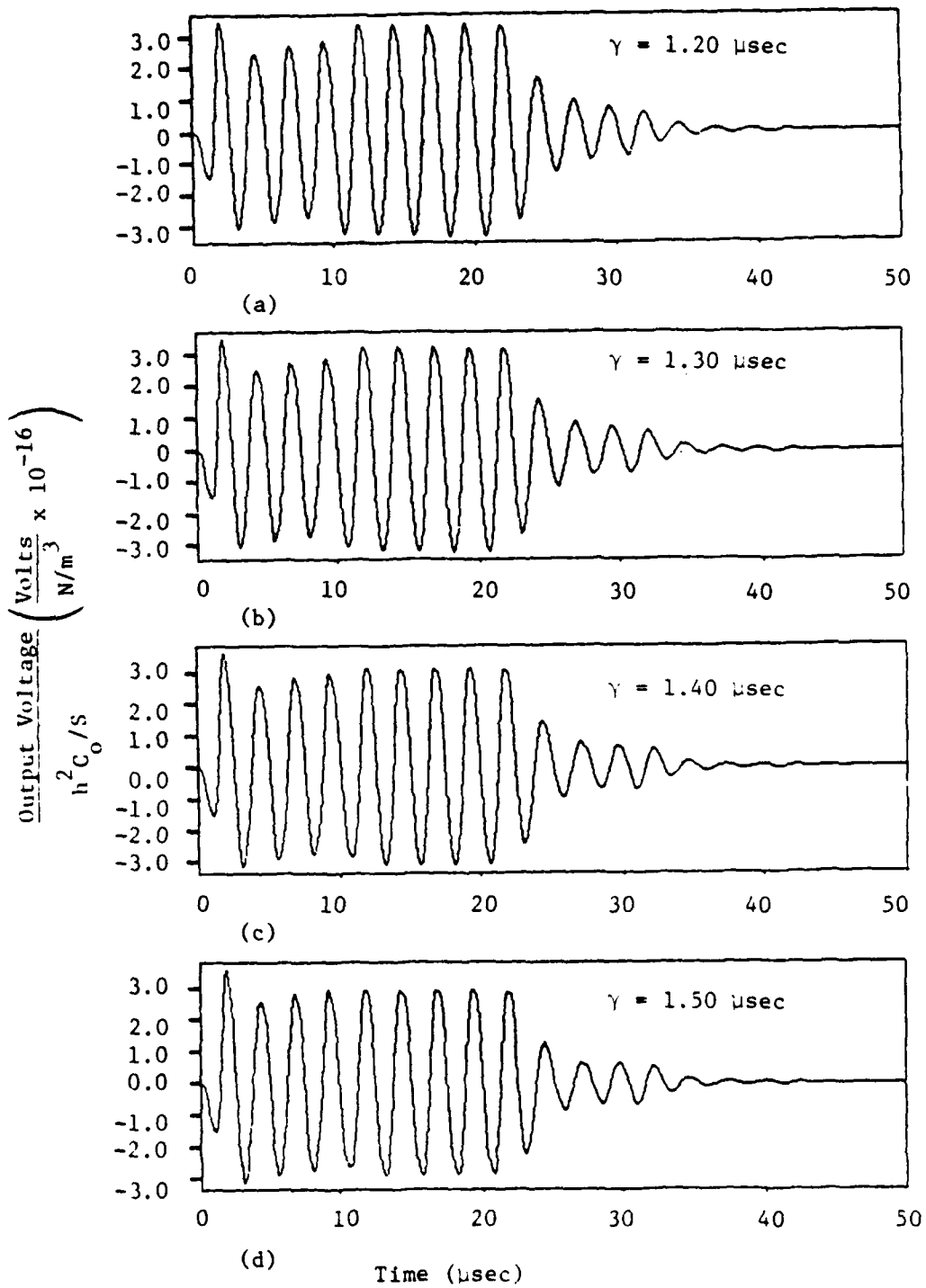

Fig. E11 Predicted response to 0.4 MHz tone burst for two FC-500 transducers clamped face-to-face as a function of time delay.

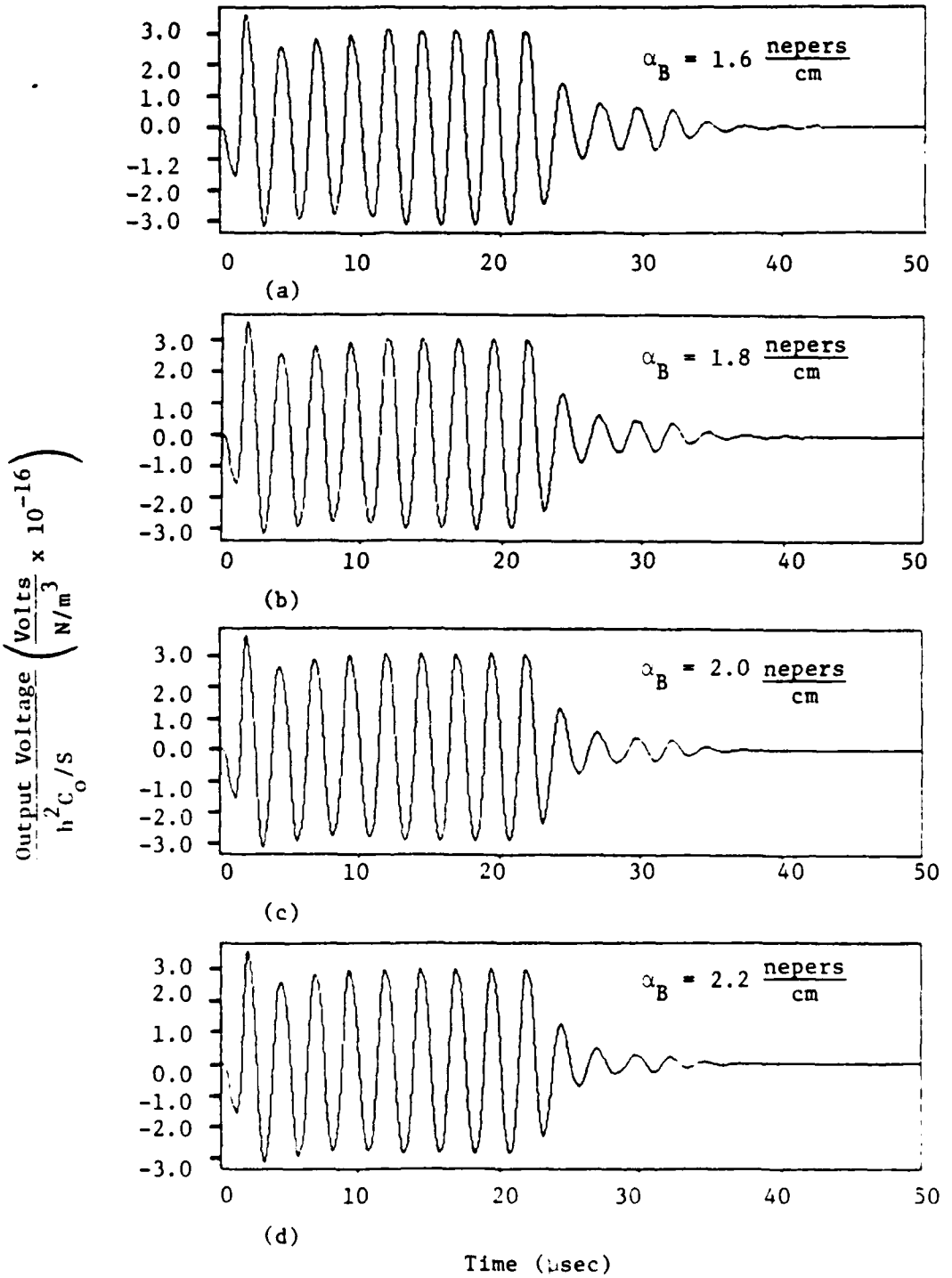

Fig. E12 Predicted response to 0.4 MHz tone burst for two FC-500 transducers clamped face-to-face as a function of the backing attenuation.

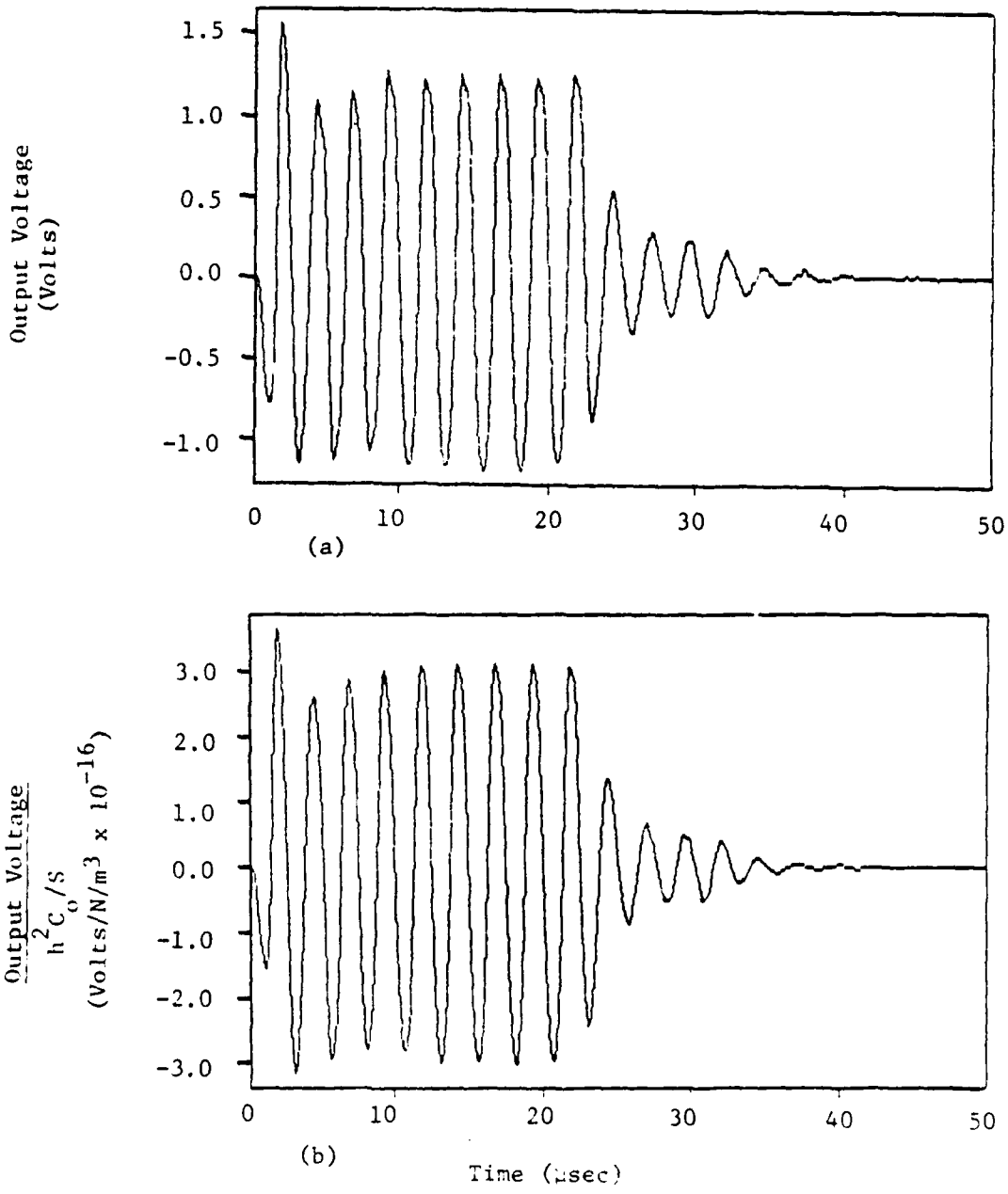

Fig. E13 Comparison of (a) measured and (b) predicted output signals corresponding to 0.4 MHz tone burst input for two FC-500 transducers clamped face-to-face (λ=1.40 μsec, α_B =1.8 nepers/cm).

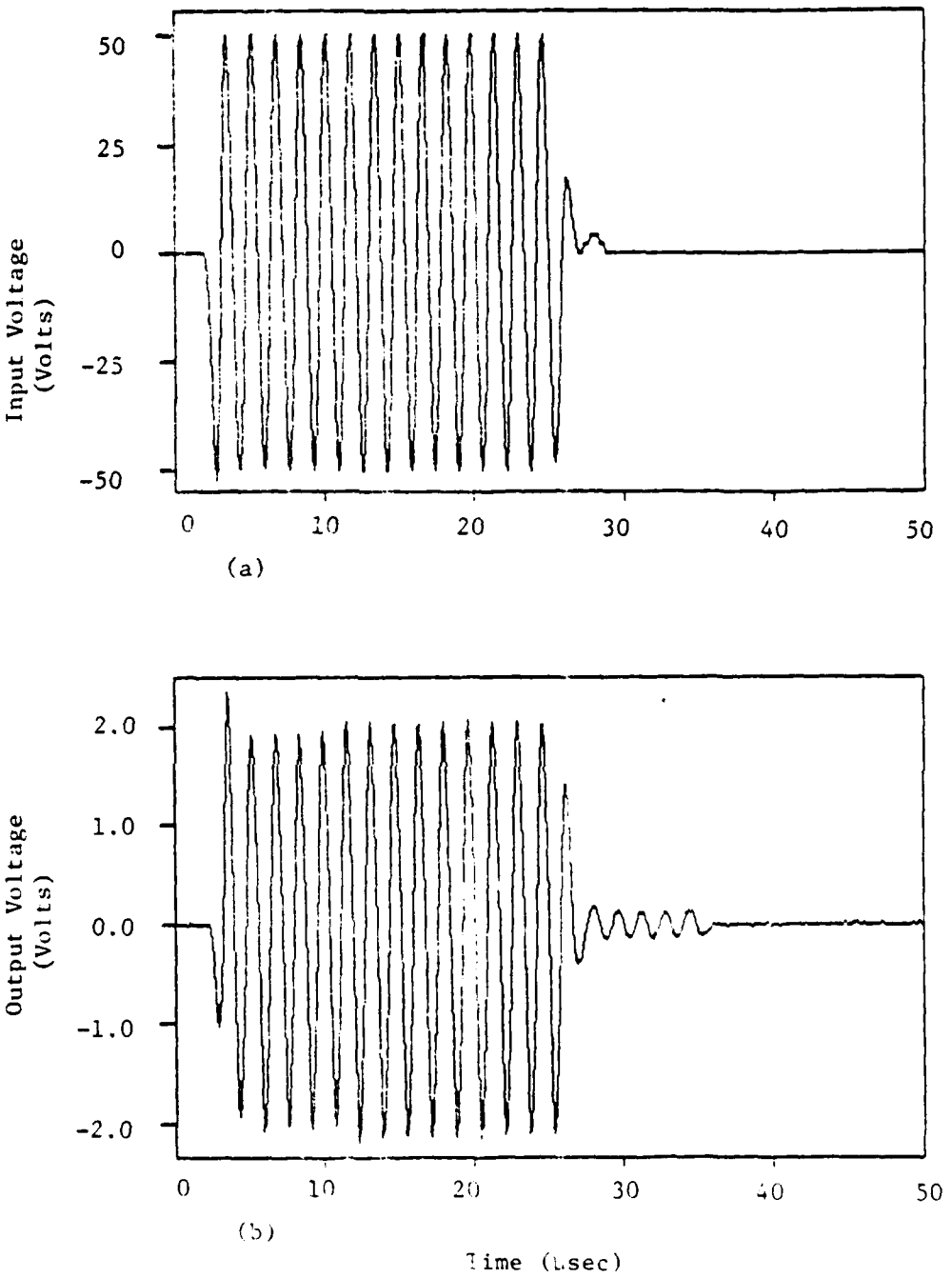

Fig. E14 Measured 0.6 MHz tone burst (a) input and (b) output signals for two FC-500 transducers clamped face-to-face.

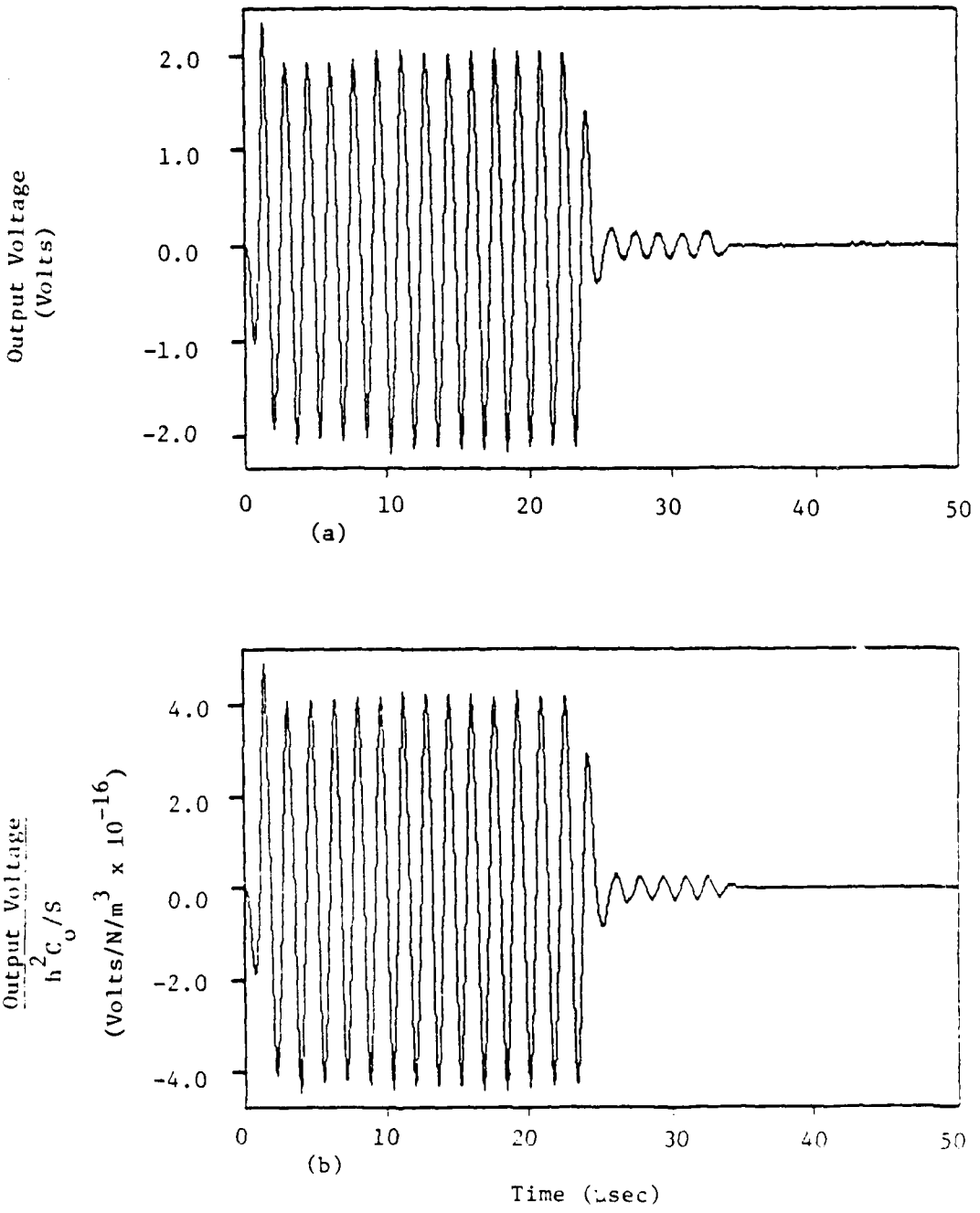

Fig. E15 Comparison of (a) measured and (b) predicted output signals corresponding to 0.6 MHz tone burst input for two FC-500 transducers clamped face-to-face (λ=1.40 μsec, α_B=2.5 nepers/cm).

APPENDIX F

DISCUSSION OF MEASURED STEADY-STATE OUTPUT AMPLITUDE

All of the transducers were clamped face-to-face and tested with 100 V peak-to-peak continuous sinusoidal input signals. The raw data are summarized in Table 7 , and are plotted against frequency in Figs. F1, F2, and F3. These three plots illustrate the effects of three different transducer parameters—backing impedance, wearplate impedance, and backing thickness—on the steady-state output amplitude of an ultrasonic test system. Each of these parameters is discussed in detail in one of the following sections.

F.1 EFFECT OF BACKING IMPEDANCE ON STEADY-STATE OUTPUT AMPLITUDE

Fig. F1 shows the steady-state output amplitude vs. frequency for both the unbacked transducer (AE-100) and the FC-500, which has an impedance-matched backing layer. This plot illustrates very clearly how the presence of a matched backing layer affects the frequency response of the transducer. The FC-500 shows a maximum peak of about 10 volts at 1.9 MHz, but the AE-100 has a peak output of over 50 volts, at about 1.6 MHz. The very large peak in the response of the unbacked transducer corresponds to a condition in the piezoelement known as standing-wave resonance.

The standing-wave (or half-wave) resonance condition occurs whenever the frequency of the oscillations within the piezoelement is equal to an even multiple of the reciprocal of the piezoelement

transit time, so that waves reflected back into the piezoelement from the surfaces of the piezoelement interfere constructively (in phase) with the waves incident upon the surfaces. A matched backing layer absorbs the incident waves at one surface of the piezoelement, so that they are not reflected back into the piezoelement, and standing waves cannot develop. It is not surprising, then, that a strong resonant peak exists in the unbacked transducer, nor that the peak is effectively damped out by the presence of the backing layer in the FC-500. This matched backing layer gives the transducer a much more flat response, so that its useful bandwidth is increased by a factor of two.

F.2 EFFECT OF WEARPLATE IMPEDANCE ON STEADY-STATE OUTPUT AMPLITUDE

Fig. F2 shows the steady-state response for the transducer with aluminum wearplate (AE-101) compared to that for the standard FC-500. The presence of the aluminum wearplate appears to increase the steady-state amplitude by a significant amount, especially at higher frequencies (greater than 1.5 MHz). In fact, the increase in amplitude is so great at the high end that the peak amplitude for the AE-101 comes at about 2.3 MHz, compared to 1.9 MHz for the FC-500.

There appear to be two different factors involved here. The difference between the steady-state amplitudes for the two transducers at relatively low frequencies (below 1.5 MHz) is due chiefly to the improved impedance-match between wearplate and piezoelement in the AE-101, which increases the transmission coefficient for stress-wave propagation across the wearplate-

piezoelement interfaces in the system. Thus, a greater portion of the stress-wave amplitude which is generated at the input piezoelement actually arrives at the output piezoelement, with the result that the output amplitude is increased. This effect alone would produce two curves of steady-state output amplitude that differed by a constant multiplicative factor at all frequencies. This is obviously not the complete picture, though, for it is clear that the aluminum wearplate has some effect on the resonant frequency of the transducer as well.

In general, an increase in resonant frequency corresponds to a decrease in piezoelement transit time. Since there are large time delays β for reflected waves which approach the wearplate-piezoelement interfaces from the outside of the piezoelement (see Chapter 4, subsection 4.1.2), it seems probable that there are time delays for waves which strike the surfaces of the piezoelement from the inside. Although these time delays could only increase the piezoelement transit time, recall that the value of β for the AE-101 was about half of the value for the FC-500. The difference between the period corresponding to 1.9 MHz and that corresponding to 2.3 MHz is 0.09 μsec, and the difference between the wearplate-piezoelement time delays for the FC-500 and the AE-101 is 0.115 μsec, larger by slightly more than 20%. It seems perfectly reasonable, then, that the increase in resonant frequency for the aluminum backing layer is due to smaller time delays at the wearplate-piezoelement interfaces.

In conclusion, then, the AE-101 shows a consistently larger steady-state amplitude than the FC-500, due to the relatively

good impedance match between the wearplate and piezoelement in the AE-101. In addition, the resonant frequency of the AE-101 is higher than that for the FC-500, due to the smaller time delays introduced at the wearplate-piezoelement interfaces in the AE-101.

F.3 EFFECT OF BACKING THICKNESS ON STEADY-STATE OUTPUT AMPLITUDE

Fig. F3 shows a plot of steady-state output amplitude vs. frequency for the AE-102, AE-103, and FC-500 transducers. These transducers are allegedly identical, except for the thickness of their backing layers. Notice that the FC-500 and the AE-102 have slightly greater amplitude than the AE-103 transducer over almost the entire frequency range of the experiments (0.4-3.0 MHz). Observe also that the peak amplitude of the prototype transducers (AE-102 and AE-103) occurs at about 1.6 MHz, while the peak in the response of the standard FC-500 comes near 1.9 MHz. In addition, the shapes of the response curves of the AE-102 and AE-103 are qualitatively similar to one another, yet the curve for the FC-500 is significantly different. These observations indicate some variations in construction between the transducers.

Since the behavior of the FC-500 is so different from the AE-102 and AE-103, the FC-500 cannot really be compared with the two other transducers here. It is still possible, though, to draw some conclusions. Recall, first, that in Chapter 4 (subsection 4.2.3) it was noted that the amplitude of the pulse response of a transducer appears to decrease for increasing backing thickness. This is also the case here, where the AE-103 (1.905 cm (0.750 in) backing) shows a characteristically lower steady-state

amplitude than the AE-102 (1.270 cm (0.500 in) backing). Thus, the correlation of backing thickness with output amplitude is substantiated. The relatively low resonance frequency of the prototype transducers, on the other hand, is much lower than would be expected based on the results for the AE-101 transducer discussed in the previous section.

In conclusion, the steady-state amplitude is observed to decrease for increasing backing thickness. No effect of backing on the resonance frequency is observed; the important variation of resonance frequency occurs between the FC-500 and the others, not between identical transducers differing only in backing thickness. Apparently, the piezoelement used in the FC-500 is different from that in the prototype transducers.

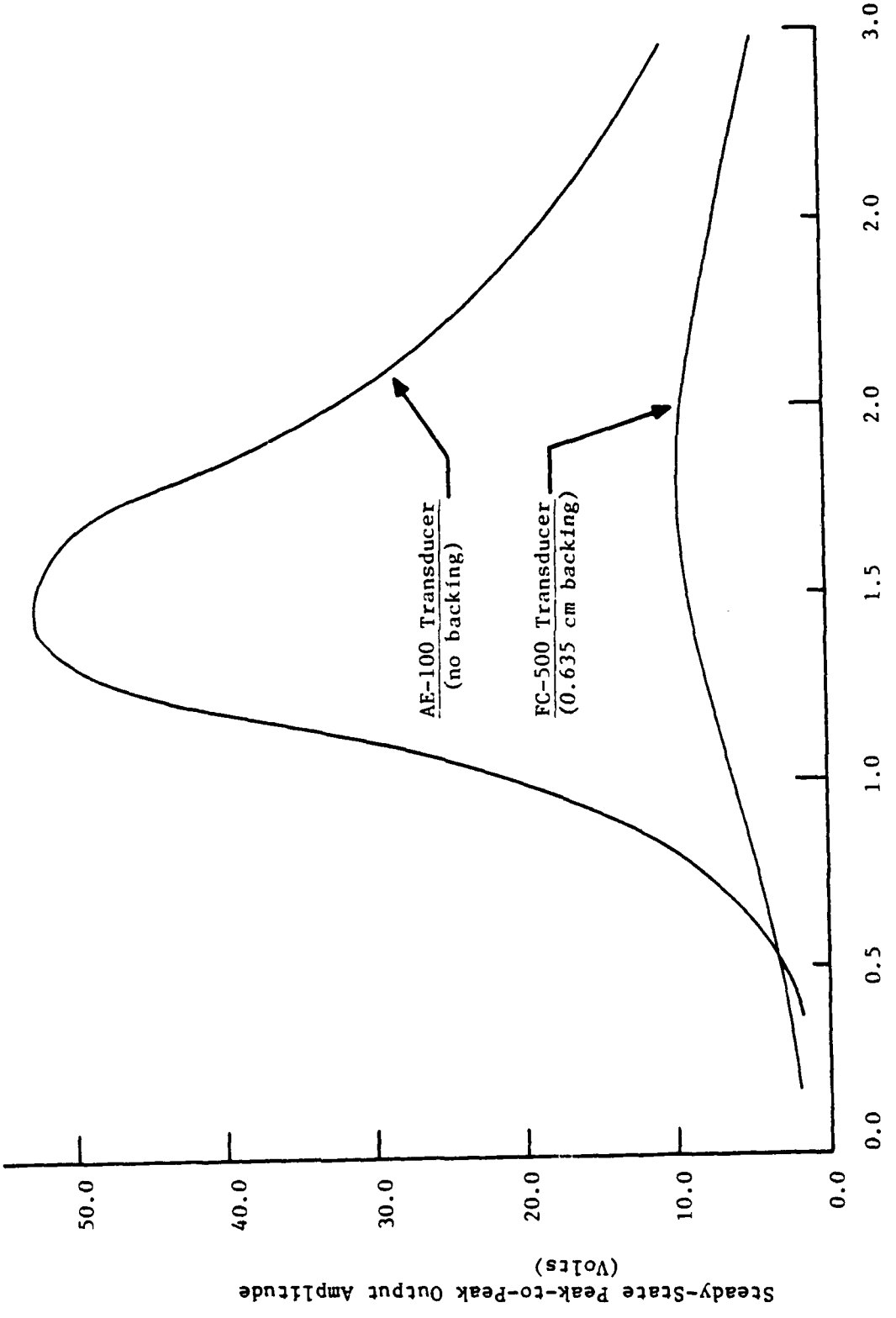

Fig. F1 Plot of steady-state output amplitude vs. frequency for AE-100 and FC-500 transducers corresponding to continuous-wave input.

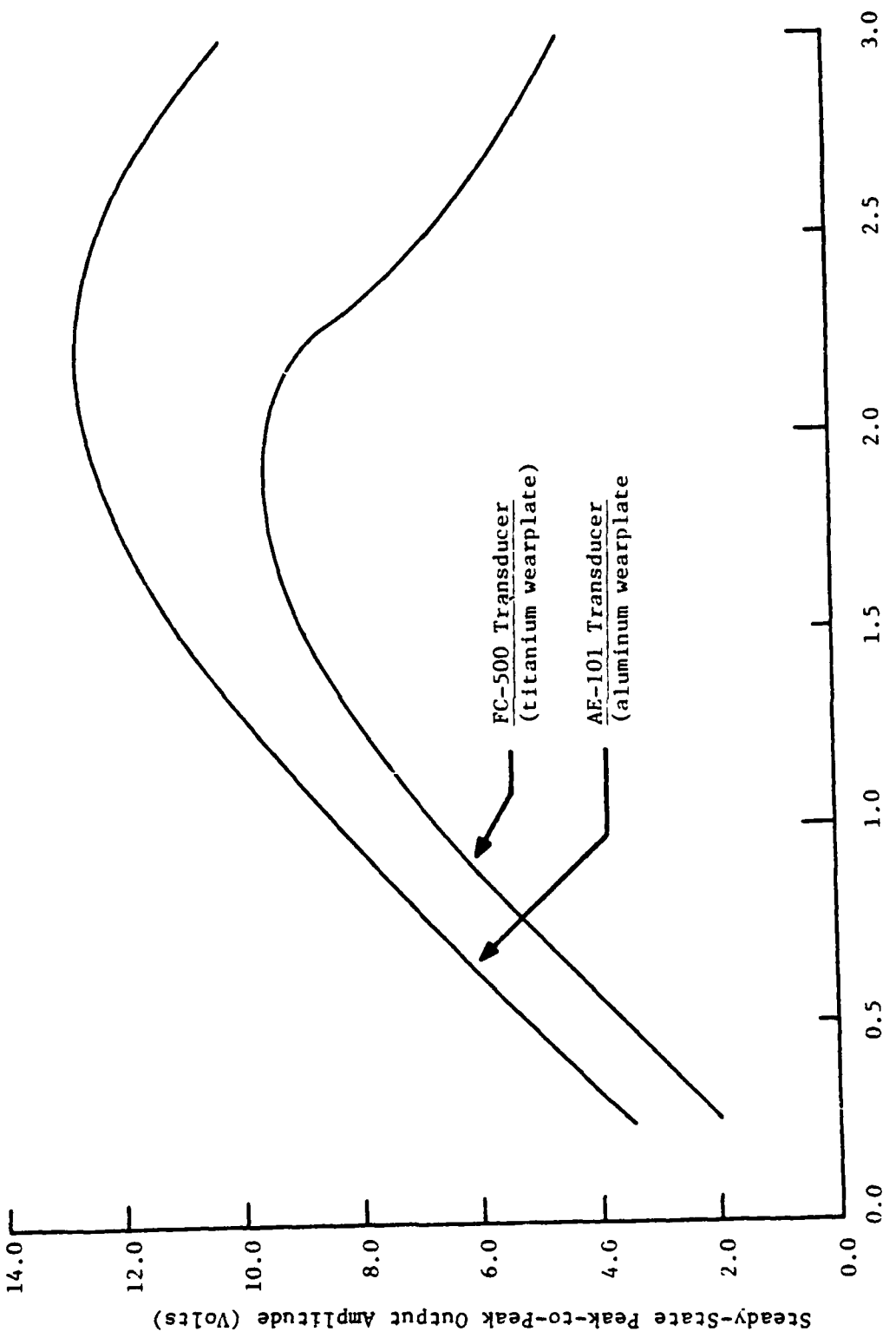

Fig. F2 Plot of steady-state output amplitude vs. frequency for AE-101 and FC-500 transducers corresponding to continuous-wave input.

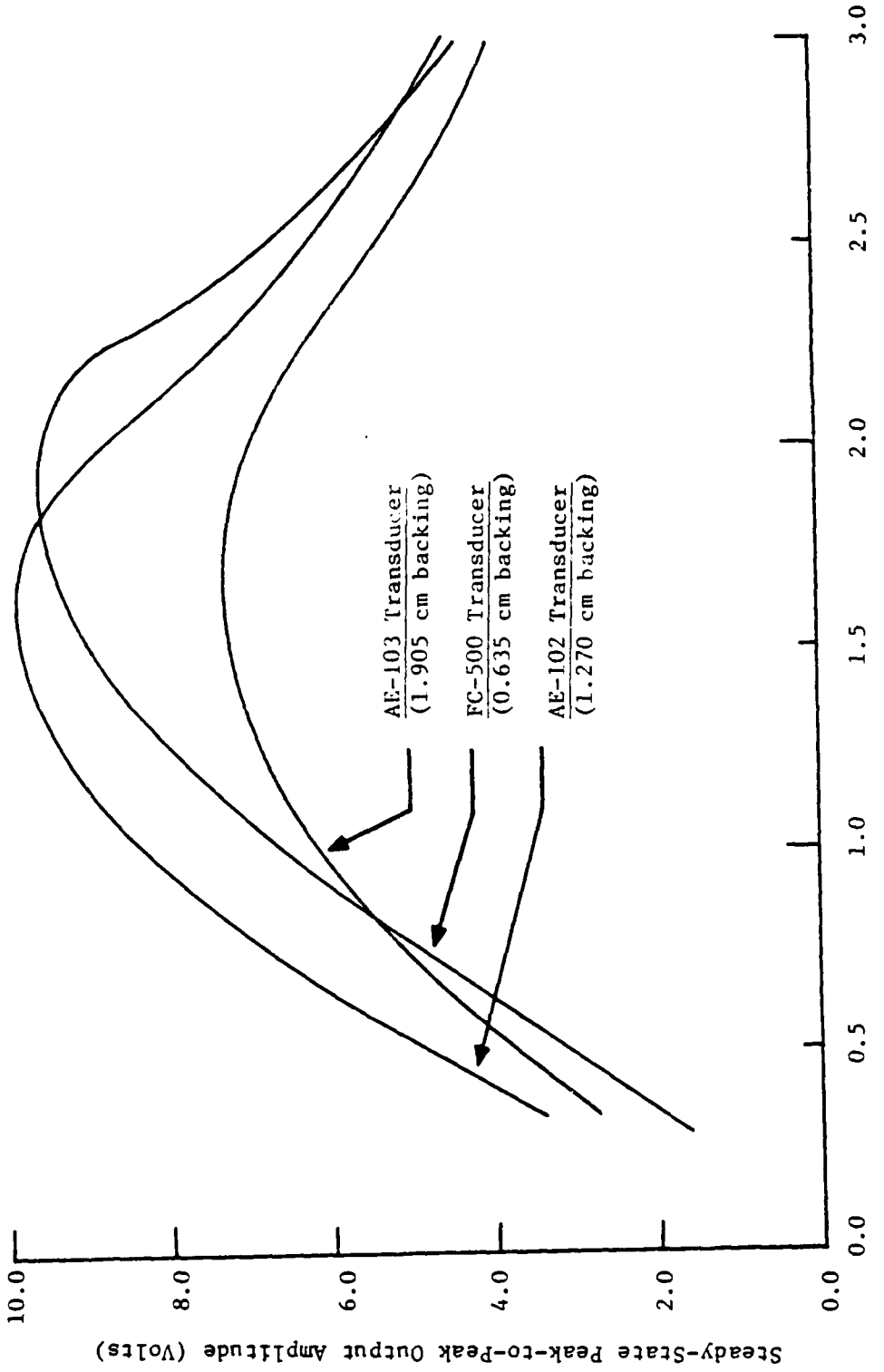

Fig. F3 Plot of steady-state output amplitude vs. frequency for AE-103, AE-102, and FC-500 transducers corresponding to continuous-wave input.

APPENDIX G

SIMULATED EFFECTS OF WEARPLATE IMPEDANCE, BACKING IMPEDANCE, AND PIEZOELEMENT THICKNESS ON TRANSDUCER RESPONSE

In this appendix, the effects of three different parameters on the broadband pulse response of a system are determined. The system consists basically of two FC-500 transducers face-to-face, except for variations in the particular parameters being studied.

G.1 EFFECT OF WEARPLATE IMPEDANCE

Fig. G1 consists of four predicted output signals which show the result of varying the wearplate impedance in the system. The standard FC-500 corresponds to case (d), where $Z_w/Z_p=2.5$. Case (b) represents transducer AE-101, which has an aluminum wearplate rather than the standard titanium carbide wearplate of the FC-500. Case (c) corresponds to a system in which the wearplates are impedance-matched to the piezoelements, and in case (a), the ratio of wearplate impedance to piezoelement impedance is the reciprocal of the standard ratio for the FC-500.

Notice that curves (a) and (d) appear to be identical. This is at first surprising, but recall that waves traversing the two wearplates must cross two wearplate-piezoelement interfaces, once from piezoelement to wearplate, and once from wearplate to piezoelement. Note that the transmission coefficient for a wearplate-to-piezoelement interface where Z_w is half of Z_p is identical to the transmission coefficient for a piezoelement-to-

wearplate interface where Z_W is twice Z_P. This means that the product of the transmission coefficients for the two interfaces should be the same, regardless of the order in which the interfaces are traversed.

The other interesting observation to be made is that the "efficiency" of the system drops significantly for large impedance mismatch between piezoelement and wearplate. An impedance ratio of 0.75, as in case (b), decreases the efficiency only slightly, but a decrease of almost 30% is observed for $Z_W/Z_P=0.4$.

In conclusion, then, the simplest and largest-amplitude output signal is obtained by impedance-matching the wearplate and pioezoelement in an ultrasonic transducer.

G.2 THE EFFECT OF BACKING IMPEDANCE

Fig. G2 shows four curves which predict the result of varying the backing impedance of the system. The standard case, of course, corresponds to $Z_B/Z_P=1.0$, where the backing is impedance-matched to the piezoelement.

The most obvious feature of Fig. G2 is the resonance which occurs when the backing is mismatched. It is interesting, however, that the resonant frequencies are not all the same. Case (a) seems to have a fairly high frequency of oscillation, while cases (c) and (d) show a much lower frequency.

In case (a), the backing has a lower impedance than the piezoelement. This means that a wave in the piezoelement which strikes the piezoelement-backing interface will be partly reflected and partly transmitted. More importantly, however, the reflected

wave will be inverted as compared to the incident wave—its amplitude will be a negative fraction of the incident amplitude (see eqns. (2-15)). When the reflected wave strikes the piezoelement-wearplate interface, it will then produce a voltage pulse which is opposite in sign to the pulse produced at the piezoelement-backing interface one piezoelement transit time earlier. Thus, the predominant frequency in plot (a) is determined by the piezoelement transit time (0.27 μsec). Note the large peak at about 2 μsec and its negative counterpart at about 2.5 μsec as evidence of this.

Figs. G2(c) and (d) are fairly similar to one another except for the rate of decay of the resonance. They both correspond to cases in which the backing has a larger impedance than the piezoelement, so that the wave reflected from the piezoelement-backing interface has the same sign as the incident wave. This means that, rather than a negative peak appearing in the output shortly after each positive peak, the positive peaks are repeated at slightly reduced amplitude. Then, since the wearplate impedance is also much larger than the piezoelement impedance, the wave is reflected from the piezoelement-wearplate interface as well, with a positive, further-reduced amplitude. This positive reinforcement accounts for the broadening of the peaks in these two output signals.

The 0.5 MHz resonance frequency in these last two cases of Fig. G2 corresponds to repeated reflection back and forth between the piezoelement-backing interfaces of the two transducers. The round-trip transit time is almost 2 μsec, which is of course

the period associated with 0.5 MHz resonance. The reason that the resonance takes longer to decay in case (d) than in case (c) is that the reflection coefficient at the piezoelement-backing interface is higher for larger backing impedance. This means that more of the energy will be reflected back into the piezoelement by a very stiff backing, so that it will take more cycles between the piezoelement-backing interfaces for the amplitude of the reflected wave to fall to a negligible level.

It is therefore clear that the only backing layer that is effective in damping transducer resonance is the impedance-matched backing.

G.3 THE EFFECT OF PIEZOELEMENT THICKNESS

Fig. G3 shows four predicted pulse output signals for four systems with piezoelements of varying thickness. Case (c) corresponds to the standard FC-500 piezoelement.

The most striking feature of Fig. G3 is the variation in "smoothness" of the output signals. Plot (a) is very rough and jagged, while plot (d) shows almost no detail whatsoever. This is a consequence of the fact that the output voltage is approximately proportional to the integral of the stress inside the piezoelement of the output transducer. A thicker piezoelement integrates over a longer time interval, so that the small, abrupt variations in the stress waveform make a lesser contribution to the output voltage.

Another consequence of integrating over a longer time interval is that the amplitude of the integral increases as the

time interval increases. Fig. G3 shows that increasing the piezoelement thickness eightfold results in a factor of twenty increase in output amplitude. This increase is highly desirable, but the tradeoff is that the bandwidth of the output signal is reduced by lengthening the piezoelement. Similarly, a very thin piezoelement produces a voltage signal that is very close to the actual stress waveform, but it is of very low amplitude. The FC-500 seems to be well suited to the particular broadband input pulse used in this study, giving enough detail in the output without creating a jagged signal that is difficult to interpret or quantify.

In conclusion, then, the proper piezoelement thickness will provide a useful amount of detail in the output signal, while also maintaining a reasonable amplitude level.

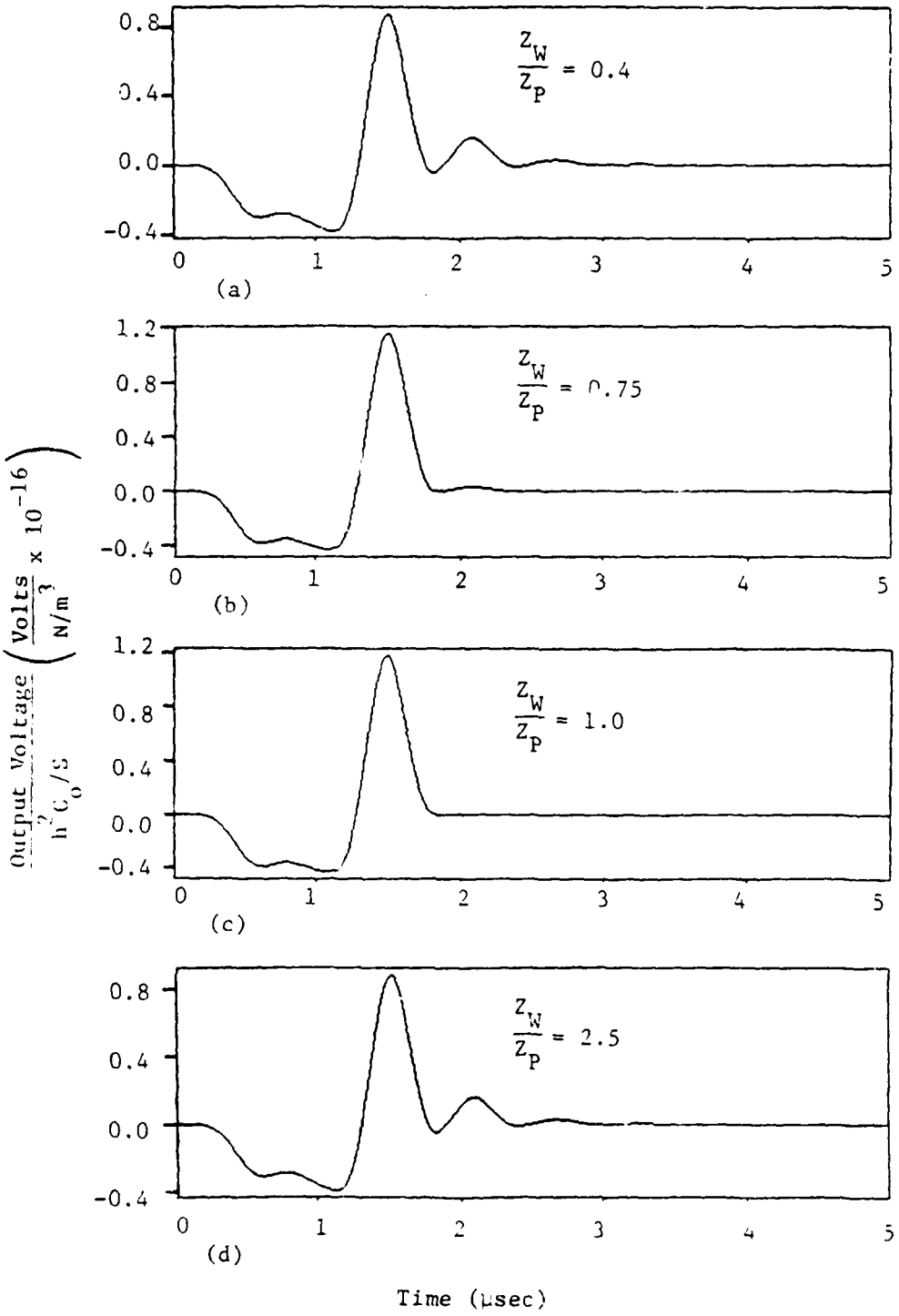

Fig. G1 Predicted broadband pulse response of two FC-500 transducers clamped face-to-face as a function of wearplate impedance.

AD-A128 965 CHARACTERIZATION OF ULTRASONIC TRANSDUCER THROUGH TRANSMISSION SYSTEMS(U) WEA CAMBRIDGE MA J C BLOUGH ET AL. DEC 82 N00014-81-C-2319

3/3

UNCLASSIFIED F/G 20/3 NL

END

DATE FILMED

DTIC

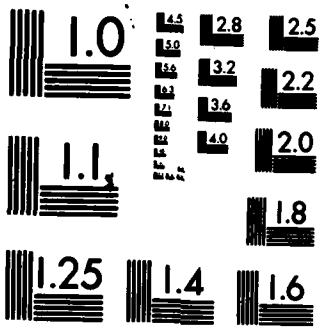

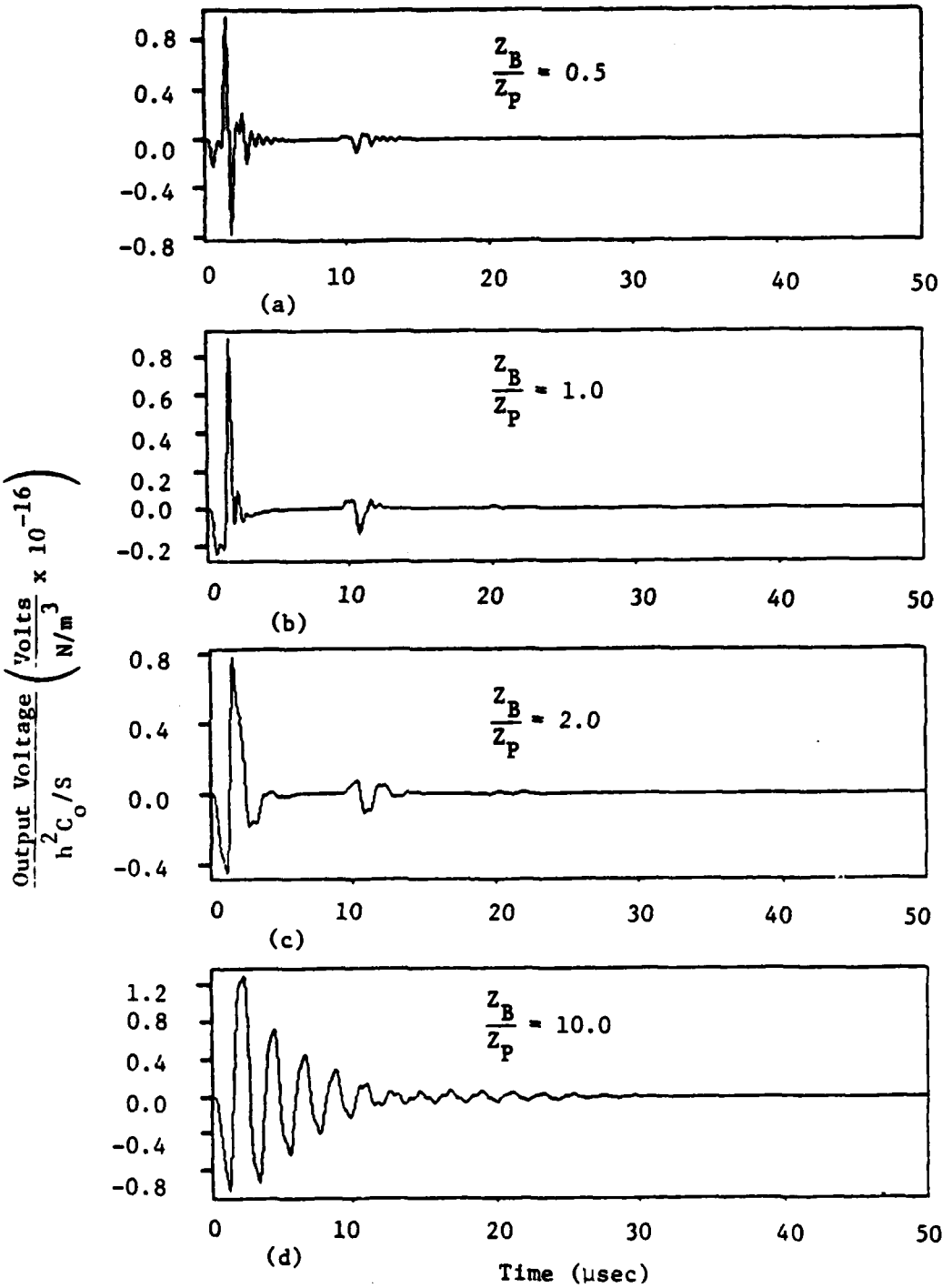

Fig. G2 Predicted broadband pulse response of two FC-500 transducers clamped face-to-face as a function of backing impedance.

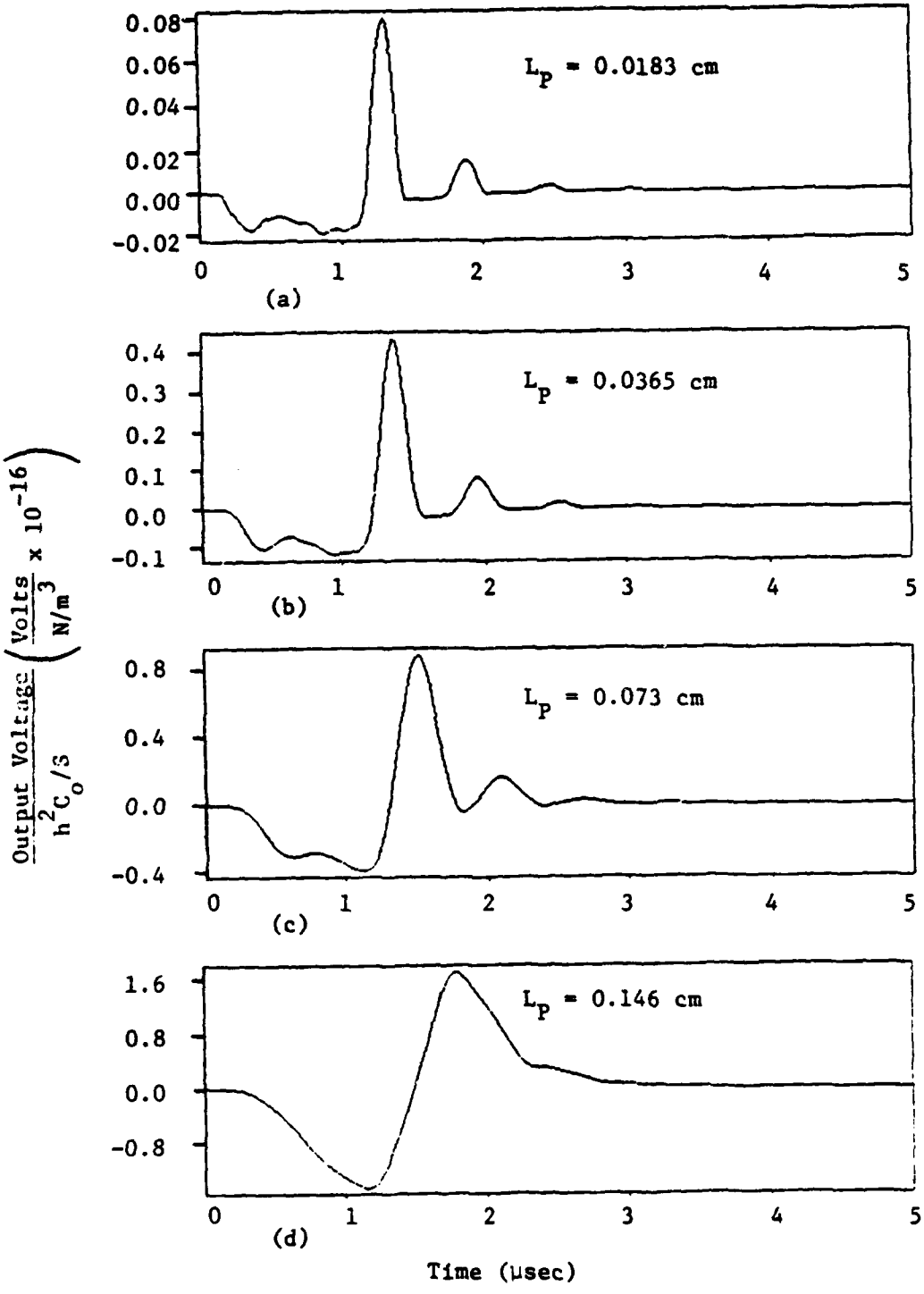

Fig. G3 Predicted broadband pulse response of two FC-500 transducers clamped face-to-face as a function of piezoelement thickness.

APPENDIX H

EXPERIMENTAL STUDY OF WAVE INTERACTION AT INTERFACES

This appendix is a discussion of experimental results which deal with the behavior of stress waves at the interfaces between the various layers in an ultrasonic test system. The effect of a thin layer of ultrasonic couplant on the output of the system is investigated for both impedance-matched and impedance-mismatched interfaces; the effect of a thin epoxy-bonding layer is also discussed.

H.1 BEHAVIOR AT IMPEDANCE-MISMATCHED COUPLANT LAYER

Fig. H1 shows two measured broadband pulse output signals. A 1.270 cm (0.500 in) thick aluminum plate serves as the specimen in each system, and two different types of transducers are used—AE-103 transducers for system A, and AE-101 transducers for system B. The significant difference between the transducers is that the AE-103 has a titanium carbide wearplate, and the AE-101 has an aluminum wearplate. Thus one wearplate is impedance-matched to the specimen, and the other is mismatched.

The two output signals are quite similar except for two important differences. First, observe the interval between 7 and 9 μsec. System B shows only a slight perturbation at 7.5 μsec, followed quickly by another plateau, but system A shows a distinct reflection arriving at that time. If this reflection is caused by the largest peak in the signal (which starts at about 3.5 μsec),

there appears to be a time delay of approximately 4 μsec between the arrival of the first peak and the arrival of the reflection. The theoretical transit time of a 1.270 cm (0.500 in) thick aluminum plate is 2.04 μsec, so that a measured time delay of 4 μsec is within 2% of the predicted value. Therefore, the reflection at 7.5 μsec in System A is clearly caused by the impedance mismatch at the wearplate-specimen interface.

The second difference between the plots is the difference in overall amplitude. System B has a peak amplitude of over 0.5 volts, while the peak value for system A is barely 0.4 volts. This may also be attributed to the reflection at the impedance-mismatched interfaces—a portion of the input energy in system A is reflected back into the input wearplate by the specimen, and another portion is reflected back into the specimen by the output wearplate. Thus, only a fraction of the energy radiated by the input piezoelement is actually transmitted to the output piezoelement, resulting in a reduced measurement of output amplitude as compared to system B. This occurs to all waves, however, so that the shape of the output signal is not really affected, except for the reflection.

Using the impedance values from Fig. C2, eqns. (2-17) predict that the amplitude should be reduced by a factor of 0.696. The observed reduction is 0.67, accurate to within 4% of the predicted value.

It seems clear, then, that the presence of a couplant layer does not affect the validity of the impedance model for wave interaction at surfaces. In addition, no time delay appears to be

introduced when waves are reflected from impedance-mismatched interfaces where a couplant layer is present. Further experiments and some wave propagation simulations of the system should be performed to confirm these conclusions.

H.2 BEHAVIOR AT IMPEDANCE-MATCHED COUPLANT LAYER

In order to isolate the effect of the couplant layer, two specimens have been prepared (see Fig. C5). One is simply the 1.270 cm (0.500 in) thick aluminum plate of the preceding experiment, and the other consists of two 0.635 cm (0.250 in) thick aluminum plates with a layer of couplant between them. The measured broadband pulse output signals corresponding to these two systems are shown in Fig. H2.

The curves are strikingly similar, qualitatively as well as quantitatively. It appears that there is no time delay introduced by the extra couplant layer in system B, as far as can be seen from the resolution of the plot (about 0.01 μsec). There is, however, a very slight reflection produced at the couplant layer—it shows up at 5.5 μsec in the output signal for system B. This is consistent with the calculated value of 1.02 μsec for the transit time of a 0.635 cm (0.250 in) aluminum plate.

The results of this experiment further reinforce the earlier conclusion that the presence of a couplant layer in an ultrasonic system does not introduce additional time delays into the system response. And, finally, although slight reflections are generated at impedance-matched interfaces where couplant is used, the quantitative impedance model for wave interaction at surfaces is

essentially unaffected by the presence of a couplant layer.

H.3 THE EFFECT OF ADHESIVE BONDING LAYERS

An experiment similar to the previous one has been performed using an adhesive bonding layer between the two 0.635 cm (0.250 in) aluminum plates, instead of a couplant layer. The measured broadband pulse response of this system is shown in Fig. H3. The output for a solid 1.270 cm (0.500 in) aluminum plate is also shown for comparison.

The output for the adhesive-bonded specimen shows some distortion that has not been observed in any of the previous experiments. The first peaks are slightly distorted near 3 μsec, and the trailing edge of the largest peak is broadened as well. The particular causes of these distortions are difficult to isolate, but perhaps the epoxy layer has a transit time or a time delay that is close enough to the piezoelement transit time to interfere with the arrival of the first three wavefronts A(11), A(21), and A(31) (see Fig. E3). Regardless of this distortion, however, there are three clear observations that can be made.

First, no additional time delay between the application of the input voltage and the arrival of the first output peak is introduced by the epoxy layer. Second, a significant reflection shows up in the measured output at 5.5 μsec. Since the calculated transit time of the 0.635 cm (0.250 in) plate is 2.04 μsec, and the transit time of the wearplate is less than 0.06 μsec, this reflection is a consequence of waves bouncing back and forth between the epoxy layer and the piezoelements. No apparent time

delay is associated with these reflections, either.

Finally, there is a difference in amplitude between the two output signals in Fig. H3. The amplitude of the largest peak (3.8 μsec) for system B is only 0.48 of the corresponding value for system A. This factor may be used to calculate the impedance of the epoxy from eqns. (2-17), giving a value $Z = 2.0 \times 10^4$ $gm/cm^2/s$. This value, an approximate wavespeed, and the measured thickness of the epoxy layer (0.005 cm) could be used to attempt to simulate the output of this system using the computer model.

In conclusion, the presence of an adhesive bond, however thin, does have a significant effect on the interaction of stress waves at an interface. In addition to generating multiple reflections, the epoxy layer reduces the amplitude of the waves transmitted across the interface. For the particular specimen tested in this study, no time delays were observed at the epoxy layer, either for reflection or transmission.

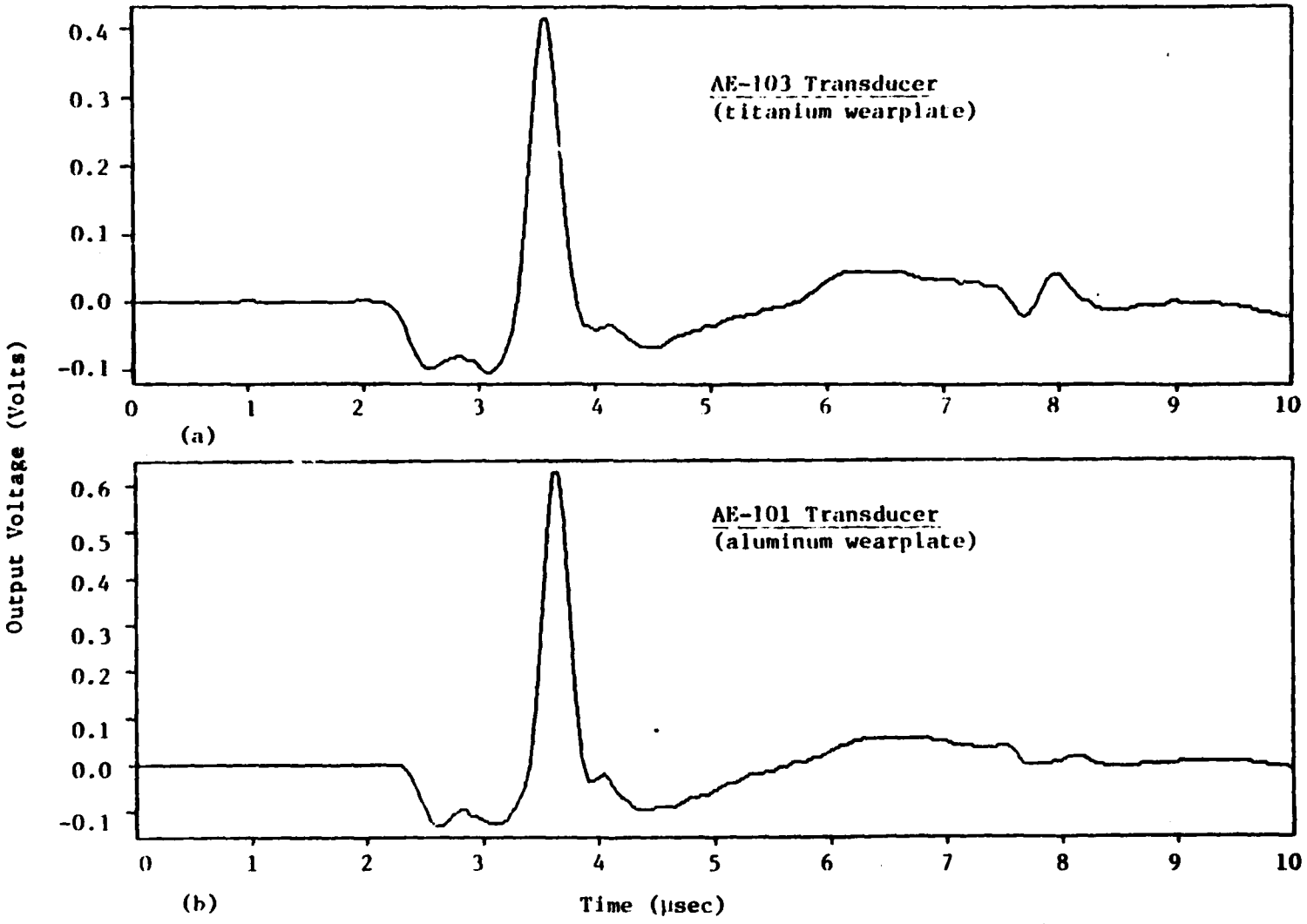

Fig. H1 Comparison of broadband pulse response for 1.270 cm (0.500 in) aluminum plate clamped between (a) AE-103 transducers and (b) AE-101 transducers.

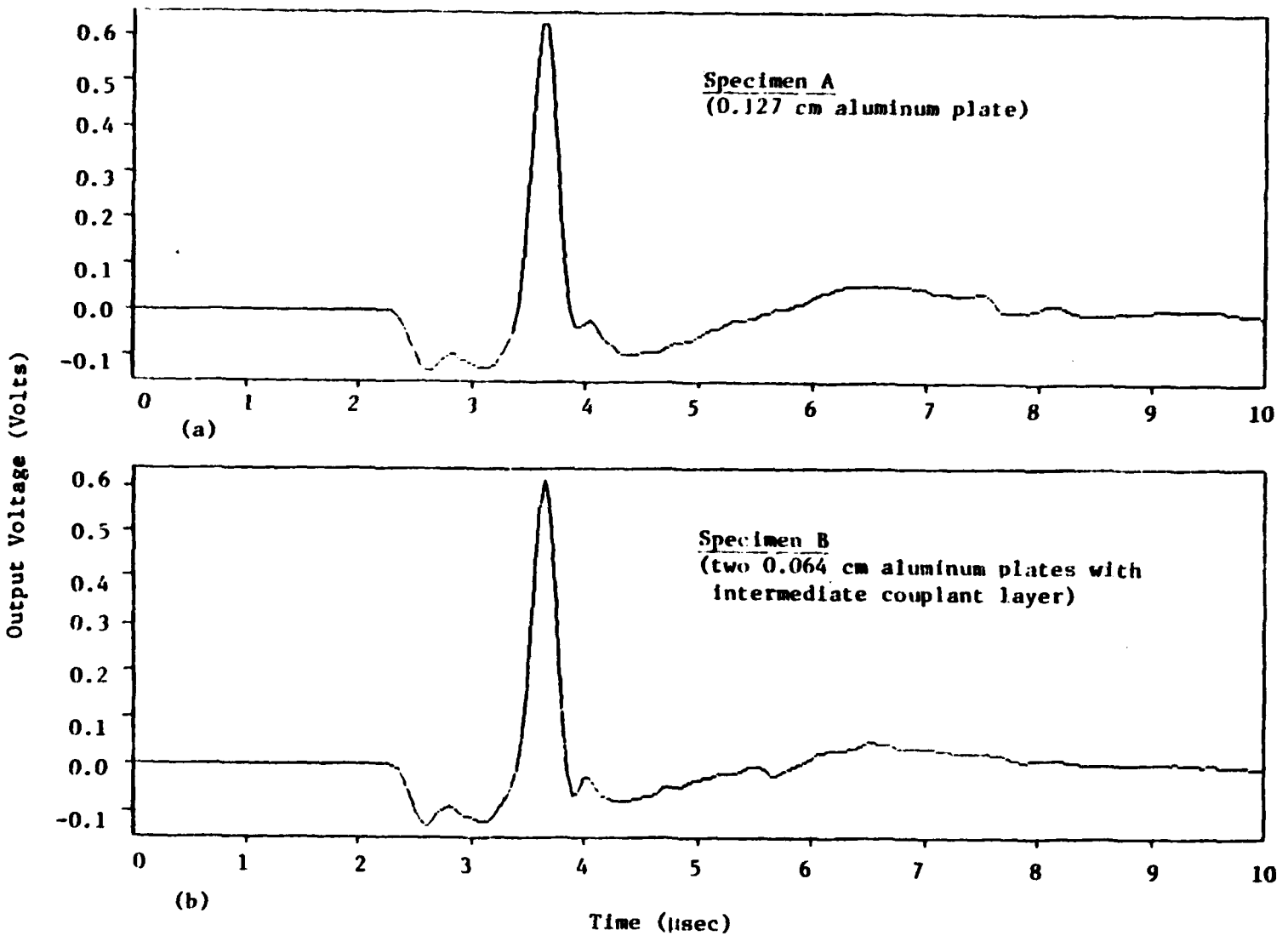

Fig. H2 Comparison of broadband pulse response for (a) 1.270 cm (0.500 in) aluminum plate and (b) two 0.635 cm (0.250 in) aluminum plates with intermediate couplant layer clamped between AE-101 transducers.

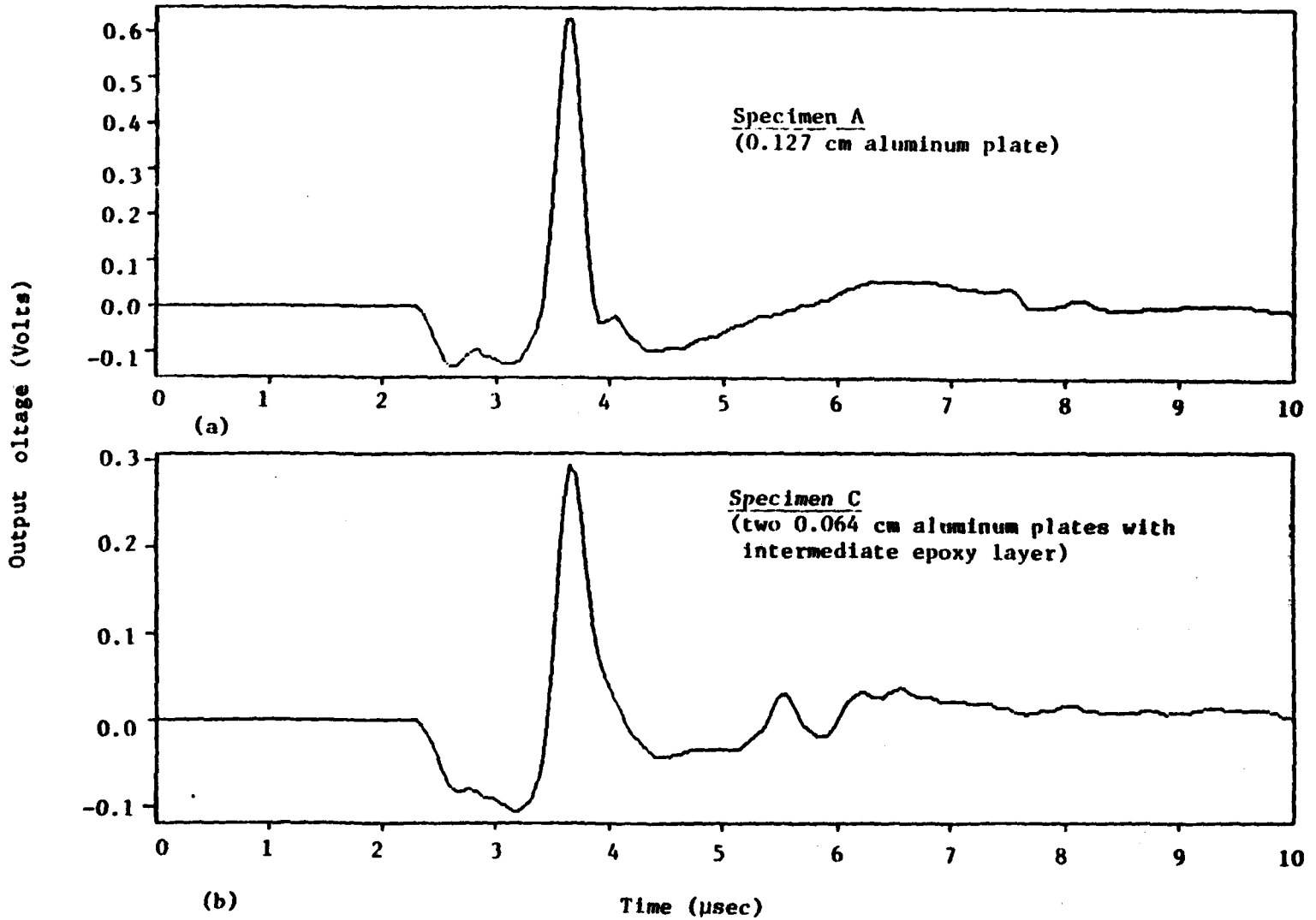

Fig. H3 Comparison of broadband pulse response for (a) 1.270 cm (0.500 in) aluminum plate and (b) two 0.635 cm (0.250 in) aluminum plates with intermediate epoxy layer clamped between AE-101 transducers.

APPENDIX I

SIMULATION OF FREQUENCY-DEPENDENT BACKING ATTENUATION USING A LOW-PASS DIGITAL FILTER

In this appendix, a scheme is proposed for the efficient simulation of the strongly frequency-dependent attenuation of the backing material used in the transducers in this study. This enables the prediction of the backing wave produced by a broadband input signal.

I.1 PRELIMINARY PREDICTION OF BACKING WAVE

Fig. I1 shows the complete measured and predicted broadband pulse response of two FC-500 transducers clamped face-to-face. The predicted output signal is based on the parameters given in Table 2 for a 0.4 MHz tone burst input. This is only a crude approximation, since the input pulse has appreciable frequency components from 0.0-1.0 MHz, and Fig. C6 shows that the backing attenuation varies significantly with frequency at the high end of that range.

The predicted output signal shows, as expected, a backing wave arriving at about 10 μsec after the application of the input voltage. It also shows a second backing wave arriving at about 20 μsec, with greatly reduced amplitude. The time delays for each of these backing waves appear to be correct, but the amplitude and shape are distinctly different from those in the measured output signal. Observe that the first backing wave in

the predicted signal is merely a reduced-amplitude, inverted version of the primary wave, while the measured output shows a very smooth backing wave, without the jagged peaks of the primary wave. This behavior can be simulated by selective filtering of the high-frequency components in the predicted backing wave.

I.2 DESIGN OF THE FILTERING ALGORITHM

A one-parameter digital low-pass filter is described by

$$T_o(t) = (1 - \Delta)T_i(t) + (\Delta)T_o(t - \Delta t) \tag{I1}$$

where T_i represents the stress wave entering the filter, T_o represents the filtered stress wave leaving the filter, Δt is the time interval of the filtering process and Δ is a dimensionless filtering parameter. This filter resists arbitrarily abrupt (high-frequency) changes in the stress by weighting the previous value of stress into the current value, so that the filtered output stress is a sort of time average of the input and output at a particular instant. Setting $\Delta=0$ means that $T_o(t) = T_i(t)$, so that no filtering is introduced at all. For $\Delta=1$, on the other hand, $T_o(t+\Delta t)=T_o(t)$, and the value of T_o remains constant regardless of variations in T_i. Thus, increasing Δ from 0 to 1 varies the cutoff frequency from infinity all the way down to 0. Note that the cutoff frequency depends on Δt as well as on the filtering parameter, Δ.

Fig. I2 shows the predicted broadband pulse response of the system for several different values of Δ. Of these four plots, curve (d), for which $\Delta=0.975$, appears to look the most like the

measured output signal.

I.3 PREDICTION OF THE BACKING WAVE USING THE FILTER

Fig. I3 shows the final prediction of the complete output signal, including the filtered backing wave. The results are very encouraging, with the predicted and measured backing waves showing excellent agreement with one another.

Fig. I4 is a plot of the attenuation of the filter versus frequency. Comparing this plot to Fig. C6 (measured backing attenuation versus frequency) shows that the predicted curve is much steeper than the measured curve, and that the predicted cutoff frequency is somewhat low. Probably a two- or three-parameter filter is required to accurately duplicate the measured frequency-dependence of the backing attenuation.

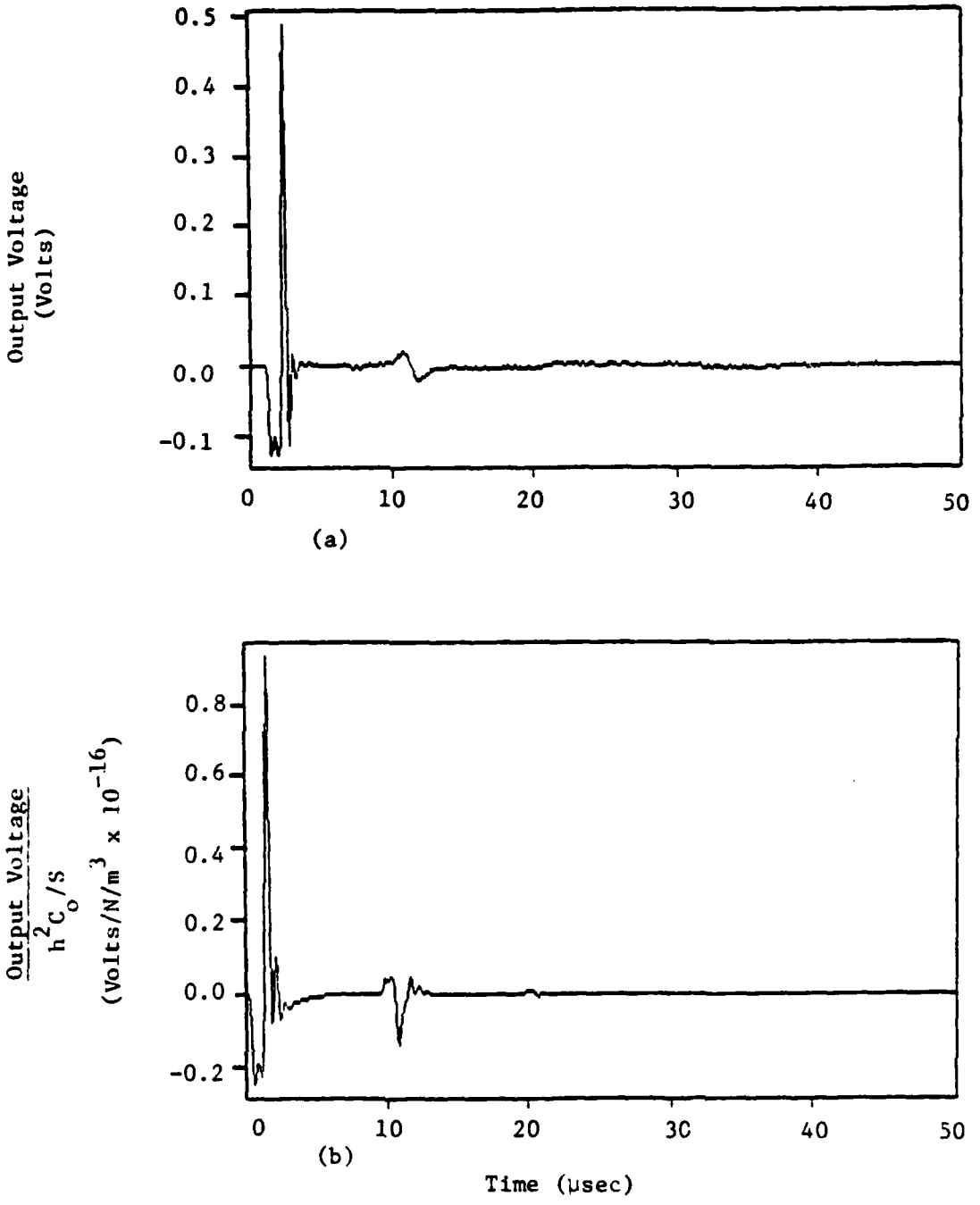

Fig. 11 Comparison of (a) measured and (b) predicted broadband pulse response for two FC-500 transducers clamped face-to-face.

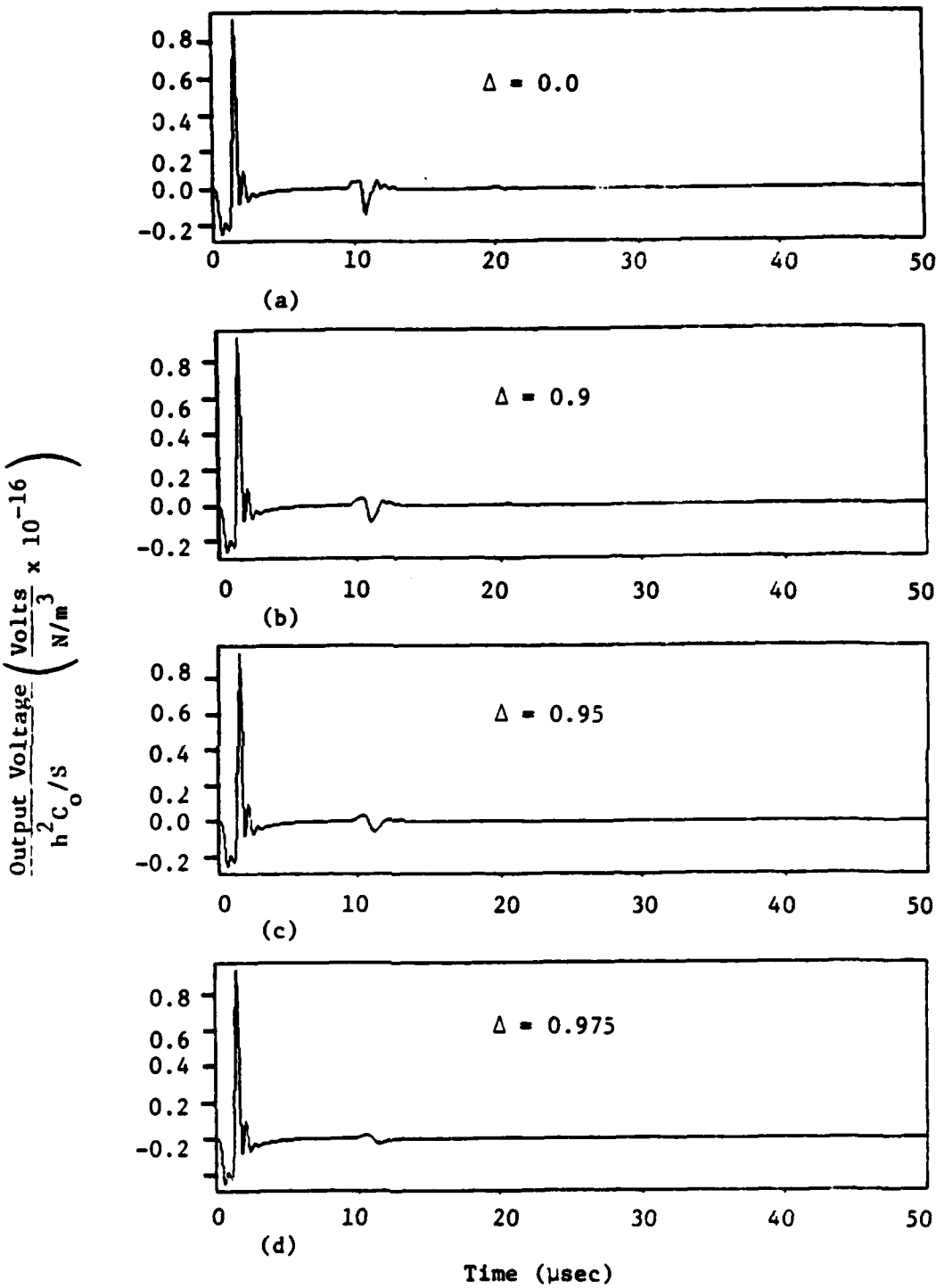

Fig. I2 Predicted broadband pulse response for two FC-500 transducers clamped face-to-face as a function of attenuation filtering parameter.

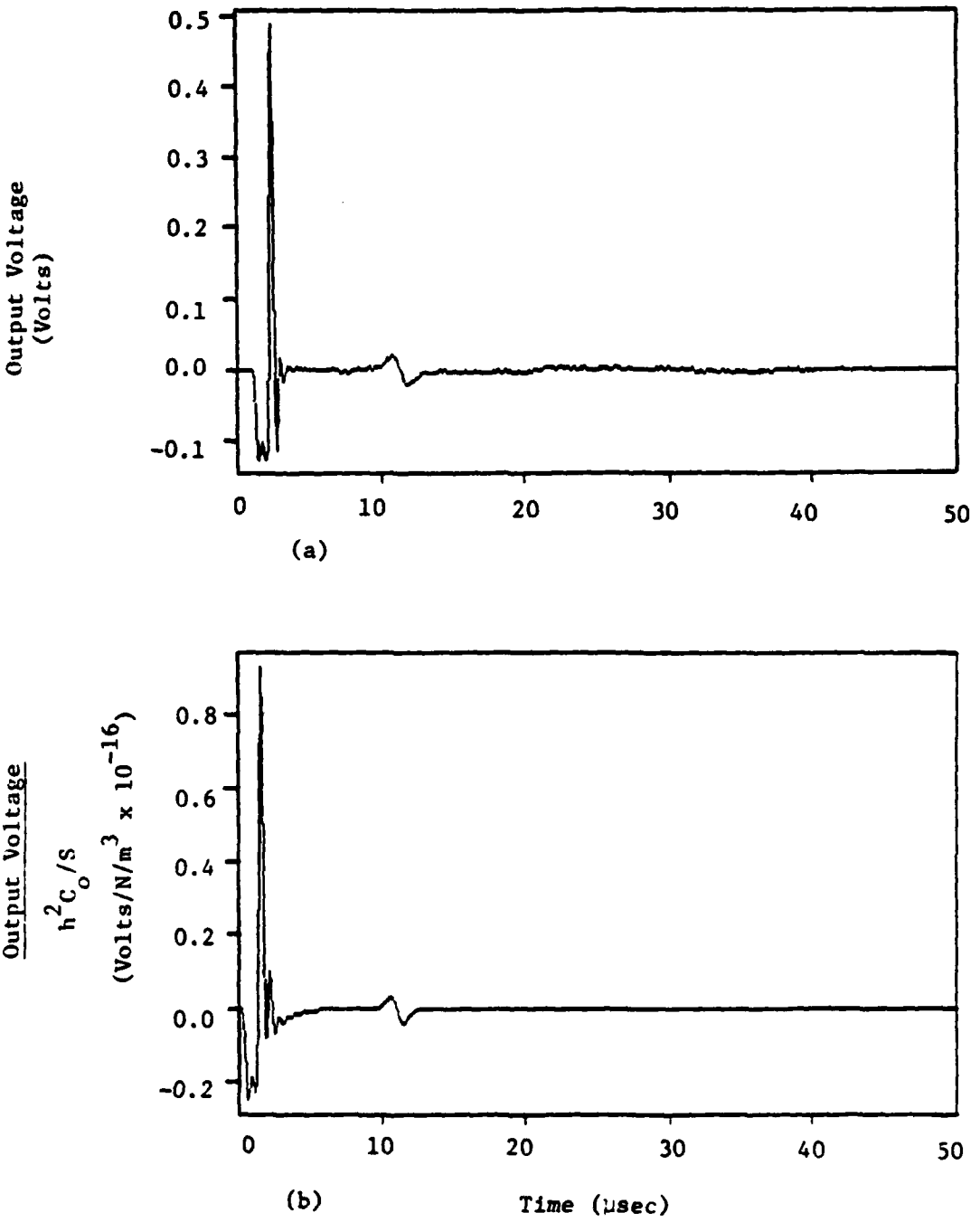

Fig. I3 Comparison of (a) measured and (b) predicted broadband pulse response for two FC-500 transducers clamped face-to-face.

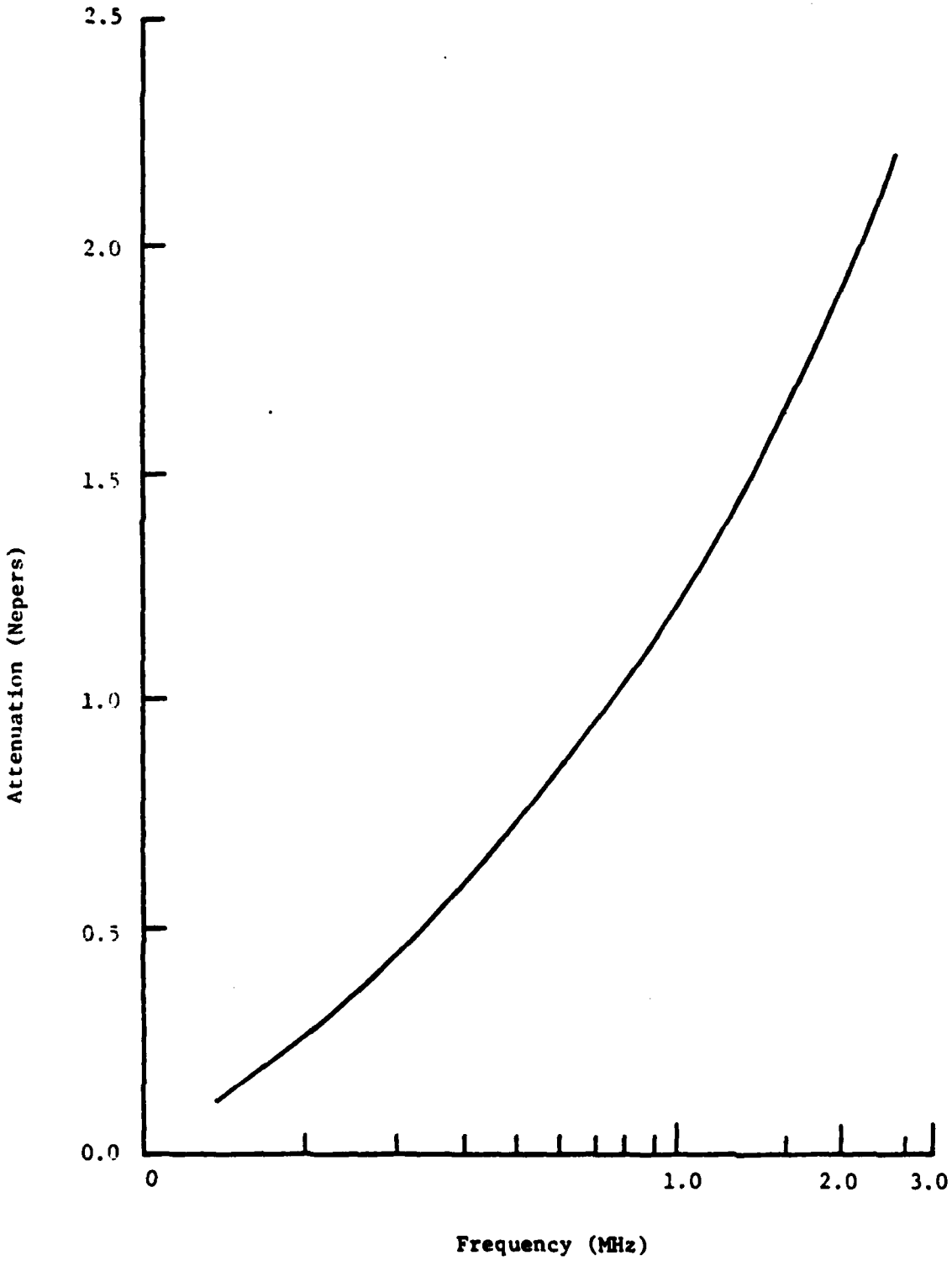

Fig. I4 Plot of attenuation vs. frequency for the one-parameter digital low-pass filter (Δ=0.975).